Exploring the impact of TGF-β superfamily cytokines on HIV-1 replication



Matthew Dickinson
Wolfson College
University of Oxford

A thesis submitted for the degree of
Doctor of Philosophy in Clinical Medicine
Trinity 2020

Abstract

The transforming growth factor (TGF)-β superfamily comprises evolutionarily conserved cytokines including TGF-β isoforms, activins and bone morphogenetic proteins (BMPs). Recent work has shown that TGF-β superfamily cytokines elicit transcriptional changes overlapping with those of type I interferons (IFNs) in hepatoma and epithelial cells and control the replication of several viruses by IFN-dependent and -independent mechanisms. Type I IFNs play a complex role in HIV-1 infection, restricting virus replication and transmission but also driving immune activation and apoptosis. However, the roles of TGF-β superfamily cytokines in HIV-1 infection are less well understood. In this thesis, both the induction of TGF-β superfamily cytokines during HIV-1 infection and their putative roles in HIV-1 control and pathogenesis were explored.

TGF-β_1 was found to be systemically induced very early in acute HIV-1 infection (prior to the innate cytokine "storm"), likely due to release from platelets; remaining upregulated throughout infection. In contrast, activins A and B, and BMP-2 were not found to be significantly perturbed during acute or chronic infection. TGF-β_1 inhibited HIV-1 replication in primary, activated $CD4^+$ T cells *in vitro*, but had no effect on HIV-1 replication in less activated cells or in macrophages. Other TGF-β superfamily cytokines did not inhibit HIV-1 replication in any of the cell types tested. Neither TGF-β_1, activin A nor BMP-2 upregulated antiviral genes or modulated type I IFN signalling genes in activated $CD4^+$ T cells. Further investigation of how TGF-β_1 restricts HIV-1 replication suggested that TGF-β_1 may reduce the proportion of Th17 cells in activated PBMC cultures. Most notably, TGF-β_1 reduced cell activation status and proliferation; and diminished transcriptional activity from the HIV-1 promoter. This study gives insight into the utility of harnessing TGF-β_1 activity for HIV-1 prophylaxis or therapy, and provides broader insight into an apparent cell type-dependent nature of innate antiviral activity of TGF-β superfamily cytokines.

Acknowledgements

I have to start by expressing my heartfelt gratitude to Prof Seph Borrow, who took a chance on me when I had barely ever picked up a pipette, and who encouraged me throughout my DPhil. On the days when I didn't believe in myself, Seph always vocally did. I really appreciated all the intellectually stimulating conversations not only about the project but also discussing HIV in great depth, which we did frequently and at a leisurely pace. Under Seph's mentorship, I can honestly say I have emerged as a new person: I *think* in different ways. It has been a truly formative experience.

I would also like to sincerely thank Prof Hal Drakesmith who has been a fantastic co-supervisor. Hal played a very active role in steering the project, giving me unlimited access to reagents, resources and advice whenever I needed them. I really appreciated him providing commiserations and humour in equal measure when things would go spectacularly wrong.

From day one, the Borrow lab has felt like home. I would like to acknowledge the following people for fostering such a positive environment that was so conducive for productive work and learning. Angharad Fenton-May for teaching me absolutely every cell culture and virological technique, mentoring me right from the beginning when I knew nothing about viral immunology. Ane Ogbe for contributing to so much of my early training in cat 3, and for the great friendship we have created outside of the lab. Anna Kliszczak for producing stocks of every virus used in this thesis and being such a kind, conscientious colleague and team player. Isabela Pedroza-Pacheco for teaching me so much about flow cytometry, generously providing tried and tested panels, and for being a fantastic role model who never cuts corners. Wayne Paes for the jokes, and so many great conversations about the natural world. Cathy Wormald for all the tissue culture chats about Oxford life, film and life beyond science. Tom Partridge for always being such a patient, approachable person to troubleshoot those joyful 7pm

problems, and for imparting wisdom about dendritic cells, travel, and maintaining a work-life balance.

I am grateful to members of the Drakesmith lab for listening to this work unfold over four years and for making the WIMM a second home. In particular, Joe Frost and Ali Preston for being such great friends, and Joe for providing so many useful suggestions and just always wanting to help, teach, share, listen, discuss. Also, with thanks to Nicki Gray in the CBRG for patiently helping with RNAseq experimental design and for analysing the data; to the McMichael, Gillespie and Peppa groups for providing feedback on my data at joint lab meetings; to Prof Paul Klenerman and Prof Jan Rehwinkel for all their input on the project throughout; and to Wolfson College and the British Society of Immunology for financial support to attend conferences. I also want to acknowledge Prof Christoph Wulfing at Bristol for my first brief exposure to research and giving me such a positive experience of supervision in his lab. I have to thank the Nuffield Department of Clinical Medicine for its generous Prize Studentship which funded all my living costs and fees of the last four years. My gratitude also goes to the anonymised donors of our samples, without whom none of this work would be possible. I write this in solidarity with those living with HIV worldwide, I have continually felt driven to work on this project in the hope that one day we will beat the HIV/AIDS pandemic and end the stigmatisation and marginalisation of those affected by it.

Outside of the lab I have been incredibly lucky to have met the most wonderful lifelong friends who made my time in Oxford so special. I would not have made it through the DPhil without them. Nicky Burt and Jonny Madelaine, the two best friends I made in this city; it was a joy to return home every night and just hang out while day turned to night and summer turned to winter. Charlie Harris and Dan Schofield for always being there for me through the best and worst of times. Dave Cain for being so down-to-earth and reminding me that we are always

vets no matter where our future paths take us. Donall Forde, for helping me through challenges and just being such a fun presence at work. Jon Stott and Ronja Becker, who will forever be the friends whose sunny dispositions got me through the pandemic lockdown in Oxford. My inspirational friends Hugh Palmer and Hoonie Feltham, for always being so supportive and interested in my life. And Katie Roche, for unconditionally supporting me in so many special ways: keeping me company in the lab on weekends, attending my talks, proof-reading this thesis, and for giving me an appreciation of so many things on my own doorstep.

Finally, my biggest gratitude has to go to my mum and dad, Christine and Trevor Dickinson, who have unwaveringly supported every decision I've ever made, without whom I would never have made it to where I am today.

Thank you.

Dedicated to Margaret Olga Tomlin, my grandma, the wisest person I have ever known, who showed me that an education is what remains when you've forgotten everything you formally learnt, and whose enduring patience and courage I hope to always emulate when facing adversity.

Table of contents

Abstract i
Acknowledgements ii
List of figures x
List of tables xiii
List of abbreviations xiv
Author's contributions xvii
Statement of impact of COVID-19 xviii

Chapter 1: Introduction 1
1.1 HIV 1
1.1.1 The HIV/AIDS pandemic 1
1.1.2 The need for prophylactic and therapeutic strategies against HIV 2
1.1.3 HIV-1 M subtypes 3
1.1.4 HIV-1 structure 3
1.1.5 HIV-1 genome 4
1.1.6 HIV-1 life cycle 5
1.1.7 Natural course of HIV-1 infection: the clinical picture 6
1.1.8 HIV-1 transmission 7
1.1.9 Acute HIV-1 infection 8
1.1.10 Chronic HIV-1 infection and the pathologic basis of HIV-1 disease 10
1.2 The immune system 12
1.2.1 Innate immunity 12
1.2.2 Type I and III interferons 14
1.2.3 Adaptive immunity 15
1.2.4 T helper differentiation and subsets 16
1.3 HIV-1 and the immune system 20
1.3.1 Innate immune responses in HIV-1 infection 20
1.3.2 Dendritic cells in HIV-1 infection 20
1.3.3 Macrophages in HIV-1 infection 22
1.3.4 Innate cytokines in HIV-1 infection 22
1.3.5 Adaptive immune responses in HIV-1 infection 26
1.3.6 Treg cells in HIV-1 infection 27
1.3.7 Th17 cells in HIV-1 infection 29
1.4 The TGF-β superfamily 30
1.4.1 TGF-β superfamily ligands 30
1.4.2 TGF-β superfamily receptors and signalling 33
1.4.3 TGF-β immunobiology 36
1.4.4 TGF-β in HIV-1 infection 38
1.4.5 Activins in immunobiology and infection 40
1.4.6 BMPs in immunobiology and infection 42
1.4.7 Cross-communication between TGF-β superfamily and type I interferon signalling pathways 44
1.5 Hypotheses and research objectives 46

Chapter 2: Materials and methods 47
2.1 Materials 47
2.1.1 Human samples 47
2.1.2 Viruses 48
2.1.3 Chemical reagents and media 49
2.1.4 Media 51

2.1.5 Cell lines 51
2.1.6 Cytokines 52
2.1.7 Antibodies for stimulation or neutralisation 53
2.1.8 Antibodies and stains for flow cytometry 53
2.1.9 Flow cytometry staining panels 54
2.1.10 Antibodies for western blotting 55
2.1.11 TaqMan probes for RT-qPCR 56
2.2 Methods 57
2.2.1 General tissue culture methodology 57
2.2.2 Production of viruses from infectious molecular clones 58
2.2.3 Isolation of peripheral blood mononuclear cells 58
2.2.4 Isolation of leukocyte subsets 59
2.2.5 Generation of monocyte-derived dendritic cells 60
2.2.6 Generation of monocyte-derived macrophages 60
2.2.7 ELISA and Luminex assays 61
2.2.8 TGF-β superfamily cytokine induction assays 64
2.2.9 Western blotting 64
2.2.10 Flow cytometry 66
2.2.10.1 General flow cytometry methodology 66
2.2.10.2 phosphoSMAD2/3 staining 67
2.2.10.3 Intranuclear FOXP3 staining 68
2.2.10.4 CellTrace Violet staining for analysis of cell proliferation 68
2.2.11 Standard HIV-1 replication assay 69
2.2.12 Monocyte-derived macrophage HIV-1 replication assay 71
2.2.13 Monocyte-derived dendritic cell-CD4$^+$ T cell co-culture HIV-1 replication assay 71
2.2.14 293FT cell HIV-1 replication assay 73
2.2.15 HIV-1 p24 AlphaLISA assay 73
2.2.16 HIV-1 NL4-3 LTR luciferase reporter assay 74
2.2.17 RNA sequencing 75
2.2.18 Quantitative real-time polymerase chain reaction 77
2.2.19 Statistical analysis and data presentation 77

Chapter 3: Analysis of the induction of TGF-β superfamily cytokines in HIV-1 infection 79
3.1 Introduction 79
3.2 Results 83
3.2.1 Circulating levels of TGF-β_1, but not activins A and B or BMP-2, are elevated in acute HIV-1 infection 83
3.2.2 Circulating levels of TGF-β_1, but not activins A and B or BMP-2, are elevated in subacute and chronic HIV-1 infection 88
3.2.3 Increased TGF-β_1 correlates with platelet degranulation at all stages of HIV-1 infection 92
3.2.4 pDCs stimulated with HIV-1 do not produce TGF-β_1, activins A and B or BMP-2 94
3.2.5 MDDCs stimulated with HIV-1 do not produce TGF-β_1, activins A and B or BMP-2 96
3.2.6 mDCs stimulated with HIV-1 do not produce TGF-β_1, activins A and B or BMP-2 98
3.2.7 PBMCs stimulated with HIV-1 do not produce TGF-β_1, activins A and B or BMP-2 99
3.3 Discussion 101

Chapter 4: The effects of TGF-β superfamily cytokines on HIV-1 replication *in vitro* 112
4.1 Introduction 112
4.2 Results 115
4.2.1 SMAD signalling in macrophages and CD4+ T cells 115
4.2.2 Lack of effect of TGF-β superfamily cytokines on HIV-1 replication in macrophages 119
4.2.3 Lack of effect of many TGF-β superfamily cytokines on HIV-1 replication in activated CD8-depleted PBMCs 121
4.2.4 TGF-β_1 inhibits HIV-1 replication in activated CD4+ T cells 125
4.2.5 TGF-β_1 and IFN-α inhibit HIV-1 replication by mechanisms independent of one-another's signalling 127
4.2.6 Transmitted founder viruses are relatively more resistant to TGF-β_1 inhibition 129
4.2.7 Establishment of an HIV-1 replication assay in less activated CD4+ T cells 135
4.2.8 No effect of TGF-β superfamily cytokines on HIV-1 replication in phenotypically less activated cells 139
4.2.9 No effect of TGF-β superfamily cytokines on HIV-1 replication in 293FT cells 142
4.3 Discussion 144

Chapter 5: Exploration of mechanisms of TGF-β_1-mediated inhibition of HIV-1 replication 153
5.1 Introduction 153
5.2 Results 159
5.2.1 TGF-β_1 modulates the expression of a distinct set of genes to IFN-α in activated CD4+ T cells, with no upregulation of canonical antiviral genes 159
5.2.2 TGF-β_1 and IFN-α do not modulate the transcription of genes involved in one-another's signalling pathways 166
5.2.3 Activin A and BMP-2 minimally alter the transcriptome of activated CD4+ T cells and do not induce the expression of antiviral genes 168
5.2.4 TGF-β_1 downregulates *IL17* expression and upregulates *CCL5* in activated CD4+ T cells 173
5.2.5 Recombinant IL-17 does not reverse TGF-β_1-mediated inhibition of HIV-1 replication 175
5.2.6 Blocking the IL-17 receptor does not inhibit HIV-1 replication 176
5.2.7 TGF-β_1 and IFN-α do not inhibit HIV-1 replication via a mechanism involving the chemokine XCL1 177
5.2.8 Analysis of the effects of TGF-β_1 on the T helper subset composition within activated CD4+ T cell cultures 178
5.2.9 Analysis of the effects of TGF-β_1 on CCR5 and CXCR4 expression 185
5.2.10 TGF-β_1 does not induce a Treg phenotype or induce FOXP3 expression in activated CD4+ T cells 188
5.2.11 TGF-β_1 attenuates transcription from the HIV-1 LTR in activated CD4+ T cells 190
5.2.12 The effects of TGF-β_1 on the NF-kB pathway in activated CD4+ T cells 192
5.2.13 TGF-β_1 decreases the phenotypic activation status of highly activated CD4+ T cells 194
5.2.14 TGF-β_1 negatively affects activated CD4+ T cell proliferation 200
5.2.15 TGF-β_1 does not affect the viability of activated CD4+ T cells 202
5.2.16 TGF-β_1-mediated inhibition of HIV-1 replication in activated CD4+ T cells may not be contingent upon its effects on T cell proliferation 204
5.3 Discussion 207

Chapter 6: Summary and future perspectives 217
6.1 Summary 217
6.2 Future perspectives 221
6.3 Final statement 228

Appendices 229
Appendix I Genes differentially expressed (adjusted P value <0.05) in activated $CD4^+$ T cells relative to non-activated cells 229
Appendix II Genes differentially expressed (adjusted P value <0.05) in IFN-α-treated activated $CD4^+$ T cells relative to untreated activated cells 230
Appendix III Genes differentially expressed (adjusted P value <0.05) in TGF-β_1-treated activated $CD4^+$ T cells relative to untreated activated cells 243
Appendix IV Genes differentially expressed (based on unadjusted P value <0.05) in activin A-treated activated $CD4^+$ T cells relative to untreated activated cells 248
Appendix V Genes differentially expressed (based on unadjusted P value <0.05) in BMP-2-treated activated $CD4^+$ T cells relative to untreated activated cells 252

References 254

Publications 295

List of figures

Figure 1.1 The structure of HIV-1 4
Figure 1.2 The HIV-1 genome 5
Figure 1.3 Typical dynamics of HIV-1 viral load and CD4+ T cell count throughout infection 9
Figure 1.4 T helper cell subset differentiation and function 17
Figure 1.5 The cytokine storm in acute HIV-1 infection 24
Figure 1.6 Processing of TGF-β superfamily precursor proteins 32
Figure 1.7 Canonical and non-canonical TGF-β superfamily signalling 35
Figure 2.1 HIV-1 viral replication assay 70
Figure 2.2 MDDC-CD4+ T cell co-culture viral replication assay 72
Figure 3.1 Analysis of the effects of anticoagulant and freeze-thawing on TGF-β superfamily cytokine concentration measured by ELISA or Luminex assay 85
Figure 3.2 Plasma concentrations of IFN-α and TGF-β superfamily cytokines at serial timepoints during AHI in three donors 86
Figure 3.3 Plasma concentrations of IFN-α and TGF-β superfamily cytokines in AHI 87
Figure 3.4 Plasma concentrations of TGF-β superfamily cytokines and IL-18 in subacute and chronic HIV-1 infection 91
Figure 3.5 Plasma concentrations of TGF-β_1 in subacute and chronic HIV-1 infection do not correlate with viral load 92
Figure 3.6 Correlation between plasma concentrations of PF4 and TGF-β_1 in HIV-1 infection 93
Figure 3.7 Analysis of TGF-β superfamily cytokines produced by pDCs cultured with HIV-1 *in vitro* 95
Figure 3.8 Analysis of TGF-β superfamily cytokines produced by MDDCs cultured with HIV-1 *in vitro* 97
Figure 3.9 Analysis of TGF-β superfamily cytokines produced by mDCs cultured with HIV-1 *in vitro* 98
Figure 3.10 Analysis of TGF-β superfamily cytokines produced by PBMCs cultured with HIV-1 *in vitro* 100
Figure 4.1 SMAD signalling in macrophages in response to TGF-β superfamily ligands 117
Figure 4.2 SMAD signalling in CD4+ T cells in response to TGF-β superfamily ligands 118
Figure 4.3 Analysis of the effects of TGF-β superfamily cytokines on HIV-1 replication in macrophages 120
Figure 4.4 Analysis of the effects of diverse TGF-β superfamily cytokines on HIV-1 replication in activated CD8-depleted PBMCs 123
Figure 4.5 Analysis of the effects of activin A and BMP-2 on IFN-α-mediated inhibition of HIV-1 replication in activated CD8-depleted PBMCs 124
Figure 4.6 The effects of TGF-β_1 on HIV-1 replication in activated CD4+ T cells and CD8-depleted PBMCs 126
Figure 4.7 The effects of inhibition of SMAD and JAK/STAT signalling on TGF-β_1- and IFN-α-mediated inhibition of HIV-1 replication 128
Figure 4.8 The effect of TGF-β_1 on the replication of TF viruses 131
Figure 4.9 The effect of TGF-β_1 on the replication of 6M viruses 132
Figure 4.10 Differential effects of TGF-β_1 and IFN-α on TF and 6M virus replication 133
Figure 4.11 The relationships between replicative efficiency and TGF-β_1- and IFN-α- mediated inhibition of TF and 6M virus replication 134
Figure 4.12 Flow cytometric analysis of activation marker expression in CD4+ T cells in a less highly activated viral replication assay compared to the standard HIV-1 replication assay 138

Figure 4.13 Analysis of viral growth in a less highly activated CD4+ T cell HIV-1 replication assay 139
Figure 4.14 Analysis of the effects of TGF-β superfamily cytokines on HIV-1 replication in an MDDC-CD4+ T cell co-culture HIV-1 replication assay 141
Figure 4.15 Differential TGF-β_1-mediated inhibition of HIV-1 replication in CD8-depleted PBMCs pre-activated with high or low concentrations of antibodies to CD3 and CD28 142
Figure 4.16 Analysis of the effects of TGF-β superfamily cytokines on HIV-1 replication in 293FT cells 143
Figure 5.1 The structure of the HIV-1 LTR 154
Figure 5.2 Canonical NF-κB pathway activation 156
Figure 5.3 Comparative analysis of gene expression in CD4+ T cells directly *ex vivo* and after activation for 72 hours with antibodies to CD3 and CD28 163
Figure 5.4 The effects of IFN-α on the transcriptome of activated CD4+ T cells 164
Figure 5.5 The effects of TGF-β_1 on the transcriptome of activated CD4+ T cells 165
Figure 5.6 qRT-PCR analysis of selected genes in TGF-β_1- and IFN-α-treated activated CD4+ T cells identified from the RNA sequencing dataset 166
Figure 5.7 qRT-PCR analysis of selected target genes in activin A- and BMP-2-treated activated CD4+ T cells identified from the RNA sequencing dataset 170
Figure 5.8 qRT-PCR analysis of the expression of genes encoding selected HIV-1 restriction factors in TGF-β superfamily and IFN-α-treated activated CD4+ T cells 171
Figure 5.9 qRT-PCR analysis of the expression of selected ISGs previously shown to be upregulated in BMP-treated hepatocytes, in TGF-β superfamily and IFN-α-treated activated CD4+ T cells 172
Figure 5.10 Pathway analysis of genes differentially expressed in TGF-β_1-treated versus non-cytokine-treated activated CD4+ T cells 174
Figure 5.11 Analysis of the effects of IL-17 on TGF-β_1-mediated inhibition on HIV-1 replication 175
Figure 5.12 Analysis of the effects of blocking IL-17 signalling on HIV-1 replication 176
Figure 5.13 Analysis of the effects of inhibiting XCL1 on TGF-β_1- and IFN-α-mediated inhibition of HIV-1 replication 178
Figure 5.14 Gating strategy for T helper subset analysis in CD4+ T cells 182
Figure 5.15 Analysis of the effects of TGF-β_1 on proportions of T helper subsets in total activated CD4+ T cells 183
Figure 5.16 Analysis of the effects of TGF-β_1 treatment of activated CD4+ T cells on proportions of Th17 and Th17-like follicular cells in total CD4+ T cell, Tcm and Tem compartments 184
Figure 5.17 Analysis of the effects of TGF-β_1 treatment of activated CD4+ T cells on expression of CCR5 and CXCR4 in total CD4+ T cell, Tcm and Tem compartments 187
Figure 5.18 Analysis of the effects of TGF-β_1 on Treg markers in activated CD4+ T cells 189
Figure 5.19 Analysis of the effects of TGF-β_1 on transcriptional activity from the HIV-1 LTR in immortalised T cell lines 191
Figure 5.20 The effects of TGF-β_1 on transcriptional activity from the HIV-1 LTR in activated primary CD4+ T cells 191
Figure 5.21 Analysis of the effects of TGF-β_1 on the NF-κB signalling pathway in activated CD4+ T cells 193
Figure 5.22 Analysis of the effects of treatment of pre-activated CD4+ T cells with TGF-β_1 for 24 hours on expression of cellular activation markers 197
Figure 5.23 The effects of TGF-β_1 on activation marker expression in activated CD4+ T cells after two and five days 198

Figure 5.24 Analysis of the effects of TGF-β_1 on activation marker expression in $CD4^+$ ..... T cells co-cultured with allogeneic MDDCs 199
Figure 5.25 The effects of TGF-β_1 on activated $CD4^+$ T cell proliferation 201
Figure 5.26 Analysis of the effects of TGF-β_1 on viability and cell numbers of ..... activated $CD4^+$ T cells.....203
Figure 5.27 Analysis of the effects of TGF-β_1 and a reduced cell activation stimulus on ..... $CD4^+$ T cell activation status, proliferation and on HIV-1 replication.....206

List of tables

Table 1.1 Selected TGF-β superfamily ligands and their receptors 33
Table 2.1 HIV-1 viruses derived from infectious molecular clones 48
Table 2.2 Chemical reagents 49
Table 2.3 Recombinant cytokines 52
Table 2.4 Antibodies for stimulation or neutralisation 53
Table 2.5 Antibodies and stains for flow cytometry 53
Table 2.6 Antibodies for western blot 55
Table 2.7 TaqMan probes for qRT-PCR 56
Table 2.8 MACS kits for leukocyte subset isolation 59
Table 2.9 ELISA and Luminex assay kits 61
Table 3.1 Clinical information for donors subacutely and chronically infected with HIV-1 90
Table 5.1 Genes differentially regulated by both TGF-β_1 and IFN-α in activated $CD4^+$ T cells 161
Table 5.2 Analysis of the effects of TGF-β_1 on expression of IFN-α signalling pathway genes in activated $CD4^+$ T cells 167
Table 5.3 Analysis of the effects of IFN-α on expression of TGF-β superfamily signalling pathway genes in activated $CD4^+$ T cells 168
Table 5.4 Analysis of the effects of TGF-β_1 on expression of NF-κB pathway genes in activated $CD4^+$ T cells 194
Table 5.5 The effects of 24 hours of TGF-β_1 treatment of pre-activated $CD4^+$ T cells on expression of T cell activation marker-encoding-genes 196

List of abbreviations

6M	6-month
ACVR	Activin receptor
AF	Alexa Fluor
AGM	African green monkey
AHI	Acute HIV-1 infection
AIDS	Acquired immunodeficiency syndrome
ALK	Activin-like kinase
ANOVA	Analysis of variance
APC	Allophycocyanin
APOBEC3G	Apolipoprotein B mRNA editing enzyme, catalytic polypeptide-like 3G
ART	Antiretroviral therapy
BB	Brilliant Blue
BMP	Bone morphogenetic protein
BMPR	Bone morphogenetic protein receptor
BSA	Bovine serum albumin
β-TG	Beta-thromboglobulin
BV	Brilliant Violet
CD	Cluster of differentiation
cDNA	Complementary DNA
CLR	C-type lectin receptor
coSMAD	Common SMAD
CPM	Counts per million
CLR	C-type lectin receptor
CTV	Cell Trace Violet
CV%	Coefficient of variation
DC	Dendritic cell
DC-SIGN	DC-specific intercellular adhesion molecule-3-grabbing non-integrin
DEG	Differentially expressed gene
DMEM	Dulbecco's Modified Eagle medium
DMSO	Dimethyl sulfoxide
dN	Deoxynucleoside
DNA	Deoxyribonucleic acid
dsDNA	Double-stranded DNA
ECL	Enhanced chemiluminescence
EDTA	Ethylenediaminetetraacetic acid
ELISA	Enzyme-linked immunosorbent assay
Env	Envelope glycoprotein
FBS	Foetal bovine serum
FITC	Fluorescein isothiocyanate
FMO	Fluorescence minus one
FOSx	Following onset of symptoms
FOXP3	Forkhead box protein 3
FS	Forward scatter
GALT	Gut-associated lymphoid tissue
GAPDH	Glyceraldehyde 3-phosphate dehydrogenase
GDF	Growth differentiation factor
gDNA	Genomic DNA
GM-CSF	Granulocyte-monocyte colony-stimulating factor
HAART	Highly active antiretroviral therapy
HAND	HIV-associated neurocognitive disorder

HBV	Hepatitis B virus
HCMV	Human cytomegalovirus
HCV	Hepatitis C virus
HIV	Human immunodeficiency virus
HPV	Human papillomavirus
HRP	Horseradish peroxidase
IFI6	Interferon-alpha-induced protein 6
IFIT3	Interferon-induced protein with tetratricopeptide repeats 3
IFITM	Interferon-induced transmembrane protein
IFN	Interferon
IFNAR	Interferon alpha/beta receptor
IKK	Inhibitor of kappa B kinase
IL-17R	Interleukin 17 receptor
IMC	Infectious molecular clone
IRF	Interferon regulatory factors
ISG	Interferon-stimulated gene
IκB	Inhibitor of kappa B
JAK	Janus kinase
KSHV	Kaposi's sarcoma-associated herpesvirus
LC	Langerhans cell
LCMV	Lymphocytic choriomeningitis virus
LLC	Large latent complex
LLOQ	Low limit of quantitation
LPS	Lipopolysaccharide
LRSC	Leukocyte reduction system chamber
LTR	Long terminal repeat
MACS	Magnetic-activated cell sorting
M-CSF	Macrophage colony-stimulating factor
MAPK	Mitogen-activated protein kinase
mDC	Myeloid dendritic cell
MDDC	Monocyte-derived dendritic cell
MDM	Monocyte-derived macrophage
MEM NEAA	Minimum essential medium non-essential amino acid
MFI	Median fluorescence intensity
MHC	Major histocompatibility complex
MMP	Matrix metalloproteinase
MOI	Multiplicity of infection
mRNA	Messenger RNA
MSM	Men who have sex with men
NaCl	Sodium chloride
Nef	Negative regulatory factor
NFAT	Nuclear factor of activated T cells
NF-κB	Nuclear factor kappa-light-chain-enhancer of activation B cells
NHP	Non-human primate
NK	Natural killer
PBMC	Peripheral blood mononuclear cell
PBS	Phosphate-buffered saline
pDC	Plasmacytoid dendritic cell
PE	Phycoerythrin
PF4	Platelet factor 4
PHA	Phytohaemagglutinin
PI3K	Phosphatidylinositol-3-kinase

PD-L1	Programmed death-ligand 1
PRR	Pattern recognition receptor
pSMAD	PhosphoSMAD
pTreg	Peripheral regulatory T cell
qRT-PCR	Quantitative real-time polymerase chain reaction
Rev	Regulator of expression of virion proteins
RM	Rhesus macaque
RNA	Ribonucleic acid
RNAseq	RNA sequencing
RORγt	Retinoic acid receptor-related orphan receptor gamma t
RPMI	Roswell Park Memorial Institute
rSMAD	Receptor-regulated SMAD
RT	Reverse transcriptase
SAMHD1	Sterile alpha motif and histidine-aspartic domains protein 1
SD	Standard deviation
SDS	Sodium dodecyl sulfate
SIV	Simian immunodeficiency virus
SMAD	Sons of mothers against decapentaplegic
SP1	Specificity protein 1
SS	Side scatter
ssRNA	Single-stranded RNA
STAT	Signal transducer and activator of transcription protein
TAK1	TGF-β-activated kinase 1
Tat	Trans-activator of transcription
TBS	Tris-buffered saline
TBST	Tris-buffered saline with 0.1% Tween
Tcm	T central memory
TCR	T cell receptor
Tem	T effector memory
Temra	$CD45RA^+$ T effector memory
TF	Transmitted founder
Tfh	T follicular helper
Tfr	T follicular regulatory
Treg	Regulatory T cell
TGF-β	Transforming growth factor beta
TGFBR	Transforming growth factor beta receptor
TGS	Tris/glycine/SDS
Th	T helper
TLR	Toll-like receptor
TNF	Tumour necrosis factor
TRIM5a	Tripartite motif-containing protein 5 alpha
tTreg	Thymic regulatory T cell
Vif	Viral infectivity factor
Vpr	Viral protein R
Vpu	Viral protein unique
VSV	Vesicular stomatitis virus

Author's contributions

All work in this thesis is original and was independently conducted by Matthew Dickinson with the following exceptions:

- Dr Anna Kliszczak (University of Oxford, UK) produced HIV-1 virus stocks including quantification of reverse transcriptase.
- Dr Eleni Giannoulatou (Victor Chang Cardiac Research Institute, Australia and University of New South Wales, Australia) created interpolation curves and carried out the statistical analysis of data in Figure 3.3.
- Nicki Gray (University of Oxford, UK) conducted bioinformatic analysis of the RNA sequencing data in Chapter 5, including mapping reads, determining differentially expressed genes and associated quality control work.
- MSc student Alexander Wicking assisted in producing some of the data in Figures 4.8-10 and Figure 4.14B.

Statement of impact of COVID-19

For the experiment shown in Figures 5.15-17, it was originally planned to assess days two and five post-TGF-β_1 treatment for consistency with other experiments in Chapter 5, and in a greater number of donors. Due to disruption caused by self-isolation, a single timepoint of day four was assessed in n=2 donors.

For Figure 5.27, a greater number of donors would have been assessed but were not, due to time lost from laboratory and building closures.

Chapter 1

Introduction

1.1 HIV

1.1.1 The HIV/AIDS pandemic

Human immunodeficiency virus (HIV) is a leukotropic lentivirus responsible for causing acquired immunodeficiency syndrome (AIDS). HIV/AIDS is an ongoing global pandemic; 38 million people currently live with the virus, 1.7 million people became newly infected with HIV in 2018, and 750,000 people died from AIDS-related illnesses in that same year[1]. The World Health Organisation considers HIV/AIDS to be among the 10 greatest threats to global health from 2019-2023[2].

HIV traces its origins to the early 20th century as a former zoonosis. Strains of simian immunodeficiency virus (SIV) were transmitted from non-human primates (NHPs) to people in spillover events, likely due to hunting and bushmeat consumption[3]. HIV can be divided into two main types: HIV-1 and HIV-2. HIV-1, the more pathogenic and virulent, is divided into three subgroups, M, N and O, the first of which is derived from the chimpanzee strain of SIV and accounts for the vast majority of all HIV infections worldwide[3]. HIV-2 is derived from the sooty mangabey monkey strain of SIV, and although also a cause of AIDS, fewer infected individuals progress to AIDS and they generally take longer to do so[4].

The current HIV pandemic gained traction in the late 1970s, exploding into global awareness in the subsequent decade[5]. HIV-1 is now a global pathogen, while HIV-2 remains predominantly in West Africa[4]. As a continent, Africa bears a significantly high amount (54%) of the global HIV/AIDS burden[1]. Globally, women are disproportionately more affected by the pandemic due to a myriad of reasons rooted in gender inequality as well as physiological factors[6].

1.1.2 The need for prophylactic and therapeutic strategies against HIV

Despite decades of research effort, no licensed vaccine exists for preventing HIV infection. The virus is predominantly a sexually transmitted pathogen, though other transmission routes include perinatal transmission and percutaneous injection[7]. Prophylactic strategies targeting these transmission routes have demonstrably slowed the progression of the pandemic. These include condom usage, education programmes, needle exchanges, and testing facilities to allow infected individuals to know their status[8]. However, despite these efforts, in 2018, there were still on average 4500 new cases of HIV occurring every day[1].

One of the greatest scientific triumphs in the fight against HIV to date is the development of antiretroviral therapy (ART), which can radically halt the progression of disease and prevent AIDS. ART drugs prevent HIV replication by inhibiting various stages of the virus life cycle. With the dawn of highly active ART (HAART), that is, combination therapy with multiple ART drugs, HIV has transformed from a slow but invariably fatal infection of the 1980s, to a manageable chronic condition in the present day[5]. Individuals on successful ART in developed countries now have a life expectancy close to that of the general population[9], providing that intervention is commenced early enough, and treatment compliance remains consistent. However, in 2018, only 62% of those living with HIV were accessing ART[1]. Reasons for this include the perceived cost of ART to individuals in some countries, social stigma, unawareness of infection, or for females, lack of access to healthcare facilities for reasons of gender inequality[10]. For those accessing ART, patients still have some immune system dysfunction[11,12] and are at a greater risk of other morbidities such as cardiovascular and renal disease[13]. And, even in those on successful treatment, drug-resistant viral mutants may emerge, which may correlate with poor adherence to treatment regimens, depending on the class of ART drug[14]. Finally, ART is not curative of infection, which is a lifelong status, so treatment must be taken indefinitely[15].

It is clear that despite world-changing scientific advances made over the last few decades, more prophylactic and therapeutic strategies to combat HIV are needed. In recent years, great leaps have been made in better understanding both protective immune responses in HIV infection as well as immunopathologic ones[16,17]. In order to inform rational and evidence-based design of new medicines, a greater understanding still of immune responses against the virus is warranted.

1.1.3 HIV-1 M subtypes

HIV-1 M can be divided into many subtypes or clades, of which clades A, B and C are the most prevalent. Clade A has a global prevalence of around 12% and is common in Eastern Europe, Central Asia and East Africa[18]. Clade B is the most prevalent strain circulating in the rest of Europe, the Americas, East Asia and Oceania[18]. Clade C is the most common subtype in Southern and Eastern Africa and India, accounting for around 50% of all cases worldwide[19]. There may be subtle differences between HIV-1 subtypes in virus transmission, replicative efficiency and drug resistance[19].

1.1.4 HIV-1 structure

Like all retroviridae, HIV-1 is an enveloped virus with a positive-sense, single-stranded diploid ribonucleic acid (RNA) genome. The viral envelope is derived from host cell membranes and carries glycoproteins gp120 (the distal head) and gp41 (the proximal stalk) as heterodimers (Fig. 1.1). Trimeric gp120-gp41 complexes form the viral surface envelope protein (Env), essential for binding host cells[20]. Underlying the envelope is p17 matrix protein. Within these protective layers, lies the distinctly conical capsid made of p24 protein arranged in hexagonal arrays. p7 nucleocapsid protein and p6, a protein necessary for late assembly of virions, bind the viral genome[21]. Packaged within the virus are also protease, reverse transcriptase (RT) and integrase enzymes, as well as accessory proteins viral protein R (Vpr), viral infectivity

factor (Vif), negative regulatory factor (Nef) and viral protein unique (Vpu); which antagonise host innate immune responses[22–24].

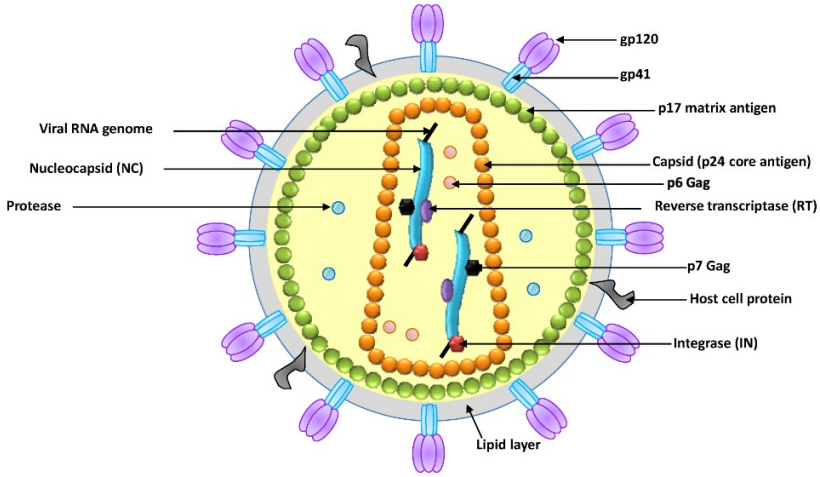


Figure 1.1 The structure of HIV-1
Figure adapted from[25]. Unlike most viruses, HIV-1 is unusual in that it possesses very few surface glycoproteins, fewer than is implied by this diagram; around 7-14 per virion, on average[26]. For comparison, influenza A virus has around 450 glycoprotein spikes per virion[27], Zika virus around 60[28] and herpes simplex virus over 600[29].

1.1.5 HIV-1 genome

The HIV-1 genome is remarkably succinct, comprising only nine genes spanning 9.7 kilobases across three reading frames (Fig. 1.2). The genome encodes three groups of genes. The structural protein genes include *gag*, encoding capsid, matrix and other major structural proteins; *pol*, encoding viral enzymes; and *env*, encoding the gp160 Env protein, cleaved into gp120 and gp41 by host proteases. The second group, the regulatory genes, include *tat* and *rev,* which are indispensable regulators of viral replication and gene expression. Accessory protein genes form the final group; *nef, vpr, vif* and *vpu* which antagonise immune responses, among other roles[30]. The genome is flanked by long terminal repeat (LTR) regions containing the viral promoter, necessary for transcription of the genome[31].

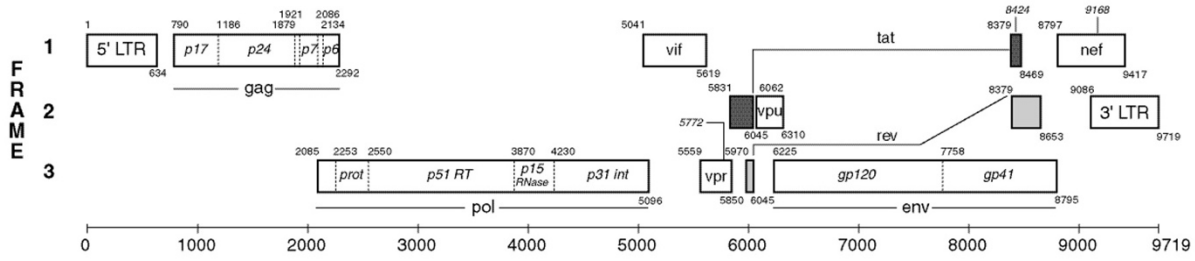


Figure 1.2 The HIV-1 genome
The HIV-1 genome schematically split to show its three reading frames. Open reading frames are enclosed in boxes. Numbers next to boxes denote start codon positions. Regulatory genes *tat* and *rev* both consist of two exons, spread apart in two reading frames. LTR=long terminal repeat, prot=protease, RT=reverse transcriptase, int=integrase. Figure taken from[32].

1.1.6 HIV-1 life cycle

HIV-1 infects cluster of differentiation 4 positive ($CD4^+$) T lymphocytes (T cells), monocytes and macrophages. The virus binds both CD4 and a host chemokine receptor as a coreceptor (usually either CCR5 or CXCR4) via the trimeric Env glycoprotein, which mediates both attachment and fusion[20]. Upon fusion between the viral envelope and the cell membrane, the capsid enters into the cytoplasm. Reverse transcription of the viral genome into complementary deoxyribonucleic acid (cDNA) begins in the capsid[33], which enshrouds viral cDNA from detection by intracellular immune sensing[34]. A pre-integration complex composed of viral cDNA complexed with host and viral proteins enters the nucleus, before viral integrase mediates integration of viral cDNA into the host genome. This frequently occurs in highly transcribed, active genes[35]. The newly resident HIV-1 genome (known as provirus in its integrated, non-replicating form) represents a virus reservoir, which may remain latent or commence active transcription[36].

In $CD4^+$ T cells, the HIV-1 genome is abundantly transcribed upon cell activation, with minimal active virus production taking place in truly resting cells[37]. Cell activation yields an increase in host transcription factors and substrates required for messenger (m)RNA synthesis, and the HIV-1 promoter contains binding sites for these factors, such as nuclear factor kappa-light-

chain-enhancer of activation B cells (NF-κB)[38], nuclear factor of activated T cells (NFAT) and specificity protein 1 (SP1)[39].

Early HIV-1 transcripts include fully spliced, short mRNAs encoding regulator of expression of virion proteins (Rev), trans-activator of transcription (Tat), and Nef. Tat ensures the transcription of longer transcripts containing structural protein genes, and Rev allows the egress of these incompletely spliced transcripts from the nucleus[40]. After translation of viral structural proteins, virion assembly occurs in the cytoplasm or at the plasma membrane[41]. Through membrane fission, encapsidated virions bud out from the cell surface membrane, taking the protective coating of lipid envelope with them. Viruses at this stage are immature and non-infectious, until viral protease cleaves the Gag and GagPol polyproteins, morphologically changing the virion and rendering it mature and infectious[41].

1.1.7 Natural course of HIV-1 infection: the clinical picture

Acute HIV-1 infection (AHI) commonly manifests as flu-like clinical signs and symptoms such as pyrexia, pharyngitis, myalgia and fatigue, known as acute retroviral syndrome, seen around two weeks into infection[42]. Following AHI, HIV-1 infection remains clinically latent for a long period (the “lente” of lentivirus means slow in Latin, referring to the timeline of disease). Many people are unaware of their HIV infection status during the latent phase. During this time, $CD4^+$ T cell count, a litmus for general immune health, gradually declines.

After a largely asymptomatic period of on average eight years in untreated individuals[43], signs of systemic immunodeficiency become apparent. These include chronic weight loss; opportunistic infections such as tuberculosis; obscure infections uncommonly or rarely seen in non-HIV infected individuals such as the parasitic cerebral toxoplasmosis, *Pneumocystis* pneumonia, *Candida* fungal infections; and cancers such as Kaposi’s sarcoma[44]. In the end

stage, neurological diseases can also arise, under a spectrum known as HIV-associated neurocognitive disorder (HAND), the worst manifestation of which is dementia[45]. Onset of AIDS is generally defined as a circulating $CD4^+$ T cell count of less than 200 cells/μl (or cells/mm^3) coupled with AIDS-defining illnesses[46].

For reasons still incompletely understood, a small number of people (1-5%[47]) either do not progress to AIDS or do so at a much slower rate than others, even without ART intervention. Some individuals also extraordinarily suppress viral replication, sometimes to even undetectable levels. Definitions of these subject groups are inconsistent in published literature, but the two most regularly used terms are “long-term non-progressors” for the former and “elite controllers” for the latter[48].

1.1.8 HIV-1 transmission

In most infected individuals, HIV-1 is present in semen, genital secretions, blood and milk, enabling sexual transmission, percutaneous inoculation and mother-to-child *in utero* (during parturition or through breastfeeding), although 70% of all infections are transmitted through heterosexual intercourse[7]. Virus present in body fluids may be cell-free or cell-associated, with transmission via the latter being more efficient[49]. The likelihood of sexual transmission of the virus is correlated with plasma viral load, with incremental increases in viral load and new infections showing a dose-response relationship[50].

HIV-1 is a relatively inefficiently transmitted virus, establishing infection an estimated four and eight times (insertive and receptive respectively) per 10,000 instances of penile-vaginal intercourse. Virus transmission is more efficient through receptive anal intercourse at 138 infections per 10,000 exposures, and damage or inflammation of mucosal sites also enhances transmission risk[51]. HIV-1 exhibits extremely high genetic diversity and exists as a

quasispecies in infected individuals[52]. Such is the vastness of the quasispecies, it is estimated that the genetic diversity of strains even in a single infected individual can exceed that of all circulating influenza A strains worldwide[53].

Despite this, new infections are often established by a single transmitted founder (TF) virion variant of the quasispecies[54]. Viruses can be CCR5 (R5)- or CXCR4 (X4)-tropic, or a combination of the two ("dual tropic"), dependent on the variant of the envelope glycoprotein present. TF viruses almost all use the coreceptor CCR5[55], are more infectious *in vitro* than non-TF viruses[56] and are more resistant to control by host innate immune responses[57,58]. X4-tropic and dual tropic viruses generally only emerge in the chronic stages of infection. Coreceptor switch is generally associated with rapid disease advancement[59], although this is not a pre-requisite for AIDS.

1.1.9 Acute HIV-1 infection

The earliest events in AHI, particularly in the microenvironment of the genital mucosa, are inferred from NHP models[60]. Rhesus macaques (RMs) (Old World monkeys native to Asia) infected with SIV (a native African primate virus) develop a pathology remarkably similar to that seen in HIV-1 infected people[61].

After crossing the mucosal epithelium, the virus establishes infection in a small population of cells and expands locally and in proximal draining lymphoid tissues[62]. In this "eclipse" period, believed to last around seven to ten days[63–65], there is no systemically detectable virus in plasma. After around one week, there are sufficient numbers of infected cells to enable the virus to spread systemically via lymph and subsequently blood, enabling replication in large numbers of target cells in lymphoid tissues throughout the body. This is associated with an exponential ramp-up of viraemia that peaks around three weeks post-infection[63]. Clinical signs

of acute retroviral syndrome generally coincide with the ramping up of high viraemic titres[66]. A latent proviral reservoir is likely established in less than three days post-infection[67,68]. The acute peak in viraemia wanes relatively rapidly, coinciding with adaptive responses (antibodies and CD8+ T cells[69,70]), and subsequently stabilises at a "viral set-point". A viral set-point of higher magnitude has long been known to herald a faster progression to AIDS[71,72].

The phases of AHI can be defined into Fiebig stages according to the cumulative appearance of various viral components and antibody responses[73]. In stage I, HIV-1 RNA is detectable in blood by PCR, and in stage II, viral p24 is detectable by ELISA. From stage III, which occurs around time of peak viraemia, HIV-1 antibody responses are observed, with IgM detectable by ELISA. In stage IV, an indeterminant western blot band appears for viral proteins that does not yet meet the criteria for positivity (two out of three bands for p24, gp41, and gp120). At stage V, these criteria are met. The dynamics of viral load and CD4+ T cell count during acute and subsequent phases of infection are shown in Figure 1.3.

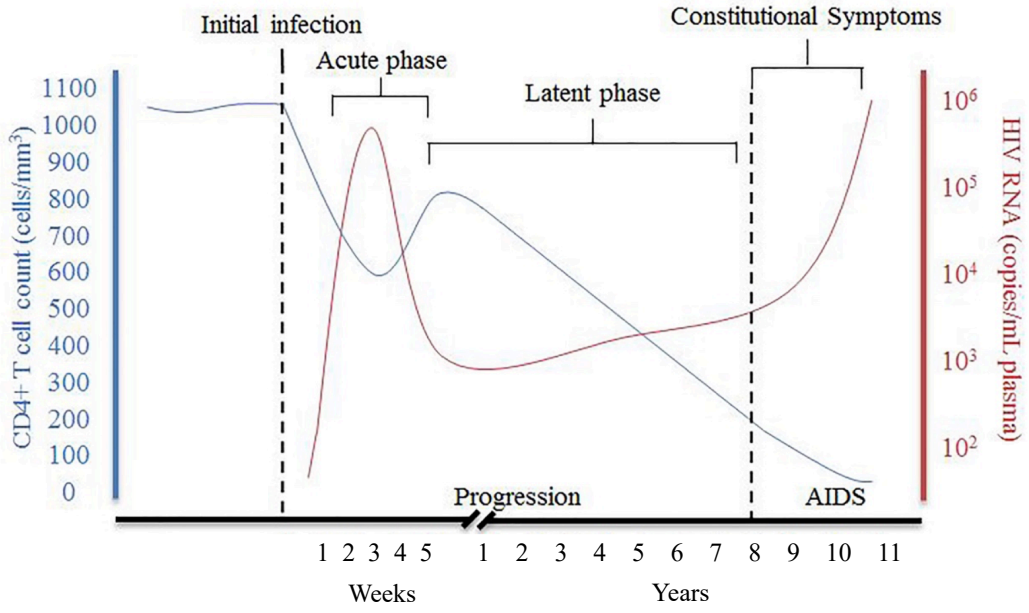


Figure 1.3 Typical dynamics of HIV-1 viral load and CD4+ T cell count throughout infection
The typical relationship between viral load and CD4+ T cell count throughout untreated HIV-1 infection in the average individual. The x-axis represents time relative to acquisition of infection. Figure modified from[74].

During AHI there is a catastrophic loss of $CD4^+$ T cells in the gut-associated lymphoid tissue (GALT)[75]. Cells are irreversibly lost here during AHI, but also at other stages of infection, as revealed by a landmark study analysing blood, lymphoid and intestinal biopsies from patients[76]. The authors of this study found a high percentage of GALT cells express activation markers and posited this could explain the preferential depletion in this compartment (the degree of $CD4^+$ T cell activation is one of the single biggest cellular determinants of permissiveness to HIV-1 infection[77]).

However, HIV-1 also successfully replicates in resting cells *in vivo*[78], and macaque work has shown that most GALT viral replication in acute infection occurs in cells that have a "resting" immunophenotype, at least by activation marker expression[79]. Preferential loss of GALT memory cells could be explained by the high expression of CCR5 in these cells[80]. Mechanisms of $CD4^+$ T cell loss include lytic infection[81], death of highly activated uninfected cells[82,83] and some destruction of infected cells by immune responses[84]. Mechanistically, productively infected activated cells are lost by apoptosis, and non-productively infected resting cells by pyroptosis[85].

1.1.10 Chronic HIV-1 infection and the pathologic basis of HIV-1 disease

After AHI, there is a partial upward rebound in $CD4^+$ T cell count, followed by steady decline (Fig. 1.3). During chronic infection, cells are lost by the same mechanisms as in AHI, but continual immune stimulation and activation is a pivotal driver of $CD4^+$ T cell loss[86,87], and both $CD4^+$ and $CD8^+$ T cells exhibit an exhausted phenotype[88]. There is also insidious dysfunction of almost all other components of the immune system due to relentless stimulation[89]. Inflammation of the intestinal mucosa leads to loss of enterocytes and tight junctions[90], permitting translocation of intestinal bacterial components into the bloodstream, exacerbating systemic inflammation[91].

Chronic immune activation is even further driven by reduced control of persisting viruses, particularly human cytomegalovirus (HCMV)[92], with which a great majority of HIV-infected individuals (and in some countries up to 100% of the general population) are coinfected[93]. In cases where viral coreceptor switch occurs in chronic infection, the virus has access extended to CXCR4-expressing blood and lymph node memory cells, naïve T cells and thymocytes[94]. As such, coreceptor switch precipitates a rapid progression of disease. After terminal $CD4^+$ T cell loss, lymphoid fibrosis and loss of lymphoid architecture accompanies the final sequela of AIDS[95].

1.2 The immune system

1.2.1 Innate immunity

The immune system comprises intrinsic, innate and adaptive defences. Intrinsic defences are pre-existing, such as physical barriers (e.g. skin and mucosae), constitutively secreted antimicrobial factors or intracellular antiviral factors. The innate and adaptive arms of the immune system are activated in response to stimuli. The innate immune system is an evolutionarily ancient set of defences, many components of which are conserved in both vertebrates and invertebrates.

Compared to the adaptive immune system, innate immunity is less specific but more rapidly induced, exemplified by the process of inflammation, an innate immune response that can be induced in seconds to minutes. Many intrinsically produced factors are further upregulated during the innate immune response. Dysregulated or overexuberant innate immune responses can also be prove harmful to the host, as is seen in the process of autoinflammation[96]. Innate leukocytes include granulocytes; monocytes and their tissue-dwelling counterparts, macrophages, both of which are mononuclear phagocytes that engulf pathogens and infected or apoptotic cells; innate lymphoid cells including natural killer (NK) cells with cytolytic function important for killing virally infected cells and cancerous cells; and dendritic cells (DCs)[97].

Innate immune responses are initiated when pathogen-associated molecular patterns or damage-associated molecular patterns (self-motifs) are detected by pattern recognition receptors (PRRs)[98]. PRRs can be membrane-bound, such as toll-like receptors (TLRs), found on the plasma membrane (TLRs 1, 2, 4, 5, and 6, which mostly detect bacterial components) and on the luminal surfaces of endosomal membranes (TLRs 3, 7, 8, and 9, which detect microbial nucleic acid motifs); and C-type lectin receptors (CLRs), a superfamily that detect motifs from an array of viruses, bacteria, fungi and many self-ligands[99]. PRRs can also be

cytosolic, such as retinoic acid-inducible gene-I-like receptors, which detect viral nucleic acids, and nucleotide-binding oligomerisation domain-like receptors, which detect bacterial peptidoglycans[100].

PRRs are expressed in every cell type, with leukocytes and epithelial cells in particular expressing a great breadth of these receptors. PRR ligation results in the initiation of immune responses, which include both cell effector responses and immunomodulatory responses[100]. These are mediated through both cell-cell interactions and through soluble factors such as innate cytokines (cytokines produced during the innate response). Examples include chemokines, which attract leukocytes; pro-inflammatory cytokines such as interleukin 6 (IL-6), tumour necrosis factor (TNF) and IL-1β, which mediate immune cell activation, degranulation or diapedesis as well as exert the systemic acute phase response[101]; type I and III interferons (IFNs) and many others.

DCs are sentinel cells found both in circulation and in tissues (e.g. Langerhans cells (LCs) in the skin and genital mucosa) that bridge the innate and adaptive immune systems through the above mechanisms, but also through antigen presentation. DCs sample their surroundings for antigens, which are processed and presented on major histocompatibility complex (MHC) molecules on the cell surface to naïve T cells, leading to initiation of adaptive immune responses[102]. MHC class II is constitutively expressed by DCs, macrophages and B cells, known as “professional” antigen presenting cells and largely presents peptides derived from outside the cell. However, other cells, such as T cells, can express MHC class II upon activation[103]. MHC class I is expressed by all nucleated cells, and presents peptides derived from the cytoplasm, though professional antigen-presenting cells can also cross-present cell-extrinsic peptides on MHC class I[104]. Upon immature DC activation through PRR ligation, they mature and switch from antigen capture to antigen presentation mode, upregulating MHC class

II and costimulatory molecules and migrating to draining lymphoid tissue[105]. Conventional myeloid DCs (mDCs) are more specialised towards the function of antigen presentation, whereas plasmacytoid DCs (pDCs) excel at soluble factor production, particularly type I IFNs.

1.2.2 Type I and III interferons

Type I IFNs are highly pleiotropic innate cytokines produced by almost all cell types, modulating cell activation, differentiation, survival as well as exerting antiviral activity[106]. Type I IFNs include IFN-α, IFN-β and six others. The transcriptional profiles induced by different type I IFN subtypes are incompletely overlapping at sub-saturating concentrations, with some genes more efficiently upregulated by certain subtypes[107]. There are 14 IFN-α subtypes with differing potencies. IFN-α_{2a} for example, is generally considered more potent than IFN-α_1[108]. After PRR stimulation, activation of the IFN regulatory factors (IRFs) 3 and 7 transcription factors induces type I IFN production[109]. pDCs have unique expertise in producing copious type I IFNs (up to 1000 times more than any other cell), owing to considerable constitutive expression of IRF7[110]. Though IRFs 3 and 7 have the most prominent role, other IRFs implicated in the transcription of type I IFNs include IRFs 1, 5, and 8[106].

Almost all cells can respond to type I IFNs[106]. Type I IFN signalling is mediated through the IFN alpha/beta receptor (IFNAR). IFNAR ligation activates Janus kinase (JAK) and signal transducer and activator of transcription proteins (STAT) signalling pathways, along with others, which leads to transcription of IFN-stimulated genes (ISGs)[106] some of which have antiviral activity. Some ISGs (e.g. *ISG15*) also negatively feedback to limit excessive IFN signalling[111]. Type I IFN action also shuts down mRNA translation via protein kinase R signalling and indirectly provides antiviral protection by increasing MHC class I expression and activating DCs, macrophages and NK cells[112].

The type III IFNs are made up of four subtypes of IFN-λ (IFN-λ_{1-4}) and have type I IFN-like antiviral activity[113], though they signal through different receptors, which are much more tissue-restricted than the ubiquitous IFNAR[114]. Although type III IFNs induce many canonical antiviral genes in common with type I IFNs, their transcriptomes are non-redundantly overlapping[115]. IFN-λ is capable of inducing an antiviral state that inhibits the replication of HIV-1 in macrophages[116] and $CD4^+$ T cells[117].

1.2.3 Adaptive immunity

The adaptive immune system is responsible for targeted, extremely specific immunity. Adaptive immune responses take days to weeks to develop and generate enduring immunity (immunological memory). Inappropriate or excessive adaptive immune responses underlie the pathological processes of allergy and autoimmunity. Adaptive immunity comprises "cell-mediated" immunity conveyed by T cells, and humoral immunity mediated by B subsets including plasma cells and the antibodies they produce. Several classes of antibodies (also known as immunoglobulins) exist: IgA, IgD, IgE, IgG and IgM. Through somatic recombination, an enormous repertoire of antibodies and T cell receptors (TCRs) can bind the breadth of possible antigen amino acid permutations[118]. The breadth of this repertoire explains the ability of the immune system to recognise the diversity of foreign antigens present in micro-organisms against which specific T and B cells can expand (clonal selection and expansion), but also underpins central tolerance, in which developing lymphocytes meet self-peptides and are deleted if the display high affinity autoreactivity[119].

T cells are classically sub-divided into those expressing CD4 and CD8. $CD8^+$ T cells exert effector activity via cytolysis or virally infected and cancerous cells, which is achieved by targeted secretion of cytotoxic proteins such as perforin and granzymes or ligation of death receptors on target cells; and via production of IFN-γ, TNF and other soluble factors[120]. $CD4^+$

T cells (also known as T helper (Th) cells) provide indispensable assistance to other leukocytes, aiding their activation and functions, as well as immunoregulatory roles. They can also mediate cytolytic activity[121], although $CD8^+$ T cells play a much more dominant role in control of most established virus infections.

1.2.4 T helper differentiation and subsets

Naïve Th cell activation begins when a professional antigen-presenting cell presents a peptide on MHC class II, which is engaged by the TCR (and its component, CD3) and the coreceptor, CD4 ("signal one")[122]. Following signal one, a co-stimulatory second signal is required for successful T cell activation and effector function. Examples of co-stimulation include interaction between antigen-presenting cell CD80 or CD86 and Th cell CD28, and between antigen-presenting cell CD40 and Th cell CD40 ligand (CD40L). Th autocrine IL-2 further drives activation and proliferation[122].

After signals one and two, Th cells differentiate into one of many Th effector subsets, depending on factors including the combination of cytokines present in the microenvironment (signal three) (Fig. 1.4). Each Th subset has a distinct role in immunity[123]. For example, Th1 cells promote cell-mediated immune responses against viruses, intracellular bacteria and tumours; Th2 cells defend against extracellular pathogens, particularly parasites; Th17 cells protect against extracellular bacteria and fungi; and T follicular helper (Tfh) cells aid B cell maturation and humoral immunity. Finally, regulatory T (Treg) cells suppress other leukocytes, regulating immune responses. Some antigen-specific Th cells adopt a long-lived memory phenotype, able to quickly clonally expand should re-exposure ever occur[124]. Due to the important role played by transforming growth factor beta (TGF-β) (one of the TGF-β superfamily cytokines on which this thesis is focused) in Treg and Th17 cell biology, these two

Th subsets are reviewed in this section in greater detail, and later again in the context of HIV-1 infection.

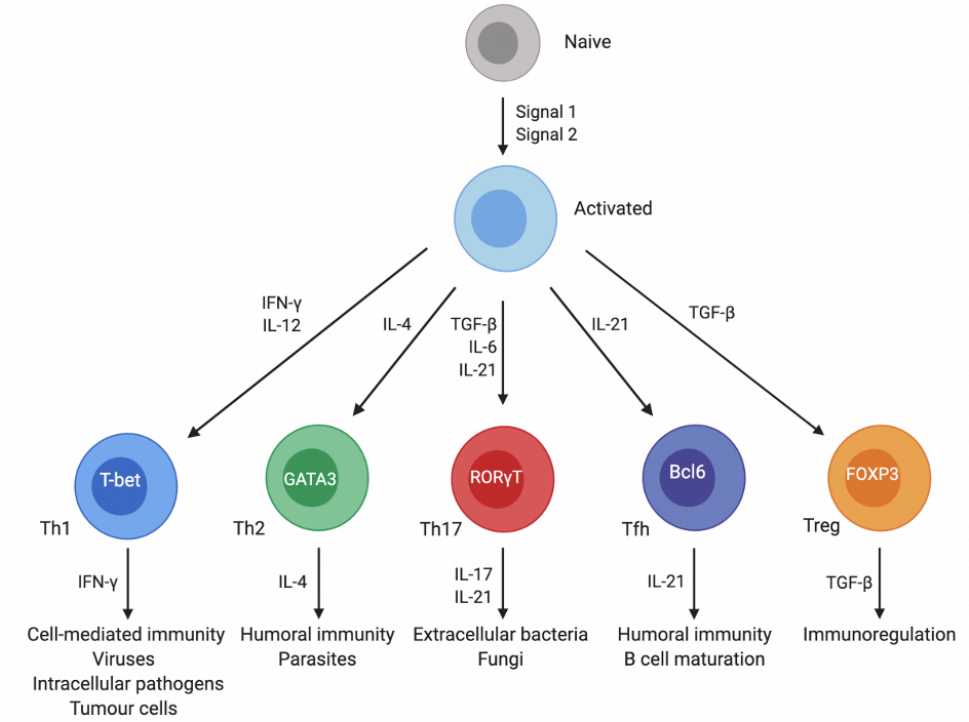


Figure 1.4 T helper cell subset differentiation and function
After activation (signals one and two), Th differentiation into effector subsets is determined by the presence of various cytokine combinations (signal three). Labelled arrows preceding effector subsets show signal three. Annotations in the centre of cells show canonical transcription factors expressed by each subset. Labelled arrows moving distal to effector cell show cytokines produced by those subsets. T-bet=T-box protein expressed in T cells, GATA3=GATA-binding protein 3, RORγt=retinoic acid receptor-related orphan receptor gamma T, Bcl6=B-cell lymphoma 6 protein, FOXP3=forkhead box P3. Figure made with BioRender, citing content from[123,125]

$CD4^+$ Treg cells (referred to as Tregs hereafter) express CD25 and the lineage-defining transcription factor forkhead box protein 3 (FOXP3)[126]. Tregs regulate immune responses by a variety of mechanisms including secretion of anti-inflammatory cytokines such as TGF-β and IL-10 among other mechanisms[127], such as through "mopping up" excess IL-2 that binds the highly expressed CD25, though this mechanism of suppression is debated[128]. Tregs are induced under the influence of TGF-β and can be of thymic origin (tTregs) or induced in the periphery (pTregs), with the term iTregs used for induced Tregs differentiated *in vitro*[129]. The transcription factor Helios and transmembrane glycoprotein neuropilin 1 are expressed in tTregs and are suggested as differentiators between these cells and pTregs[129,130].

Th17 cells (referred to as Th17s hereafter) are abundantly found at mucosal surfaces and defend against bacteria and fungi, but are also implicated in autoimmune disease[131]. Th17s are homeostatically maintained by IL-23[132]; express the transcription factors RAR-related orphan receptor gamma T (RORγt), STAT3 and IRF4; have the surface marker CCR6 (and sometimes CCR4); and produce IL-17, IL-21, IL-22 and CCL20[133].

The combination of cytokines inducing Th17 differentiation is complex and is also tied to a protective or autoimmune/pathogenic phenotype. Th17s were first identified as being induced by the curious combination of TGF-β and IL-6, anti- and pro-inflammatory cytokines respectively[134]. Alternatively, IL-21 can replace IL-6[135]. Th17s induced under these conditions have low pathogenic potential[136]. The presence of IL-23 and IL-1β at differentiation induces a pathological phenotype[136,137]. As TGF-β is an arbiter of both Th17 and Treg lineage commitment, a fine balance exists between the induction of the two. At lower TGF-β concentrations, IL-23 receptor expression is promoted, favouring Th17 differentiation. At higher concentrations, FOXP3 expression prevails over RORγt, the IL-23 receptor is downregulated, and iTregs are induced[138].

Some evidence exists showing that Th17s develop under TGF-β-independent conditions[139,140], and this has been a hotly debated area of immunology[141,142]. Some authors have asserted that TGF-β dependence is a murine, but not a human phenomenon[140]. However, later studies argued that some “TGF-β-independent” work had not accounted for endogenous serum levels of TGF-β in culture media, and that use of serum-free media shows the essential contribution of TGF-β to Th17 differentiation[143,144]. Later work still, using serum-free conditions, has supported TGF-β independence[145], but more recent data has demonstrated that autocrine T cell-derived TGF-β promotes Th17 differentiation, and that Th17s also produce TGF-β[146]. In

conclusion, TGF-β is likely instrumental in human Th17 differentiation, but in certain environments, Th17 differentiation in its absence may be possible[141,142].

1.3 HIV-1 and the immune system

1.3.1 Innate immune responses in HIV-1 infection

Innate immune responses shape the course of HIV-1 infection. The fact that HIV-1 exposure often does not result in establishment of systemic infection is due in part to the activity of innate responses, which play an important role in locally eliminating the virus before it can undergo systemic spread. However, innate immune responses are both beneficial and deleterious at all stages of infection[147]. In chronicity, persistent innate immune responses heavily underpin immunopathogenesis. Subsections that follow cover the contributions of selected components of the innate immune system to HIV-1 immunity and pathogenesis. Those innate leukocytes not covered by the work in this thesis (e.g. NK cells) are beyond the scope of review here.

1.3.2 Dendritic cells in HIV-1 infection

From the first moments when HIV-1 encounters the genital mucosa, DCs are instrumental in the transmission process[148]. This is a most fragile time for the virus, it must overcome a physical barrier, seek target $CD4^+$ T cells (a relatively sparsely populous cell at mucosal sites) and avoid local host immune responses capable of extinguishing it.

In the RM SIV infection model, vaginal epithelial cells exposed to the virus rapidly produce CCL20, which attracts pDCs to the site of infection[149]. pDCs express TLRs 7 and 9, which sense single-stranded RNA (ssRNA) and double-stranded DNA (dsDNA) viral motifs respectively[150]. pDC endosomal TLR7 senses HIV-1 ssRNA following viral endocytosis[151], leading to production of vast amounts of type I IFNs, as well as the chemokines CCL3 and CCL4[149]. Although HIV-1 uses multiple strategies to avoid triggering type I IFN induction in cells that it infects[152–154], HIV-1 has not evolved strategies for impairing pDC activation, despite the fact that pDCs produce high levels of type I IFNs as well as CCL3 and CCL4, the latter two being ligands of the viral coreceptor CCR5 also with anti-HIV-1 activity[155]. This is likely because

CCL3 and CCL4 recruit $CD4^+$ T cells to the exposure site[149], stimulating local inflammation and providing the virus with valuable new targets, without which it may otherwise be unable to expand sufficiently to enable subsequent more widespread dissemination. The activation of pDCs by HIV-1 contrasts with hepatitis C virus (HCV), which inhibits type I IFN from pDCs[156]. The detection of HIV-1 by pDCs is so exquisitely sensitive that their increased frequency in an activated form precedes the reappearance of replicating virus in chronically infected individuals who interrupt ART, before any rebound viraemia can be detected by current methods[157].

Conventional mDCs may also facilitate HIV-1 transmission. Through binding DC-specific intercellular adhesion molecule-3-grabbing non-integrin (DC-SIGN), a CLR substantially expressed on mucosal mDCs, the virus is transited to draining lymph nodes, where it can infect $CD4^+$ T cells undergoing interaction with these DCs in a process known as trans-infection[158]. In contrast, LCs, a non-conventional type of mDC among the earliest cells to encounter HIV-1 at the mucosal surface, combat transmission of the virus. The LC CLR Langerin captures HIV-1 virions before internalising them into cytoplasmic Birbeck granules for destruction[159].

Despite the roles DCs play in HIV-1 transmission, their professional antigen-presenting function is indispensable for setting up adaptive immune responses against the virus. DCs present HIV-1 antigens to both $CD8^+$[160] and $CD4^+$ T cells[161]. In AHI, there is systemic activation of both mDCs and pDCs, and circulating frequencies of both drop precipitously as viraemia increases due to recruitment to lymphoid tissues. This is followed by some restoration of mDC numbers over time, but pDCs remain heavily reduced[162]. Nonetheless, compared to seronegative controls, both the frequency[163,164] and functionality[165,166] of both DC subsets are eroded by HIV-1 infection, and are not restored to normality by ART[163,164]. One study however, reports hyperresponsive cytokine production of DCs from HIV-infected individuals in response to TLR stimulation[162]. The continual systemic presence of factors that drive pDC and mDC

activation (e.g. HIV-1 antigens, LPS, TNF) likely enhances turnover of these cells, which fail to adequately replenish over time. In a vicious circle, activated DCs in turn produce more soluble factors including pro-inflammatory cytokines[167], contributing to further detrimental immune activation of other cells.

1.3.3 Macrophages in HIV-1 infection

As professional antigen-presenting cells, although macrophages are not generally the main initiators of naive T cell priming, they nonetheless drive adaptive immune responses to HIV-1[160]. However, macrophages express CD4 and are readily infected with the virus[168]. Not all HIV-1 strains replicate proficiently in macrophages, and despite some historical nomenclature inaccuracies to the contrary, HIV-1 macrophage tropism is a lot more complicated than simply virus coreceptor (R5/X4) specificity[169].

Macrophages transmit HIV-1 to $CD4^+$ T cells[170]. However, although mucosal macrophages can be infected[171], transmitted founder viruses do not replicate efficiently in macrophages, suggesting that they are not a major site of initial virus expansion[172]. Tissue-resident macrophages are long-lived cells[173], and are believed to be among the key cellular sites of HIV-1 latency in chronic infection (as well as a variety of $CD4^+$ T cell populations, particularly central memory T cells[174]). At least in NHPs, macrophages are a primary source of the chronic SIV viral load[175]. The accumulation of inflammatory macrophages in the brain is thought to contribute to the pathogenesis of HAND[45].

1.3.4 Innate cytokines in HIV-1 infection

The first systemic perturbations in AHI are induction of acute phase proteins as early as seven days prior to the onset of detectable viraemia[176]. Following the eclipse period, AHI induces a systemic cytokine storm[63,177] (Fig. 1.5). The earliest elevations appear around six days post-

first detection of viraemia, and comprise increases in IL-15, IFN-α, CCL3 and TNF, the first two of which show a sharp kinetic, rising and falling to baseline much faster than the others. These analytes are predominantly generated by pDCs, which represent their likely source. IFN-γ-induced protein 10 also rises in this first wave, a chemokine secreted by many cell types, but particularly monocytes, in response to stimulation with type I and type II IFNs[178]. It is likely that the first wave of cytokines in AHI triggers secondary waves of immune activation and induction of other analytes. At around seven to nine days there is sustained production of IL-18 and TNF[63], both of which are secreted by mDCs and macrophages. IL-6 and IL-10 also appear in this second wave. The type II IFN, IFN-γ, also appears around day eight, a cytokine produced in particular by NK cells, Th1 cells and $CD8^+$ T cells, but also by other cells[179]. Following AHI, many innate cytokines remain slightly elevated in chronic HIV-1 infection[180], being both an indicator and a further driver of immune activation. ART, though highly effective at reducing viral load to undetectable levels, fails to perfectly restore these disturbances to normal[11,12,181].

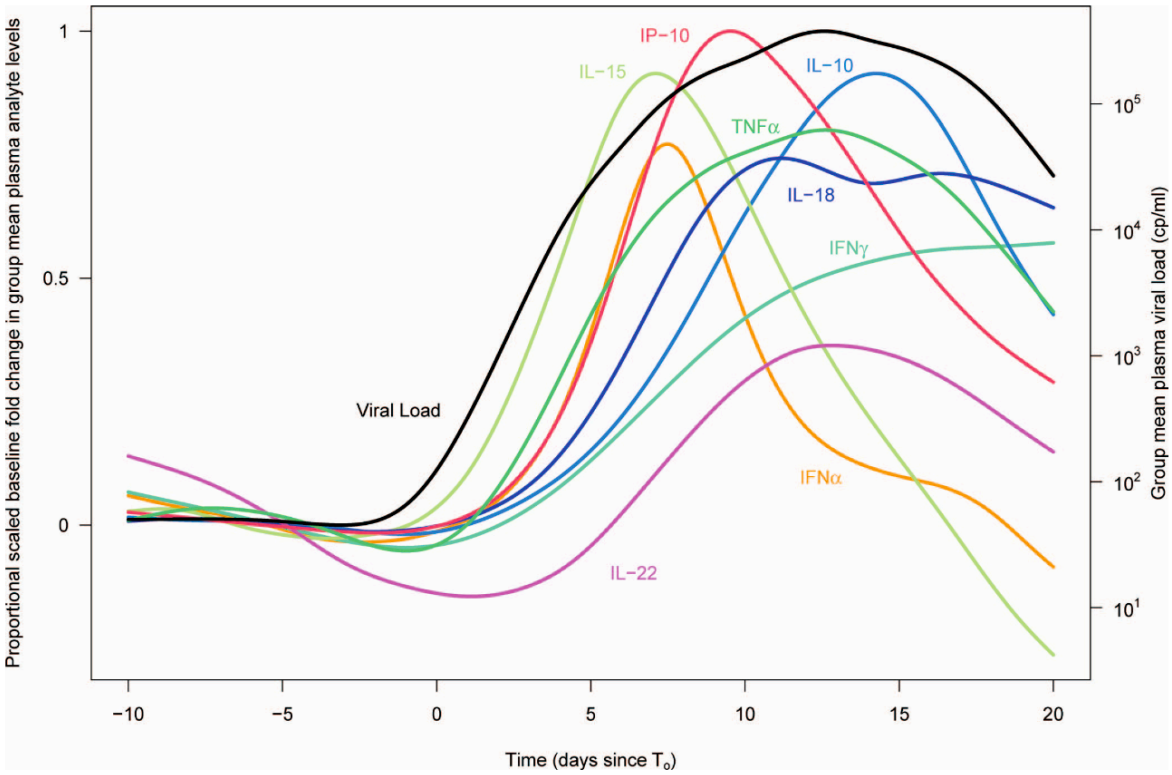


Figure 1.5 The cytokine storm in acute HIV-1 infection
Kinetics of elevations in selected cytokines during AHI, scaled proportionally to show fold changes relative to pre-viraemia baseline concentrations. Viral load is represented by a black line. Cp/ml = viral RNA copies/ml; T_0= time relative to first detection of viraemia with a low limit of detection of 100 copies/ml. Figure taken from[63].

Induction of type I IFNs and/or their downstream gene signatures can be seen in the very early stages of infection (as early as 24 hours post-infection in some studies) in NHP models[182–184]. Type I IFNs suppress HIV-1 replication and create a stringent transmission bottleneck, as evidenced by the greater IFN-α resistance of TF viruses compared to viruses from the same patient in chronic infection[57], and compared to viruses from the chronically infected donor who infected the recipient, in virologically linked transmission pairs[58]. In RMs, administration of recombinant type I IFN initially protects from SIV infection[185]. Furthermore, blockade of IFN signalling in acute infection, either through a drug antagonist or desensitisation of the IFN system through prolonged administration of recombinant type I IFN prior to challenge results in higher viral loads, lower $CD4^+$ T cell count and worse prognosis in these animals[185]. These data reveal the real relevance of type I IFNs in restricting HIV-1 transmission and viral replication in AHI.

One way by which type I IFNs exert anti-HIV-1 activity is through upregulation of antiviral genes, many of which are constitutively expressed in cells to provide a basal level of intrinsic resistance to infection, but that is amplified further by type I IFNs. Well-described HIV-1 antiviral genes (known as restriction factors) include apolipoprotein B mRNA editing enzyme, catalytic polypeptide-like 3G (APOBEC3G), a G-to-A mutation-inducing cytidine deaminase[186] whose activity is enhanced by IFN-α[187]. Whilst many mutations induced by host cytidine deaminases induce stop codons in HIV-1 transcripts, they are also in part responsible for the enormous genetic diversity of the viral quasispecies in infected individuals[52]. The intrinsic restriction factor tripartite motif-containing protein 5 alpha (TRIM5α) is also upregulated by type I IFNs[188]. Although human TRIM5α was previously believed to be only a potent restriction factor to non-human lentiviruses, with minimal anti-HIV-1 activity, it has recently been demonstrated that type I IFNs promote HIV-1 restrictive activity of this factor through immunoproteasomal activation[189]. Other HIV-1 restriction factors upregulated by type I IFNs include MX2[190]; ISG15[191]; interferon-induced transmembrane protein (IFITM) genes[192]; and tetherin, which hinders virus exit from the cell[193]. Some restriction factors are directly antagonised by HIV-1 accessory proteins[30].

In contrast to AHI, weighing up the utility of type I IFNs in chronic HIV-1 infection is a muddier task, and the cytokine causes many detrimental effects to the host[194]. Murine models have shown that under conditions of low $CD4^+$ count, prolonged type I IFN exposure disrupts $CD4^+$ T cell homeostasis and further promotes the loss of these cells[195]. Clinical trials have shown type I IFN administration lessens viral load in chronic infection[196–198]. Historically, IFN-α has also been licensed for treating Kaposi's sarcoma in AIDS patients, though has since fallen out of favour[199]. However, when comparing non-pathogenic NHP models of SIV infection to macaques, the former resolve ISG and other inflammatory gene expression early in infection, whereas the latter do not[182,183,200]. In chronically infected RMs, plasma IFN-α correlates with

viral load[201], a finding corroborated by human data, where IFN-α concentration also correlates positively with markers of immune activation, and negatively with $CD4^+$ T cell count[202]. The pDCs of women secrete more IFN-α than those of men when stimulated with HIV-1[203]. In women in AHI, viral load is on average lower than that of men[204], but women have a greater risk of later progressing to AIDS than men of similar viral set-points[205].

Boosting or blocking type I IFNs provides a further case for a negative role of these cytokines in chronic infection. In HIV-1 clinical trials, recombinant IFN-α reduces $CD4^+$ T cell count[198,206], which may be due to apoptosis of $CD4^+$ T cells[201]. In HIV-1 infected humanised mice, blocking the type I IFN receptor lowers viral replication and revitalises the HIV-1 specific $CD8^+$ T cell response, both alone and greater still with ART[207]. In chronically SIV-infected macaques, a similar intervention to that used in mice shows no effect on viral load but does decrease IFN-mediated inflammatory pathways[208].

1.3.5 Adaptive immune responses in HIV-1 infection

The first detectable humoral immune responses against HIV-1 appear around three weeks post-exposure, though these have no neutralising activity[209]. Neutralising antibodies appear from 12 weeks post-infection though these have only autologous activity – they are strain specific[210]. Broadly neutralising antibodies appear on average 2.5 years into infection, and only in around 25% of infected individuals[211]. Induction of these antibodies is the primary focus of the global effort to develop a broadly protective HIV-1 vaccine[16]. In chronic infection, B cells become exhausted and functionally weakened[212].

The first effective adaptive immune responses in HIV-1 infection are $CD8^+$ T cell responses, which reach peak frequencies within a few days of peak viraemia[213]. In addition to mediating cytotoxicity, $CD8^+$ T cells also produce incompletely understood factors that curb viral

replication[214]. In AHI, the $CD8^+$ T cell response exerts a harsh selection pressure, which makes an important contribution to containing viral replication to the viral set-point persisting level. In RMs acutely infected with a chimeric SIV/HIV virus, depletion of $CD8^+$ T cells results in rapid loss of viraemic control[215]. During AHI, selection of T cell escape mutant viruses compromises $CD8^+$ T cell control of the virus[84,216], and this is further compounded by $CD8^+$ T cell exhaustion in the face of ongoing stimulation by persisting virus. By chronic infection, virus-specific CD8 T cell function is significantly impaired[217]; nonetheless $CD8^+$ T cells do continue to mediate partial control of viral replication throughout infection, as evidenced by enhanced viraemia upon depletion of these cells in macaques with chronic SIV infection[218].

Virus-specific $CD4^+$ T cell responses are also induced during AHI[219]. Although these responses are relatively poorly studied, they may contribute to control of viral replication[220]. However, the recruitment of $CD4^+$ T cells supplies the virus with target cells, and there is evidence that the virus preferentially infects HIV-1 specific $CD4^+$ T cell *in vivo*[221].

1.3.6 Treg cells in HIV-1 infection

The role of Tregs in HIV-1 infection is contentious; they may work to limit pathological immune activation but may also impair antiviral adaptive immune responses[222]. $CD4^+$ Tregs are susceptible to HIV-1 infection[223]. In both acute[224] and chronic HIV-1 infection[224–226], absolute Treg numbers are decreased compared to those in seronegative individuals. Changes in Treg frequencies (Tregs as a percentage of $CD4^+$ T cells) appear more complicated. In acute infection, data is conflicting[224,225,227], which may be explained by inconsistent use of defining Treg markers between studies, a common cause of controversy in the Treg field.

In chronic infection, studies have generally consistently found that circulating Treg frequency is greater than in seronegative individuals[222,225,228,229], a finding also seen in GALT[230,231]. One

explanation for this may be preferential loss of other Th subsets, such as Th17s[232]. Data from NHPs infected with SIV or rhesus CMV show that Treg induction is more influenced by degree of immune activation than by viral replication, though viral replication is a driver of immune activation in SIV infection[233]. In line with this, ART-treated HIV-1 patients with fully suppressed viral loads but greater T cell activation than seronegative individuals also have increased frequencies of circulating Tregs[234], though patient $CD4^+$ T cell counts were much lower than those of controls in this study, so this may be due to other Th subset preferential loss, rather than true net Treg induction. Finally, it is important to note that apparent increases in Treg frequency may also be due to the inclusion of non-Treg populations in Treg gates due to increased immune activation in chronic HIV-1 infection, as the commonly used Treg markers CD25 and FOXP3 are also T cell activation markers[235]. Treg function may be impaired in HIV-1 infection, though there is a contradiction of evidence[223,225].

Some literature favours a protective role of Tregs in HIV-1 infection. In one study, HIV-specific Tregs with highly functioning suppressive capacity *in vitro* were derived from patients with the highest $CD4^+$ T cell counts, the most suppressed viral loads and clinically asymptomatic infections[236]. In addition, when comparing LTNPs and elite controllers to progressors, a greater proportion of Tregs from the former two groups show an activated phenotype compared to the progressors[237]. Finally, *in vivo* NHP data has shown a rapid (within 24 hours) increase in the percentage of circulating Tregs (of total lymphocytes) in a non-pathogenic model of infection in African green monkeys (AGMs)[238].

In support of a negative role of Tregs in HIV-1 infection, Tregs from infected individuals suppress HIV-specific $CD8^+$ T cell responses *ex vivo*[239,240]. *In vivo* data from RMs show that an increased frequency of Tregs inversely correlates with the strength of the anti-SIV $CD8^+$ T cell response[233]. The authors of this study argue that a rapid, early induction of Tregs in AGMs

may dampen immune activation and prevent disease, but that persistent infection still occurs owing to inhibition of SIV-specific immune responses, which could be judged an undesirable outcome. *In vitro,* pDCs stimulated with HIV-1 produce indoleamine 2,3-dioxygenase, causing differentiation of naïve $CD4^+$ T cells into Tregs, which in turn suppress maturation of bystander mDCs, stifling adaptive immunity[241]. Taken together, these data indicate that Tregs may serve to attenuate pathological immune hyperactivation in HIV-1 infection but may hinder immune control of the virus.

1.3.7 Th17 cells in HIV-1 infection

Th17s represent around 10% of $CD4^+$ T cells in the GALT[242], and GALT Th17s are preferentially lost during both HIV-1 infection[232] and in SIV-infected macaques[242]. Depletion of this key mucosal defence renders the host susceptible to gastrointestinal tract microbial translocation, leading to systemic immune activation and associated immunopathology[91]. In ART-treated individuals, a hybrid Th subset, Th1/17 cells (which express both Th1 and Th17 transcription factors and cytokines), may be a long-lived latent viral reservoir[243].

Despite early assertions to the contrary[244], Th17s probably are more susceptible to HIV-1 infection than other Th subsets[243,245–247]. Their enhanced susceptibility (the allowance of entry) may have several explanations. Compared to non-Th17s, these cells express relatively higher levels of CD4, CXCR4[245] and, more subtly, of CCR5[245,246]. Th17s also do not produce CCR5 ligands CCL3 and CCL4[245,246], and transfection of Th17s with CCL4 increases resistance to infection *in vitro*[245]. Th17s are also more permissive to HIV-1 replication. When using pseudotyped HIV-1 carrying envelope glycoproteins from broad tropism non-HIV viruses that bind widely expressed receptors, thus bypassing differences in the efficiency of viral entry into different Th subsets, Th17s produce more virions than non-Th17s[246,247]. This may be due to decreased expression of antiviral RNAse A proteins in these cells[247].

1.4 The TGF-β superfamily

1.4.1 TGF-β superfamily ligands

The TGF-β superfamily is a large group of evolutionarily conserved pleiotropic cytokines that regulate diverse cellular processes such as differentiation, proliferation, migration, embryogenesis, and play roles in immune system regulation[248]. The TGF-β superfamily consists of the eponymous TGF-β, activins, inhibins, bone morphogenetic proteins (BMPs), growth differentiation factors (GDFs) and others. Most members of the TGF-β superfamily are hetero- or homodimeric proteins.

TGF-β was discovered in the early 1980s, as a growth factor secreted from a virally transformed neoplastic mesenchymal cell line that contributed to the transformation of neighbouring cells[249]. It is now known that TGF-β can be produced and responded to by virtually all cell types, playing varied physiological roles not limited to effects on embryonic cell development and differentiation[250,251], cell migration[252], apoptosis[253], cellular homeostasis[254], wound healing and fibrosis[255], and in the immune system[256].

TGF-β exists in three isoforms in mammals, TGF-$\beta_{1\text{-}3}$[257], with TGF-β_5 also being described in frogs[258]. TGF-β_4 was once described in birds[259] but has subsequently been found to be avian TGF-β_1[260]. TGF-β_1 receives the majority of research attention, being the most abundant isoform of the three in tissues and plasma[261]. Although all isoforms play similar biological roles, they are not entirely mutually redundant. Examples include pulmonary fibrosis mediated by TGF-β_1, but not TGF-β_3[262] and the roles of TGF-β_3 in palatal formation[263] and pathogenic Th17 cell development[137]. In mammals, heterodimeric TGF-β consisting of combinations of subunits from the three isoforms have been identified[264,265].

Activins and inhibins have traditionally been studied for their place in reproductive physiology. Activins stimulate follicle-stimulating hormone release[266] and inhibins do the opposite, both regulating the menstrual cycle. Activins are produced in a wide variety of cell types during embryogenesis[267] and in differentiated cells throughout life, regulating physiology from glucose homeostasis and adipogenesis to erythropoiesis and immune function[268].

Activins are dimeric proteins formed from combinations of inhibin beta subunits, of which there are four identified in mammals: βA, βB, βC and βE. Activin A is made up of βA-βA, activin B of βB-βB and activin AB of βA-βB. Inhibins are composed of an inhibin alpha subunit and either a βA or a βB subunit, the former constituting inhibin A and the latter inhibin B. The activin isoforms have many similar functions, but some are distinct[269]. The non-overlapping functions of the activin/inhibin subunits can be demonstrated in knockout mice. Mice lacking βA suffer severe craniofacial defects and die within 24 hours of birth[270], whereas those lacking βB are viable, with different anatomical defects[271]. Of the activin isoforms, activin A is the most well-studied. An enzyme-linked immunosorbent assay (ELISA) for activin B only first became available in 2009[272].

The BMPs were first identified as 30kDa factors able to induce bone formation[273] and have been extensively studied in the context of bone biology. Unsurprisingly, just like the many other pleiotropic cytokines within the TGF-β superfamily, BMPs are now also known to affect a range of cellular processes[274]. There are around 20 members of the BMP family, making it the largest group of the TGF-β superfamily[274], and heterodimers between isoforms occur[275]. The main members of the BMP family can be subdivided into five subgroups based on structural similarity: BMPs -2 and -4; BMP-3 alone; BMPs -5, -6, -7 and -8; BMPs -9 and -10; and BMPs -12, -13 and -14; with BMP-1 not belonging to the TGF-β superfamily[274,276].

TGF-β superfamily cytokines are initially produced as precursor proteins, comprising a C-terminal mature ligand, and an N-terminal prodomain that is essential for correct protein folding and the later export of mature dimers[277]. The prodomain is cleaved from the mature domain by proteases such as furin[278] but remains non-covalently bound to the mature peptide. Disulphide bonds between mature regions link two polypeptides together in the dimeric form (Fig. 1.6).

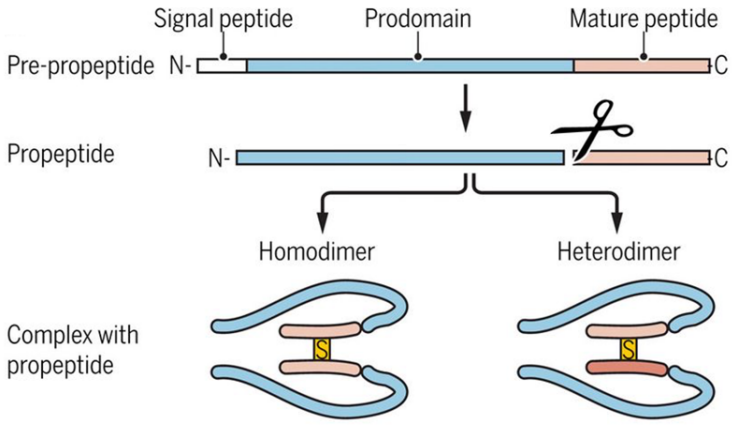


Figure 1.6 Processing of TGF-β superfamily precursor proteins
TGF-β superfamily cytokines are initially translated as precursor proteins. After loss of the signal peptide, the prodomain is cleaved from the mature domain, but they remain non-covalently associated. Hetero- or homodimers form by disulphide linkage between the mature regions. Figure taken from[278].

Upon secretion, the prodomains remain associated with the mature proteins, and in the case of TGF-β, GDFs -8 and -11, and BMP-10, render them non-biologically active[277]. In contrast, activins and most BMPs are unaffected by the presence of the prodomain and are effectively secreted in active form. In the case of TGF-β, the prodomain (referred to as latency-associated peptide) is bound to latent TGF-β-binding proteins, forming a large latent complex (LLC), a biologically inactive structure that is secreted from the cell[279]. The secretion of this 25kDa ligand in a cumbersome, inactive 270kDa complex[280] is testament to the enormous number of homeostatic and regulatory functions of TGF-β. Commensurately, TGF-β activation must be tightly regulated.

Latent TGF-β is activated by a variety of stimuli. These include low pH[281], thrombospondins[282], matrix metalloproteinases (MMPs)[283], reactive oxygen species[284] and integrin interaction. Integrin-mediated activation can be mediated through physical force (integrins $\alpha_v\beta_5$ and $\alpha_v\beta_6$[285,286]), by which the LLC is bound between the extracellular matrix and cell surface integrins and physically pulled apart through actin-driven cell contraction, relinquishing the active ligand. Alternatively, integrins can mediate activation in a force-independent manner (integrin $\alpha_v\beta_8$) that depends on MMP activity[287].

1.4.2 TGF-β superfamily receptors and signalling

TGF-β superfamily ligands signal through type I and II transmembrane receptors, of which vertebrates possess seven of the former and five of the latter[288]. Although referred to as serine/threonine kinase-linked receptors, phosphorylation of tyrosine residues also occurs[289]. Receptor usage by selected TGF-β superfamily ligands is shown in Table 1.1, with content adapted from[290]. Type I receptors have the nomenclature activin-like kinase (ALK). In addition, there exists a type III TGF-β receptor (TGFBR3 or betaglycan), a proteoglycan coreceptor for type I and II TGF-β receptors, that does not directly signal itself but supports some TGF-β isoforms in binding TGFBR2[291], as well as aiding BMP signalling[292]. TGF-β superfamily ligands compete with one another for type II receptors in common. For example, activin A has a higher affinity for activin receptor type-2A (ACVR2A) than does BMP-7, resulting in antagonism of BMP-7 signalling in hepatoma cells[293]. In *Xenopus* embryos, BMP-3 inhibits activin A signalling by blocking ACVR2B[294].

Table 1.1 Selected TGF-β superfamily ligands and their receptors

Ligand	Type I receptors	Type II receptors
TGF-β	ALK1, ALK5	TGFBR2
Activins	ALK4, ALK7	ACVR2A, ACVR2B
BMPs	ALK2, ALK3, ALK6	ACVR2A, ACVR2B, BMP receptor type 2 (BMPR2)

Type I and II TGF-β superfamily receptors are widely expressed in most tissues, and no receptor of the superfamily is truly exclusive to one cell type or tissue[295]. However, ALK1 is predominantly expressed by endothelial cells[296] and ALK7 is found mostly in the central nervous system, pancreas and colon[297].

TGF-β superfamily cytokines canonically signal through the sons of mothers against decapentaplegic (SMAD) pathway[288], as well as through non-SMAD pathways including mitogen-activated protein kinase (MAPK), phosphatidylinositol-3-kinase (PI3K), and Rho-like guanosine triphosphatase signalling pathways[298]. SMAD proteins contain an N-terminal MH1 domain, a C-terminal MH2 domain and a connecting linker region. The MH1 domain binds DNA, whilst the versatile MH2 domain is phosphorylated by receptors, and binds other SMADs and a large selection of transcription factors[299].

TGF-β superfamily ligands bind to heterotetrameric receptor complexes of two type I and two type II receptors, which can occur in many combinations to allow the signal transduction of the large number of superfamily ligands[290]. The type II receptor has constitutionally active kinase activity and phosphorylates the type I receptor, which in turn recruits and phosphorylates receptor-regulated SMADs (rSMADs) at the C-terminal MH2 domain[288]. rSMADs are signal transducers and can be divided into the TGF-β-like pathway: SMADs 2 and 3, and the BMP-like pathway: SMADs 1, 5 and 8. The type I receptor phosphorylated dictates the rSMADs recruited. ALKs 4, 5 and 7 use TGF-β-like pathway SMADs, whereas ALKs 1, 2, 3 and 6 use those of the BMP-like pathway[288]. After rSMAD phosphorylation, two rSMADs from the same pathway form a trimeric complex with the common SMAD (coSMAD) 4 (Fig. 1.7). Trimeric SMAD complexes enter the nucleus where they bind GC-rich regions in promoter and enhancer regions of target genes[299] and interact with transcription factors to co-initiate or co-repress gene expression. Examples include forkhead box O3, p53 and runt-related

transcription factor 2[300]. Another SMAD group, the inhibitory SMADs, comprising SMAD6 and SMAD7, inhibit transduction of the SMAD signalling pathway[301].

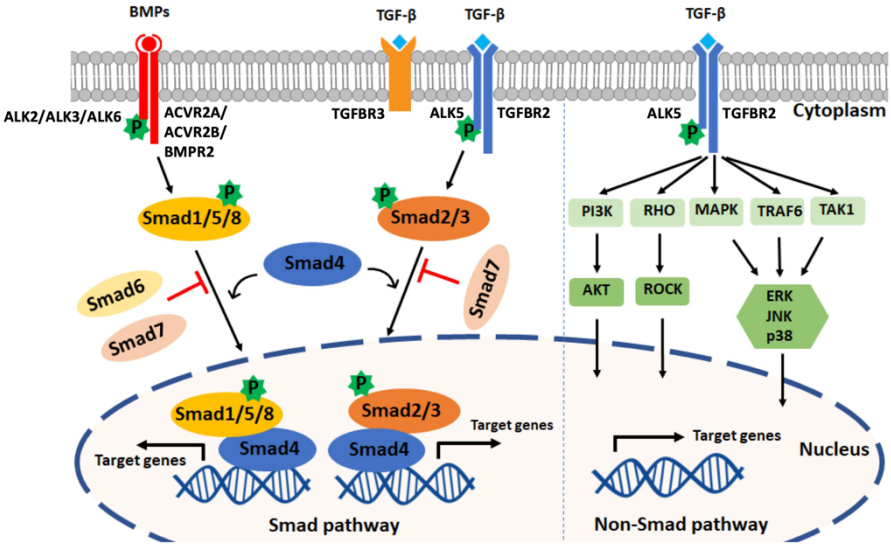


Figure 1.7 Canonical and non-canonical TGF-β superfamily signalling
TGF-β superfamily ligands bind heterotetrameric complexes consisting of two type I and type II receptors each. Type I BMP receptors include ALKs 2, 3 and 6, and type II BMP receptors include ACVR2A, ACVR2B and BMPR2. The principal type I TGF-β receptor is ALK5, and the type II receptor TGFBR2. TGFBR3 is a ligand-presenting receptor to other receptors and does not directly signal itself. After ligand binding at the cell surface, the type II receptor phosphorylates the type I receptor. In canonical signalling (left panel), this results in recruitment and phosphorylation of rSMADs of two distinct pathways (1/5/8 for BMP signalling, or 2/3 for TGF-β and activin signalling), which form trimeric complexes with SMAD4. SMAD trimers enter the nucleus and bind DNA as well as with DNA-binding proteins and recruit other activators and repressors of transcription to act on target genes. Inhibitory SMADs 6 and 7 block the signal transduction process. In non-canonical, non-SMAD signalling (right panel), alternative signalling pathways are activated, also resulting in downstream transcription of target genes. RHO=Rho-like guanosine triphosphatase signalling pathway. TRAF6=TNF receptor-associated factor 6. TAK1=TGF-β-activated kinase 1. AKT=protein kinase B. ROCK=Rho-associated protein kinase. ERK=extracellular signal-related kinase. JNK=c-Jun N-terminal kinase. Figure adapted from[302].

There are exceptions to the above dogma. As TGF-β can bind ALK1 (which uses the BMP-like pathway, SMADs 1, 5 and 8), it can therefore trigger two different pathways, which are mutually antagonistic in endothelial cells and yield contrasting functional outcomes depending on which predominates[303]. Some epithelial cells also break the rules, where TGF-β has been shown to use both ALK 5 and also classically BMP-associated ALKs, but unlike in endothelial cells, both pathways work co-operatively to form mixed rSMAD complexes containing combinations of SMADs 2/3 and 1/5 with unique outcomes[304].

The SMAD protein linker region is an underappreciated modulator of SMAD activity. In classical (C-terminal phosphorylation) SMAD pathway activation, nuclear translocation is either blocked or promoted through additional phosphorylation of linker region serine/threonine residues by kinases such as MAPK, PI3K and others, depending on the kinase pathway responsible. However, in experiments blocking type I receptor activity (and thus SMAD C-terminal phosphorylation), phosphorylation of the linker region alone can lead to upregulation of some genes, making this an independent, non-classical SMAD signalling pathway in itself[305].

1.4.3 TGF-β immunobiology

TGF-β is a master regulator of leukocyte immunobiology and immune responses[254]. TGF-β is prominently produced by CD4+ Tregs but is also made by DCs[248], macrophages[306] monocytes and neutrophils[307]. CD8+ regulatory T cells and B regulatory cells also exist, and produce TGF-β[308,309].

TGF-β signalling is required for the development of CD8+ T cells[310], tTregs[311], NKT cells[310,312] and B cells[313]. TGF-β is also important for T cell homeostasis. TGFBR2 expression maintains splenic and lymph node CD4+ T cell numbers, and in particular for cells with low affinity TCRs, acts though promotion of high expression of IL-7Rα[314]. IL-7 is a crucial mediator of T cell survival and homeostasis[315]. TGF-β signalling negatively homeostatically restricts CD8+ T cell populations[316,317]. It has been suggested that TGF-β impedes T cell TCR-driven T cell proliferation but stimulates IL-7-mediated homeostatic expansion[257].

TGF-β is involved in the differentiation of CD4+ Tfh[318], Treg and Th17 cells[138]. TGF-β is vital for the differentiation of LCs from monocytes, and once differentiated, for their homeostasis[319]. Conversely, it inhibits differentiation of Th1[320] and Th2 cells[321]. TGF-β also conditions naïve

CD8+ T cells towards a tissue-resident memory phenotype after DC-T cell interaction in lymph nodes[322].

TGF-β is crucial for immune tolerance and is a fundamental dampener of T cell activity. For example, TGF-β inhibits TCR signalling in naïve cells[323], and TGF-β-mediated SMAD signalling suppresses expression of major cytolytic protein genes in CD8+ T cells[324]. TGF-β stems T cell proliferation by inhibiting IL-2 production in these cells[325], an effect further compounded by CD4+ Tregs that bind up IL-2 with CD25[127]. The earliest work examining TGF-β function revealed that in *TGFB1*$^{-/-}$ knockout mice, of those that make it to full term (50% die prenatally due to yolk sack maldevelopment[326]), all die in the first few weeks of life, due to severe systemic multiorgan inflammation[327]. Subsequent data showed that *TGFB1*$^{-/-}$ mice lacking CD4+[328] and CD8+[329] T cells do not suffer the same marked inflammation. Later studies deleting either TGFBR1[311] or TGFBR2[310,330] within the T cell compartment reproduced the severe disease phenotype, confirming the vital contribution TGF-β makes in T cell tolerance in particular.

The immunosuppressive activity of TGF-β is not only limited to T cells. TGF-β inhibits IFN-γ production in NK cells[331] and decreases expression of activating receptors required for NK killing[332]. TGF-β-exposed DCs generally adopt a tolerogenic phenotype, with reduced expression of maturation markers and of pro-inflammatory cytokines[248]. And in macrophages, the cytokine promotes an “M2” phenotype, that is, one with a more anti-inflammatory phenotype[333]. TGF-β is also involved in regulation of chemotaxis of multiple leukocyte subsets[334,335].

TGF-β may, in some specific contexts, exert pro-inflammatory effects[336]. Transgenic mice overexpressing TGF-β_1 in keratinocytes develop an inflammatory skin condition resembling

psoriasis[337], and, as previously reviewed, TGF-β is involved in the differentiation of Th17 cells, which can be of an inflammatory, pathogenic phenotype[137].

In summary, TGF-β regulates leukocyte development, homeostasis and differentiation. TGF-β exerts broad immunosuppressive action through the following mechanisms: promotion of Treg differentiation, prevention of Th1 and Th2 differentiation, constraint of lymphocyte proliferation and effector function, inhibition of proinflammatory cytokine secretion, and inhibition of innate immune cell activity.

1.4.4 TGF-β in HIV-1 infection

TGF-β is woven into both HIV-1 immunity and immunopathology. Circulating levels of TGF-β are elevated in HIV-1 infection[338,339] even when viral replication is suppressed[340–346] (reviewed in greater detail in Chapter 3). In RMs, TGF-β expression in lymphoid tissues correlates with rapidity of disease progression[347], a finding corroborated in studies measuring circulating TGF-β in HIV-infected individuals[338,342]. HIV-1 virions can carry biologically active TGF-β, likely bound to host-derived CD36[348].

TGF-β plays roles in HIV-1 infection that are detrimental to the host, which could collectively causatively explain its correlation with disease progression. TGF-β mediates fibrosis, and its expression is correlated with the presence of type I collagen in lymph nodes in HIV-1 infection[349]. Treatment of SIV-infected macaques with an antifibrotic agent that decreases SMAD2/3 phosphorylation decreases paracortical collagen deposition and preserves peripheral and lymphoid tissue $CD4^+$ T cell numbers[350].

TGF-β may also restrict HIV-specific adaptive immune responses. In the lymphocytic choriomeningitis virus (LCMV) murine viral infection model, high TGF-β expression

differentiates $CD8^+$ T cells in persistently infected mice from those in animals acutely infected with virus isolates/doses that are cleared. This was found to be due to TGF-β-dependent apoptosis of LCMV-specific $CD8^+$ T cells. Attenuation of TGFBR2-mediated signalling enabled accrual of greater numbers of these cells and control of infection that would otherwise have persisted[351]. In SIV-infected RMs, upregulation of TGF-β-stimulated genes in gastrointestinal tissues negatively correlates with the size of Gag-specific $CD4^+$ and $CD8^+$ T cell responses in those same tissues, and inhibitory SMAD7 positively correlates with those responses[184]. In HIV-infected people, regulatory $CD8^+$ T cells are induced that can produce TGF-β when stimulated with HIV antigens, which suppresses IFN-γ production by other $CD8^+$ T cells[352].
In humoral immunity, gp120 stimulates B cells to produce TGF-β, blunting B cell proliferation[353]. Antigen-stimulated B cells from HIV-1 infected individuals poorly proliferate *ex vivo*, and this can be partly reversed by TGF-β neutralisation[354].

Finally, TGF-β is prominently found in semen at concentrations approximately five-fold greater than in plasma, with a greater proportion of the cytokine in active form, significantly contributing to the capacity of semen to modulate local vaginal mucosal immune responses to seminal antigens[355,356]. This could have implications for mucosal immunity to HIV-1.

However, TGF-β may also mediate some beneficial effects in HIV-1 infection. This anti-inflammatory cytokine may counter harmful immune activation, given its early induction in SIV-infected AGMs, which do not suffer SIV-related disease[238]. In peripheral blood mononuclear cells (PBMCs) from HIV-infected individuals, TGF-β treatment of cells *in vitro* may enhance the frequency of a subset of $CXCR5^+$ $CD8^+$ T cells and their expression of IFN-γ and the degranulation marker CD107a[357]. $CXCR5^+$ $CD8^+$ T cells have unique access to B cell follicles in lymphoid tissue and kill persistently LCMV-infected Tfh cells[358] and therefore may aid control of HIV-1. At the cellular level, there is conflicting data on the effects of TGF-β on HIV-1

replication *in vitro* depending on cell type, TGF-β concentration, timing relative to infection, and other cytokines present; there is however, some evidence for an antiviral effect in macrophages (reviewed in Chapter 4).

In summary, TGF-β circulates at elevated concentrations in HIV-1 infection, regardless of ART status, where it is a negative prognostic marker and mediates lymphoid fibrosis. However, as touched upon previously with Treg cells (the regulatory activity of which heavily relies on TGF-β[359]), the effects of TGF-β in HIV-1 infection are complex, due to its ability to hamper host immune responses to the virus in an already immunodeficient host, but yet stem harmful immune hyperactivation.

1.4.5 Activins in immunobiology and infection

The roles played by activins in immunity are only recently starting to become appreciated[360–362]. Very recent work has identified antiviral activity of the activins *in vitro*. Activin A inhibits replication of hepatitis B virus (HBV), HCV and Zika virus, and activin B inhibits HCV replication[363]. Activin A also stems reactivation of HCMV in DCs *in vitro*[364].

Activin A is a regulator of inflammation. The first evidence for this came from observing a rapid and transient elevation in plasma activin A in sheep injected intravenously with LPS, undergoing an acute phase response[365]. Similar results were later obtained in mice; furthermore, the pre-administration of follistatin, a naturally occurring activin-binding and neutralising protein[366], reduced the mortality rate by half[367]. Follistatin also blunted TNF-α and IL-1β, and enhanced IL-6 production, and changed the timing of maximal upregulation of some of these cytokines[367]. The source of activin A in this acute inflammatory context appears to be predominantly neutrophils[368].

Neutrophils are a major leukocyte source of activin A, and unlike mononuclear cells, store pre-formed activin A in copious amounts, which is released upon neutrophil stimulation by TNF[369]. Activin A acts on neutrophils to promote IL-6 and reactive oxygen species production, as well as promoting phagocytosis[370]. As well as in neutrophils, activin A is an active participant in the biology of almost every other type of leukocyte subset in which it has been studied. In innate immunity, activin A promotes immature DC migration through induction of CXCL12 and CXCL14[371]. Activin A promotes the differentiation of monocytes to DCs[372], and can substitute for TGF-β in LC differentiation[373]. DCs secrete activin A after activation[372,374], and also when making cell contact with NK cells; the activin A produced acts as a negative feedback mechanism to regulate DC pro-inflammatory cytokine production and maturation[375]. Activin A also suppresses NK cell IFN-γ production[376], proliferation[376,377], granzyme B production and tumour killing[377].

Macrophages generate activin A upon activation by TLR stimulation[378]. Microglia produce both activin A and B after LPS stimulation[379]. Activin A has contrasting effects on monocytes and macrophages depending on their activation state and the presence of other cytokines. In a non-inflammatory steady state, activins generally activate macrophages, triggering the NF-κB pathway[380], upregulating MHC class II[381] (though this was not seen in one study[382]), enhancing phagocytosis[381–383] and stimulating production of pro-inflammatory mediators[381,382,384,385]. However, where there is pre-existing inflammation, in LPS-activated macrophages, the converse effects are seen on pro-inflammatory mediator production[385–387], phagocytosis[383,387], and MHC class II expression[387].

In adaptive immunity, activin A is critical for differentiation of Tfh cells in humans[388]. Activin A may be thought of as a Th2 cytokine. Th2 cells highly express the βA gene and produce substantially more activin A protein than Th1 cells[389]. Activin A is implicated in Th2-driven

disease, such as asthma, where it can be found elevated locally in the airway[390] and systemically[391]. The Th2 cytokine IL-13 induces activin A secretion in this setting[392]. Although one study shows systemic activin A administration to alleviate allergic airway disease *in vivo*, this is mediated through induction of circulating $CD4^+$ Tregs capable of suppressing both Th1 and Th2 responses[393]. These data together confirm that locally, activin A acts as a Th2-like cytokine, but in circulation is capable of inducing regulatory T cells with anti-inflammatory action. Data from other authors has confirmed activin promotion of iTreg differentiation in synergy with TGF-β, but not alone[394]. Also in concert with TGF-β, activin A plays a role in fibrosis in lung injury models[395] and airway remodelling in asthma[391]. B cells can produce and respond to activin A, where it boosts IgA and IgG production[396,397].

In summary, many leukocytes secrete activin A upon activation, and activin A is a regulator of inflammatory cytokine cascades *in vivo*. Playing a part in Treg and LC differentiation and fibrosis, as well as dampening down the activity of some innate leukocyte subsets, activin A clearly has a lot in common with TGF-β, with which it shares the SMAD2/3 signalling pathway. However, activin A also has divergent unique actions. These include pro-inflammatory action in resting macrophages, and anti-inflammatory activity in those that are activated; and promotion of local Th2 immune responses. Activins A and B have inherent antiviral activity against several RNA and DNA viruses. There is a scarcity of literature on activin B and inhibins in immunity.

1.4.6 BMPs in immunobiology and infection

BMPs 2 and 4 are involved in thymocyte development[398], and BMP signalling is necessary for IL-7-mediated naïve T cell homeostasis and survival[399]. Similar to activin A, BMPs 2 and 4 synergise with TGF-β in iTreg differentiation but do not do so in the absence of the latter[400].

BMP-7 signalling is essential for LC development, where it promotes epithelial translocation of precursor cells, before TGF-β signalling completes the differentiation process[401].

Naïve $CD4^+$ T cells produce BMPs 2, 4 and 6 during activation[399]. BMP-2 induces IL-2 production in activated $CD4^+$ T cells[402], but appears to reduce cell proliferation, though not at high doses, where the response is lost[403]. BMP-6 inhibits proliferation of an immortalised $CD4^+$ (Jurkat) T cell line[404], and BMP-4 may inhibit $CD4^+$ T cell proliferation at low doses but enhance it at high doses[403]. Overall however, inhibition of endogenous BMP signalling in $CD4^+$ T cells diminishes IL-2 production and proliferation[399,402]. In B cells, BMPs 2, 4, 6 and 7 inhibit CD40L-mediated production of IgA, IgG and IgM[405]. BMP-6 inhibits B cell proliferation[406].

BMP-7 suppresses chemotaxis of monocytes by repressing expression of monocyte chemoattractant protein-1, as well as repressing expression of IL-6 and IL-1β by epithelial, mesangial and arterial smooth muscle cells[407–409]. DCs produce BMP-4 during maturation, and inhibition of BMP signalling in DCs reduces expression of inhibitory receptor ligands programmed death-ligand 1 (PD-L1) and PD-L2, with subsequent enhancement of NK cell killing and T cell proliferation in co-cultures of DCs with these cells[410]. In NK cells, in contrast with activin A, constitutive BMP signalling is essential for IFN-γ production, killing and proliferation[411].

Like activins, BMPs have antiviral activity. BMPs 4, 6 and 9 inhibit HCV replication, and BMP-6 inhibits HBV replication[363]. In this study, BMP-6 was found to upregulate transcription of various ISGs in both a hepatoma cell line and primary cells. In addition, in a hepatoma cell line, BMP-6 was found to boost IFN-α-mediated expression of seven ISGs, such as *TRIM14* and IFN-α-induced protein 6 (*IFI6*), and to bolster HCV inhibition in combination with IFN-α. One conflicting study shows BMP-4 enhances HCV replication[412]. However, other authors

have demonstrated inhibition of HCV replication by BMP-7[413] and that of a murine gammaherpesvirus by BMP-2[414]. BMP induction of IFN-like transcriptional signatures including antiviral genes is also well-corroborated[415,416].

In addition, viral antagonism of BMP signalling has been documented. HIV-1 infection of a myeloid cell line leads to downregulation of BMPR2, which may be mediated by Tat[417]. HCV disrupts BMP signalling, and in chronically infected individuals, impaired BMP-6 activity is associated with a worse response to treatment[363]. Kaposi's sarcoma-associated herpesvirus (KSHV) encodes a gene silencing micro RNA that targets SMAD5[418]; KSHV also possesses a K5 lytic gene that ubiquitinates BMPR2 for lysosomal destruction[419]. Finally, HBV core and x proteins heavily antagonise SMAD1/5/8 signalling[420].

In summary, BMPs are essential for the development, homeostasis, activation and proliferation of $CD4^+$ T cells, but suppress B cells. BMPs appear to regulate DCs, NK cells and some innate cytokines, though there are very few studies in these areas. There is a substantial body of evidence showing that BMPs induce an antiviral state active against several viruses (with most data to date on hepatotropic viruses), in their own right and in concert with type I IFNs.

1.4.7 Cross-communication between TGF-β superfamily and type I interferon signalling pathways

The signalling pathways of TGF-β superfamily and type I IFNs intersect and demonstrate cross-communication, particularly between SMADs, STATs and IRFs. SMAD proteins are structurally homologous to IRFs, and both SMAD1 and IRF1 bind many genome-wide loci in common[363]. Moreover, in hepatoma cells, BMP-6 upregulates *JAK1*, *STAT2*, *IRF1, IRF2*, *IRF7* and *IRF9*[363], and in immature DCs, BMP-6 upregulates *IRF1*[410]. In $CD4^+$ type 1 regulatory cells (a unique subset of Tregs), activin A induces transcription of *IRF4* and activation of IRF4

protein[421]. The haematopoietic cell-specific IRF4 principally regulates the development of leukocytes, but has also been implicated in the induction of some ISGs[422], indicating a role in the type I IFN response.

Structural similarity also means IRFs and SMADs can complex together, with functional outcomes. IRF3 binds to SMAD3, preventing its association with TGFBR1 and modulating SMAD signalling[423]; and SMAD3 interaction with IRF7 positively regulates downstream IFN-β transcription[424].

In murine mammary epithelial cells, TGF-β and activin-mediated SMAD2, 3 and 4 activation inhibit STAT5 activation and transcription of STAT5 target genes[425]. Although not as well-studied as other STAT proteins in the context of type I IFN signalling, STAT5 does mediate type I IFN responses[426]. STAT3, an inhibitor of type I IFN activity[427], co-operates with SMAD2 to activate transcription of the RORγt gene, *RORC*[428], explaining why both TGF-β and IL-6 co-operate to induce Th17 cells[134] (IL-6 signalling involves STAT3[429]). In lung adenocarcinoma cells, STAT3 signalling represses transcription of *SMAD3*[430], and in a hyperplastic prostate epithelial cell line SMAD2/3 inhibits STAT3 phosphorylation[431].

1.5 Hypotheses and research objectives

HIV-1 replication, immunopathology and disease progression are profoundly influenced by cytokines, many of which are significantly systemically perturbed in HIV-1 infection. There is a strong case for better understanding these proteins and harnessing them for novel prophylactics and therapies, or to complement those in current use. Members of the TGF-β superfamily play important roles in immune function. They are induced by some viral infections and can control the replication of some viruses. However, the impact of TGF-β superfamily cytokines on HIV-1 replication is either poorly explored or unknown, depending on the cytokine in question. Based on the above, I hypothesised that TGF-β superfamily cytokines are likely systemically induced in HIV-1 infection *in vivo*; and that members of the superfamily, particularly BMPs and activins, have antiviral activity against HIV-1 *in vitro* likely mediated through the induction of canonical antiviral genes and/or enhancement of type I IFN activity, in $CD4^+$ T cells (the principal HIV-1 target cell type).

In my DPhil research, I aimed to address:

1) Whether TGF-β superfamily cytokines are induced in HIV-1 infection *in vivo*, and whether stimulation of putative leukocyte subset sources of these cytokines with HIV-1 leads to their induction *in vitro* (**Chapter 3**).
2) Whether TGF-β superfamily cytokines have any effect on HIV-1 replication *in vitro,* and if so, whether these effects are contingent upon viral strain or cell type (**Chapter 4**).
3) For TGF-β superfamily cytokines that do impact HIV-1 replication, what are the mechanism(s) by which their effects are mediated? (**Chapter 5)**.
4) Given the overlap between the antiviral defence afforded by some TGF-β superfamily cytokines and type I IFNs against non-HIV-1 viruses in non-leukocytes, is there any intersection of these two systems in acting on HIV-1 replication in $CD4^+$ T cells? (**Chapters 4 and 5**).

Chapter 2

Materials and methods

2.1 Materials

2.1.1 Human samples

Longitudinal plasma samples from US plasma donors who became infected with HIV-1 during a serial time-course of regular plasma donation were purchased from Zeptometrix Corporation, USA. Samples were acquired by plasmapheresis into 4% sodium citrate and cryopreserved. Serial samples spanned timepoints both before detectable viraemia and during the phase of exponentially increasing viraemia during AHI. Viral load was determined by Quest Diagnostics Incorporated, USA using a Roche Amplicor HIV Ultra assay (lowest level of detection 100 viral copies/ml) as part of a prior study[63]. These samples were collected with ethical approval for research use, and donors gave written informed consent.

Patients presenting with AHI to clinics at the Mortimer Market Sexual Health Clinic (London, UK) were recruited and followed prospectively by Dr Ian Williams and Dr Pierre Pellegrino (Centre of Sexual Health and HIV Research, University College London, UK). Peripheral blood samples were collected in ethylenediaminetetraacetic acid (EDTA) anticoagulant, and plasma was isolated by centrifugation and cryopreserved. Cross-sectional samples collected in subacute and/or chronic infection from these subjects were studied here. Patient samples were kindly provided by Dr Ian Williams and Dr Pierre Pellegrino (Centre of Sexual Health and HIV Research, University College London, UK). Plasma samples from demographically matched HIV-seronegative control subjects recruited from the same clinics were provided by Dr Dimitra Peppa (University of Oxford, UK). Ethical approval for these studies was obtained from relevant NHS ethics committees (Camden and Islington Local Research Ethics Committee (98/60) and South Central-Berkshire Research Ethics Committee (6/SC/0265)) and all donors gave written informed consent.

Leukocytes from HIV-seronegative individuals obtained from leukocyte reduction system chambers (LRSCs) derived from HIV-seronegative donors during the process of platelet donation were obtained from NHS Blood & Transplant, UK. Approval for supply of this material for research use was obtained by NHSBT, and donors gave written informed consent.

2.1.2 Viruses

HIV-1 stocks were generated as described below from infectious molecular clones (IMCs), that is, plasmids containing the full-length HIV-1 genome, the sequence of which corresponded to that of the deduced transmitted-founder (TF) virus of subjects recently infected with HIV-1, or their 6-month consensus virus sequence (6M) (as described in[56,57,432]) or lab-adapted HIV-1 strains. Viruses are shown in Table 2.1. These IMCs were kindly provided by Drs John Kappes and Christina Ochsenbauer, University of Alabama at Birmingham, USA and Dr Beatrice Hahn, University of Pennsylvania, USA.

Table 2.1 HIV-1 viruses derived from infectious molecular clones

Virus	Clade	Tropism	Patient transmission risk group
CH042 TF [A]	C	CCR5	Heterosexual
CH042 6M [B]			
CH058 TF	B	CCR5	MSM [C]
CH058 6M			
CH077 TF	B	CCR5/CXCR4	MSM
CH077 6M			
CH164 TF	C	CCR5	Heterosexual
CH164 6M			
CH236 TF	C	CCR5	Heterosexual
CH236 6M			
CH470 TF	B	CCR5	MSM
CH470 6M			
CH850 TF	C	Data not available	Heterosexual
CH850 6M			
NL4-3	B	CXCR4	Lab-adapted strain
NL4-3 BaL	B	CCR5	Lab-adapted strain

[A] TF: transmitted founder virus
[B] 6M: consensus sequence of the quasispecies present at 6 months post infection
[C] MSM: men who have sex with men

An additional non-replication competent virus, VSV G NL4-3 luc was used for experiments analysing transcriptional activity from the HIV-1 LTR. This single-round luciferase reporter virus (pNL4-3.Luc.R-E-, the plasmid encoding which was obtained from the NIH AIDS Reagent Program, USA, cat no. 3418) contains firefly luciferase inserted in *nef*, with frameshifts cancelling Env and Vpr expression. Expression of the reporter gene is driven by transcriptional activity from the HIV-1 LTR. The virus was pseudotyped with vesicular stomatitis virus (VSV) envelope glycoprotein. Stocks of this reporter virus (the concentration of which were not quantitated) were kindly provided by Dr Andrea Magri and James Harris (University of Oxford, UK) in this form.

2.1.3 Chemical reagents and media

All chemical reagents and media are listed in Table 2.2.

Table 2.2 Chemical reagents

Chemical	Manufacturer	Catalogue number
2-Mercaptoethanol (50mM)	Thermo Fisher Scientific, USA	31350-010
2-Propanol (isopropanol)	Thermo Fisher Scientific, USA	10754191
Bovine serum albumin (BSA) 7.5% solution	Sigma-Aldrich, USA	A8412-100ML
Dulbecco's Modified Eagle medium (DMEM) with D-glucose and pyruvate	Thermo Fisher Scientific, USA	31966-021
Dimethyl sulfoxide (DMSO)	Thermo Fisher Scientific, USA	190186
Enhanced chemiluminescence substrate (ECL)	PerkinElmer, Inc, USA	NEL103E001EA
EDTA	Thermo Fisher Scientific, USA	15575-038
Ethanol, absolute	Thermo Fisher Scientific, USA	10428671
Foetal bovine serum (FBS)	Sigma-Aldrich, USA	F9665-500ML
G418 (Geneticin) (50mg/ml)	Thermo Fisher Scientific, USA	10131-027
Human AB serum	Sigma-Aldrich, USA	H4522-100ML
Hydrochloric acid solution (1N)	Sigma-Aldrich, USA	H9892-100ML
HEPES buffer solution (1M)	Thermo Fisher Scientific, USA	15630-056
Histopaque-1077	Sigma-Aldrich, USA	10771-500ML
L-glutamine (GlutaMAX) (100X)	Thermo Fisher Scientific, USA	35050-038
Laemmli sample buffer (4X)	Bio-Rad Laboratories, Inc, USA	1610747
LDN193189	MedChemExpress, LLC, USA	HY-12071
Lipofectamine 2000	Thermo Fisher Scientific, USA	11668-019
Lipopolysaccharide (LPS) from *E.coli* 055:B5	Sigma-Aldrich, USA	L2880-10MG

Methanol	Thermo Fisher Scientific, USA	10214490
Milk powder	AppliChem GmbH, Germany	A0830,0500
Minimum essential medium non-essential amino acids (MEM NEAAs) (100X)	Thermo Fisher Scientific, USA	11140-035
ODN 2216	InvivoGen, USA	tlrl-2216
Opti-MEM I	Thermo Fisher Scientific, USA	31985-062
Phosphate buffered saline (PBS)	Sigma-Aldrich, USA	D8537-500ML
PBS tablets	Sigma-Aldrich, USA	P4417-100TAB
Pen Strep	Thermo Fisher Scientific, USA	15140-122
Ponceau stain	G-Biosciences, USA	786-575
Protease-phosphatase inhibitor cocktail (100X)	Thermo Fisher Scientific, USA	78440
Sodium pyruvate solution (100mM)	Sigma-Aldrich, USA	S8636-100ML
Imiquimod (R837)	InvivoGen, USA	tlrl-imqs
Pierce radioimmunoprecipitation assay (RIPA) buffer	Thermo Fisher Scientific, USA	89900
Resiquimod (R848)	InvivoGen, USA	tlrl-r848
Restore Western Blot Stripping Buffer	Thermo Fisher Scientific, USA	21059
Roswell Park Memorial Institute (RPMI)-1640 medium with no glutamine	Thermo Fisher Scientific, USA	31870-025
Nuclease-free water	Thermo Fisher Scientific, USA	AM9937
SB431542	Bio-Techne Corporation, USA	1614
Sodium chloride (NaCl) 0.9% solution	VWR International, USA	A1671.0100
Sucrose	Sigma-Aldrich, USA	S0389
Towbin, without sodium dodecyl sulfate (SDS) (10X)	Santa Cruz Biotechnology, Inc, USA	sc-24955
Tris-buffered saline (TBS) (10X)	Santa Cruz Biotechnology, Inc, USA	sc-24951
Tris/glycine/SDS (TGS) running buffer (10X)	Bio-Rad Laboratories, Inc, USA	161-0732
Trypan blue solution	Sigma-Aldrich, USA	T8154-100ML
Trypsin-Versene solution	Lonza, Switzerland	LZBE17-161E
Tween 20	Sigma-Aldrich, USA	P1379-100ML
Water (distilled)	Sigma-Aldrich, USA	W4502-1L
X-VIVO-15 serum-free hematopoietic cell medium	Lonza, Switzerland	BEBP04-744Q

2.1.4 Media

"R10" medium consisted of RPMI-1640 medium, hereafter referred to as "RPMI", supplemented with 10% heat-inactivated FBS, 2mM L-glutamine, and 100 IU/ml penicillin plus 100µg/ml streptomycin. FBS was passed through a 0.22µm pore filter on occasions where a precipitate could be seen in the bottle upon thawing. "R10 complete" medium consisted of R10 with the addition of 1% NEAAs, 1mM sodium pyruvate, and 50 µM 2-mercaptoethanol. "R2 complete" medium consisted of R10 complete medium, diluted 1 part in 5 in RPMI.

"D10" medium comprised DMEM with 10% heat-inactivated FBS, 2mM L-glutamine, 1% NEAAs, 0.5mg/ml G418 and 100 IU/ml penicillin plus 100µg/ml streptomycin.

"RAB5" medium consisted of RPMI with 5% heat-inactivated, 0.22µm filtered human AB serum 2mM L-glutamine, 100 IU/ml penicillin and 100µg/ml streptomycin, and 10mM HEPES.

For serum-free medium, 100 IU/ml penicillin and 100µg/ml streptomycin were added to X-VIVO 15 serum-free hematopoietic cell medium.

"Freezing medium" consisted of FBS with 10% DMSO.

2.1.5 Cell lines

293FT cells were sourced from Thermo Fisher Scientific, USA, cat no. R70007. Jurkat.CCR5, MOLT-4.CCR5 and CEM-NKR-CCR5 cells were sourced from the Centre for AIDS Reagents, National Institute for Biological Standards and Control, UK, cat nos. 0094, 0099 and 5039 respectively. Immortalised cells lines were confirmed to be negative of *Mycoplasma* before use, with a MycoAlert PLUS luminescence assay (Lonza, Switzerland, cat no. LT07-710), and

read on a PHERAstar platereader (BMG Labtech, Germany). *Mycoplasma* testing was carried out in-house by Chris Dodds (University of Oxford, UK).

2.1.6 Cytokines

Cytokines were stored and reconstituted according to manufacturers' instructions. Activins A and B, BMPs 2 and 6 and TGF-β_1 were reconstituted in 4mM hydrochloric acid solution with 1mg/ml BSA. After initial reconstitution, aliquots were made and frozen at -20°C or -80°C. Aliquots were never thawed more than twice. Cytokine details are shown in Table 2.3.

Table 2.3 Recombinant cytokines

Cytokine	Manufacturer	Cat no.
Activin A	Bio-Techne Corporation, USA	338-AC-050
Activin B	Bio-Techne Corporation, USA	659-AB-005
BMP-2	Bio-Techne Corporation, USA	355-BM-050
BMP-6	Bio-Techne Corporation, USA	507-BP-020
GDF-15	Bio-Techne Corporation, USA	957-GD-025
Granulocyte-monocyte colony-stimulating factor (GM-CSF)	Miltenyi Biotec, Germany	130-093-865
IFN-α_{2a}	PeproTech, UK	No longer available
	Miltenyi Biotec, Germany	130-093-874
IL-2 (Aldesleukin/Proleukin)	Clinigen, UK	N/A
IL-4	Miltenyi Biotec, Germany	130-093-921
IL-17	Miltenyi Biotec, Germany	130-093-958
Inhibin A	Bio-Techne Corporation, USA	8506-AB-010
Macrophage colony-stimulating factor (M-CSF)	Miltenyi Biotec, Germany	130-096-489
TGF-β_1	Bio-Techne Corporation, USA	240-B-010
XCL1	Bio-Techne Corporation, USA	695-LT

2.1.7 Antibodies for stimulation or neutralisation

Antibodies used for stimulation or neutralisation are described in Table 2.4.

Table 2.4 Antibodies for stimulation or neutralisation					
Target [A]	**Clone**	**Species**	**Working concentration**	**Manufacturer**	**Cat no.**
CD3 epsilon	UCHT1	Mouse	10-50ng/ml [B]	Bio-Techne Corporation, USA	MAB100
CD28	CD28.2	Mouse	20-100ng/ml [B]	Thermo Fisher Scientific, USA	16-0289-85
IL-17RA/ IL-17R	133617	Mouse	10µg/ml	Bio-Techne Corporation, USA	MAB177
IFNAR2	MMHAR-2	Mouse	10µg/ml	PBL Assay Science, USA	21385-1
XCL1	Polyclonal IgG	Goat	10µg/ml	Bio-Techne Corporation, USA	AF695

[A] All antibodies target human epitopes
[B] Varied depending on the experiment. Exact concentrations are specified in figure legends

2.1.8 Antibodies and stains for flow cytometry

Antibodies and stains used for flow cytometry are described in Table 2.5.

Table 2.5 Antibodies and stains for flow cytometry					
Target [A]	**Fluorophore**	**Clone**	**Working concentration (µg/ml)**	**Manufacturer**	**Cat no.**
CCR5	Phycoerythrin (PE)-Dazzle 594 (Texas Red)	J418F1	0.25	BioLegend, USA	359125
CCR6	PE	11A9	1	BD Biosciences, USA	551773
CCR7	Brilliant Violet (BV)650	G043H7	1	BioLegend, USA	353234
CD14	BV510	M5E2	3	BioLegend, USA	301842
CD25	PE-Cy7	2A3	0.125	BD Biosciences, USA	335824
CD3	Allophycocyanin (APC)	SK7	1	BD Biosciences, USA	345767
CD3	Pacific Blue	SP34-2	2	BD Biosciences, USA	558124
CD3	PE Texas Red	7D6	0.5	Thermo Fisher Scientific, USA	MHCD0317

CD38	Alexa Fluor (AF)488	HIT2	2	BioLegend, USA	303512
CD38	BV785	HIT2	1.5	BioLegend, USA	303530
CD38	PE-Cy5	HIT2	0.2	BioLegend, USA	303507
CD4	APC-H7	SK3	0.24	BD Biosciences, USA	641398
CD4	PE	SK3	0.06	BD Biosciences, USA	345769
CD45RA	BV711	HI100	0.125	BioLegend, USA	304138
CD69	Fluorescein isothiocyanate (FITC)	FN50	0.5	BD Biosciences, USA	555530
CXCR3	PE-Cy5	1C6/CXCR3	1	BD Biosciences, USA	551128
CXCR4	BV605	12G5	0.5	BioLegend, USA	306521
CXCR5	Brilliant Blue (BB)515	RF8B2	0.24	BD Biosciences, USA	564624
FOXP3	APC	PCH101	4	Thermo Fisher Scientific, USA	17-4776-42
HLA-DR	BV421	L243	0.2	BioLegend, USA	307636
Live/Dead Aqua	-	-	Master stock [B] diluted 1 in 500	Thermo Fisher Scientific, USA	L34957
Live/Dead Near Red	-	-	Master stock [B] diluted 1 in 1250	Thermo Fisher Scientific, USA	L10119
phosphoSMAD (pSMAD)2/3	PE	O72-670	0.08	BD Biosciences, USA	562586

[A] All antibodies target human epitopes

[B] As reconstituted per the manufacturer's guidelines. The concentration of stock reconstituted in this manner is unavailable Thermo Fisher Scientific proprietary information.

2.1.9 Flow cytometry staining panels

- Panel 1: CD4 APC-H7, CD3 APC, Live/Dead Aqua, pSMAD2/3 PE.
- Panel 2: CD25 PE-Cy7, CD3 PE Texas Red, CD38 PE-Cy5, CD4 APC-H7, CD69 FITC, HLA-DR BV421, Live/Dead Aqua.

- Panel 3: CCR5 PE Texas Red, CCR6 PE, CCR7 BV650, CD14 BV510, CD25 PE-Cy7, CD3 Pacific Blue, CD38 BV785, CD4 APC-H7, CD45RA BV711, CXCR3 PE-Cy5, CXCR4 BV605, CXCR5 BB515, FOXP3 APC, Live/Dead Aqua.
- Panel 4: CD25 PE-Cy7, CD3 PE Texas Red, CD38 AF488, CD4 PE, FOXP3 APC, Live/Dead Near Red.
- Panel 5: CD25 PE-Cy7, CD3 PE Texas Red, CD38 AF488, CD4 PE, Live/Dead Near Red.

2.1.10 Antibodies for western blotting

Antibodies used for western blotting are described in Table 2.6.

Table 2.6 Antibodies for western blotting

Target [A]	Clone	Species	Working concentration (µg/ml)	Manufacturer	Cat no.
Beta-actin horseradish peroxidase (HRP)	AC-15	Mouse	0.3	Sigma-Aldrich, USA	A3854-200UL
Beta-tubulin	9F3	Rabbit	0.006	Cell Signaling Technology, USA	2128
Glyceraldehyde 3-phosphate dehydrogenase (GAPDH) HRP	1E6D9	Mouse	0.1	Proteintech Group, USA	HRP-60004
IκBα	44D4	Rabbit	0.326	Cell Signaling Technology, USA	4812
p65 (RelA)	D14E12	Rabbit	0.201	Cell Signaling Technology, USA	8242
Phospho(p)-p65	93H1	Rabbit	0.057	Cell Signaling Technology, USA	3033
pSMAD1/5/8	D5B10	Rabbit	0.348	Cell Signaling Technology, USA	13820
pSMAD2/3	1074A	Rabbit	2	Bio-Techne Corporation, USA	MAB8935
Rabbit IgG HRP	N/A	Donkey	0.4	Santa Cruz Biotechnology, USA	sc-2313 (discontinued)
SMAD1	D59D7	Rabbit	0.665	Cell Signaling Technology, USA	6944
SMAD2/3	D7G7	Rabbit	0.066	Cell Signaling Technology, USA	8685

[A] All antibodies target human epitopes

2.1.11 TaqMan probes for qRT-PCR

TaqMan probes (Thermo Fisher Scientific, USA) used for quantitative real-time polymerase chain reaction (qRT-PCR) are shown in Table 2.7.

Table 2.7 TaqMan probes for qRT-PCR

Gene	Protein encoded	Cat no.
APOBEC3G	APOBEC3G	Hs00222415_m1
CCL5	CCL5	Hs00982282_m1
CD38	CD38	Hs01120071_m1
CYC1	Cytochrome c1	Hs00357717_m1
ID3	Inhibitor of DNA binding 3	Hs00171409_m1
IFI6	IFI6	Hs00242571_m1
IFITM3	IFITM3	Hs03057129_s1
IL17A	IL-17A	Hs00174383_m1
IL17F	IL-17F	Hs01028648_m1
IRF9	IRF9	Hs00196051_m1
ISG15	ISG15	Hs01921425_s1
JAK1	JAK1	Hs01026983_m1
MMP2	MMP2	Hs01548727_m1
MX2	MX2	Hs01550814_m1
OAS1	2'-5'-oligoadenylate synthetase 1	Hs00973635_m1
SMAD7	SMAD7	Hs00998193_m1
STAT2	STAT2	Hs01013123_m1
TGFBR2	TGFBR2	Hs00234253_m1
TRIM5	TRIM5	Hs01552558_m1
XCL1	Chemokine C motif ligand	Hs00751481_s1

2.2 Methods

2.2.1 General tissue culture methodology

For thawing cells, cryogenic vials were rapidly thawed in a 37°C water bath before mixing the vial contents with room temperature PBS or RPMI at a minimum dilution of 1 part in 8, to reduce DMSO-mediated cytotoxicity. Diluted cells were then spun down and resuspended in relevant media before counting. For pelleting cells, unless otherwise noted, centrifugation was carried out at 520G in a Heraeus Megafuge 40R (Thermo Fisher Scientific, USA) for 5 minutes.

For counting and viability checking, a TC-20™ cell counter was used (Bio-Rad Laboratories, Inc, USA) using trypan blue at a 1:1 ratio with cell suspensions. When setting up all experiments, numbers of cells used always refers to live cells, not total (live and dead) cells.

All cells were cultured at 37°C in 5% CO_2. Unless otherwise noted, PBMCs and purified $CD4^+$ T cells were cultured at a density of $2x10^6$ cells/ml in R10 complete medium. Jurkat.CCR5, MOLT-4.CCR5 and CEM-NKR-CCR5 cells were cultured in R10 except with G418 500µg/ml instead of penicillin and streptomycin, at a density of $0.5x10^6$ cells/ml, splitting back down to this density upon reaching $3x10^6$ cells/ml, which usually occurred every 3 days. Adherent 293FT cells were seeded in D10 medium at a density of $5x10^4$ cells/cm^2 flask surface area and split back down to this density when 90% confluent, which usually occurred every 3 days.

When freezing and storing cells, cells were resuspended at 30-$100x10^6$ cells/ml in freezing medium before dispensing 1 ml aliquots into 2ml cryogenic vials and storing in liquid nitrogen tanks. Freezing was completed gradually at -1°C/minute by placing vials in isopropanol-filled "Mr Frosty" containers (Thermo Fisher Scientific, USA, cat no. 5100-0001) and storing at -80°C for no more than 3 days, before transferring vials to liquid nitrogen cryostorage.

2.2.2 Production of viruses from infectious molecular clones

293FT cells were transfected with IMC plasmids to produce high titre virus stocks. IMCs were grown up in MAX Efficiency Stbl2 competent cells (Thermo Fisher Scientific, USA, cat no. 10268019), plasmid confirmed by restriction enzyme digest, and quantified by Nanodrop; all conducted by Dr Anna Kliszczak (University of Oxford, UK) the protocol of which is not described here.

To produce virus stocks, the day before transfection, 10^7 293FT cells were seeded in T75 flasks in D10 medium with no G418. On transfection day, 12µg of HIV-1 DNA was diluted in 1ml Opti-MEM I. Separately, 25µl of Lipofectamine 2000 (hereafter known as Lipofectamine) was diluted in 1ml Opti-MEM I and left for 5 minutes. Both solutions were combined and left for 30 minutes at room temperature to allow Lipofectamine-DNA complexes to form. Old media was removed from the cells, and replaced with 8ml of D10 without G418, plus 2ml of the Lipofectamine-DNA complexes in Opti-MEM. Cells were incubated for 72 hours before spinning at 1000G for 5 minutes to pellet and remove the cells. Virus-containing supernatant was taken and concentrated by adding 30ml supernatant to a 5ml sucrose cushion comprising PBS with 20% sucrose and 0.2mM EDTA before spinning at 23,000 RPM for 2 hours at 4°C in a Beckman Optima XL-80K ultracentrifuge (Beckman Coulter, Inc, USA). The virus-containing pellet was resuspended in 2ml R10, before freezing in aliquots at -80°C. RT activity of viruses was measured with a colorimetric Reverse Transcriptase Assay (Roche Life Science, Switzerland, cat no. 11468120910). The production of virus stocks from IMCs was conducted by Dr Anna Kliszczak (University of Oxford, UK).

2.2.3 Isolation of peripheral blood mononuclear cells

PBMCs from HIV-seronegative donors were isolated by Histopaque-1077 density gradient centrifugation from LRSCs from NHS Blood & Transplant, UK. LRSCs were rinsed clean with

0.9% NaCl solution, before further diluting the leukoconcentrated blood up to a 70ml volume. In two tubes, 35ml of diluted blood was slowly laid on top of 15ml Histopaque-1077, and then spun for 25 minutes at 935G with no centrifuge brake applied, and the PBMC buffy coat of each tube removed with a Pasteur pipette and re-diluted up to 50ml in NaCl. Tubes were spun at 750G for 7 minutes with no brake applied, before the pellets were resuspended in 20ml NaCl each and both tubes combined. That tube was then spun at 330G for 7 minutes with the brake applied. PBMCs were resuspended in NaCl and counted, before pelleting and resuspending in freezing medium before cryopreservation in 1ml volumes at a density of between 30-100x10^6 cells/ml.

2.2.4 Isolation of leukocyte subsets

Leukocyte subsets were isolated from HIV-seronegative donor PBMCs by magnetic separation with magnetic-activated cell sorting (MACS) bead kits (Miltenyi Biotec, Germany). Kits are shown in Table 2.8. All kits were used according to the manufacturers' instructions, before separation using an AutoMACS Pro Separator (Miltenyi Biotec, Germany, cat no. 130-092-545). Buffer for all separations consisted of PBS containing 3% FBS and 2mM EDTA.

Table 2.8 MACS kits for leukocyte subset isolation

Procedure	Type of selection	Kit	Catalogue no.
$CD4^+$ T cell isolation	Negative	$CD4^+$ T cell isolation kit, human	130-096-533
$CD8^+$ T cell depletion	Positive	$CD8^+$ microbeads, human	130-045-201
mDC [A] isolation	Negative	Myeloid dendritic cell isolation kit, human	130-094-487
Monocyte [B] isolation	Negative	Pan monocyte isolation kit, human	130-096-537
pDC isolation	Negative	Plasmacytoid dendritic cell isolation kit II, human	130-097-415

[A] $CD1c^+$/$CD141^+$ mDCs.
[B] Classical ($CD14^{hi}$ $CD16^-$), non-classical ($CD14^+$ $CD16^{hi}$) and intermediate ($CD14^{hi}$ $CD16^+$) monocytes.

2.2.5 Generation of monocyte-derived dendritic cells

To generate monocyte-derived dendritic cells (MDDCs), $1x10^6$ PBMCs/cm^2 or $0.3x10^6$ purified monocytes/cm^2 from HIV-seronegative donors (isolated as previously described) were seeded into T75 or T175 tissue culture flasks in 8ml or 10ml RAB5 respectively and incubated for 2 hours, after which, adherence was confirmed using a light microscope. Non-adherent cells were removed, and adherent cells were washed 5 times with room temperature RPMI, before culturing in the same volume of RAB5 with 300IU/ml IL-4 and 100IU/ml GM-CSF for 5 days, with a fresh media change on day 3. When changing the media, old media was spun first to preserve non-adherent MDDCs, which were re-added to the flask. After 5 days, MDDCs were used for experiments.

2.2.6 Generation of monocyte-derived macrophages

To generate monocyte-derived macrophages (MDMs), purified monocytes from HIV-seronegative donors (isolated as previously described) were seeded in flat-bottomed 24-well microplates at a density of $0.5x10^6$ cells/well in 2ml of RPMI. After 2 hours of incubation, adherence was confirmed under a light microscope. The plate was tilted, and media slowly removed, and 2ml R10 complete medium plus 50ng/ml M-CSF was added to each well. After 4 days, media was removed and replaced afresh. After a total of 7 days, differentiated MDMs were used for experiments.

2.2.7 ELISA and Luminex assays

ELISA and Luminex assay kits used are listed in Table 2.9.

Table 2.9 ELISA and Luminex assay kits

Kit	Manufacturer	Cat no.
Activin A ELISA	Bio-Techne Corporation, USA	DAC00B
Activin B ELISA	Cloud-Clone Corp, USA	SEA170Hu
BMP-2 ELISA	Bio-Techne Corporation, USA	DBP200
IFN-α ELISA	PBL Assay Science, USA	41100-1
Total IL-18 ELISA	Bio-Techne Corporation, USA	DL180
Platelet factor 4 (PF4) ELISA	Bio-Techne Corporation, USA	DPF40
TGF-β_1 ELISA (cell culture supernatants) [A]	Bio-Techne Corporation, USA	DB100B
TGF-β_1 Luminex assay (plasma) [A]	Bio-Techne Corporation, USA	LTGM00

[A] The manufacturer reports no substantial cross-reactivity of TGF-β_2 or TGF-β_3 when measuring TGF-β_1 concentration in these assays.

All ELISAs used are sandwich assays, in which samples are added to a 96-well microplate with wells containing a biotinylated capture antibody bound to the streptavidin-coated plate. After a wash step, an HRP-conjugated antibody also specific for the analyte of interest is added, followed by another wash step, before adding an HRP substrate that generates a colorimetric reaction. Optical density is read using a microplate reader and compared against a standard curve of known concentrations to infer analyte concentrations in the sample.

The TGF-β_1 Luminex assay involves the use of colour-coded magnetic microparticles that are bound to antibodies specific for the analytes of interest. Microparticles and samples are combined in a 96-well microplate, before a wash step, then the addition of a biotinylated antibody also specific for the analytes of interest (of which there are several, as the major benefit of Luminex assays is the ability to multiplex many analytes). After a further wash, streptavidin-PE is added, before another wash, then samples are run on a Luminex machine.

The machine captures the beads with a magnet, before using light-emitting diodes that help identify firstly which analyte is present, and secondly, the intensity of the signal from the excitation of PE. The other analytes that were measured by this assay are not discussed in this thesis, thus this assay is referred to as a "TGF-β_1 Luminex assay" throughout. For both ELISA and Luminex assays, the manufacturer's guidelines were exactly followed, further details of which (as well as any exceptions) are provided below.

For plasma samples, activin A, activin B, BMP-2, IL-18, and PF4 were measured by ELISA, and TGF-β_1 by Luminex assay. To prepare plasma samples for the ELISA/Luminex assays: for the activin A, activin B, BMP-2 and IL-18 ELISAs, samples were diluted 1 in 2 in the same diluent used for the standard curves prior to the assay. For the PF4 assay, the same was done at a dilution of 1 in 50. For the TGF-β_1 Luminex assay, plasma samples were subjected to an acid activation step followed by base neutralisation, before diluting to a final dilution of 1 in 15, as directed in the datasheet instruction. All ELISAs and Luminex assays measuring plasma were set up in technical duplicate or triplicate.

For cell culture supernatants, activin A, activin B, BMP-2 and IFN-α and TGF-β_1 were all measured by ELISA. To prepare cell culture supernatants for all assays, samples were initially diluted 1 in 5 in the same diluent used for the standard curves. The IFN-α assay offers two standard curve options, of "low" and "high" sensitivity covering different concentration ranges. The lower sensitivity option (which has a concentration range reaching a higher magnitude, but a higher low limit of quantitation (LLOQ)) was used as a default. For the TGF-β_1 ELISA, plasma samples were subjected to an acid activation step followed by base neutralisation, resulting in a dilution of 1 in 1.4, on top of the initial sample dilution. Experiments generating cell culture supernatants for analysis by ELISA were already in technical duplicate, so these

technical duplicates were run in this fashion on the ELISA plate – they were not further split into technical ELISA replicates.

Microplates were read on a FLUOstar Omega plate reader (BMG Labtech, Germany) and raw optical densities read alongside a standard curve using four-parameter logistic regression using MARS Data Analysis software (BMG Labtech, Germany). Luminex microplates were run on a Bio Plex 200 (Bio-Rad Laboratories, Inc, USA, cat no. 171000201), with a doublet discriminator gate of 5000 to 25,000 (as a recommendation for magnetic beads from Bio-Rad Laboratories) and analysed by five-parameter logistic regression using Bio Plex Manager 4.1. For plasma, the coefficient of variation (CV%) was measured for all technical replicates, and only readings with an intra-well CV% of <20% were accepted.

For cell culture supernatants, further dilution (up to 1 in 10) was applied to samples whose readings were above the range of the standard curve, before re-running the ELISAs. Plasma samples did not exceed the higher limits of the standard curves, so no further dilution was necessary.

For readings that were below the LLOQ, several courses of action were applied. For the IFN-α ELISA, samples were re-run against the higher sensitivity standard curve option. For the BMP-2 ELISA when measuring plasma, a linear regression analysis was frequently selected instead of a four-parameter logistic regression, to extrapolate below the LLOQ, as many plasma samples contained only a very low concentration of BMP-2. For all other samples (plasma or cell culture supernatant) that fell below the LLOQ, a concentration of half of the LLOQ was arbitrarily assigned.

When measuring cytokines in patient plasma from the cross-sectional subacute/chronic HIV-1 cohort, at the time of blood processing to obtain plasma, around half of these samples were diluted in a 1:1 ratio of blood to 0.9 % NaCl solution. Therefore, the exact degree of dilution of the plasma derived from these samples was unknown, but an assumption of an average packed cell volume of 46% for European Caucasian males was made to calculate an estimated dilution factor, based on extensive haematological survey data[433]. This was in addition to the dilution done in standard curve diluents prior to the assays, as previously described above.

2.2.8 TGF-β superfamily cytokine induction assays

PBMCs, pDCs or mDCs from HIV-seronegative donors were isolated as described previously. For these experiments, MDDCs were generated through the adherence of PBMCs, without prior isolation of purified monocytes. $0.4x10^6$ PBMCs, $0.2x10^6$ MDDCs, $0.3\text{-}1.5x10^5$ pDCs or $0.3\text{-}0.7x10^5$ mDCs were plated per well into duplicate wells into flat-bottomed 96-well microplates (DCs) or round-bottomed 96-well microplates (PBMCs). All leukocyte subsets were cultured in 200µl R10 in this assay (including MDDCs that had been previously cultured in RAB5 medium) with/without the following stimuli: HIV-1 NL4-3 (50ng RT/ml); PR8 influenza virus (multiplicity of infection (MOI) 10, calculated using plaque-forming units/ml), LPS (100ng/ml), R837 (5µg/ml), R848 (10µg/ml) or ODN 2216 (5µM). After incubation for 24 hours, microplates were spun, and supernatants were harvested and frozen at -80°C. Cytokine concentrations were analysed by ELISA and duplicate values averaged. PR8 influenza virus was a gift from Prof Alain Townsend (University of Oxford, UK), and had been made in MDCK-SIAT1 cells[434,435].

2.2.9 Western blotting

$1x10^6$ MDMs or $10\text{-}30x10^6$ $CD4^+$ T cells from HIV-seronegative donors were washed with cold PBS and transferred into Eppendorf tubes, pelleted at 600G in a Microstar 17R microcentrifuge

(VWR International, USA) and cell pellets lysed in 100uL (MDMs) or 60uL ($CD4^+$ T cells) of RIPA buffer containing 1X protease-phosphatase inhibitor and left on ice for 20 minutes. Lysates were clarified by centrifugation at 14000G at 4°C for 15 minutes, before being transferred to a new Eppendorf tube. Protein concentration of each lysate was calculated using a Pierce BCA Protein Assay Kit (Thermo Fisher Scientific, USA, cat no. 23227) according to the manufacturer's instructions, in technical duplicate.

After denaturing samples at 95°C for 5 minutes in a heat block, lysates were returned to ice and combined with Laemmli sample buffer (Laemmli was pre-combined with 2-mercaptoethanol at a 9:1 ratio) at a 3:1 ratio, and around 7.5µg (macrophages) or 15-60µg ($CD4^+$ T cells) of protein was loaded per well on 10% SDS precast gels (Bio-Rad Laboratories, Inc, USA, cat no. 4561036EDU) as well as 7µl of a stained protein ladder (Thermo Fisher Scientific, USA, cat no. LC5800). Gels were run in 1X TGS running buffer for 45 minutes at 160 volts, before being transferred to a nitrocellulose membrane in 4°C 1X Towbin transfer buffer with 20% methanol for 1 hour at 100 volts. Efficiency of transfer was judged using Ponceau stain before blocking membranes with 1X TBS containing 5% milk powder on an orbital shaker at 200RPM for 1 hour.

Antibodies used for western blots are described in Table 2.6. Membranes were probed with primary antibodies in TBS with 5% milk overnight at 4°C, or for HRP-conjugated antibodies not requiring secondary antibody probing, at room temperature for 1 hour. Membranes requiring secondary probing were first washed 3 times in TBS with 0.1% Tween (TBST) on an orbital shaker at 200RPM for 10 minutes each time, before probing for 1 hour at room temperature with a secondary donkey anti-rabbit HRP-conjugated antibody. To develop blots, membranes were again washed 3 times in TBST, before submerging in ECL substrate for 1 minute. Blots were then read manually using x-ray film or with an iBright CL1500 Imaging System (Thermo

Fisher Scientific, USA, cat no. A44240). To probe membranes for multiple proteins, blots were cut with scissors where possible. For very similarly sized proteins where this was not possible (e.g. phosphoSMAD and SMAD), blots were stripped with stripping buffer for 15 minutes, before re-blocking and re-probing as above. Membranes were never stripped more than once. β-actin and GAPDH were used as housekeeping loading control proteins. Where densitometric analysis of bands was performed, ImageJ (NIH, USA) was used, and only on blots developed digitally using the iBright Imaging System.

2.2.10 Flow cytometry

2.2.10.1 General flow cytometry methodology

All flow cytometry staining was carried out as follows, unless otherwise noted in specific staining protocols. Antibody working concentrations are shown in Table 2.5.

0.2-0.5x10^6 cells were aliquoted per well into 96-well round-bottomed microplates, pelleted by spinning the plates at 750G, and washed with 200µl PBS. All spins were carried out at 4°C. Pelleted cells were surface stained (all antibodies except those against CD3, pSMAD2/3 and FOXP3) with fluorochrome-conjugated antibodies and co-stained with a Live/Dead amine-reactive viability dye in a volume of 50µl PBS for 15 minutes at room temperature (or in the incubator when using “flow cytometry panel 3”, to improve the staining of CCR5 and CXCR4) in the dark. Cells were washed once with PBS, before fixing in 100µl of Cytofix/Cytoperm (BD Biosciences, USA, cat no. 51-2090KZ) for 15 minutes at room temperature in the dark, followed by two washes with Perm/Wash (BD Biosciences, USA, cat no. 51-2091KZ). Cells were then stained with anti-CD3 antibody in 50µl PBS for 15 minutes at room temperature in the dark, followed by 2 more washes with Perm/Wash.

After all staining and fixing, cells were resuspended in 200µl PBS and run on the flow cytometer. Where cell numbers were counted using flow cytometry, CountBright beads were used (Thermo Fisher Scientific, USA, cat no. C36950) to calculate absolute cell numbers. Where samples could not be run on the same day, they were refrigerated at 4°C and left no more than 24 hours before running. Samples were run on a CyAn ADP benchtop flow cytometer (Beckman Coulter, Inc, USA) with Summit software (Beckman Coulter, Inc, USA) (staining panels 1, 2, 4 and 5), or an LSRFortessa X-20 flow cytometer (BD Biosciences, USA) (staining panel 3). Data were analysed and plotted using FlowJo 9 and 10 (FlowJo LLC, USA).

Single stain controls for compensating samples were run using anti-mouse compensation beads (BD Biosciences, USA, cat no. 51-90-9001229) or anti-rat compensation beads (BD Biosciences, USA, cat no. 51-90-9001189) or an AbC total antibody compensation bead kit (mouse or rat) (Thermo Fisher Scientific, USA, cat no. A10497). For Live/Dead single stains, an ArC amine-reactive compensation bead kit was used (Thermo Fisher Scientific, USA, cat no. A10346). All compensation bead staining was carried out according to the manufacturers' protocols. Fluorescence minus (FMO) stains were used for T cell activation markers and viral coreceptors.

2.2.10.2 phosphoSMAD2/3 staining

Recombinant TGF-β_1-treated cells at a density of 10^6 cells per well in a 96-well round-bottomed microplate were pelleted and washed once with PBS after 5 minutes of TGF-β_1 treatment. Cells were Live/Dead stained as previously described, but for a reduced time of 7 minutes, before washing and fixing for 10 minutes at 37°C with 100µl of pre-warmed 37°C Cytofix (BD Biosciences, USA, cat no. 554655) mixed with PBS at a 1:1 ratio. Cells were pelleted, the supernatant removed, and were then permeabilised using 50µl of cold (previously stored at -20°C) 80% methanol, with the plate left on ice for 30 minutes. Cells were then washed by

adding 150µl of Stain Buffer (BD Biosciences, USA, cat no. 554656) and pelleting and removing supernatants, followed by another two washes with 200µl of Stain Buffer. Cells were then stained with pSMAD2/3 antibody as well as with any surface markers, in a 50µl volume for 1 hour at room temperature in the dark, before washing once with 200µl of Stain Buffer, before resuspending in 200µl of Stain Buffer before analysis by flow cytometry.

2.2.10.3 Intranuclear FOXP3 staining

For experiments involving staining of FOXP3, the following protocol, using an eBioscience FOXP3/Transcription Factor Staining Buffer Set (Thermo Fisher Scientific, USA, cat no. 00-5523-00) was employed. Cells were washed, surface stained, Live/Dead stained and washed as described previously, before fixing in 100µl of eBioscience FOXP3 Fixation/Permeabilisation Buffer for 15 minutes at room temperature. 100µl of FOXP3 Permeabilisation Buffer was then added to cells before pelleting and washing once more with 200µl with the same buffer. Cells were then stained for FOXP3 in a 50µl staining volume for 45 minutes at room temperature in the dark, using FOXP3 Permeabilisation Buffer instead of PBS to make up the antibody cocktail. CD3 staining was also included with the FOXP3 stain. Cells were then washed twice with FOXP3 Permeabilisation Buffer before resuspending in 200µl of PBS and analysing by flow cytometry.

2.2.10.4 CellTrace Violet staining for analysis of cell proliferation

To stain leukocytes to measure proliferation, a CellTrace Violet (CTV) cell proliferation kit was used (Thermo Fisher Scientific, USA, cat no. C34557). Cells were suspended in PBS at a concentration of 10^7 cells/ml in a 50ml Falcon tube. In parallel, CTV was prepared in an equal volume of PBS at a concentration of 4µM. The cells and CTV solution were combined at a 1:1 ratio, producing a CTV concentration of 2µM. Cells were vortexed briefly and placed in the incubator for 10 minutes. The reaction was then quenched by adding FBS to the cells at a ratio

of 3:1. Cells were then pelleted and resuspended in the relevant assay medium before activation.

2.2.11 Standard HIV-1 replication assay

PBMCs pooled from 3 HIV-seronegative donors were used for most HIV-1 replication assays owing to the high amount of variability in levels of virus replication in cells from different donors (referred to as "donor trios"), to enable generation of more consistent data from different experiments (Fig. 2.1). Equal numbers of PBMCs from 3 donors were pooled and depleted of $CD8^+$ T cells as previously described. Cells were cultured in R10 complete medium with 50IU/ml IL-2 and activated with 50ng/ml soluble anti-CD3 and 100ng/ml soluble anti-CD28 for 72 hours before infection. At 24 hours prior to infection, replicate sets of cells were treated with TGF-β superfamily cytokines or IFN-α_{2a} (hereafter referred to as IFN-α) or left untreated as a control.

IFN-α was used as a positive control of viral inhibition, typically at a concentration of 1000IU/ml. Recombinant IFN-α from Peprotech, UK at 1000IU/ml was used for initial experiments, but when this became unavailable, IFN-α from Miltenyi Biotec, Germany was instead used at an equivalently active quantity that was determined with dose-response viral inhibition experiments comparing both batches (data not shown). 2000IU/ml of the latter batch was required to match inhibition elicited by 1000IU/ml of the former. However, throughout this thesis, a concentration of 1000IU/ml has been described for continuity.

On the day of infection, cells were pelleted and resuspended in R10 complete medium, before being plated in technical triplicate at a density of $0.2x10^6$ cells in 50µl in 96-well round bottomed microplates. HIV-1 resuspended in R2 complete medium was added to each well, at 0.25ng RT/10^6 cells in a volume of 50µl, taking the total infection volume to 100µl per well. Cells were

spinoculated at 1050 G for 2 hours at 21°C, before pelleting and washing twice with RPMI. Cells were then resuspended in 200µl R10 complete medium containing 50IU/ml IL-2 and medium alone or containing the relevant TGF-β superfamily cytokine or IFN-α. Supernatant samples (20µl/well) were taken 90 minutes later as a "day 0" baseline (used to measure any residual unbound virus not removed from the wash step), and then on days 3, 5, 7 and 10. On each occasion the 20µl of medium per well was replaced with the same volume of cytokine-containing media. Cytokines were not replenished by re-spiking during time courses. However, in experiments using blocking/neutralising antibodies (e.g. for the type I IFN receptor, the IL-17 receptor or against XCL1), antibodies were replenished by spiking once at day 3. Supernatants were frozen at -80°C and later analysed for p24 concentration.

Variants of this standard HIV-1 replication assay were also carried out. These included the same protocol but with single donors rather than donor trios, with purified $CD4^+$ T cells rather than CD8-depleted PBMCs, or with anti-CD3/anti-CD28 activation stimuli of a lower concentration. Details of these exceptional experiments are provided in the text of the relevant results chapters.

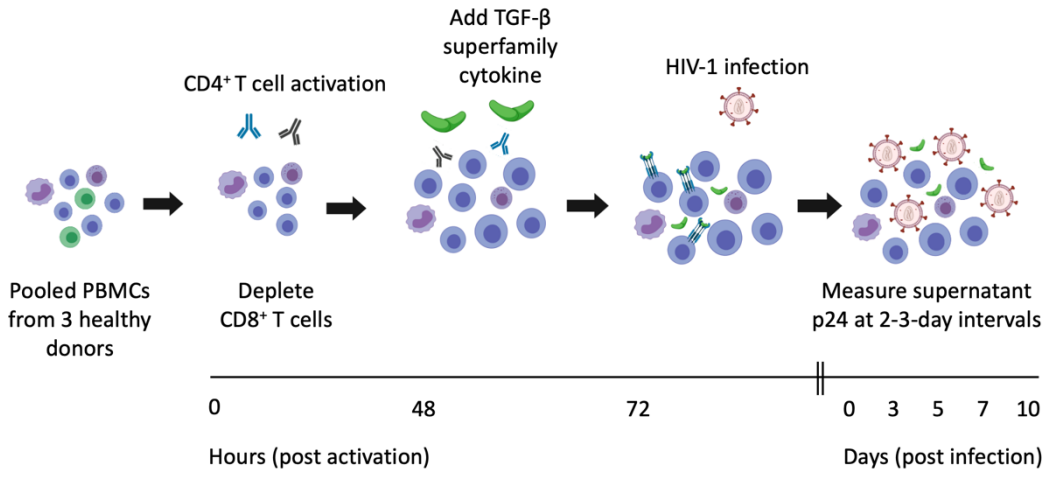


Figure 2.1 HIV-1 replication assay
PBMCs from 3 distinct HIV-seronegative donors were pooled together and depleted of $CD8^+$ T cells. Cells were activated with anti-CD3 and anti-CD28 soluble antibodies for 48 hours. 24 hours before infection, cells were pre-treated with TGF-β (or other cytokines). After 72 hours of activation, the activation stimulus was removed. Cells were infected with HIV-1 before washing and re-plating in fresh media including $TGF\text{-}\beta_1$ or other cytokines. Supernatant was sampled every 2-3 days and measured for viral p24 concentration.

2.2.12 Monocyte-derived macrophage HIV-1 replication assay

MDMs from healthy donors were generated as described previously, and $0.5x10^6$ cells were plated/well into 24-well microplates in 1ml R10 complete medium with 50ng/ml M-CSF and TGF-β superfamily cytokines or IFN-α were added to triplicate wells, after which plates were incubated for 24 hours. HIV-1 NL4-3 BaL (HIV-1 NL4-3, with an R5-tropic virus (BaL) envelope glycoprotein) was then added at 5ng RT/10^6 cells in the 1ml infection volume, before incubating for 5 hours. Wells were washed 3 times with room temperature RPMI, and 2ml R10 complete medium with 50ng/ml M-CSF added, also containing relevant TGF-β superfamily cytokines or IFN-α. After 90 minutes, baseline day 0 supernatant samples were taken, and 20µl samples of supernatant were taken again at 2-3-day intervals. On each occasion the 20µl of medium per well was replaced with the same volume of cytokine-containing media. Supernatants were frozen at -80°C and later analysed for p24 concentration.

2.2.13 Monocyte-derived dendritic cell-$CD4^+$ T cell co-culture HIV-1 replication assay

MDDCs were generated as described previously. MDDCs were infected with HIV-1 NL4-3 BaL. Concurrently, 24 hours prior to infection of MDDCs, PBMCs from individual HIV-seronegative donors allogeneic to the donor from whom MDDCs were derived were depleted of $CD8^+$ T cells as described previously and cultured in R10 complete medium with 5IU/ml IL-2 and treated with TGF-β superfamily cytokines or IFN-α (Fig. 2.2). To infect MDDCs, cells were scraped from flasks and seeded into 96-well flat-bottomed microplates at a density of $0.1x10^6$ cells in 200µl RAB5/well in technical triplicate, spun at 230G for 3 minutes and left for 90 minutes to adhere. The volume of each well was then reduced to 50µl for infection, and 50µl of R2 complete medium containing virus was added/well to allow exposure of MDDCs to 5ng RT/10^6 cells in a total volume of 100µl. Control conditions of CD8-depleted PBMCs alone (no MDDCs) and MDDCs alone (no CD8-depleted PBMCs) were also infected with the same amount of virus.

Cells were spinoculated at 1050 G for 2 hours at 21°C, then transferred to the incubator for a further 2 hours, before being spun and carefully washed three times with RPMI. After washing, 0.2x10^6 CD8-depleted PBMCs that had been pre-treated for 24 hours with TGF-β superfamily cytokines or IFN-α were added to the virus-pulsed MDDCs to form a coculture, in a volume of 200µl R10 complete medium with 5IU/ml IL-2 plus relevant TGF-β superfamily cytokines or IFN-α. Co-cultures were spun at 230G for 3 minutes to bring cells together. After 90 minutes, baseline day 0 supernatant samples (20µl/well) were taken, and further samples were taken at 3-day intervals. On each occasion the 20µl of medium per well was replaced with the same volume of cytokine-containing media. Supernatants were frozen at -80°C and later analysed for p24 concentration.

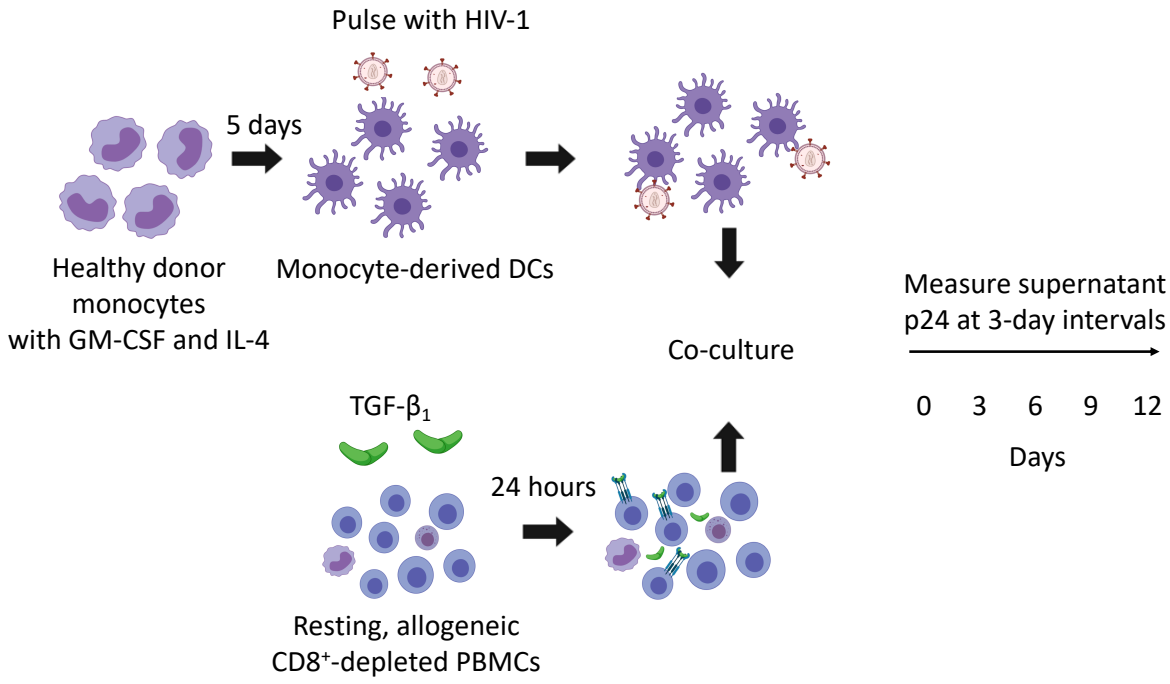


Figure 2.2 MDDC-CD4$^+$ T cell co-culture HIV-1 replication assay
MDDCs were generated from monocytes from an HIV-seronegative donor by culture with GM-CSF and IL-4 for 5 days, then were pulsed with HIV-1 NL4-3 BaL. Concurrently, 24 hours prior to the pulsing of MDDCs with virus, PBMCs from a different, allogeneic HIV-seronegative donor were CD8$^+$ T cell-depleted and pre-treated with TGF-β$_1$ or other cytokines for 24 hours. MDDCs were then washed and re-plated in fresh medium and co-cultured with CD8-depleted PBMCs. Individual controls of MDDCs alone (no CD8-depleted PBMCs) and CD8-depleted PBMCs alone (no MDDCs) were also infected in the same manner. Supernatant was sampled every 3 days and measured for viral p24 concentration.

2.2.14 293FT cell HIV-1 replication assay

24 hours prior to infection, 90% confluent 293FT cells cultured in D10 in T75 flasks had a media change to D10 without G418 and were treated with TGF-β superfamily cytokines or other treatment conditions. After 24 hours, cells were trypsinised for 5 minutes at room temperature, and $6x10^4$ cells/well seeded into a 96-well flat-bottomed microplate, with each condition in technical triplicate in a volume of 150µl of D10 without G418 and containing relevant TGF-β superfamily cytokines or other treatment conditions. The concentration of cytokines was adjusted to account for dilution by the impending addition of 50µl more liquid. Microplates were spun to bring cells to the bottom of the wells and left in the incubator for 2 hours to allow the cells to adhere. For each well, 0.3µg HIV-1 NL4-3 DNA was added to 25µl Opti-MEM I, and in parallel, 0.63µl Lipofectamine added to another 25µl Opti-MEM I and left for 5 minutes at room temperature, scaled up for the number of wells required. The equal volume DNA and Lipofectamine solutions were then combined in a 1:1 ratio and left for 30 minutes at room temperature to form DNA-Lipofectamine complexes. 50µl of the combined solution was then added to each well, and cells were placed in the incubator. Supernatant samples (20µl/well) were taken at various intervals over a 72-hour timeframe, and each time replaced with the same type of medium with the relevant cytokines. Supernatants were frozen at -80°C and later analysed for p24 concentration. In a repeat of this experiment, half the amount of HIV-1 NL4-3 DNA was used (0.15µg), and correspondingly, half the volume of Lipofectamine (0.315µl) was used, both in 25µl volumes.

2.2.15 HIV-1 p24 AlphaLISA assay

HIV-1 p24 capsid protein was measured in cell culture supernatants with a bead-based high sensitivity p24 AlphaLISA Detection Kit (PerkinElmer, Inc, USA, cat no. AL291F) according to the manufacturer's instructions. Briefly, the assay uses a biotinylated anti-p24 antibody that binds streptavidin-coated "donor" beads. p24 is also targeted by another "acceptor" bead-

conjugated antibody. When the donor and acceptor beads come together, the former are excited by the latter, and light is emitted at 615nm which can be detected by a plate reader.

Plates were read on a FLUOstar Omega plate reader (BMG Labtech, Germany) and raw AlphaScreen values read alongside a standard curve using 4 parameter logistic regression using MARS Data Analysis software (BMG Labtech, Germany). Where samples exceeded the range of the standard curve, supernatants were diluted in the same type of medium (D10 or R10 complete), up to 1 part in 14 for the highest titre samples.

2.2.16 HIV-1 NL4-3 LTR luciferase reporter assay

This assay used the single-round non-replication-competent luciferase reporter virus VSV G NL4-3 luc. Between 5-30x10^6 primary $CD4^+$ T cells from HIV-seronegative donors were isolated as described previously and activated by culture in complete R10 medium with 50IU/ml IL-2 plus 50ng/ml soluble anti-CD3 and 100ng/ml soluble anti-CD28 for 72 hours. In 50ml Falcon tubes, cells were pelleted and resuspended in a volume of 50µl medium. A volume of virus stock was added to the cells that would produce a 1 in 500 dilution of virus (the stock of which was not concentration quantitated) in media after the cells had been resuspended up to a concentration of 2x10^6 cells/ml. Cells were incubated in the 50µl volume for 2 hours with virus, before adding a volume of R10 complete medium with 50IU/ml IL-2 to suspend them at 2x10^6 cells/ml.

After 72 hours, cells were divided into two for a 50ng/ml recombinant TGF-β_1 treatment or a control receiving no cytokine, before plating 0.4x10^6 cells per well in a 96-well round-bottomed microplate, with each condition for each donor in minimum of technical quadruplicate, up to a maximum of 16 technical replicate wells. After 24 hours, cells were lysed for 10 minutes using 75µl of lysis buffer from a Luciferase Assay System kit (Promega Corporation, USA, cat no.

E1500), and freezing at -80°C to aid the lysis process. Cells were then thawed, and 45µl cell lysate combined with 45µl substrate solution from the same kit, before immediately reading on a FLUOstar Omega plate reader (BMG Labtech, Germany). Results for technical replicate wells were averaged to produce a single value.

For cell lines (Jurkat.CCR5, MOLT-4.CCR5 cells and CEM-NKR-CCR5), the same protocol was employed with some changes:

- Cells were not activated, owing to their transformed status.
- $20x10^6$ cells were infected. After 2 hours of initial infection, cells were resuspended at a more dilute volume of 0.5 $x10^6$ cells/ml to allow for expansion.
- After 72 hours of infection, cells were plated at a density of $1x10^6$ cells/ml in 2ml volumes per well, in 24-well microplates in technical quadruplicate.
- 24 hours after TGF-β_1 treatment and before cell lysis, all wells were counted and an even number of live cells were lysed for both control and TGF-β_1 conditions.

2.2.17 RNA sequencing

RNA sequencing (RNAseq) was utilised to analyse the effects of TGF-β superfamily cytokines and IFN-α on $CD4^+$ T cells. $CD4^+$ T cells from n=5 HIV-seronegative donors were purified from PBMCs as previously described, before activating for 48 hours with 50ng/ml anti-CD3, 100ng/ml anti-CD28 and 50IU/ml IL-2. Cells were then treated with TGF-β_1 (50ng/ml), activin A (5nM), BMP-2 (25nM), IFN-α (1000IU/ml) or no treatment as a control, for a further 24 hours before RNA extraction.

RNA was extracted from 10^7 $CD4^+$ T cells per donor per condition, using an RNeasy Plus Mini kit (Qiagen, Netherlands, cat no. 74134), according to the manufacturer's guidelines. Briefly, the protocol involves lysis of cells with an RNase-inactivating guanidine-isothiocyanate buffer.

Contaminating genomic DNA (gDNA) is then removed with a gDNA elimination spin column, before passing the RNA-containing flow-through through an RNA-binding column, which is finally washed of other contaminants. The protocol isolates enriched mRNA, size excluding other forms of RNA that are less than 200 nucleotides long.

After RNA elution, samples were stored at -80°C, thawed once to aliquot, then re-frozen. RNA quality and concentration were determined from one of the aliquots using a 4200 TapeStation System (Agilent Technologies, Inc, USA, cat no. G2991AA), with RNA ScreenTape (cat no. 5067-5576), RNA ScreenTape Sample Buffer (cat no. 5067-5577) and RNA ScreenTape Ladder (cat no. 5067-5578). All samples had a RNA integrity number of at least 8.6, with the vast majority being greater than 9.0.

Another aliquot of each sample was shipped on dry ice to Novogene Co, Ltd, China, for mRNA sequencing. Each shipped aliquot contained 2-17µg RNA. Libraries were sequenced on an Illumina HiSeq platform at a depth of 30 million 150bp paired-end reads per sample by Novogene. Raw data of FASTQ files were supplied in return from Novogene. Reads were mapped to the reference genome GRCh38/hg38 (UCSC Genome Browser) using the RNAseq aligner STAR[436]. The Bioconductor package *edgeR* was used to count reads and determine differentially expressed genes (DEGs) by combining data from biological replicates[437]. All analysis as far as the determination of DEGs was conducted by Nicki Gray, University of Oxford, UK. Pathway analysis of DEGs was conducted using Ingenuity Pathway Analysis (Qiagen, Netherlands). Volcano plots were generated using Bioconductor package *EnhancedVolcano*.

2.2.18 Quantitative real-time polymerase chain reaction

qRT-PCR was performed to validate genes of interest identified from RNAseq. RNA was first converted to cDNA using a High Capacity RNA-to-cDNA kit (Thermo Fisher Scientific, USA, cat no. 4387406) according to the manufacturer's guidelines, including negative controls lacking RNA and lacking reverse transcriptase respectively. Briefly, the kit provides RT and an appropriate buffer to be combined with RNA, which is subjected to 37°C for one hour to facilitate the reverse transcription reaction, before inactivating the enzyme with a 95°C step for 5 minutes. It was assumed that RNA was converted to cDNA in a 1:1 ratio.

For qRT-PCR, TaqMan probes (0.25µl/well) were combined with TaqMan Gene Expression Mastermix (2.5µl/well) (Thermo Fisher Scientific, USA, cat no. 4369016) and an amount of cDNA in nuclease-free water that gave a total well volume of 5µl, with the cDNA at a resultant concentration of 4ng/µl. TaqMan probes are shown in Table 2.7. All samples were run in technical duplicate. Microplates were run on a 384-well QuantStudio 7 Flex Real-Time PCR System (Thermo Fisher Scientific, USA, cat no. 4485695). Data were analysed comparing cycle threshold (C_T) values between a stably expressed reference gene, *CYC1*, and genes of interest using the formula $\Delta C_T = 2^{(HK - GOI)}$, according to published methods[438]. *CYC1* is a commonly used reference gene for qRT-PCR[439], and prior analysis performed in our lab had shown this to be the most stably expressed candidate (across a range of cell activation states) in $CD4^+$ T cells from a panel of commonly used reference genes (data not shown).

2.2.19 Statistical analysis and data presentation

Statistical analysis was carried out using either GraphPad Prism version 8 (GraphPad Software Inc, USA) or using publicly available packages for the statistical programming language R using RStudio (RStudio, Inc). Statistical tests used are noted in individual figure legends and were not performed on sample sizes of n=4 or fewer. For sample sizes of n=5 or

greater, normality was checked by Shapiro-Wilk and Kolmogorov-Smirnov tests before choosing parametric or non-parametric tests. Data were plotted using GraphPad Prism version 8 and R studio.

To specifically analyse perturbations in cytokine concentrations in AHI using the longitudinal US plasma donor cohort, data from each donor was aligned based on T_0 (the timepoint when viraemia first reached 100 RNA copies/ml plasma), which was estimated using linear mixed-effects modelling as previously described[63]. For each analyte, data from all donors were combined into smoothed curves using cubic spline interpolation with the R package *fields* as previously described[440]. Samples were assigned bins according to T_0, and linear mixed-effects analysis was used to compare pre-day -7 samples to those in post-day -7 bins using R packages *nlme* and *lme4* as previously described[440]. This analysis was carried out by Dr Eleni Giannoulatou (Victor Chang Cardiac Research Institute and the University of New South Wales, Australia).

Chapter 3

Analysis of the induction of TGF-β superfamily cytokines in HIV-1 infection

3.1 Introduction

As described in Chapter 1, AHI is associated with a systemic cytokine storm that begins prior to the peak in plasma viral load[63]. Less pronounced cytokine perturbations also persist into chronic infection[180], regardless of suppression of viraemia with ART[11,12,181]. The cytokines induced during HIV-1 infection have both protective and pathogenic effects, one or other of which can predominate at different stages of infection. For example, type I IFNs mediate important antiviral activity that contributes to control of viral replication in AHI, evidenced by the fact that the virus has evolved several strategies to evade triggering type I IFN production[152–154] and TF viruses are selected for their resistance to IFN-α[57]. In chronic infection, however, type I IFNs contribute to immune activation and pathogenesis, as evidenced by the reversal of a type I IFN gene signature in non-pathogenic animal models after acute SIV infection that persists in macaques[182,183,200].

Furthermore, greater upregulation of IL-12 and IFN-γ during AHI is predictive of establishment of a lower viral set-point, with the converse seen for IL-7 and IL-15[441]. IL-12 drives NK cell activation and promotes Th1 cell development, important for HIV-1 control[442]. However, although IL-15 expands NK cells and CD8 T cells[443], it promotes activation and proliferation of memory $CD4^+$ T cells[444], key targets of the virus, which may explain its association with poorer prognosis in HIV-1 infection. Notably, cytokines not only have direct and indirect effects on levels of viral replication during HIV-1 infection, but also play important roles in HIV-associated comorbidities, including cardiovascular disease[445], HAND[446] and HIV-associated nephropathy[447].

Cytokines can be harnessed (or down-modulated) during infection for therapeutic gain. Administration of recombinant IL-12 to acutely SIV-infected RMs lowers viral load and improves survival times[448] whilst IL-15 treatment does the opposite[449]. However, again timing is important, because in chronic infection IL-15 has no effect on viral load, and in ART-treated chronic RMs, IL-15 in fact boosts $CD4^+$ and $CD8^+$ T effector memory cell populations[450]. Indeed, IL-15-treated NK cells show improved killing of latency-reversed HIV-infected cells *ex vivo*[451]. In a similar issue of timing, administration of IFN-α to healthy RMs gives some resistance to SIV challenge, but after repeated administration the IFN pathway becomes desensitised, and animals that become subsequently infected in fact do clinically worse than those not receiving the treatment[185]. In prophylaxis, cytokines could also be considered as adjuvants to improve vaccine efficacy[452,453].

Given the key roles played by cytokines in HIV-1 infection, defining the dynamics of innate cytokine induction during infection is of key importance to inform understanding of the contributions they may be making to protection and/or pathogenesis and identify opportunities for exploiting or down-modulating their activity for therapeutic benefit. In contrast to other innate cytokines, TGF- β superfamily members are relatively poorly studied in HIV-1 infection.

Animal data in RMs reveal rapid plasma TGF-β induction[233] within 24 hours of SIV inoculation[184,238]. TGF-β is also induced in non-pathogenic AGM infection with the same rapid kinetics, and in fact, to a much greater magnitude[238]. However, a notable difference is a complete return to baseline in AGMs within days, contrasted with sustained elevation for at least two weeks in RMs, indicating that TGF-β could play a crucial function in limiting immunopathology, but that timing and concentration are key. It could be the case that in the pathogenic model, a lack of response to TGF-β drives its persistence. In RMs, transcription of inhibitory SMAD7 is concurrently persistently upregulated, which is not seen in AGMs[454]. The

opposite appears true for SMAD4[454], a positive contributor to the TGF-β signalling pathway. Human studies to date have compared single timepoint samples from patients at varying stages of infection against seronegative demographically matched controls, leaving the kinetics of plasma TGF-β in the earliest stages of acute infection still to be elucidated.

In chronic HIV-1 infection, TGF-β is found in greater concentrations in the plasma of infected individuals than in seronegative controls, and correlates with T cell activation marker expression[339], as well as with disease progression and $CD4^+$ T cell loss[338,342]. A small number of studies have either failed to show greater circulating TGF-β in HIV-1 infection compared to seronegative controls[455,456] or in one study, showed the opposite[457], though these studies appear to be a minority exception.

TGF-β can be directly induced from PBMCs[458] and B cells[353] by HIV-1 Env, and from glial cells[459] and macrophages by Tat[460] (though historically, recombinant proteins were not always tightly controlled for possible endotoxin contamination), but systemic induction is likely also driven by immune activation and pro-inflammatory cytokine induction. In line with this, one *in vitro* study demonstrated that recombinant Tat-mediated TGF-β_1 induction in monocytes is at least in part likely due to IL-6 induction[461]. This is also evidenced by the fact that TGF-β remains heightened even in virally suppressed individuals on ART[338,340–346].

There exists no published data on whether HIV-1 induces activins or BMPs *in vivo* or *in vitro*, despite the growing body of evidence for the involvement of these cytokines in viral infections and immunity. Unsurprisingly, given its involvement in regulating inflammation[366,367], activin A is systemically induced in a range of infectious and non-communicable diseases. These include ischaemic tissue injury[462], asthma[391], mammary neoplasia[463], septicaemia[464], and HBV and HCV infections[465,466]. In more localised compartments, elevations are also noted in urine

in inflammatory kidney disease[467], in cerebrospinal fluid of patients with bacterial meningitis[468], and in synovial fluid in rheumatoid arthritis[469].

The cellular sources of cytokines produced in HIV-1 infection are predominantly leukocytes and epithelial cells, as these cell types express a range of PRRs and are capable of secreting high levels of many cytokines. DCs in particular are key sources of many innate cytokines with effects on HIV-1 replication, such as IFN-α (pDCs)[151], IL-12[470] and IL-15 (mDCs)[471]; and DCs from HIV-1 infected individuals produce a large repertoire of cytokines upon stimulation, indicating that infection might not impair this aspect of DC functionality[162].

pDCs possess TLRs 7 and 9[150], which sense ssRNA and dsDNA respectively. Human mDCs negligibly express TLR7 and do not express TLR9, but express most other TLRs[472,473]. Although mDCs can sense GU-rich ssRNA (which HIV-1 possesses) through TLR8[474], HIV-1 alone does not activate mDCs[167]. Rather, pDC-derived IFN-α and TNF produced following HIV-1 stimulation is responsible for subsequent mDC activation[167]. TGF-β superfamily cytokines are keenly involved in DC biology[248], and mDCs produce BMPs[410] and activins[372,374] during maturation.

In this chapter I aimed to explore:

- Whether TGF-β superfamily cytokines are systemically induced in the earliest stages of AHI and, if so, the kinetics of these perturbations.
- Whether TGF-β superfamily cytokines are systemically induced in subacute and chronic HIV-1 infection.
- Whether stimulation of leukocyte subsets with HIV-1 induces TGF-β superfamily cytokines *in vitro*, with a view to identifying potential cellular sources of those cytokines induced *in vivo*.

3.2 Results

3.2.1 Circulating levels of TGF-β_1, but not activins A and B or BMP-2, are elevated in acute HIV-1 infection

To determine the kinetics of any perturbations in circulating levels of TGF-β superfamily cytokines during AHI, longitudinal plasma samples from regular plasma donors who acquired HIV-1 infection during the time-frame or serial plasma donation were analysed for concentrations of TGF-β_1, activins A and B, and BMP-2 by ELISA or Luminex assay. TGF-β_1 was selected owing to it being the most abundant of the TGF-β isoforms in the body[261]. Activins A and B are the best-studied of the activins in terms of systemic induction in the context of inflammation and infectious disease[391,463,465,466] and similarly, BMP-2 is documented to play important roles in leukocyte biology[399,400], so was selected as a good representative of the BMP subgroup in this regard.

Initial quality control experiments examined possible effects of freeze-thawing and anticoagulant on the measured cytokine concentrations. No substantial impact was found from anticoagulant (EDTA, lithium heparin or 4% sodium citrate) on the measured concentrations of TGF-β_1, BMP-2, activin A or activin B (Fig. 3.1A); nor from freeze-thawing on the concentrations of TGF-β_1 or activins A and B (Fig. 3.1B).

The panel of serial time-course samples allowed investigation of perturbations in circulating levels of cytokines and other analytes in the very earliest stages of HIV-1 infection. Samples were taken at two to five-day intervals into 4% sodium citrate anticoagulant and included timepoints from up to 132 days before viraemia first reached detectable levels (100 copies/ml viral RNA, referred to as the "time origin" or T_0), and timepoints up to a maximum of 41 days post T_0. Plasma viral loads had been measured as part of previously published work[63]. Previous work has revealed disturbances in acute phase proteins up to 7 days before the first

onset of detectable viraemia in AHI[176]. Thus, donors were selected based on the availability of at least one timepoint prior to -7 days pre-T_0 to give insight into baseline analyte levels at timepoints that were highly likely prior to acquisition of infection.

Data from three representative donors are shown in Fig. 3.2, together with IFN-α data, measured as part of a previous study[63], which is shown as an example of an innate antiviral cytokine known to be systemically upregulation in early AHI. Some minor fluctuation was observed in plasma levels of all analytes in each individual over time, consistent with findings made for other analytes in prior studies. A transient increase in IFN-α was apparent in two donors, but a similar increase was not observed in the third donor, indicative of donor-to-donor variation and/or a failure to capture transient IFN-α upregulation in the third individual. A trend was also observed for TGF-β_1 to increase in two donors in AHI, but there was no obvious change in activins A and B, or BMP-2 during the time-frame analysed (Fig. 3.2).

To draw more meaningful conclusions with statistical analysis, cytokine concentrations and viral load data from n=10-15 donors (depending on the cytokine) were pooled and plotted as smoothed curves using spline interpolation. For statistical analysis, data were also grouped into bins relative to T_0, and linear mixed-effects models were fitted on the data accounting for inter-sample variability. All samples before day -7 were considered as a baseline bin, against which the other bins were compared. When considering all donors together, plasma TGF-β_1 was found to be significantly elevated 1-4 days post-T_0 and remained so throughout AHI. Concentrations of activins A and B and BMP-2 were largely unchanged over the course of AHI. BMP-2 was slightly elevated at 9-12 days post-T_0 (Figure 3.3). However, this bin contained only a small number of samples, which may have skewed the data.

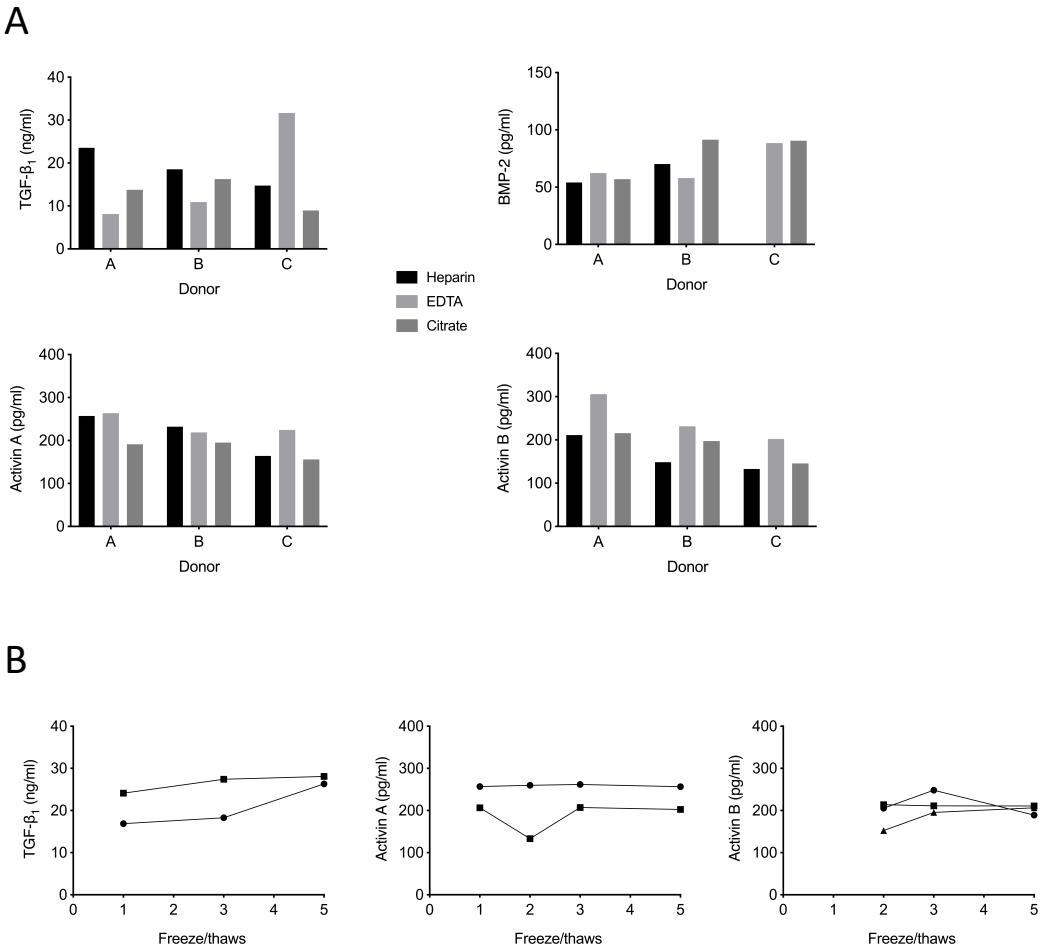


Figure 3.1 Analysis of the effects of anticoagulant and freeze-thawing on TGF-β superfamily cytokine concentration measured by ELISA or Luminex assay
A. Plasma separated from blood samples from HIV-seronegative donors collected in heparin, EDTA or 4% sodium citrate was measured for TGF-β_1 (Luminex assay), BMP-2, activin A or activin B (ELISA). Samples were assayed in technical duplicate and the results averaged. CV percentages of greater than 20% between technical replicates were rejected, resulting in the omission of one sample (BMP-2, heparin, donor C). **B.** Plasma samples from blood collected into heparin anticoagulant were spiked with recombinant TGF-β_1 (5ng/ml), activin A (100pg/ml) or activin B (100pg/ml), then freeze-thawed a number of times before measurement of those cytokines by Luminex assay or ELISA. Each unique shape represents a donor.

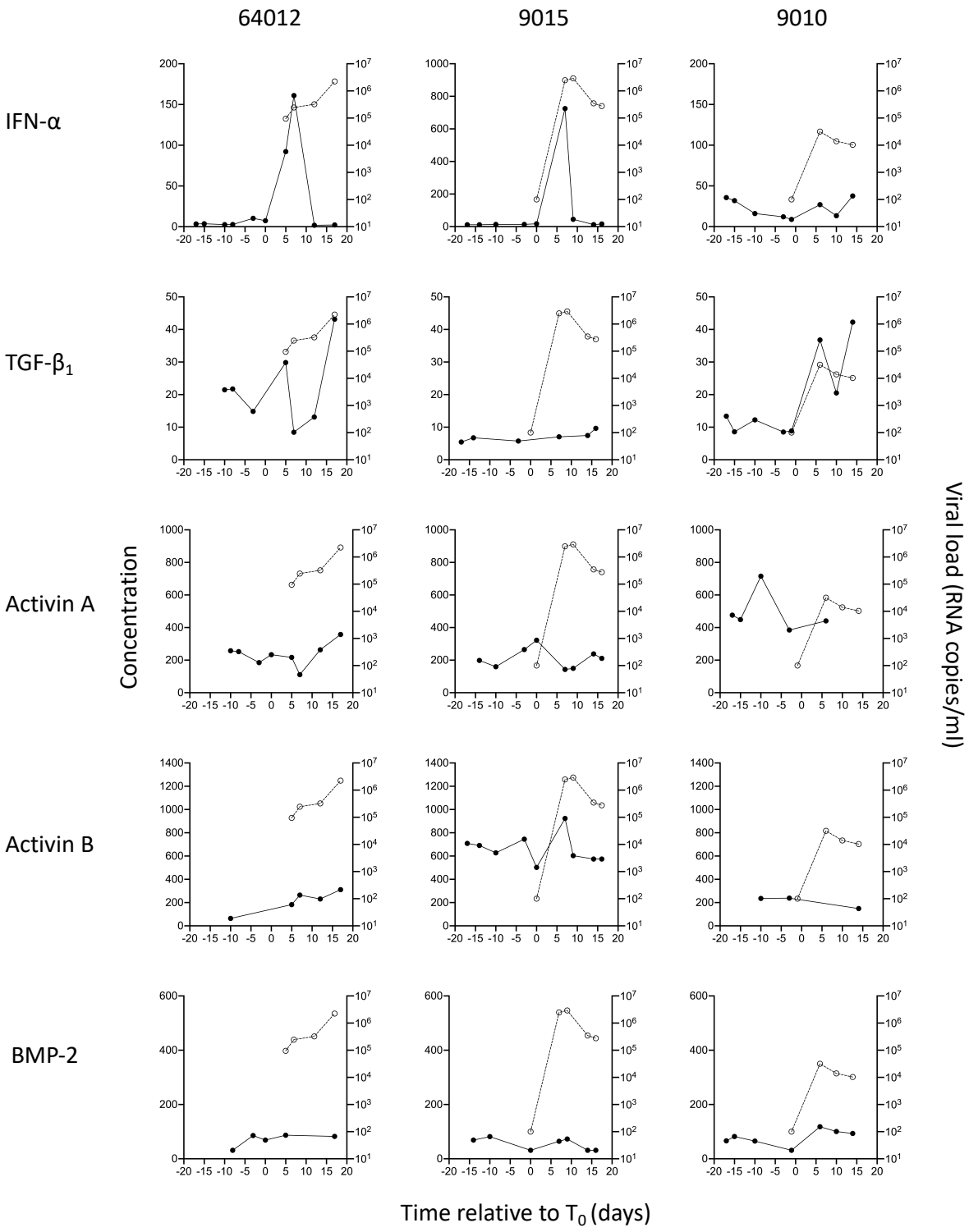


Figure 3.2 Plasma concentrations of IFN-α and TGF-β superfamily cytokines at serial timepoints during AHI in three donors

Longitudinal plasma samples from 10-15 donors were analysed for concentrations of TGF-β_1, activins A and B, and BMP-2; data from three representative donors (64012, 9015 and 9010) are shown here, together with plasma viral load data from each individual. T_0 represents the time at which viral load first reached detectable levels (100 RNA copies/ml). IFN-α is shown as a positive control and was measured as part of a prior study[63]. Closed circles/solid lines=cytokine concentration (pg/ml, except TGF-β_1, which is in ng/ml). Open circles/dashed lines=viral load (RNA copies/ml).

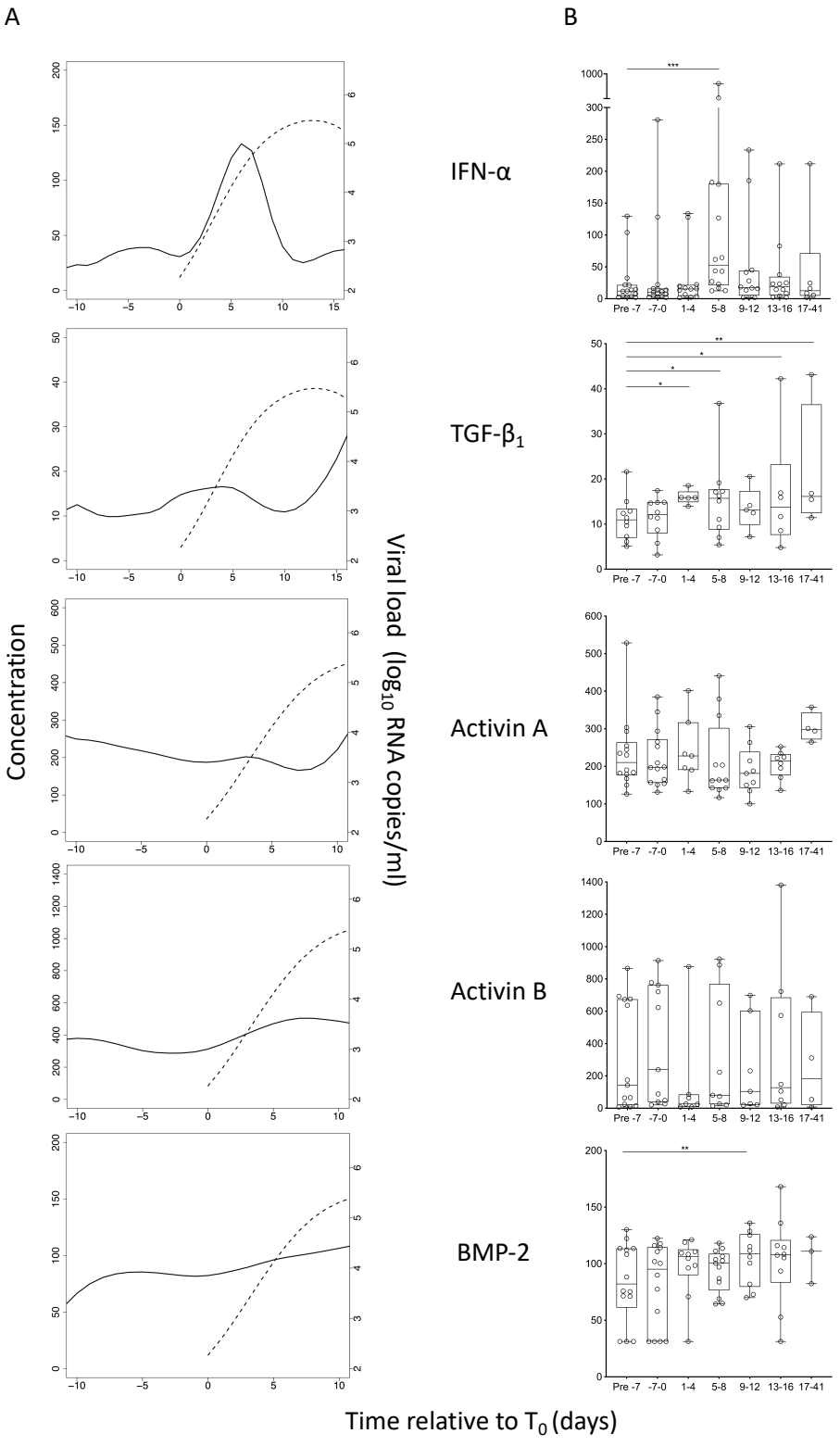


Figure 3.3 Plasma concentrations of IFN-α and TGF-β superfamily cytokines in AHI
A. Data from n=15 (IFN-α), n=10 (TGF-β_1), n=14 (activin A), n=13 (activin B) and n=14 (BMP-2) donors were combined and smoothed using cubic interpolation. For any given day relative to T_0, up to seven donors contributed a sample. Solid lines=cytokine concentration (pg/ml, except TGF-β_1, which is ng/ml). Dashed lines=viral load (RNA copies/ml). IFN-α data were measured as part of a prior study[63]. **B.** Pooled data were assigned into bins, and linear mixed-effects analysis was used compare each bin to the baseline (pre-day -7) bin (*P<0.05, **P<0.01, ***P<0.001). Boxes show the median and the 25th and 75th percentiles, whiskers show the range. All cytokines are pg/ml, except TGF-β_1, which is ng/ml.

3.2.2 Circulating levels of TGF-β_1, but not activins A and B or BMP-2, are elevated in subacute and chronic HIV-1 infection

To examine possible perturbations in systemic TGF-β superfamily cytokine concentrations during subacute and chronic HIV-1 infection, plasma samples were obtained from a cohort of patients recruited during AHI and followed prospectively until they chose to commence ART. Subacute infection was defined as up to 30 days post-onset of acute retroviral syndrome symptoms (FOSx), and chronic as more than two years post-FOSx. Plasma from n=21 patients sampled in subacute infection, n=26 donors sampled during chronic infection and n=20 demographically matched seronegative controls was analysed for concentrations of TGF-β_1, activins A and B, and BMP-2 by Luminex assay or ELISA. Plasma was separated from blood collected into EDTA anticoagulant. Clinical information for subacutely and chronically infected donors is shown in Table 3.1. Analysis was cross-sectional, although n=8 patients provided a sample in both the subacute and chronic infection, allowing paired analysis of these samples. IFN-α was evaluated in a subset of samples from both patient groups but was mostly found to be below the assay LLOQ (data not shown), in line with prior studies that have shown IFN-α is only transiently elevated prior to the peak in viraemia in AHI[63] and is typically not systemically elevated during subacute or chronic infection[440,475,476]. IL-18, reported to be elevated in subacute and chronic infection[340,475], was selected as an alternative positive control.

As shown in Figure 3.4A, TGF-β_1 was found to be significantly elevated in subacute and chronic HIV-1 infection (as was IL-18) compared to seronegative controls. There was a trend for activin B to be elevated in chronic infection compared to seronegative controls, but this did not reach statistical significance. In contrast, activin A and BMP-2 appeared relatively unchanged throughout infection. In subacute infection BMP-2 levels were statistically significantly higher than in chronic infection, although the difference was very subtle (Fig. 3.4A).

When comparing paired data from n=8 patients providing a sample in both subacute and chronic infection, TGF-β_1 was elevated in chronic infection compared to subacute infection, and there was a trend for increased activin A in chronic relative to subacute infection, though not of statistical significance. Activin B and BMP-2 levels in subacute and chronic infection did not differ significantly (Fig. 3.4B).

Viral load correlates positively with immune activation in HIV-1 infection[477], and both variables positively correlate with speed of disease progression[478]. As TGF-β_1 was elevated in subacute and chronic HIV-1 infection, whether TGF-β_1 correlated with viral load in these samples was examined, but no correlation was found (Fig. 3.5A, B).

Group	Subject ID	Days following onset of symptoms	Plasma viral load (RNA copies/ml)	CD4 count (cells/μl)
Subacute	MM12	16	1,555,700	500
	MM19	13	5,678,900	400
	MM20	16	2,253,700	220
	MM22	12	9,059,000	ND[B]
	MM23[A]	9	11,105,300	330
	MM24	16	157,700	580
	MM28	6	4,337,100	560
	MM31	20	324,000	370
	MM32	10	147,640,000	320
	MM33	12	1,451,400	940
	MM36	6	38,417,000	320
	MM38	29	2,721,100	410
	MM39	5	350,600	610
	MM41	14	3,172,500	190
	MM65	10	5,000,000	500
	MM67	24	8,300,000	90
	MM69	12	5,100,000	480
	MM70	18	2,500,000	260
	MM72	5	2,100,000	510
	MM73	11	3,700,000	510
	MM75	9	30,000,000	320
Chronic	MM1	1370	29,700	1020
	MM4	1222	233,400	490
	MM8	801	105,200	240
	MM9	945	217,600	160
	MM12	900	304,800	200
	MM13	1125	8,800	240
	MM14	1394	19,700	340
	MM23	1064	45,700	240
	MM24	1322	ND	220
	MM27	1329	336,300	310
	MM28	1381	15,900	290
	MM31	1220	153,000	750
	MM33	1441	30,000	440
	MM34	1396	14,000	490
	MM36	1395	216,500	ND
	MM39	1206	280,000	190
	MM40	1530	310,000	250
	MM45	1570	1,200	410
	MM46	938	160,000	240
	MM47	1263	24,000	210
	MM51	906	27,000	560
	MM55	1299	11,000	490
	MM56	802	300	620
	MM57	971	130,000	350
	MM62	1173	20,000	1200
	MM65	753	18,000	880

Table 3.1 Clinical information for donors subacutely and chronically infected with HIV-1
Clinical information for individuals sampled during subacute and/or chronic HIV-1 infection. Subacute samples were collected from 5-29 (median 12) days post-onset of acute retroviral syndrome symptoms. Chronic samples were collected at 753-1570 (median 1243) days. All donors had never received ART prior to or at the timepoints analysed. All patients were male. The majority of patients were of Caucasian ethnicity, infected through sex with men, with a clade B virus.
[A] Where donors provided a sample in both subacute and chronic infection, these paired data are indicated in bold
[B] Not determined

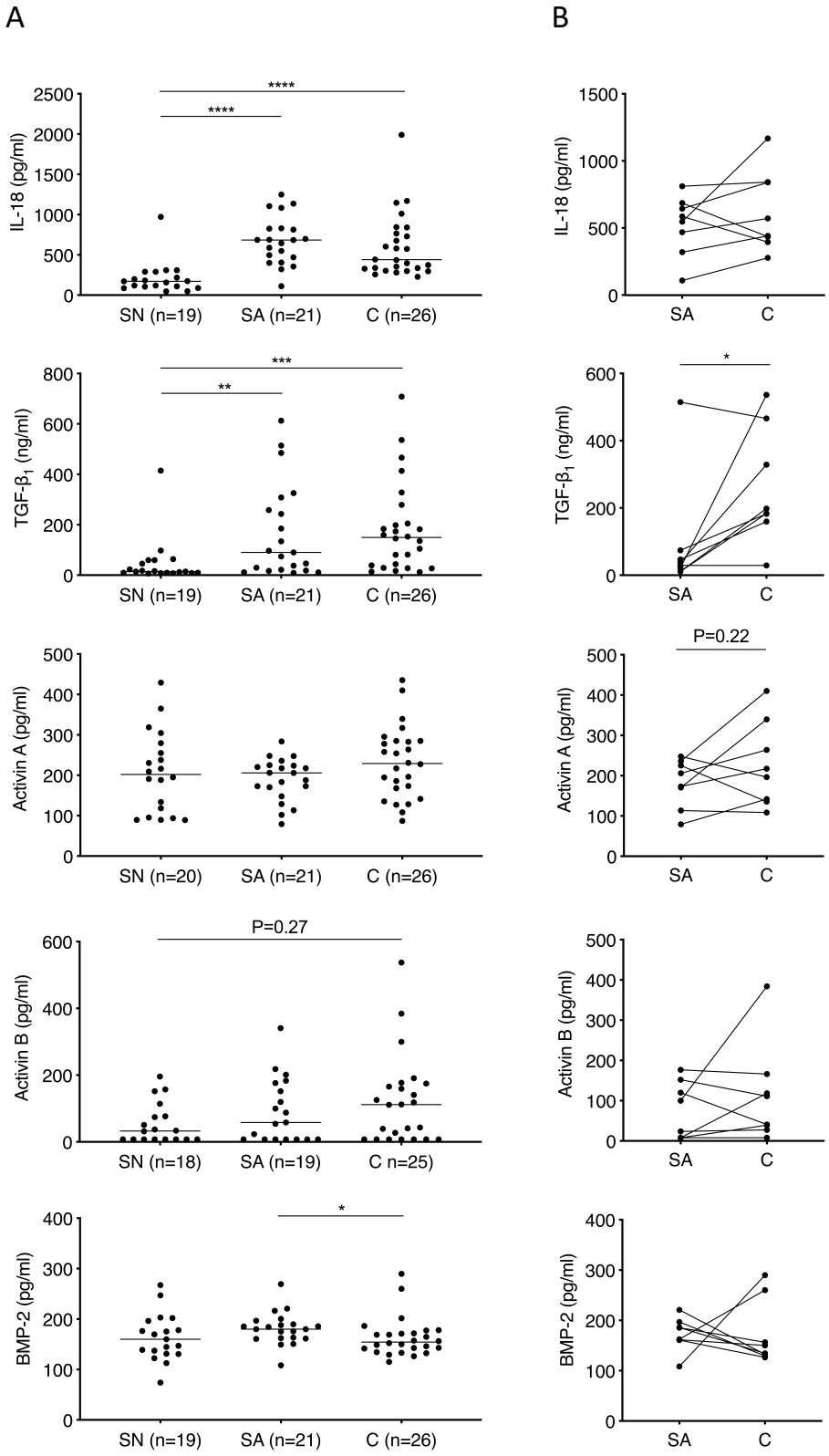


Figure 3.4 Plasma concentrations of TGF-β superfamily cytokines and IL-18 in subacute and chronic HIV-1 infection

A. Concentrations of IL-18, TGF-β_1, activins A and B, and BMP-2 were investigated cross-sectionally in donors sampled in subacute (n=19-21) or chronic (n=25-26) HIV-1 infection, as well as seronegative controls (n=18-20). Horizontal lines denote group medians. Kruskal-Wallis test with Dunn's post-test, *P<0.05, **P<0.01, ***P<0.001, ****P<0.0001. SN=seronegative, SA=subacute, C=chronic. **B.** n=8 patients provided a sample in both subacute and chronic infection. Paired t-test (IL-18, activin A), Wilcoxon signed-rank test (all others).

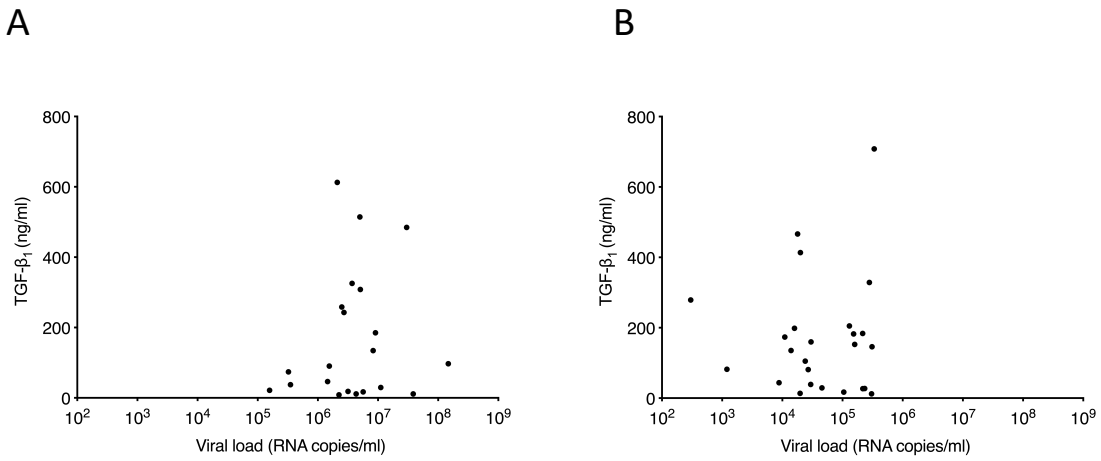


Figure 3.5 Plasma concentrations of TGF-β_1 in subacute and chronic HIV-1 infection do not correlate with viral load
A. Plasma TGF-β_1 concentration and viral load were measured in n=21 samples from individuals subacutely infected with HIV-1. Spearman's rank correlation coefficient, r=0.09, P=0.69. **B.** Plasma TGF-β_1 concentration and viral load were measured in n=25 samples (for one of the 26 samples, viral load data was unavailable) from individuals chronically infected with HIV-1. Spearman's rank correlation coefficient, r=0.06 , P=0.76.

3.2.3 Increased TGF-β_1 correlates with platelet degranulation at all stages of HIV-1 infection

Platelets store large amounts of TGF-β_1 as a component of alpha-granules, along with chemokines such as PF4 (also known as CXCL4) and these analytes are secreted when the cells are activated and undergo degranulation[479]. PF4 was measured in samples from Fig. 3.4 as a marker of platelet degranulation.

In subacute and chronic HIV-1 infection, plasma PF4 concentrations were significantly higher than those in HIV-seronegative donors (Fig. 3.6A). There was also a trend for the presence of a higher PF4 concentration in chronic infection than in subacute infection in donors sampled at both timepoints, although the difference did not reach statistical significance (Fig. 3.6B). When PF4 and TGF-β_1 data from the subacute group were plotted against one another, a strong positive correlation (r=0.94, P<0.0001) was observed (Fig. 3.6C). This was also seen with the chronic group (r=0.94, P<0.0001) (Fig. 3.6D). PF4 was also analysed in samples from plasma donors longitudinally sampled during AHI (Fig. 3.3), and when data from all timepoints

analysed in n=9 donors were combined, a similar positive correlation was seen (r=0.71, P<0.0001) (Fig. 3.6E). These data reveal that platelet degranulation occurs at all phases of HIV-1 infection and suggest that platelets are likely to be a major source of systemic TGF-β_1 in HIV-1 infection.

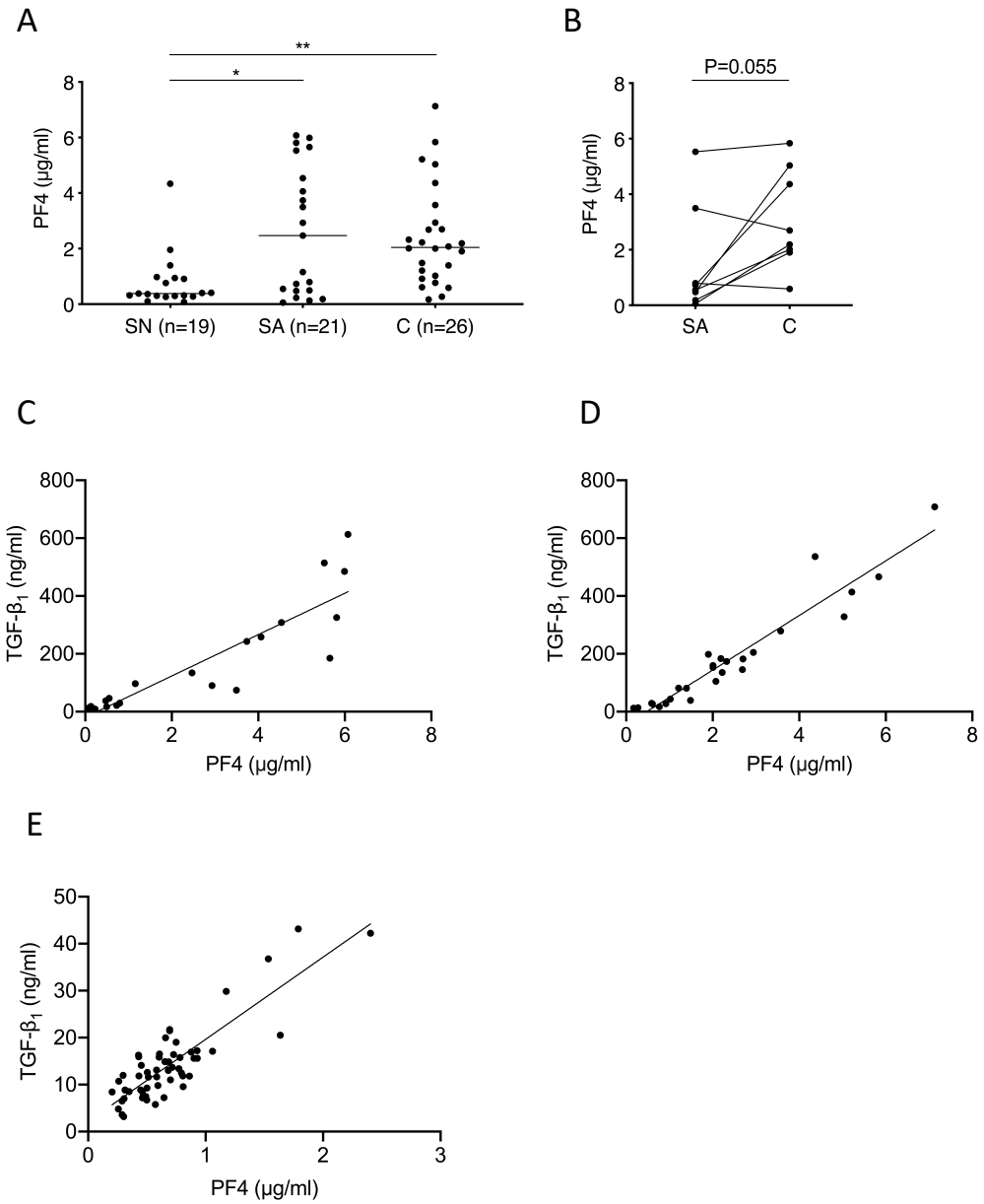


Figure 3.6 Correlation between plasma concentrations of PF4 and TGF-β_1 in HIV-1 infection
A. Plasma PF4 concentration was investigated in subacute (n=21) and chronic (n=26) HIV-1 infection, as well as seronegative controls (n=19). Horizontal lines denote group medians. Kruskal-Wallis test with Dunn's post-test, *P<0.05, **P<0.01. SN=seronegative, SA=subacute, C=chronic. **B.** n=8 patients provided a sample in both subacute and chronic infection. Wilcoxon signed-rank test. **C.** Correlation of TGF-β_1 and PF4 concentrations in n=21 samples from individuals subacutely infected with HIV-1. Spearman's rank correlation coefficient, r=0.94, P<0.0001. **D.** Correlation of TGF-β_1 and PF4 concentrations in n=26 samples from individuals chronically infected with HIV-1. Spearman's rank correlation coefficient, r=0.94, P<0.0001. **E.** Correlation between TGF-β_1 and PF4 levels in n=56 samples from n=9 individuals acutely infected with HIV-1. Spearman's rank correlation coefficient (r=0.71, P<0.0001).

3.2.4 pDCs stimulated with HIV-1 do not produce TGF-β_1, activins A and B or BMP-2

To explore other potential sources of TGF-β_1 production during HIV-1 infection, and to gain insight into whether activins and BMP-2 may be produced by leukocytes in response to HIV-1 at tissue sites of viral infection despite not being detectably elevated in plasma, an *in vitro* assay was devised.

pDCs copiously produce type I IFNs upon stimulation with HIV-1, and given the early upregulation of these cytokines in the earliest stages of the cytokine storm in AHI[63], these cells likely represent the leukocyte subset to be stimulated earliest in infection *in vivo*[149]. However, whether production of TGF-β superfamily cytokines is also triggered by HIV-1 in pDCs has not previously been addressed. pDCs were therefore cultured with HIV-1 NL4-3; or with positive controls TLR7 agonist R837, TLR9 agonist ODN2216 or PR8 influenza virus (an ssRNA virus sensed by TLR7); all known to induce IFN-α from pDCs[480]. Supernatant levels of IFN-α, TGF-β_1, activins A and B, and BMP-2 were measured 24 hours later.

IFN-α was induced by HIV-1, as well as by influenza virus, R837 and ODN2216. However, pDCs stimulated with HIV-1 were not induced to produce TGF-β_1, activins A and B, or BMP-2. (Fig. 3.7).

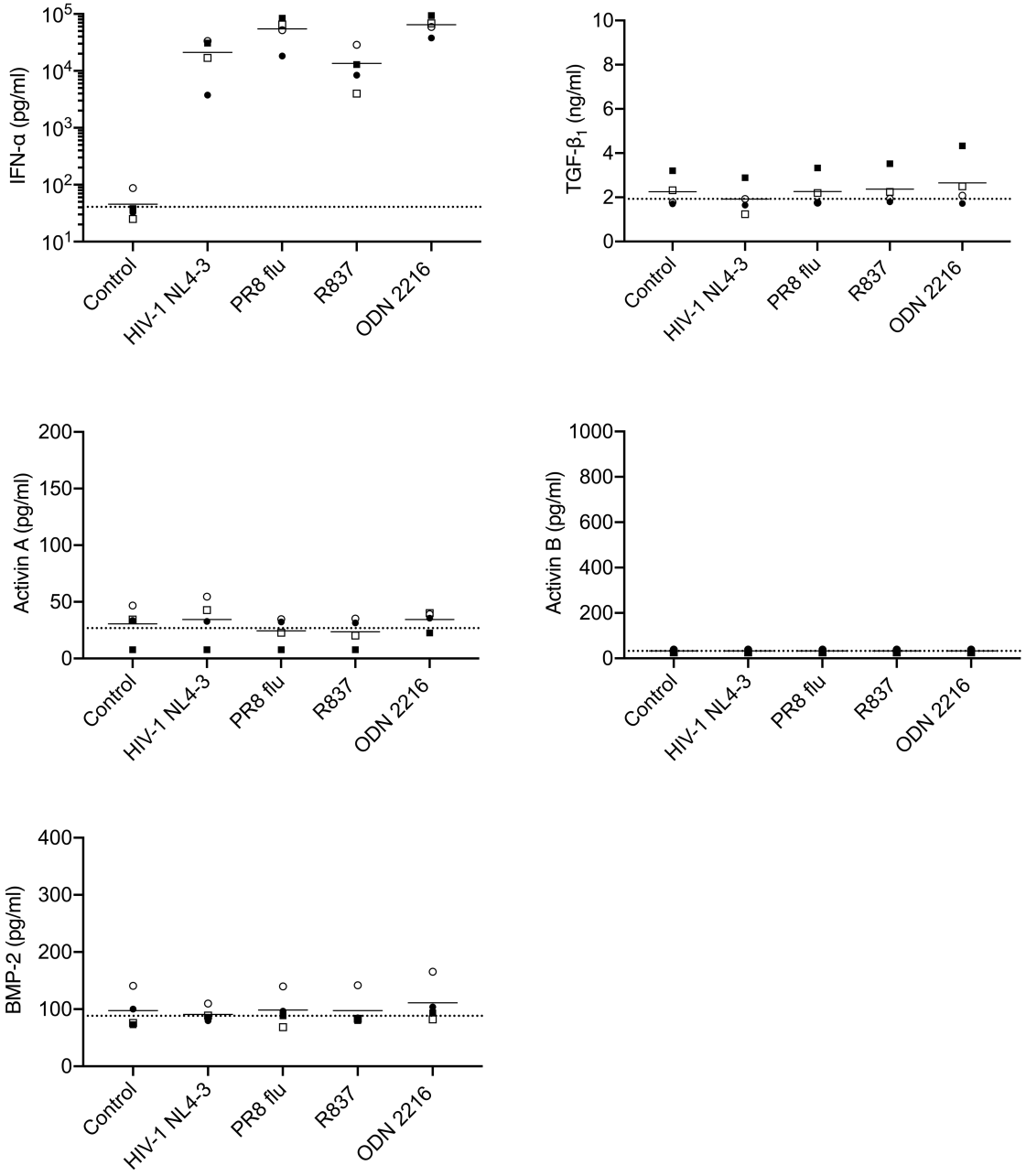


Figure 3.7 Analysis of TGF-β superfamily cytokines produced by pDCs cultured with HIV-1 *in vitro*
pDCs from n=4 HIV-seronegative donors were cultured with medium only as a negative control, or HIV-1 NL4-3 (50ng RT/ml), PR8 influenza virus (MOI 10), R837 (5μg/ml), or ODN 2216 (5μM) for 24 hours before measuring IFN-α, TGF-β_1, activins A and B, or BMP-2 in cell culture supernatants. Levels of each analyte were also measured in the serum-containing medium used for each experiment, an average of values from which is shown as a horizontal dotted line. Shapes represent each unique donor; solid lines represent group means.

3.2.5 MDDCs stimulated with HIV-1 do not produce TGF-β_1, activins A and B or BMP-2

mDCs both produce and respond to a large selection of TGF-β superfamily cytokines[248]. As the first choice due to ease of cultivation over primary cells, MDDCs were generated from HIV-seronegative donors and cultured with HIV-1 and the same TLR ligands as the PBMC experiment, with the exception of R837 and influenza virus, as conventional DCs do not express TLR7[472,473]. TLR ligands known to induce production of activin A from mDCs and MDDCs include TLR4 agonist LPS and TLR7/8 agonist R848[372,374], so these positive controls were included. Although primary human mDCs also do not express TLR9[472,473], MDDCs often do[481,482], so ODN2216 was also included as one of the positive control stimuli.

MDDCs stimulated with HIV-1 were not induced to produce TGF-β_1, activins A and B or BMP-2. R848 induced marked release of activin A, with a slightly smaller magnitude of activin A from LPS and ODN2216 (Fig. 3.8), as anticipated based on findings reported in the literature[372,374].

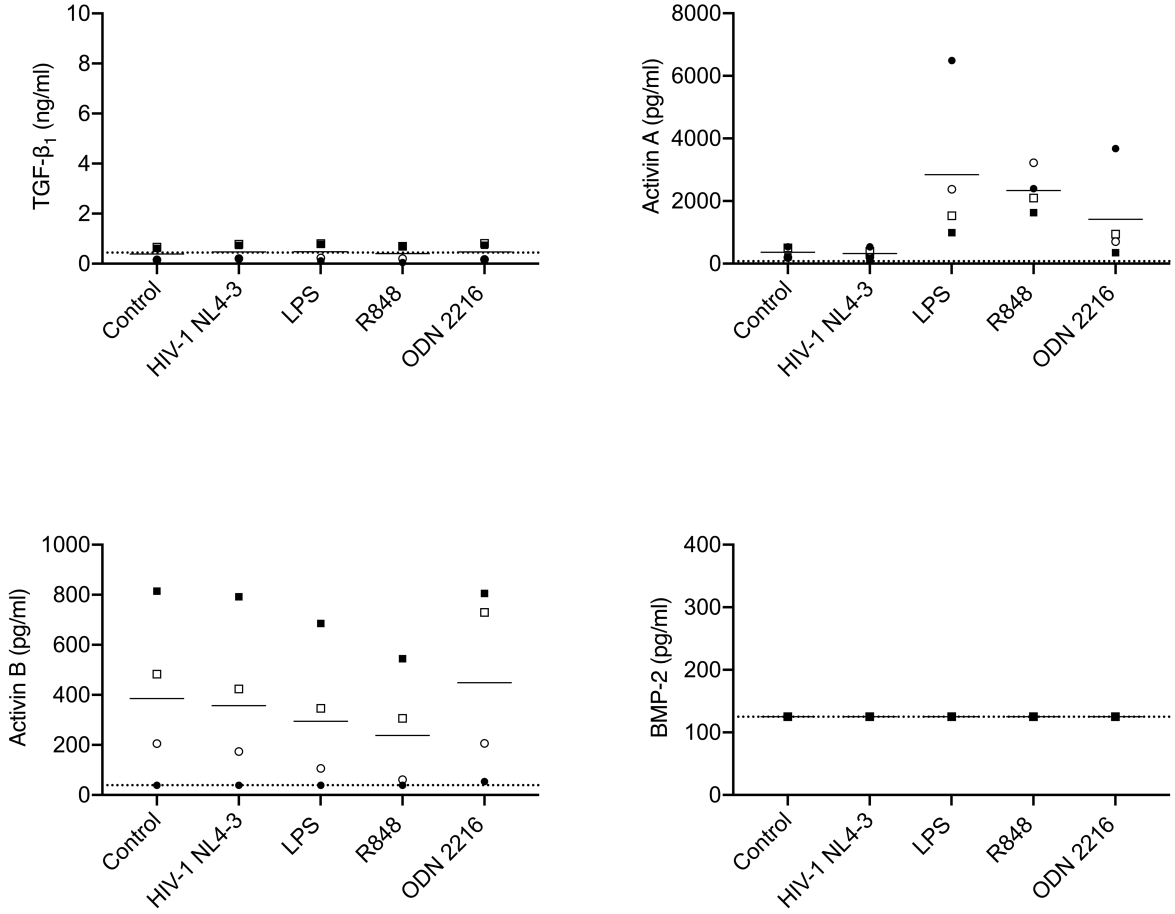


Figure 3.8 Analysis of TGF-β superfamily cytokines produced by MDDCs cultured with HIV-1 *in vitro*
MDDCs from n=4 HIV-seronegative donors were cultured with medium only as a negative control, or HIV-1 NL4-3 (50ng RT/ml), LPS (100ng/ml), R848 (10μg/ml), or ODN 2216 (5μM) for 24 hours before measuring TGF-β_1, activins A and B, or BMP-2 in cell culture supernatants. Levels of each analyte were also measured in the serum-containing medium used for each experiment, an average of values from which is shown as a horizontal dotted line. Shapes represent each unique donor; solid lines represent group means.

3.2.6 mDCs stimulated with HIV-1 do not produce TGF-β_1, activins A and B or BMP-2

To examine whether the findings in MDDCs are reflected in primary cells, mDCs were subjected to the same assay conditions, except ODN 2216 was excluded. HIV-1 did not induce TGF-β_1, activins A and B or BMP-2 release from mDCs, unlike the positive controls LPS and R848 that induced production of activin A (Fig. 3.9).

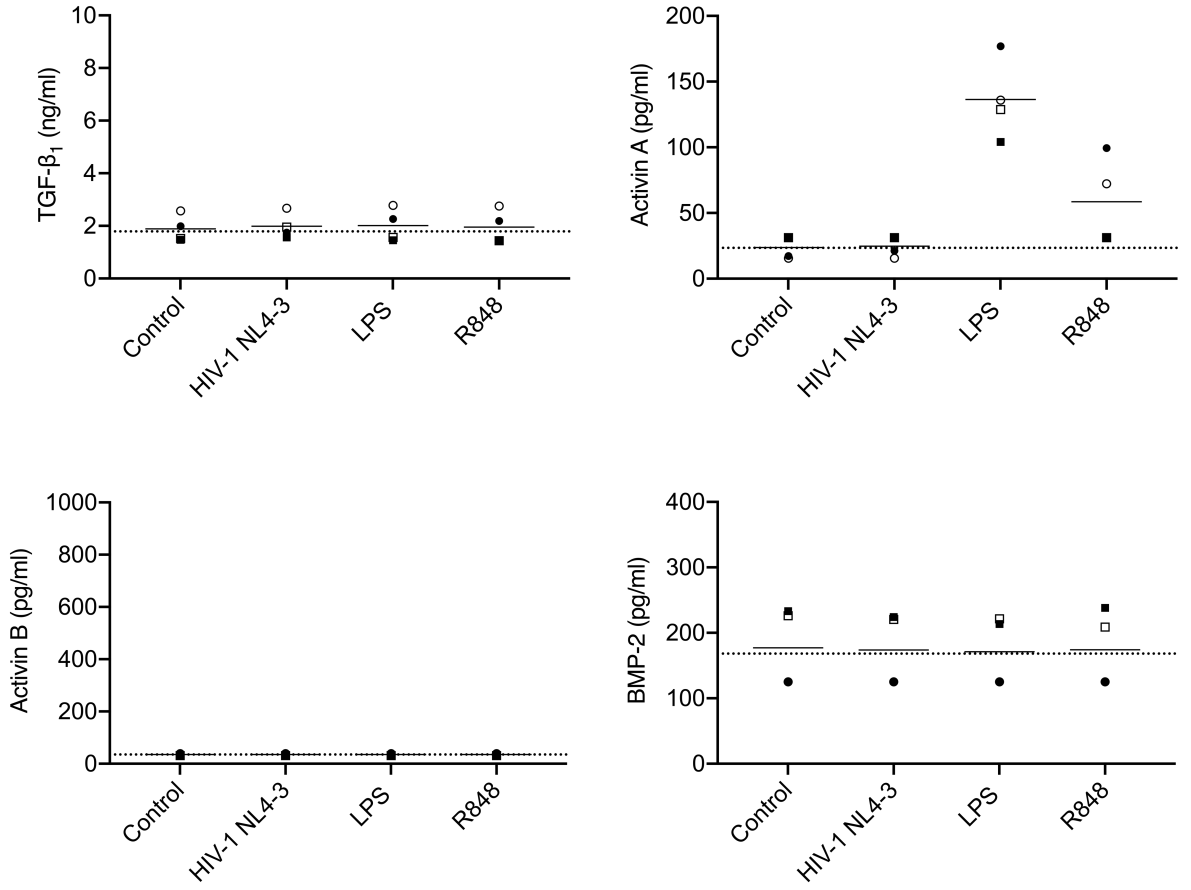


Figure 3.9 Analysis of TGF-β superfamily cytokines produced by mDCs cultured with HIV-1 *in vitro*
mDCs from n=4 HIV-seronegative donors were cultured with medium only as a negative control, or HIV-1 NL4-3 (50ng RT/ml), LPS (100ng/ml) or R848 (10µg/ml) for 24 hours before measuring TGF-β_1, activins A and B, or BMP-2 in cell culture supernatants. Levels of each analyte were also measured in the serum-containing medium used for each experiment, an average of values from which is shown as a horizontal dotted line. Shapes represent each unique donor; solid lines represent group means.

3.2.7 PBMCs stimulated with HIV-1 do not produce TGF-β_1, activins A and B or BMP-2

Whilst DC subsets do not produce TGF-β_1, activins A and B or BMP-2 upon direct stimulation with HIV-1, it was next considered whether diverse leukocyte subsets may stimulate one another to produce these cytokines after HIV-1 stimulation. Therefore, to gain insight into the potential for HIV-1 to elicit production of TGF-β superfamily cytokines via indirect as well as direct mechanisms, total PBMCs were subjected to the same *in vitro* assay, comprising both HIV-1 NL4-3 as well as all aforementioned TLR ligands.

Consistent with observations made in prior studies[483,484], stimulation of PBMCs with HIV-1, influenza virus and ODN2216, though surprisingly not R837, induced some production of IFN-α (likely from pDCs); and stimulation of PBMCs with LPS and R848 induced production of activin A (likely from mDCs) (Fig. 3.10).

PBMCs stimulated with HIV-1 were not induced to produce detectable levels of TGF-β_1, activin B or BMP-2, although there was a trend for low-level induction of activin A by HIV-1, as well as by other TLR7 and 9 agonists R837, influenza virus and ODN2216 (Fig. 3.10). This could be explained by stimulation of pDCs, with subsequent production of TNF leading to activation of mDCs, which produce copious activin A but lack TLRs 7 and 9.

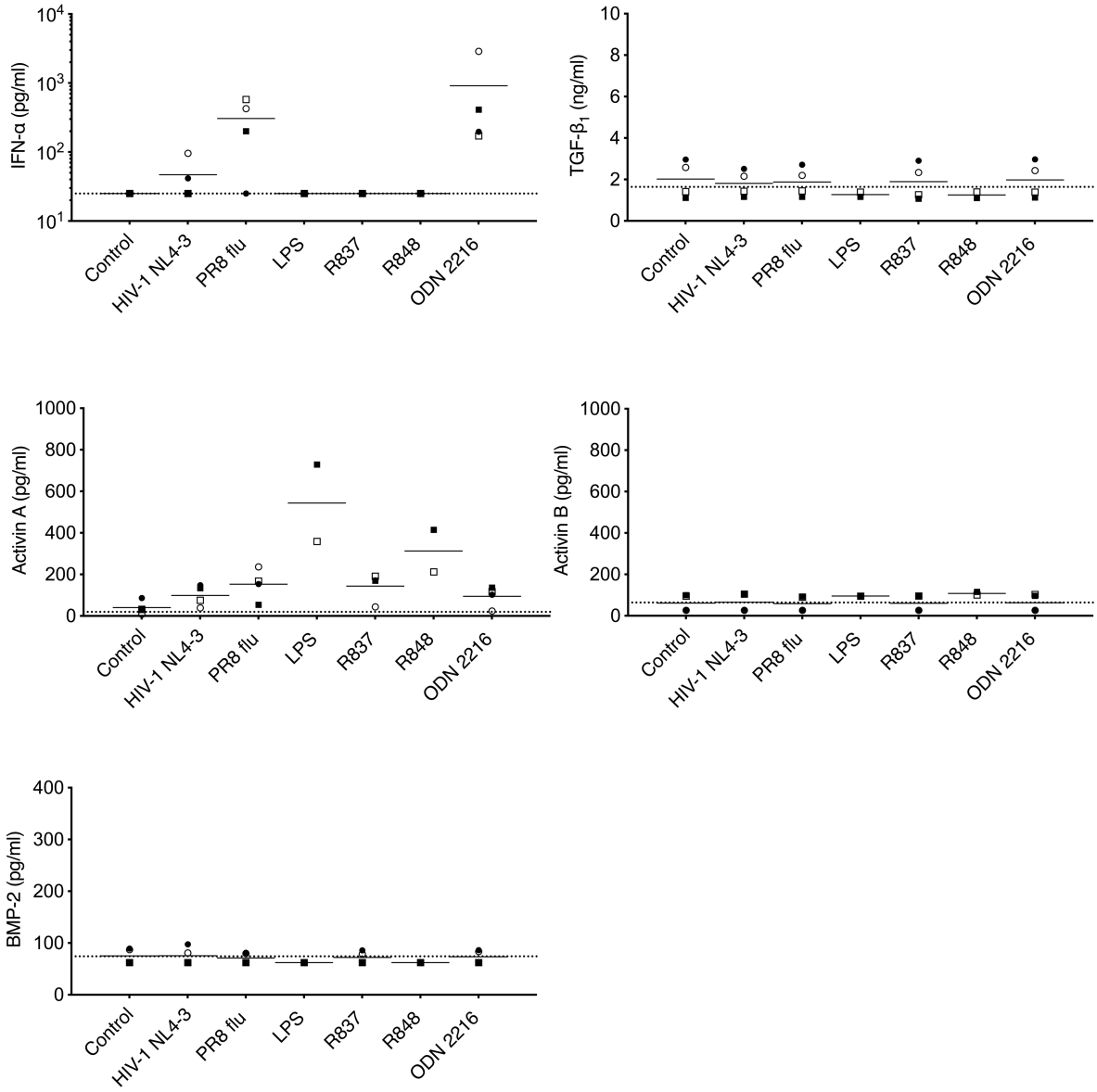


Figure 3.10 Analysis of TGF-β superfamily cytokines produced by PBMCs cultured with HIV-1 *in vitro*
PBMCs from HIV-seronegative donors were cultured with medium only as a negative control, or HIV-1 NL4-3 (50ng RT/ml), PR8 influenza virus (MOI 10), LPS (100ng/ml), R837 (5µg/ml), R848 (10µg/ml), or ODN 2216 (5µM) for 24 hours before measuring IFN-α, TGF-β_1, activins A and B, or BMP-2 in cell culture supernatants. Data are shown from n=4 donors (except LPS and R848, which were assessed in n=2 donors). Levels of each analyte were also measured in the serum-containing medium used for each experiment, an average of values from which is shown as a horizontal dotted line. Shapes represent each unique donor; solid lines represent group means.

3.3 Discussion

The work in this chapter addressed circulating concentrations of several TGF-β superfamily cytokines (TGF-β_1, activins A and B and BMP-2) at different stages of HIV-1 infection. AHI is associated with a cytokine storm from around 7 days after T_0[63], which mostly abates by subacute and chronic infection, although some analytes normalise at levels slightly above those present in HIV-seronegative individuals thereafter[475]. In contrast, results obtained here show that circulating TGF-β_1 concentrations increase modestly 1-4 days after T_0 and remain similarly elevated throughout AHI, whilst no substantial systemic perturbations occur in activins A and B and BMP-2. In line with the former observation, studies with SIV-infected RMs have detailed a rapid (one day post-infection) increase in circulating TGF-β_1 that persists throughout acute infection[238] and increased transcription of genes downstream of TGF-β signalling in as little time[184].

TGF-β_1 was found to be elevated at later stages of HIV-1 infection, in agreement with findings made in another study[339]. TGF-β_1 has also been analysed in the later stages of infection in patients receiving ART, where it has been found to be elevated[338,340–346]. In subacute and chronic HIV-1 infection, no correlation was found between TGF-β_1 and viral load, in agreement with other studies[338,342,343].

The contrast of systemic TGF-β kinetics between pathogenic immunodeficiency virus infections (where modest, rapid onset, persistent elevations occur) and non-pathogenic models (where rapid onset elevations of higher magnitude are initially triggered and are then down-modulated)[238] mirrors that seen with type I IFNs. Transcription of ISGs in blood and lymph node $CD4^+$ T cells is induced within 24 hours of infection with SIV in both pathogenic and non-pathogenic models, but in non-pathogenic models, this resolves before the chronic stage of infection[182,183,200]. This raises the possibility that similar to type I IFNs, TGF-β may

have predominant protective and pathogenic effects in early versus late infection respectively. Limitation of excessive immune activation in this fashion may be due to upregulation of immunomodulatory genes such as the gene encoding PD-L1[183]. Despite persistent ISG expression in pathogenic NHP models, plasma IFN-α peaks only ephemerally in AHI, and it is generally not detectable in the circulation in chronic infection[440,475,476]. Given the observations in this chapter of persistent systemic TGF-β_1 induction in both acute and chronic HIV-1 infection, it could be speculated that TGF-β_1 drives the expression of inflammatory gene signatures that are known to pervade chronic infection. In support of this, TGF-β induces *IFITM3* in glioma cells, and increases expression of ISGs in human papillomavirus (HPV)-infected keratinocytes by inciting autocrine release of cell-specific type I IFNs[486]. Furthermore, the induction of ISGs by BMPs, other members of the TGF-β superfamily, is documented[363,416]. Regarding TGF-β_1 activity, one limitation of the data in this chapter is the measurement of total TGF-β_1, comprising both latent and active forms, rather than solely active TGF-β_1. Measurement of the latter is considerably more difficult and relies on the development of bioassays to measure biological activity[487], something not done by most authors.

By contrast to TGF-β_1, plasma concentrations of other superfamily cytokines analysed did not change substantially during acute infection. During subacute and chronic infection, circulating levels of these cytokines were also not substantially different from those in HIV-seronegative controls. There was a trend for activin A to be increased in chronic compared to subacute infection, when considering paired samples from the same donors, and a trend for activin B to be increased in chronic infection compared to seronegative controls. On one hand, these trends fit with other infectious/inflammatory disease states in which activins A and/or B are systemically induced[391,463,465,466]. But on the other hand, it is surprising that in HIV-1 infection these trends are only mild, particularly for activin A, concentrations of which in chronic infection were not seen to exceed 250pg/ml. Other studies have noted an average circulating activin A

concentration three to four-fold greater than this in asthma[391], malignant mammary neoplasia[463], and chronic HCV infection[466], mostly with similar values for healthy controls to those in this chapter, allowing for a reasonably fair comparison between the absolute activin A concentrations between studies. Overall, despite minor trends, it is interesting that no statistically significant induction of the activins or BMP-2 should be seen, given the induction of so many other innate cytokines in AHI[63,177,441,475,476]. However, despite a lack of systemic induction of activins and BMPs in HIV-1 infection, the induction of their target genes due to low-level cytokine production in tissues is still a possibility, as is seen for IFN-α, which, as discussed, only briefly peaks in plasma in AHI but whose gene signatures persist throughout chronicity.

When measuring cytokine concentrations in plasma, care must be taken to minimise artefacts of sample processing or storage[488]. Long term plasma cryostorage affects cytokine measurements[489], as does freeze-thawing, though this is cytokine dependent[489–491]. Anticoagulants have variably reported effects on measured cytokine concentrations, depending on the cytokine and anticoagulant[489,490,492]. In this chapter, quality control experiments found no influence from freeze-thawing or anticoagulants. Published data also indicate no impact of age or sex on circulating TGF-β concentrations[493], though a C->T single nucleotide polymorphism in the *TGFB1* gene significantly impacts plasma TGF-β_1 concentration[494].

The marker of platelet activation and degranulation, PF4, was found to be elevated in subacute and chronic HIV-1 infection. Platelets mediate haemostasis, but also immunomodulate innate and adaptive immune responses through cell-to-cell contact with leukocytes and through release of pro- and anti-inflammatory cytokines found within alpha granules. Consequently, platelets are heavily involved in both immunity and immunopathology[495,496]. In HIV-1 infection,

platelets can bind the virus through expression of DC-SIGN and CLR-2. Platelet-bound HIV-1 remains infectious for several days, so platelets may have a role in dissemination and transmission of the virus to target cells[497]. Platelet alpha granule contents are known to have broadly virucidal properties[498], with PF4 both inhibiting and enhancing HIV-1 infection of target cells at low and high concentrations respectively[499]. Platelets possess TLRs including TLRs 1, 2, 4, 6, 7, 8 and 9[495,500] and are capable of sensing viral antigens, which initiates platelet activation and immunomodulatory activity[500,501].

In this chapter, the plasma PF4 concentration was found to be correlated with TGF-β_1 at all stages of infection, indicating that platelets may represent a key cellular source of TGF-β_1 in HIV-1 infection. Platelets are an abundant source of TGF-β_1 that is released upon activation and degranulation[493]. Platelets are also known to produce BMPs 2, 4 and 6[502], and release BMP-9 upon activation[503]. However, there is significant inter-donor variability in BMP production by platelets[504], and, given the lack of induction of BMP-2 in HIV-1 infection in plasma samples in this chapter, it is unlikely that HIV-1 induces significant production of this cytokine from these cells.

When measuring TGF-β_1, the possibility of *ex vivo* platelet degranulation and artefactual elevations in TGF-β_1 must always be considered, something not done in many TGF-β_1 studies. Sample processing can encompass a platelet depletion step; however, platelets degranulate with rough phlebotomy technique, physical sample agitation, incorrect sample storage or improper platelet depletion during processing[505]. In addition, most common anticoagulants have been found to cause platelet activation (sodium citrate[506], EDTA[506] and heparin[507]) although quality control experiments performed at the start of this study revealed no effect of anticoagulants on the TGF-β_1 concentrations measured in plasma.

To control for *ex vivo* platelet degranulation, at least three published methods exist. The first[508] involves measuring PF4 alongside another alpha-granule protein, beta thromboglobulin (β-TG). The authors of the method posit that both proteins are stored and released from platelets in a roughly 1:1 ratio. PF4 is rapidly cleared *in vivo*[509] in a biphasic pattern, whereby whole intact protein has a half-life of around two minutes through binding to endothelia[510], and C-terminal PF4 peptides have a half-life of around 40 minutes through uptake by hepatocytes[511]. In contrast, β-TG has a half-life of 100 minutes[508]. As such, owing to rapid PF4 clearance, the authors of this method assert that in true *in vivo* degranulation, the β-TG:PF4 ratio is around 3, whereas in samples that degranulate *ex vivo*, accumulation of PF4 reduces the ratio. Thus, this method can purportedly reject samples with excess *ex vivo* degranulation. This has erroneously led to some authors describing PF4 alone as a "marker" of *ex vivo* degranulation[512,513], despite the fact that a ratio between the two proteins must be measured[508]. Some have provided evidence that invalidates the primary assumption of this method however, demonstrating heterogeneity in the ratios of alpha-granule proteins released from activated platelets depending on the stimuli[514,515].

In a second published method[516], TGF-β and PF4 concentrations are measured in both serum and optimally handled plasma samples (in serum samples, effectively all platelets degranulate *ex vivo*). A factor is then calculated to account for and remove platelet-derived TGF-β from subsequent measurements in plasma. For proof of concept, the authors variably mishandled plasma samples from a single donor and accurately removed artefactual noise in the measured TGF-β concentrations using the factor. Similarly, in a third method[505], plasma TGF-β is simply expressed as a factor of β-TG. The obvious flaw of these two methods is that all platelet-derived TGF-β is discounted including that released *in vivo*, which may be a novel finding in the disease state studied.

Overall, measurement of TGF-β in plasma is complex and no perfect method of measurement exists. The samples used in this chapter are historic and it is unknown if platelet depletion steps were undertaken. Whilst it is the case that concentrations of PF4 in these samples (in the order of μg/ml) by far exceeds those normally recorded physiologically by most studies (in the order of ng/ml), likely indicating at least some *ex vivo* degranulation, such artefacts would be expected to affect both seronegative and patient groups stochastically. It is therefore highly unlikely that the findings reported are solely a consequence of *ex vivo* degranulation. Furthermore, systemically elevated TGF-β_1 has been documented in HIV-1 patients in at least one other study using a stringent platelet depletion protocol[338]. Finally, platelet activation in HIV-1 infection is documented in other studies[517–520], including in ART-naïve individuals[521] (some ART drugs are associated with increased platelet activation[522,523]), as well as in other viral infections[524–526]. An animal study using SIV infection of RMs has shown increased platelet activation 10 days post-inoculation[527], and in AHI, circulating levels of fibrinogen alpha chain increase before T_0[176]. Fibrinogen is released from activated platelets in alpha granules[528].

There are several possible mechanistic explanations by which HIV-1 infection may stimulate platelet activation and degranulation. A direct mechanism is the stimulation of platelets by HIV-1 Tat[529], which causes a profound increase in circulating PF4 in mice injected with the protein in recombinant form[530,531]. Murine platelets are capable of sensing HIV-1 through TLR7, resulting in their activation and degranulation[532]. Other viruses are sensed through platelets in a similar manner, including picornaviruses through TLR7[500] and Dengue virus through TLR4[526].

Indirect mechanisms for elicitation of platelet activation could include via stimulation by pro-inflammatory cytokines such as TNF, which is abundantly produced in AHI[63,533] and activates platelets[534]. Systemic TNF levels also correlate with platelet activation in HIV-1 infection[519]. As already mentioned, platelets possess TLR4, which could theoretically be bound by circulating

LPS present in HIV-1 infection, leading to indirect activation. However, some studies have contested the ability of LPS to classically activate platelets[535], where resultant secretion of TGF-β is not reliably always seen[536]. Finally, platelet-activating factor, whose biologically active derivatives are increased by the state of HIV-1 infection[537] could also underlie activation of these cells.

To identify other possible cellular sources of TGF-β_1 in HIV-1 infection, DC subtypes and PBMCs from HIV-seronegative donors were stimulated with HIV-1 or a range of TLR ligands *in vitro*. Although TGF-β_1 is produced in particular by Treg cells[127], DCs produce a myriad of cytokines in HIV-1 infection[162] and are known to be capable of producing TGF-β_1[248], although generally the maturation process has been observed to either not influence DC TGF-β_1 production[538] or to decrease it[539,540]. pDCs sense HIV-1 after viral endocytosis through TLR7 ligation[151], and pDC-derived pro-inflammatory cytokines then stimulate and activate mDCs which, in lacking TLR7 and 9, are not directly activated by HIV-1[162]. Although activins A and B and BMP-2 were not found to be systemically elevated during HIV-1 infection it was considered that if production was of a low magnitude, or focal to areas of viral replication (e.g. at the genital mucosa in early infection), analysing plasma may not reveal *in vivo* cytokine induction. Therefore, these cytokines were also measured, as well as IFN-α as a positive control known to be induced from pDCs by HIV-1.

IFN-α was induced from pDCs and PBMCs by HIV-1 and other TLR7 and 9 ligands, as observed in prior studies[151,483] (although one limitation of these findings was the lack of a non-CpG-containing ODN2216 control). However, although HIV-1 is capable of activating cytokine release from pDCs, it did not induce production of detectable levels of TGF-β_1 from pDCs or total PBMCs (or from MDDCs or primary mDCs) in a 24-hour culture. This could indicate that leukocytes do not substantially contribute to the earliest TGF-β_1 induction in AHI (days 1-4

post T_0). However, it is possible that following rapid *in vivo* triggering of platelet activation after HIV-1 infection and initial TGF-β_1 release, pDCs are stimulated to contribute to TGF-β_1 production (given that TGF-β-stimulated pDCs are documented to further produce more TGF-β[541]) and also that regulatory T cell activation occurs, providing an additional cellular source of TGF-β_1 production. In SIV infection of AGMs, in which plasma concentrations of TGF-β are significantly elevated within 24 hours post-infection, the induction of $CD4^+$ and $CD8^+$ regulatory cells is one highly implicated source, given the correlation of the frequency of $CD4^+CD25^+$ and $CD8^+CD25^+$ T cells with plasma TGF-β[238] (though the former was not quite statistically significant in that study). Although increased expression of CD25, a T cell activation marker, could reflect overall increased activation of all $CD4^+$ and $CD8^+$ T cell subsets, *FOXP3* gene expression was also noted to be increased in PBMCs[238], raising the possibility that the major source of systemic TGF-β in the earliest stages of SIV and HIV-1 infections could be regulatory T cells. Other work has shown induction of $CD8^+$ T cells in HIV-1 infection that produce large amounts of TGF-β when cultured with HIV-1 antigens *in vitro*[352], though it is unknown whether these cells are induced as rapidly as 1-4 days post T_0 *in vivo*.

A further source of TGF-β_1 *in vivo* could include monocytes, which in one *in vitro* study, have been observed to produce TGF-β_1 in response to stimulation with HIV-1 Tat, which could be at least in part via the induction of IL-6[461]. In AHI, IL-6 has been seen to initially increase from around day 8 after the first detection of viraemia[63], so this mechanism would likely contribute to the later, sustained systemic induction of TGF-β_1 rather than the earliest elevations. In the aforementioned *in vitro* study[461], substantial TGF-β_1 induction followed that of IL-6 and took at least 48-72 hours, possibly explaining why induction of TGF-β_1 from PBMCs in response to stimulation with HIV-1 was not seen in this chapter. Similarly, studies have documented TGF-β production from PBMCs[458] and B cells[353] stimulated *in vitro* with HIV-1 glycoproteins, but 48-hour timepoints were analysed, again possibly explaining a lack of induction from HIV-1-

stimulated PBMCs in this chapter. Furthermore, studies working with purified leukocyte subtypes (e.g. B cells[353] or monocytes[461]) may be more sensitive at detecting cytokine induction due to the potentially greater concentration of cells than in PBMC cultures. Further work on data covered in this chapter should cover a greater range of timepoints, in case subtle differences are noted earlier or later than 24 hours.

Significant levels of activin A production were not induced by HIV-1 from DC subsets or PBMCs. However, the virus, as well as other TLR7 and 9 ligands showed a subtle trend towards inducing activin A in PBMC cultures. Given the most probable source of activin A is mDCs, but mDCs lack TLR7 and 9, this could reflect HIV-1 stimulation of pDCs with subsequent bystander mDC activation. Upon HIV-1 stimulation of pDCs, the principal pDC-derived cytokine responsible for mDC activation is TNF[167]. In one study analysing a range of maturation stimuli for mDCs, TNF was found to induce the least amount of activin A production (approximately four-fold less than LPS)[372]. This may explain the trend for mild upregulation of activin A by HIV-1 in PBMCs *in vitro*. It may also explain why no induction of activin A was seen in AHI *in vivo*, with only a subtle, non-statistically significant trend for induction in chronic infection in paired donor data, especially given that the *in vitro* study in question treated DCs with a 1000-fold greater concentration of TNF than that seen in plasma in AHI[63,533] and still found TNF to be the relative weakest activin A-inducing stimulus[372].

The lack of activin A induction by HIV-1 or other TLR7 or 9 ligands in monocultures of MDDCs, mDCs or pDCs provides further evidence for a two-cell mechanism of induction in PBMCs and also underlying the subtle, non-statistically significant upregulation seen *in vivo*. Although, exceptions to this could include mDC-intrinsic activin A release stimulated by circulating LPS from bacterial translocation in chronic infection[91]; or mDC maturation by IL-18[542], which was analysed as a positive control in this chapter and found to be upregulated in chronic infection.

Non-DC leukocytes known to produce activin A in an inflammatory context could also be the source of the subtle non-statistically significantly elevated activin A in chronic infection and/or the small amount produced *in vitro* PBMC cultures, such as Th2 cells[389], macrophages[378] or neutrophils[368,369].

Activin B and BMP-2 were not induced by HIV-1 in pDCs, MDDCs, mDCs or PBMCs. Although limited published data exist on activin B, LPS has been shown to stimulate production of both activins A and B from macrophages[379], making the lack of observation of release of activin B from LPS-stimulated MDDCs and mDCs in this study somewhat unexpected. On one hand, these negative results may help to explain the lack of statistically significant systemic upregulation of these cytokines in HIV-1 infection *in vivo*. On the other hand, the subtle trend towards an increase in circulating levels of activin B in chronic infection may reflect LPS-stimulated release of activin B from macrophages.

In summary, results presented in this chapter demonstrate that a very rapid modest systemic upregulation of TGF-β_1 occurs in AHI, and TGF-β_1 then remains elevated throughout subacute and chronic infection. By contrast, levels of other TGF-β superfamily cytokines were not substantially perturbed at any stage of infection, although activins A and B trended towards being induced in chronic infection. Platelet degranulation was significantly correlated with elevated TGF-β_1 and platelets likely represent a major cellular source of circulating TGF-β_1 *in vivo*, although other cell types may also contribute to its production. Further work is needed to understand the potential protective or pathogenic nature of TGF-β_1 in HIV-1 infection. As there are clear differences in TGF-β kinetics between non-pathogenic and pathogenic animal models, the latter of which are corroborated by data in this chapter in HIV-1 infection, there could be potential to harness TGF-β_1 as part of prophylactic or therapeutic strategies. For example, if TGF-β_1 is contributing to expression of inflammatory/ISG signatures in chronic

infection, blocking induction of this cytokine could be considered to decrease excessive immune activation and associated pathology. Given the precedent set by others demonstrating the effects of TGF-β superfamily cytokines against other viruses *in vitro,* work in the next chapter of this thesis focused on addressing whether these cytokines have the ability to restrict HIV-1 replication.

Chapter 4

The effects of TGF-β superfamily cytokines on HIV-1 replication *in vitro*

4.1 Introduction

In recent years, there has been a growing appreciation of the roles activins and BMPs play in immunity[248,360,361] and in particular, antiviral immunity (reviewed in Chapter 1). However, there are no published data on the impact of these cytokines on HIV-1 replication. Notably, BMPs and activins are documented to inhibit the replication of HCV and HBV in hepatoma cell lines[363,413] and Zika virus in epithelial cells[363] through type I IFN-dependent and type I IFN-independent mechanisms. Work in Chapter 3 of this thesis demonstrated early, modest TGF-β_1 induction in AHI that is sustained throughout infection, but no significant systemic upregulation of activins or BMPs at any stage of HIV-1 infection. This provides an opportunity to exploit these cytokines therapeutically, should they have any beneficial effect against the virus.

There is no clear consensus on the effects of TGF-β on HIV-1 replication *in vitro*, with variation being observed between cell types and even within a certain cell type by conflicting studies. In non-mitogen-stimulated PBMCs, one study reported inhibition of HIV-1 replication by TGF-β[543], whilst another reported enhancement of HIV-1 replication at low TGF-β concentrations but inhibition at higher concentrations in phytohaemagglutinin (PHA)-activated PBMCs[544], indicating cell activation status may also play a role. Other studies showed no effect of TGF-β on HIV-1 replication in a T cell line[545] or primary T cells[546,547].

In macrophages, there are at least four studies showing TGF-β-mediated enhancement of HIV-1 replication[546,548–550]; one study documenting both enhancement and inhibition of

replication, depending on the timing of the cytokine application relative to infection[551]; and at least two studies showing inhibition[545,552]. In LCs, recent work has identified a post-entry block to replication induced by TGF-β, which is dependent on SMAD2 signalling[553] and independent of sterile alpha motif and histidine-aspartic domains protein 1 (SAMHD1), an HIV-1 restriction factor[554].

A number of studies have also explored the effects of TGF-β on the replication of other viruses. Overall, TGF-β appears to enhance the replication of respiratory viruses that infect epithelial cells. These include respiratory syncytial virus[555], rhinovirus[556,557], and influenza A[558]. In most of these studies, TGF-β diminishment of endogenous and virus-induced type I IFN production was responsible.

Contrastingly, TGF-β has been shown to inhibit HBV replication in hepatoma cell lines[559] due to induction of activation-induced cytidine deaminase (a member of the APOBEC family)[560] but possibly also through regulation of microRNA expression[561]. TGF-β also inhibits replication of a HCV replicon in hepatoma cell lines[562]. Interestingly in the studies performed with hepatotropic viruses, there was no evidence to suggest the antiviral activity of TGF-β is mediated via induction of antiviral ISGs or enhancement of the type I IFN response, as was seen with the activins and BMPs in hepatocytes[363]. And in fact, one of these studies ruled out TGF-β-driven stimulation of transcription from sequences found in the promoters of ISGs in a hepatoma cell line[562]. TGF-β was recently also reported to inhibit HPV replication through induction of IFN-κ, a type I IFN subtype that is selectively expressed in keratinocytes[486].

In summary, data from a breadth of studies performed with different viruses illustrate the potential for TGF-β, BMPs and activins to inhibit or potentially enhance virus replication via multiple different mechanisms, including modulation of host cell production of and/or response

to type I IFNs, IFN-independent upregulation of ISGs or other antiviral factors, and other effects on host cells. The effects observed may be contingent on the virus, host cell type, whether cells are activated, and cytokine concentration. Importantly, the effects of TGF-β superfamily cytokines on HIV-1 replication are very poorly understood, with a lack of consensus as to the effects of TGF-β on HIV-1 replication in primary $CD4^+$ T cells and macrophages, and no prior data on the impact of activins and BMPs on HIV-1 replication or the ability of TGF-β superfamily cytokines to modulate the antiviral type I IFN response.

In this chapter I aimed to explore:

- The effects of TGF-β superfamily cytokines on HIV-1 replication *in vitro* in primary $CD4^+$ T cells, macrophages, and other cell types.
- How virus strain impacts on these effects (lab-adapted vs patient viruses, strains from early vs later infection, X4-tropic vs R5-tropic viruses).
- Whether TGF-β superfamily cytokines influence type I IFN-mediated inhibition of HIV-1 replication.
- Whether the activation status of $CD4^+$ T cells influences the effects of TGF-β superfamily cytokines on HIV-1 replication in these cells.

4.2 Results

4.2.1 SMAD signalling in macrophages and CD4+ T cells

Based on the aforementioned precedent of other studies showing TGF-β, activins and BMPs to modulate the replication of other viruses, cytokines from these families were assessed for their effects on HIV-1 replication *in vitro*. Cytokines analysed in HIV-1 infection in Chapter 3 were initially selected, that is, TGF-β_1, activin A and BMP-2, therefore representing one member of the TGF-β superfamily seen to be systemically induced in HIV-1 infection *in vivo* and two that are not. Experiments were carried out in macrophages and primary CD4+ T cells, the main sites of *in vivo* HIV-1 infection. However, it was first confirmed that these cell types respond to these cytokines.

Given the variable expression levels of TGFBRs and BMPRs in CD4+ T cells depending on cell activation status[399,563] as well as a relative paucity of commercially available reagents to assess these receptors, downstream SMAD signalling was instead assessed as a means of measuring cellular responsiveness to these cytokines. MDMs and activated CD4+ T cells were treated with TGF-β superfamily ligands before analysing subsequent pSMAD expression by western blot.

MDMs were found to be responsive to TGF-β_1 and activin A as evidenced by the presence of a strong pSMAD2/3 band in cells harvested two hours after cytokine addition, indicative of SMAD signalling. Specificity of the effect being mediated through type I receptors bound by TGF-β_1 and activin A (ALKS 4, 5 and 7) was demonstrated by blocking these receptors with the small molecular inhibitor SB431542[564], which ablated the pSMAD2/3 bands (Fig. 4.1A).

Responsiveness to BMP-2 was provided by evidence of pSMAD1/5/8 signalling in MDMs incubated for 2 hours with this cytokine (Fig. 4.1B), and similarly to above, diminishment of this

signalling using the small molecular inhibitor LDN193189, which blocks BMP receptors ALKs 2, 3 and 6[565].

When a similar approach was employed to assess cytokine signalling in activated $CD4^+$ T cells (here reading out responses to TGF-β_1 and activin A two hours after cytokine addition, but culturing cells with BMPs for a longer period of 10 hours prior to analysis, based on findings from a prior study[404]), responsiveness to TGF-β_1 (Fig. 4.2A) and activin A (Fig. 4.2B), including diminishment of the response in the presence of SB431542, was observed. Similarly, responsiveness to BMP-2 was also observed (Fig. 4.2C).

Published data indicate that demonstrating BMP signalling may be challenging in activated cells and/or serum-containing media owing to high levels of endogenous BMPs[404], so for BMP-6, signalling was assessed in resting $CD4^+$ T cells cultured in serum-free medium (Fig. 4.2D): here too, signalling was observed in cells harvested 10 hours after cytokine addition, which was diminished in the presence of LDN193189. Activated $CD4^+$ T cells were also analysed for pSMAD2/3 signalling in response to TGF-β_1 by flow cytometry (Fig. 4.2E). A substantial increase in the median fluorescence intensity (MFI) of pSMAD2/3 staining was observed five minutes after cytokine addition, providing additional evidence of cytokine responsiveness.

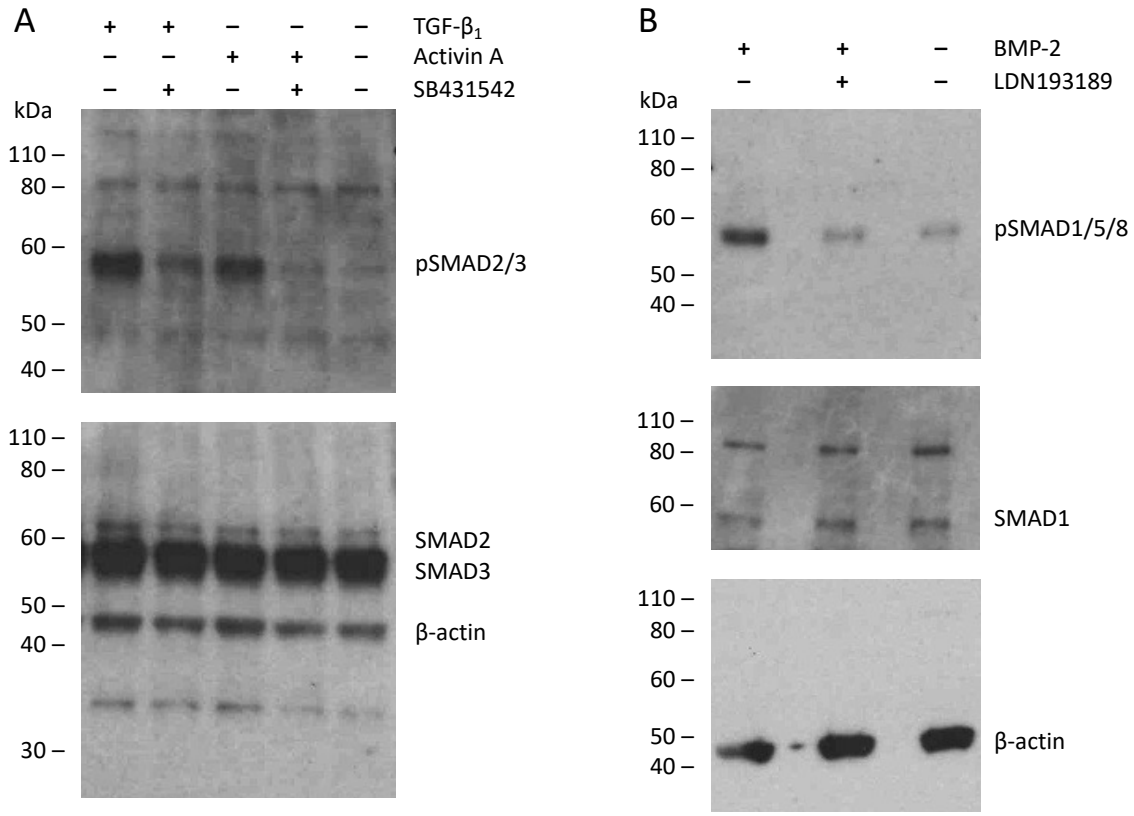


Figure 4.1 SMAD signalling in macrophages in response to TGF-β superfamily ligands
MDMs from HIV-seronegative donors were treated with TGF-β superfamily cytokines for two hours before western blot for SMAD signalling. The small molecule inhibitors SB431542 (10μM) (blocks ALKs 4, 5 and 7) and LDN193189 (100nM) (blocks ALKs 2, 3 and 6) were added to the cells one hour prior to cytokine treatment. **A.** TGF-β_1 (50ng/ml) and activin A (5nM) signalling. Results shown are representative of those obtained in experiments using MDMs from n=3 donors. **B.** BMP-2 (25nM) signalling. Representative results obtained with MDMs from one of n=4 donors tested are shown.

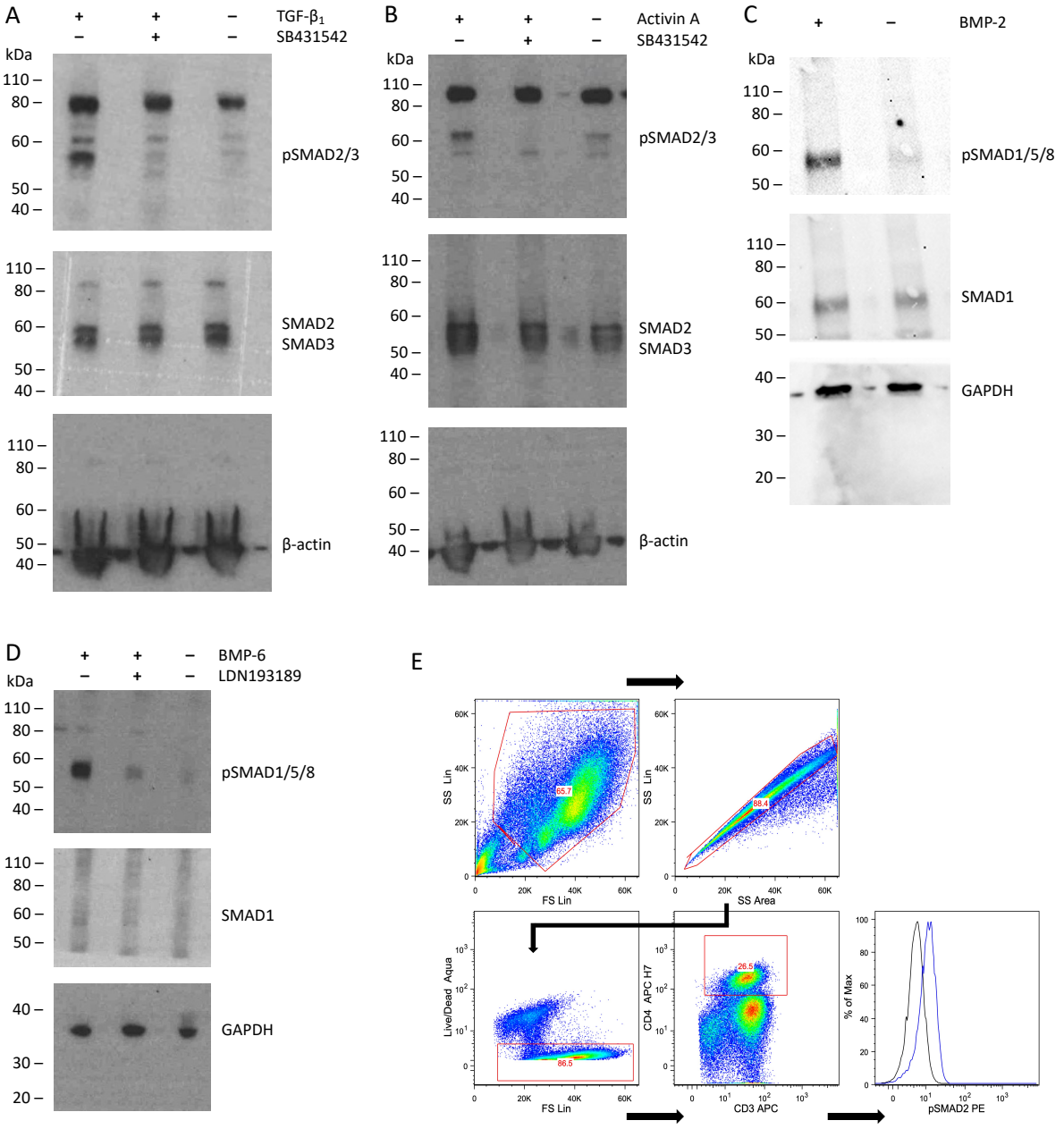


Figure 4.2 SMAD signalling in CD4⁺ T cells in response to TGF-β superfamily ligands
CD4⁺ T cells from two HIV-seronegative donors were combined to decrease inter-donor variability (a "donor pair"), activated for 48 hours in serum-containing medium with 50ng/ml anti-CD3, 100ng/ml anti-CD28 and 50IU/ml IL-2 and treated with TGF-β superfamily cytokines for 2 or 10 hours before western blot for SMAD signalling. SB431542 (10μM) and LDN193189 (100nM) were added to some samples for one hour prior to cytokines. **A.** TGF-β_1 (50ng/ml) signalling after two hours. Data from one donor pair representative of n=3 tested. **B.** Activin A (5nM) signalling after two hours. Data from one donor pair representative of n=3 tested. **C.** BMP-2 (25nM) signalling after 10 hours. Data from one donor pair representative of n=2 tested. **D.** Resting CD4⁺ T cells from single HIV-seronegative donors were treated with BMP-6 (25nM) for 10 hours in serum-free medium before western blot. Data from one donor representative of n=2 tested. **E.** TGF-β_1 signalling was verified by flow cytometry using "flow cytometry panel 1" (Chapter 2). PBMCs from single HIV-seronegative donors were activated as above and treated with TGF-β_1 (50ng/ml) for five minutes before staining. pSMAD2/3 signalling in CD4⁺ T cells in one representative of n=2 donors is shown. A wide initial gate on linear forward scatter (FS) and side scatter (SS) was used to allow for the heterogeneity of lymphocyte size during activation, followed by sequential gating on single, live, CD4⁺ T cells. Black=cells to which no TGF-β_1 was added, blue=TGF-β_1-treated cells.

4.2.2 Lack of effect of TGF-β superfamily cytokines on HIV-1 replication in macrophages

To assess the effects of TGF-β superfamily members on HIV-1 replication in macrophages, MDMs from HIV-seronegative donors were treated with TGF-β superfamily cytokines for 24 hours before infecting with HIV-1 NL4-3 BaL, an R5-tropic strain. Cytokines remained present throughout the infection time course. Cytokine concentrations were selected roughly based on published work with the same cytokines, at which effects on viral replication had been maximally or peri-maximally observed. These were 50ng/ml TGF-β_1 (10ng/ml TGF-β_1 has been observed to significantly enhance HIV-1 replication macrophages[550] and inhibit it in PBMCs[544]), 25nM BMP-2 (Between 18 and 52nM BMP-6 has been seen to maximally inhibit HCV *in vitro*[363]) and 5nM activin A (4nM activin A being shown to exert maximal restrictive activity against HCV[363]).

HIV-1 p24 was analysed in supernatants at serial timepoints post-infection as a measure of viral growth, after prior $CD4^+$ T cell experiments by others in the lab using flow cytometric analysis of intracellular p24 revealed that at this MOI, only a small percentage of cells (around 2-3%) became detectably infected by days three and five post-infection (data not shown), making this an insensitive readout for detecting cytokine-induced changes in the extent of viral replication.

IFN-α_2 (herein referred to as IFN-α) was used as a control inhibitor of viral replication, and ablated viral growth in macrophages when added at a high concentration (1000IU/ml) (Fig. 4.3A), consistent with previously published data[566]. In contrast, TGF-β_1, activin A, BMP-2, or the small molecule inhibitor of BMP signalling LDN193189 (tested to address any effects of endogenous BMP production by macrophages on HIV-1 replication in these cells) all had no significant effect on HIV-1 replication in these cells (Fig. 4.3B) (macrophages are documented to constitutively produce BMP-2[567,568]). To assess whether TGF-β superfamily cytokines

enhanced IFN-α-mediated inhibition (despite having no effect alone), a suboptimal concentration of IFN-α was used (10IU/ml) concurrently with activin A. No additional inhibition was observed (Fig. 4.3C).

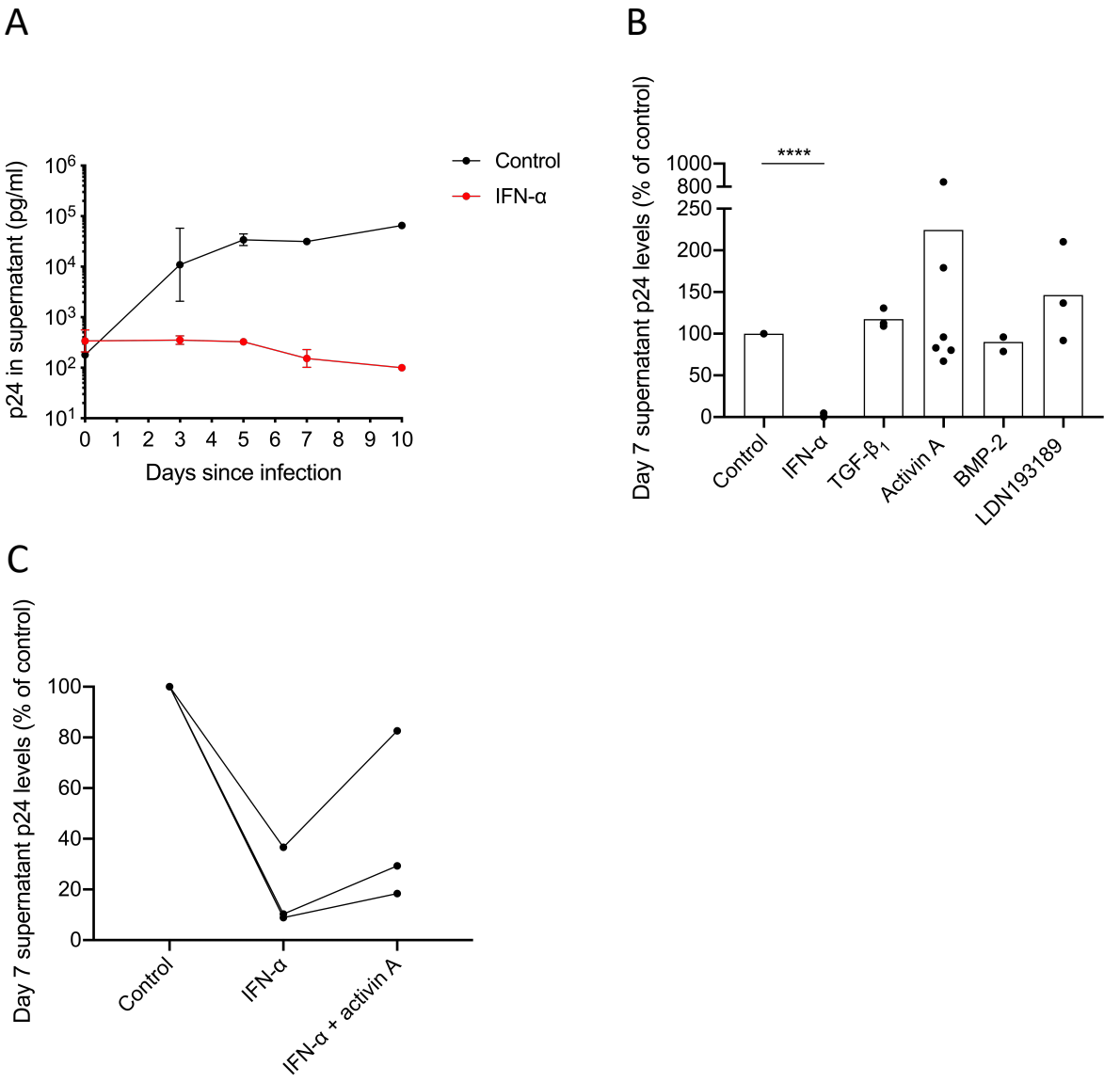


Figure 4.3 Analysis of the effects of TGF-β superfamily cytokines on HIV-1 replication in macrophages
MDMs from HIV-seronegative donors were treated with TGF-β superfamily cytokines for 24 hours before (and continuously after) infection with HIV-1 NL4-3 BaL, and viral replication was assessed by analysis of supernatant p24 levels over time. IFN-α (1000IU/ml) was used as a positive control for viral inhibition. **A.** Viral growth curve and the effect of IFN-α addition: data from MDMs from one representative donor of n=6. Error bars represent geometric standard deviation (SD) between triplicate wells. **B.** Summarised data showing the effects of IFN-α, TGF-β_1 (50ng/ml), activin A (5nM), BMP-2 (25nM) or LDN193189 (100nM) on viral replication in MDMs from n=6 (IFN-α and activin A) and n=3 (all others) donors (supernatant p24 levels at day seven as a percentage of untreated control). Bars represent the group mean. Mixed-effects analysis with Dunnett's post-test comparing to control, ****P<0.0001. **C.** Summarised data showing the effects of IFN-α (10IU/ml) alone or in combination with activin A (5nM) on viral replication in MDMs from n=3 donors (supernatant p24 levels at day seven post-infection as a percentage of untreated control).

4.2.3 Lack of effect of many TGF-β superfamily cytokines on HIV-1 replication in activated CD8-depleted PBMCs

The effects of selected TGF-β superfamily ligands were next assessed on HIV-1 replication in activated $CD4^+$ T cells, the primary target of the virus *in vivo*[75]. Although analysis of HIV-1 replication in purified $CD4^+$ T cells is feasible, isolated $CD4^+$ T cells often survive poorly *in vitro* after infection with HIV-1, making analysis of virus replication over time difficult. The majority of experiments assessing virus replication thus employed activated PBMCs (depleted of $CD8^+$ T cells to prevent non-specific $CD8^+$ T cell-mediated inhibition of HIV-1 replication), and prior work in the laboratory had shown that activated $CD4^+$ T cells are the predominant cell type in these cultures.

CD8-depleted PBMCs pooled from three HIV-seronegative donors (to minimise inter-assay variation) were activated for 72 hours and infected with HIV-1 stocks generated from IMCs corresponding to primary TF or 6M consensus virus sequences (see "standard HIV-1 replication assay" in Chapter 2). As in experiments with macrophages, cells were treated with TGF-β superfamily cytokines 24 hours prior to infection.

First, the effects of activin A on HIV-1 replication were assessed, with a representative example of results obtained in one pooled "trio" of cells from three HIV-seronegative donors shown in Fig. 4.4A. In experiments performed with the CH058 6M virus (an IFN-α-sensitive virus representative of those replicating in chronically infected individuals) in several donor trios, activin A was found to have no substantial effect on HIV-1 replication (Fig. 4.4B). Similar observations were made in additional experiments using 6M consensus sequence viruses from several other patients (Fig. 4.4C). Activin A also did not enhance the inhibitory activity of IFN-α when the two cytokines were used concurrently (Fig. 4.4A).

The effects of BMP-2 on HIV-1 replication were also assessed: data from one representative donor trio infected with the CH58 6M virus is shown in Fig. 4.4D. Overall, in several donor trios, BMP-2 had no substantial effect on viral replication (Fig. 4.4E) and did not enhance the inhibitory activity of IFN-α when the two cytokines were used concurrently (Fig. 4.4D). Likewise, no inhibition of HIV-1 replication was seen in experiments performed with activin B, BMP-6, inhibin A or GDF-15, assessed to cover a wider breadth of members of the TGF-β superfamily, and none of these cytokines enhanced IFN-α-mediated HIV-1 inhibition (Fig. 4.4F-I).

Next, whether activin A or BMP-2 potentiate the anti-HIV-1 activity of type I IFNs was addressed. CD8-depleted PBMCs were treated with activin A 48 hours pre-infection and IFN-α 24 hours pre-infection, or vice versa (Fig. 4.5A). In both scenarios, activin A did not boost IFN-α inhibition of HIV-1 replication (Fig. 4.5B, C). The same result was seen with BMP-2 (Fig. 4.5D, E).

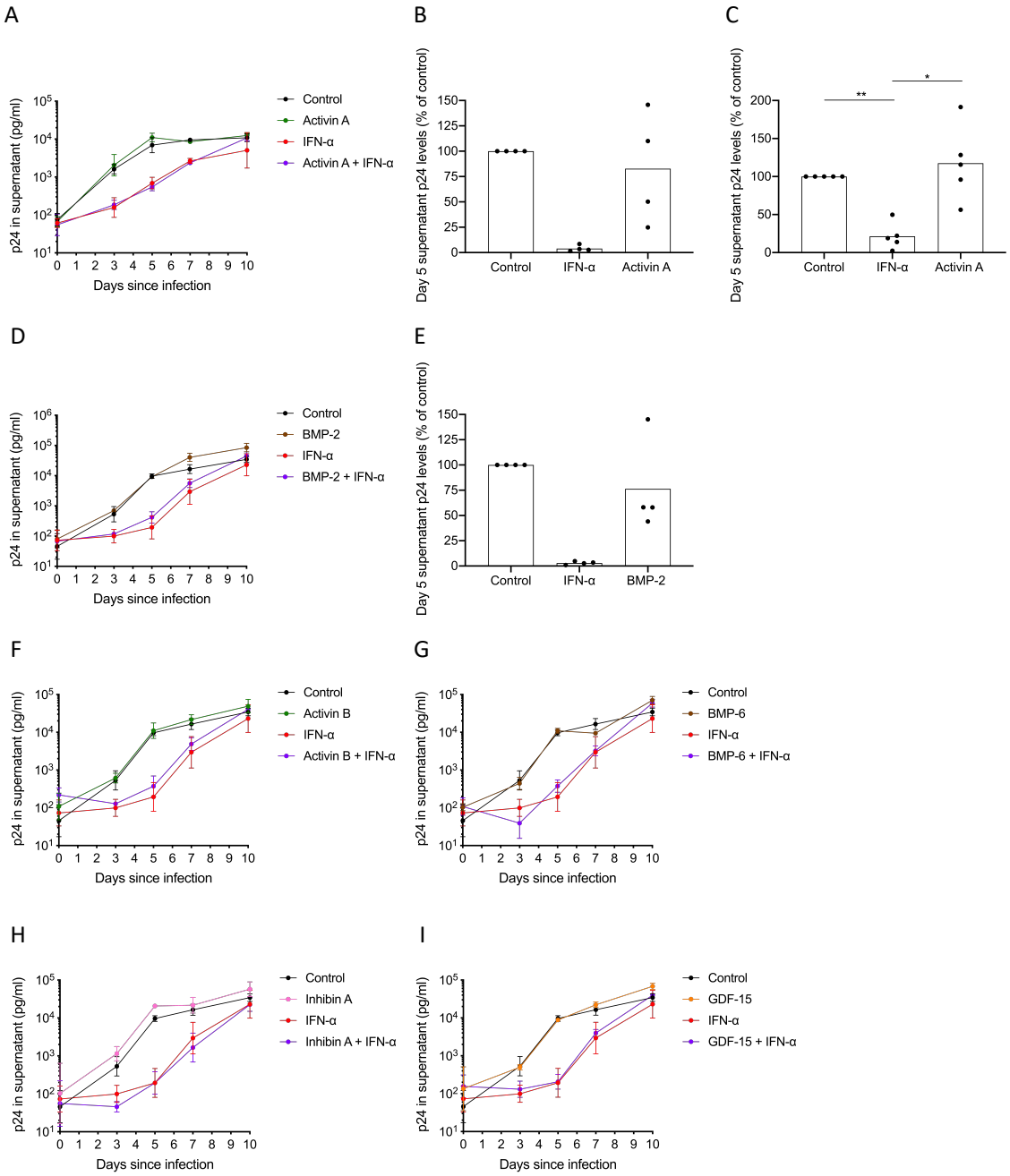


Figure 4.4 Analysis of the effects of diverse TGF-β superfamily cytokines on HIV-1 replication in activated CD8-depleted PBMCs

CD8-depleted PBMCs from three HIV-seronegative donors ("donor trios") were pooled and activated for 48 hours with 50ng/ml anti-CD3, 100ng/ml anti-CD28 and 50IU/ml IL-2 before treatment with TGF-β superfamily cytokines for 24 hours before (and continuously after) infection with HIV-1 strain CH058 6M. On growth curves, error bars represent the geometric SD of triplicate wells. **A.** Representative data from an experiment in which the effect of activin A (5nM) on viral replication, alone or in combination with IFN-α (1000IU/ml), was analysed in one donor trio. **B.** The effect of activin A on CH058 6M virus replication in n=4 donor trios (supernatant p24 at day five as a percentage of untreated control). Bars represent the group mean. **C.** In one donor trio, the effect of activin A on the replication of 6M viruses from n=5 other patients (CH042 6M, CH164 6M, CH236 6M, CH470 6M and CH850 6M) was assessed (supernatant p24 values at day five as a percentage of untreated control). Bars represent the group mean. One-way analysis of variance (ANOVA) with Tukey's post-test, *P<0.05, **P<0.01. **D.** Representative data from an experiment in which the effect of BMP-2 (25nM) on CH058 6M virus replication, alone or in combination with IFN-α, was analysed in one donor trio. **E.** The effect of BMP-2 on CH058 6M virus replication in n=4 donor trios (supernatant p24 at day five as a percentage of untreated control). Bars represent the group mean. **F-I.** The effects of activin B (5nM), BMP-6 (25nM), inhibin A (50ng/ml) and GDF-15 (200ng/ml) on CH058 6M virus replication alone or in combination with IFN-α, in n=1 donor trio.

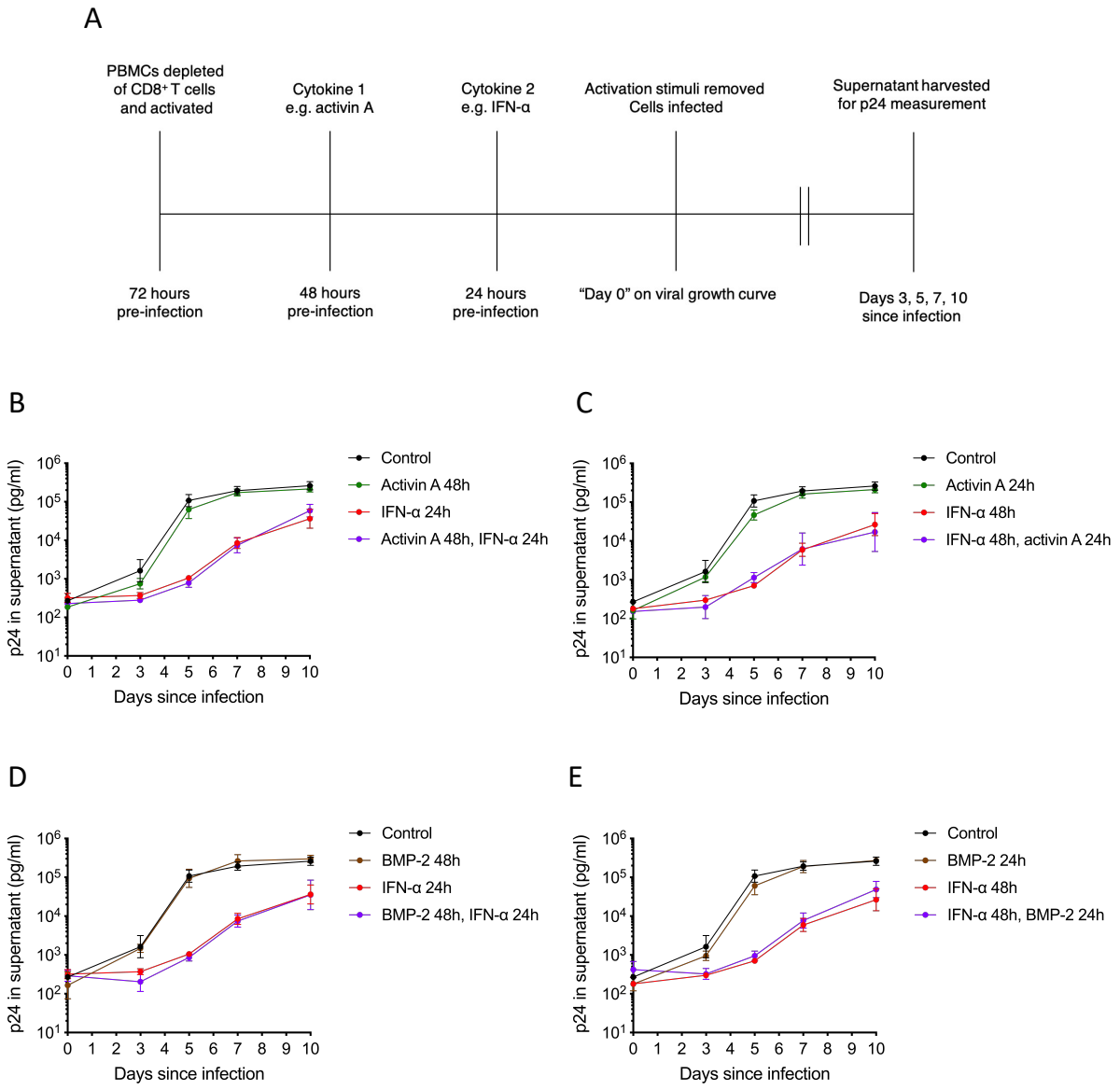


Figure 4.5 Analysis of the effects of activin A and BMP-2 on IFN-α-mediated inhibition of HIV-1 replication in activated CD8-depleted PBMCs

Activated donor trios of CD8-depleted PBMCs were treated with activin A (5nM) or BMP-2 (25nM) before or after IFN-α (1000IU/ml), before (and continuously after) infecting with HIV-1 CH058 6M. The two treatment time points were 48 and 24 hours before infection. Single controls of only the 48-hour or only the 24-hour treatment were also included. For all subfigures, one representative example of results obtained using cells from n=2 donor trios is shown. Error bars represent the geometric SD of triplicate wells. **A.** Schematic of the experimental design. **B.** The effect of activin A on IFN-α-mediated viral inhibition, where activin A was applied first. **C.** The effect of activin A on IFN-α-mediated viral inhibition, where IFN-α was applied first. **D.** The effect of BMP-2 on IFN-α-mediated viral inhibition, where BMP-2 was applied first. **E.** The effect of BMP-2 on IFN-α-mediated viral inhibition, where IFN-α was applied first.

4.2.4 TGF-β_1 inhibits HIV-1 replication in activated CD4$^+$ T cells

TGF-β_1 is the best-studied member of the TGF-β superfamily in the context of the immune system. To assess whether this cytokine influences HIV-1 replication in activated CD4$^+$ T cells, either isolated CD4$^+$ T cells or CD8-depleted PBMCs from HIV-seronegative donors were activated for 72 hours, treating with TGF-β_1 for the last 24 hours of the activation period, and then infected with HIV-1 CH058 6M. TGF-β_1 inhibited HIV-1 replication in both isolated CD4$^+$ T cells (Fig. 4.6A) and CD8-depleted PBMCs (Fig. 4.6B). All further viral replication data shown is from experiments using CD8-depleted PBMCs.

Analysis of the effects of TGF-β_1 on HIV-1 CH058 6M replication in a greater number (n=8) of donor trios revealed that the cytokine reduced the amount of virus by around three-fold during the exponential growth phase (Fig. 4.6C). IFN-α inhibited replication to a greater degree (around ten-fold) than TGF-β_1 (Fig. 4.6C). There was a consistent trend for the combination of TGF-β_1 and IFN-α (added concurrently, 24 hours prior to infection) to inhibit more than TGF-β_1 alone (Fig. 4.6C). Next, TGF-β_1 was titrated, and was shown to inhibit HIV-1 replication in a dose-dependent manner (Fig. 4.6D). As HIV-1 CH058 6M is an R5-tropic virus representative of primary viruses present in many subjects in early chronic infection, the effect of TGF-β_1 on the replication HIV-1 NL4-3, an X4-tropic, lab-adapted strain, was also assessed. TGF-β_1 also inhibited HIV-1 NL4-3 replication (Fig. 4.6E), indicating that it is active against both R5- and X4-tropic strains.

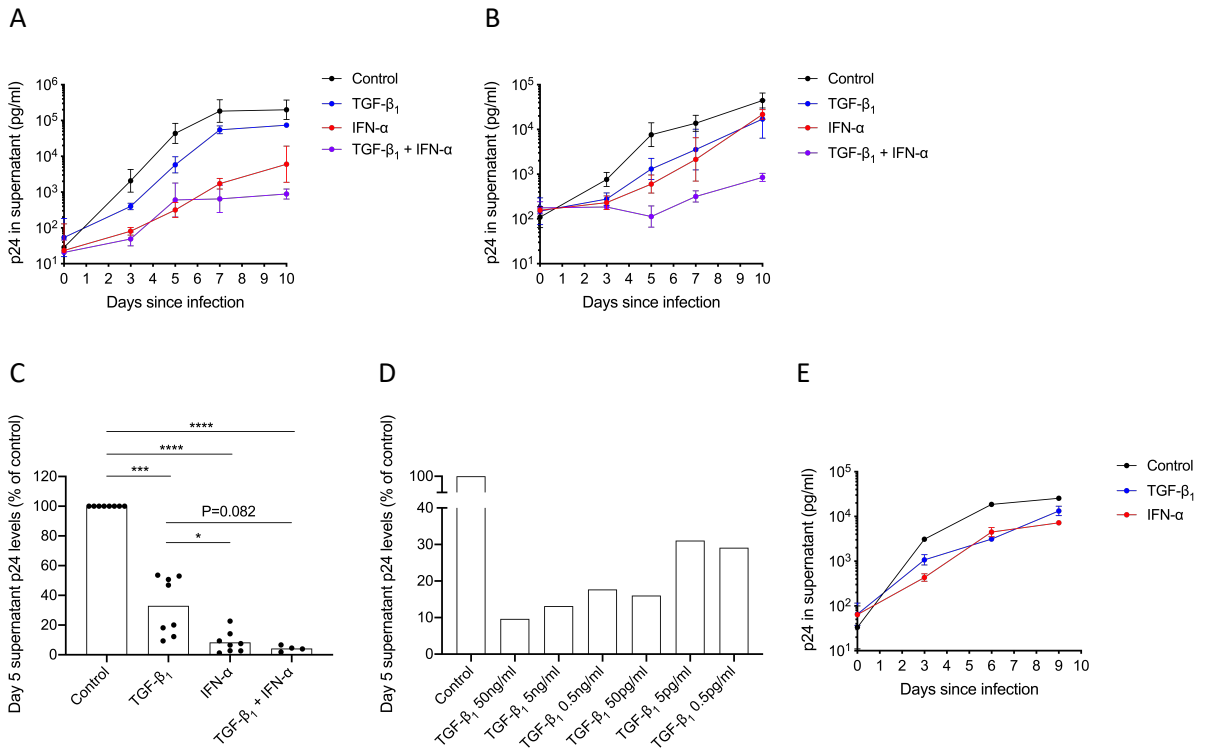


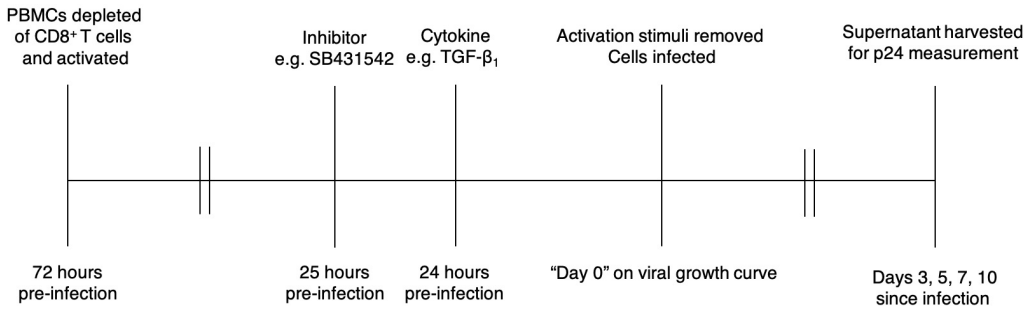
Figure 4.6 The effects of TGF-β$_1$ on HIV-1 replication in activated CD4$^+$ T cells and CD8-depleted PBMCs
Activated donor trios (or single donors, where noted) of CD4$^+$ T cells or CD8-depleted PBMCs were treated with TGF-β$_1$ (50ng/ml) or IFN-α (1000IU/ml) for 24 hours before (and continuously after) infecting with HIV-1 CH058 6M. On growth curves, error bars represent the geometric SD of triplicate wells. **A.** The effects of TGF-β$_1$ and IFN-α on viral replication in CD4$^+$ T cells (data from one representative experiment of n=2 donor trios. The findings were also seen in an additional, distinct n=2 single donors). **B.** The effects of TGF-β$_1$ and IFN-α on viral replication in CD8-depleted PBMCs (data from one representative donor trio). **C.** The effects of TGF-β$_1$ (n=8 donor trios), IFN-α (n=8 donor trios), or both (n=4 donor trios) in CD8-depleted PBMCs (p24 values at day five as a percentage of untreated control). Bars represent the group mean. Mixed-effects analysis with Tukey's post-test, *P<0.05, ***P<0.001, ****P<0.0001. **D.** Effect of different concentrations of TGF-β$_1$ on viral replication (supernatant p24 values at day five); results are representative of those obtained in experiments performed with cells from n=3 donor trios. Bars represent the mean of values from triplicate wells. **E.** The effect of TGF-β$_1$ on HIV-1 NL4-3 replication in cells from a single donor (data representative of n=2 single donors. The findings were also seen in n=1 donor trio).

4.2.5 TGF-β_1 and IFN-α inhibit HIV-1 replication by mechanisms independent of one-another's signalling

Owing to previous work demonstrating the upregulation of expression of components of the type I IFN signalling pathway in hepatoma cells treated with BMP-6[363], it was next explored whether TGF-β_1 and IFN-α exert their antiviral activity independently, or through crosstalk between the SMAD and JAK/STAT signalling pathways respectively. TGF-β_1 signalling in activated CD8-depleted PBMCs was blocked using an inhibitor of the type I TGF-β receptors ALKs 4, 5 and 7; or IFN-α signalling was inhibited using a blocking antibody against IFNAR2, before treating cells with either TGF-β_1 or IFN-α and infecting with HIV-1 CH058 6M (Fig. 4.7A).

Inhibition of either TGF-β_1 or IFN-α signalling had no effect on HIV-1 replication in control, non-cytokine-treated cells, indicating that this was not modulated by endogenous production of either of these cytokines. IFNAR2 blockade substantially reduced IFN-α-mediated inhibition of HIV-1 replication (although limitations on the amount of antibody it was feasible to add precluded achievement of complete blockade of the effects of the high concentration of IFN-α employed here), but had no effect on TGF-β_1-mediated inhibition of viral replication; similarly type I TGF-β receptor blockade ablated TGF-β_1-mediated inhibition of viral replication but had no effect on that exerted by IFN-α (Fig. 4.7B). These data indicate that type I IFN signalling is not required for TGF-β_1 inhibition of HIV-1 replication, and SMAD signalling is not required for that mediated by IFN-α.

A



B

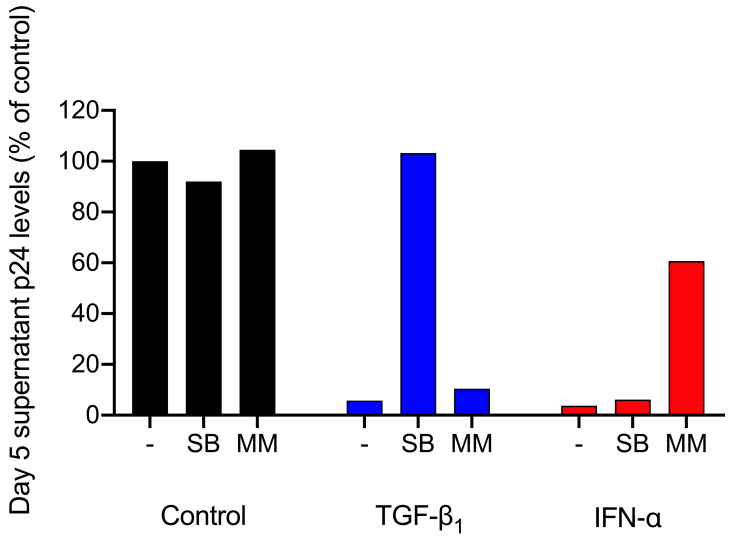


Figure 4.7 The effects of inhibition of SMAD and JAK/STAT signalling on TGF-β$_1$- and IFN-α-mediated inhibition of HIV-1 replication

Activated donor trios of CD8-depleted PBMCs were treated with inhibitor of SMAD2/3 signalling SB431542 (SB) (10μM) or IFNAR2-neutralising monoclonal antibody MMHAR-2 (MM) (10μg/ml) for one hour prior to the addition of TGF-β$_1$ (50ng/ml) or IFN-α (250IU/ml), and incubated for 24 hours before (and continuously after) infecting with HIV-1 CH058 6M. **A.** Schematic of the experimental design. **B.** Supernatant p24 values at day five are plotted as a percentage of the untreated control. Bars show the mean (of triplicate wells) values from one experiment representative of n=2 donor trios.

4.2.6 Transmitted founder viruses are relatively more resistant to TGF-β_1 inhibition

TF viruses are relatively more resistant to type I IFN inhibition than viruses that evolve later in the course of infection, consistent with the hypothesis that type I IFN resistance confers a transmission advantage on HIV-1, but that this resistance declines as virus undergoes subsequent replication in the presence of selective pressure exerted by adaptive immune responses[57,58]. Using a panel of n=7 patient-derived TF viruses and n=7 6M consensus sequence viruses from the same patients, the question of potential TGF-β_1-mediated inhibition of TF and 6M viruses was interrogated, to investigate whether TGF-β_1 resistance could confer a transmission advantage.

TGF-β_1 was found to inhibit the replication of TF viruses, and TGF-β_1 in combination with IFN-α to inhibit replication to a greater extent than TGF-β_1 alone (Fig.4.8A). When examining each TF virus in more than one donor trio, there was some variability in the degree of inhibition (Fig. 4.8B). When considering the data from n=3 donor trios, across all n=7 TF viruses, TGF-β_1 was found to mediate significant inhibition of TF virus replication, there was a trend for greater inhibition by IFN-α, and virus replication was inhibited to a significantly greater extent by TGF-β_1 in combination with IFN-α than by TGF-β_1 alone (Fig. 4.8C). Similar observations were made with 6M viruses (Fig. 4.9A-C). However, six out of seven TF viruses were found to be relatively more resistant to the effects of TGF-β_1 than their 6M paired counterpart, and overall, TF viruses were inhibited less well by TGF-β_1 than their 6M counterparts (Fig. 4.10A). Consistent with data from prior studies, TF viruses were also found to be more significantly more resistant to IFN-α inhibition than their 6M counterparts (Fig. 4.10B). TF and 6M viruses did not differ significantly in the extent to which their replication was inhibited by TGF-β_1 and IFN-α combined, although five of the seven TF viruses were inhibited less well by this combination of cytokines than their 6M counterparts (Fig. 4.10C).

Analysis of the relative resistance of different HIV-1 strains to cytokine-mediated inhibition can be confounded by differences in viral fitness. The degree of cytokine-mediated inhibition of the replication of any individual virus is dependent on the number of rounds of virus replication that the virus undergoes[566], hence viruses that are fitter and undergo more rounds of replication during *in vitro* assays appear more sensitive to the inhibitory effects of type I IFN. When considering all viruses (TF and 6M viruses from all donors) together, this was apparent, as a significant negative correlation was observed between the slope of the increase in p24 values in the exponential growth phase between days three and seven post-infection in non-cytokine treated cells and IFN-α resistance (Fig. 4.11A) or TGF-β_1 resistance (Fig. 4.11B). Accordingly, in the *in vitro* assay employed in this chapter, TF viruses had statistically significantly less replicative efficiency than 6M viruses overall, as measured by slope in the exponential growth phase (Fig. 4.11C), supporting the observation of greater resistance of TF viruses to TGF-β_1-mediated inhibition, relative to 6M viruses. To calculate slope for each virus in each donor trio (as a measure of viral replication efficiency), the p24 concentration values of non-cytokine treated cells at days three, five and seven were natural log (ln) transformed, before using the "simple linear regression" option on GraphPad Prism version 8 (GraphPad Software Inc, USA) on the three transformed values to calculate the slope between days three and seven.

TF viruses often carry mutations for type I IFN resistance through increased resistance to certain antiviral ISGs[569] and exhibit varying levels of resistance to type I IFN[58]. Accordingly, in comparing the relationship between slope and IFN-α resistance in TF viruses (in the same way as in in Figs. 4.11A and B with all viruses), no significant relationship was observed between IFN-α-mediated inhibition and viral replication (Fig. 4.11D). In contrast to this, TF virus replication efficiency did show a significant negative correlation with TGF-β_1 resistance (Fig. 4.11E), indicating that these viruses do not exhibit specific TGF-β_1 resistance.

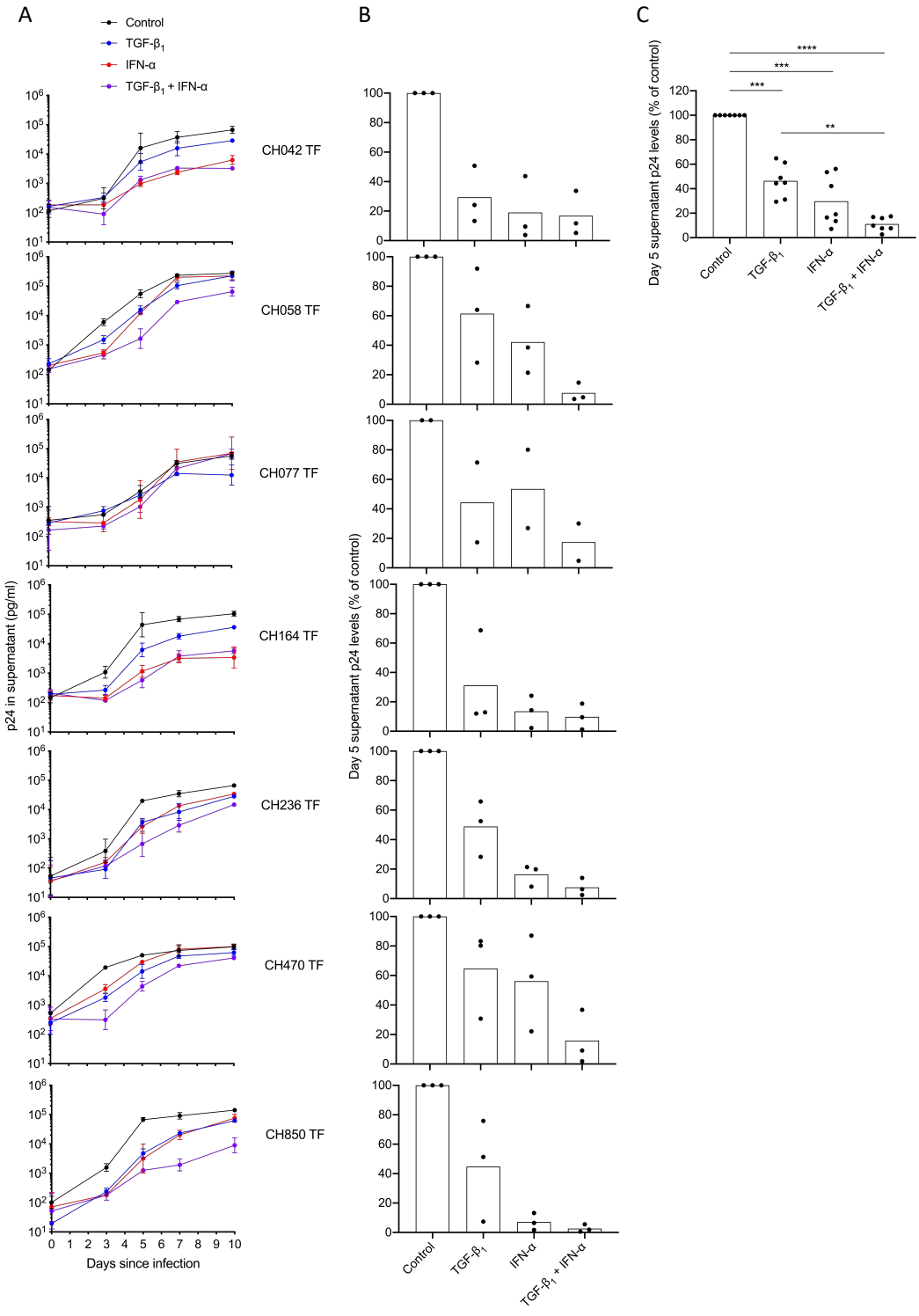


Figure 4.8 The effect of TGF-β1 on the replication of TF viruses
Activated donor trios of CD8-depleted PBMCs were treated with TGF-β1 (50ng/ml), IFN-α (1000IU/ml or both, for 24 hours before (and continuously after) infecting with n=7 TF strains of HIV-1. **A.** Examples of growth curves for each TF virus, illustrating cytokine-mediate inhibition in one representative experiment of n=3 performed with each virus in different donor trios. Error bars represent the geometric SD of triplicate wells. **B.** Results from analysis of the effect of TGF-β1 and IFN-α on the replication of each TF virus in cells from n=3 donor trios tested (except CH077 TF, where n=2) (p24 values at day five as a percentage of untreated control). Bars represent group means. **C.** Summarised data from experiments addressing the effect of TGF-β1 and IFN-α on the replication of all TF viruses (p24 values at day five as a percentage of untreated control). Each data point (n=7) represents the average of all donor trios for n=7 viruses. Bars represent group means. One-way ANOVA with Tukey's post-test, **P<0.01, ***P<0.001, ****P<0.0001.

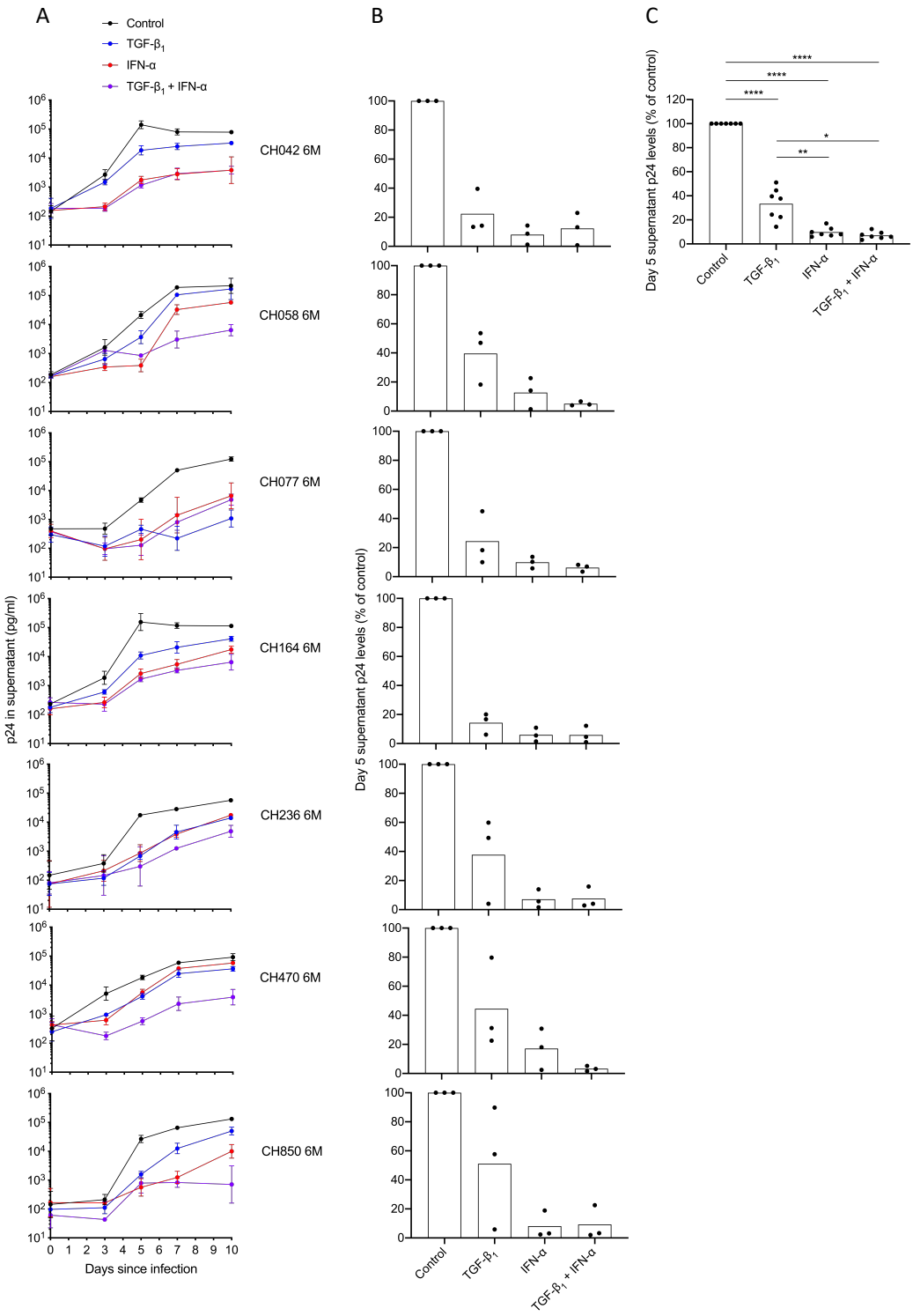


Figure 4.9 The effect of TGF-β1 on the replication of 6M viruses
6M viruses (n=7) derived from the same patients as TF viruses from Fig. 4.8 were assessed in the same way. The same donor trios were also used within each TF-6M pair. **A.** Examples of growth curves for each 6M virus, illustrating cytokine-mediate inhibition in one representative experiment of n=3 performed with each virus in different donor trios. Error bars represent the geometric SD of triplicate wells. **B.** Results from analysis of the effect of TGF-β1 and IFN-α on the replication of each 6M virus in cells from n=3 donor trios tested (p24 values at day five as a percentage of untreated control). Bars represent group means. **C.** Summarised data from experiments addressing the effect of TGF-β1 and IFN-α on the replication of all 6M viruses (p24 values at day five as a percentage of untreated control). Each data point (n=7) represents the average of all donor trios for n=7 viruses. Bars represent group means. One-way ANOVA with Tukey's post-test, *P<0.05, **P<0.01, ****P<0.0001.

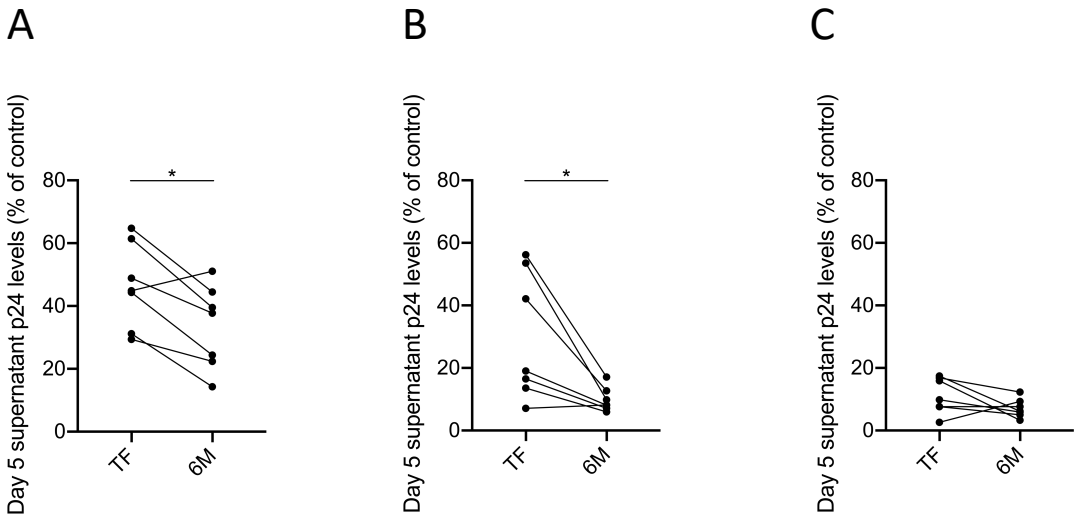


Figure 4.10 Differential effects of TGF-β$_1$ and IFN-α on TF and 6M virus replication
The resistance of n=7 TF and patient-matched 6M viruses to TGF-β$_1$ and IFN-α (shown in Figs. 4.8 and 4.9) were compared. **A.** Comparison of effect of TGF-β$_1$ on TF and 6M virus replication (supernatant p24 values at day five as a percentage of untreated control). Paired t-test, *P<0.05. **B.** Comparison of the effect of IFN-α on TF and 6M virus replication (supernatant p24 values at day five as a percentage of untreated control). Paired t-test, *P<0.05. **C.** Comparison of the effect of TGF-β$_1$ and IFN-α combined on TF and 6M viruses (supernatant p24 values at day five as a percentage of untreated control).

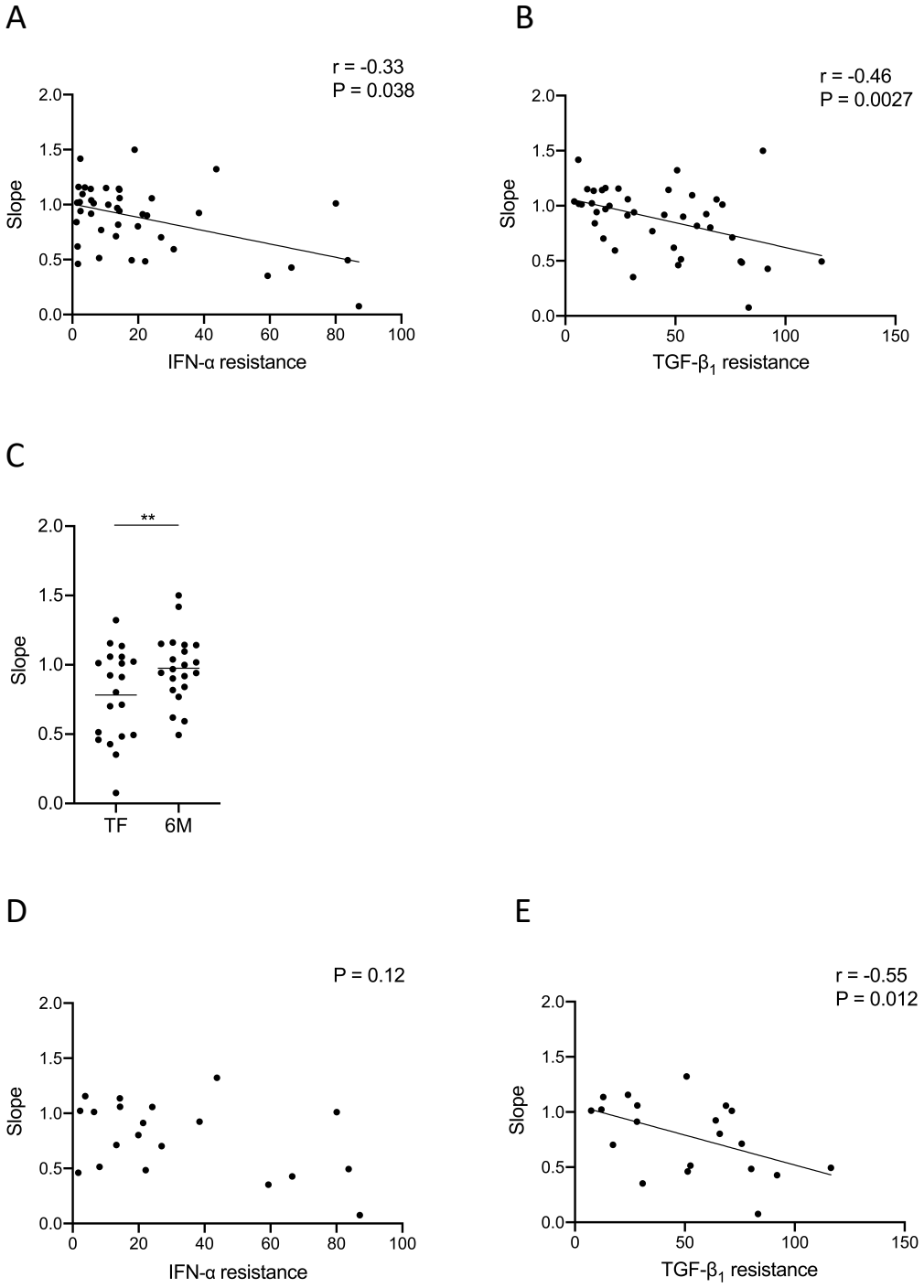


Figure 4.11 The relationships between replicative efficiency and TGF-β$_1$- and IFN-α-mediated inhibition of TF and 6M virus replication

A and **B.** The growth of all viruses (TF and 6M, shown in Figs. 4.8 and 4.9), assessed on the basis of the slope of increase in supernatant p24 values in the exponential growth phase (days three to seven) in control untreated cells in all donor trios (total n=41 data points) was plotted against their IFN-α resistance (A) and TGF-β$_1$ resistance (B) (supernatant p24 values from cytokine treated cells as a percentage of the untreated control at day five). Correlations were analysed by Spearman's rank. **C.** Comparison of the slope of the increase in supernatant p24 values from days three to seven in control untreated cells in all donor trios between TF (n=20 data points) and 6M (n=21 data points) viruses. Paired t-test, **P<0.01. **D** and **E.** The growth of TF viruses (assessed on the basis of the slope of increase in supernatant p24 values in the exponential growth phase (days three to seven) in control untreated cells) in all donor trios (total n=20 data points) was plotted against their IFN-α resistance (D) and TGF-β$_1$ resistance (E) (supernatant p24 values from cytokine treated cells as a percentage of the untreated control at day five). Correlations were analysed by Spearman's rank.

4.2.7 Establishment of an HIV-1 replication assay in less activated CD4+ T cells

The degree to which a CD4+ T cell is activated positively correlates with cellular susceptibility to HIV-1 infection[77] and with virion production[570], particularly *in vitro*. However, *in vivo,* the virus also infects and replicates in cells with very low levels of phenotypic activation markers[78,79]. In addition, resting CD4+ T cells (both naïve and previously activated memory cells that have since reverted to a resting state) form a key source of the latent HIV-1 reservoir *in vivo*[571,572].

Cell activation increases transcription of many ISGs[573–576], creating a very different baseline transcriptional landscape on which to examine viral replication compared to resting cells. In order to assess the impact of TGF-β_1 and other members of the TGF-β superfamily on HIV-1 replication in more phenotypically resting CD4+ T cells, an alternative HIV-1 replication assay was sought.

Productive HIV-1 replication in resting cells is difficult to achieve *in vitro*. Barriers to replication in resting CD4+ T cells include SAMHD1[577] and decreased availability of deoxynucleosides (dNs). To facilitate infection of resting cells, some studies have provided exogenous dNs[578], or have blocked the action of transcription factors that promote cell quiescence such as forkhead box protein O1, to promote cell cycle progression and decrease expression of SAMHD1[579]. In pilot experiments, both of these methods were attempted with no success. Instead, a system was devised utilising DC-mediated virus transfer to CD4+ T cells.

CD8-depleted PBMCs from HIV-seronegative donors that had not been pre-activated *in vitro* were co-cultured with MDDCs from allogeneic HIV-seronegative donors (to promote CD4+ T cell-DC interaction), the latter of which had been pre-pulsed with HIV-1 NL4-3 BaL. Recombinant IL-2 was provided, but at a 10-fold lower concentration than with the standard HIV-1 replication assay. HIV-pulsed MDDCs, and an aliquot of CD8-depleted PBMCs that had

been pre-pulsed with the same quantity of virus as that added to the DCs were each cultured alone in parallel.

The phenotypic activation status of $CD4^+$ T cells in this system were compared to those highly activated under conditions of the standard HIV-1 replication assay using flow cytometry for activation markers CD69, CD25, CD38 and HLA-DR. CD69 is an early activation marker, induced within a few hours of T cell stimulation and peaking at around 24 hours. CD25 is a later marker, elevating from 24 hours onwards, and HLA-DR an even later marker, usually peaking several days post-activation[580]. CD38 is upregulated within 24 hours of activation and upregulation is often sustained for several days[581]. Sample gating on these markers in $CD4^+$ T cells at "baseline" (before *in vitro* activation or co-culture with allogeneic MDDCs), after 72 hours of anti-CD3/anti-CD28 and high IL-2 activation stimulation as is used in the standard HIV-1 replication assay, or after eight days of co-culture with virus-pulsed allogeneic MDDCs as in the alternative system, are displayed in Fig. 4.12A.

Overall in this assay, there was some inter-donor variability. But on average at baseline, only around 5% of cells expressed CD69, while around 20-30% expressed CD25, CD38 and HLA-DR. After 72 hours of standard high activation, around 20% expressed CD69, over 90% expressed CD25 and CD38, and almost 40% expressed HLA-DR. In contrast, co-cultured $CD4^+$ T cells expressed low levels of all four activation markers, all around 10-20% of $CD4^+$ T cells at any time point analysed (days two, five and eight post-DC co-culture) (Fig. 4.12B). When analysing the MFI of the activation markers within the $CD4^+$ T cell population, all four markers (but particularly CD25 and CD38) increased in activated cells, with the MFI in cells cultured with DCs remaining essentially the same as baseline cells at all timepoints of co-culture (Fig. 4.12C).

Taken together, these data indicate that in the MDDC-CD4$^+$ T cell co-culture HIV-1 replication assay system, both the percentage of cells positive for CD69, CD25, CD38 and HLA-DR and the intensity of their expression did not appreciably change from cells at baseline, in comparison to the conditions of the standard HIV-1 replication assay in which cells substantially upregulated these markers after 72 hours.

Next, HIV-1 replication was examined using the co-culture assay system, as measured by supernatant p24 titres. A very small amount of productive viral replication occurred in each cell population (MDDCs or CD4$^+$ T cells) when cultured alone, evidenced by a slow, relatively low-level increase in p24 over time. However, much more rapid and pronounced productive HIV-1 replication was observed in the co-cultures (Fig. 4.13). The two logs of virus growth observed in the co-cultures after 10 days are consistent with that seen by another study using a similar method[582].

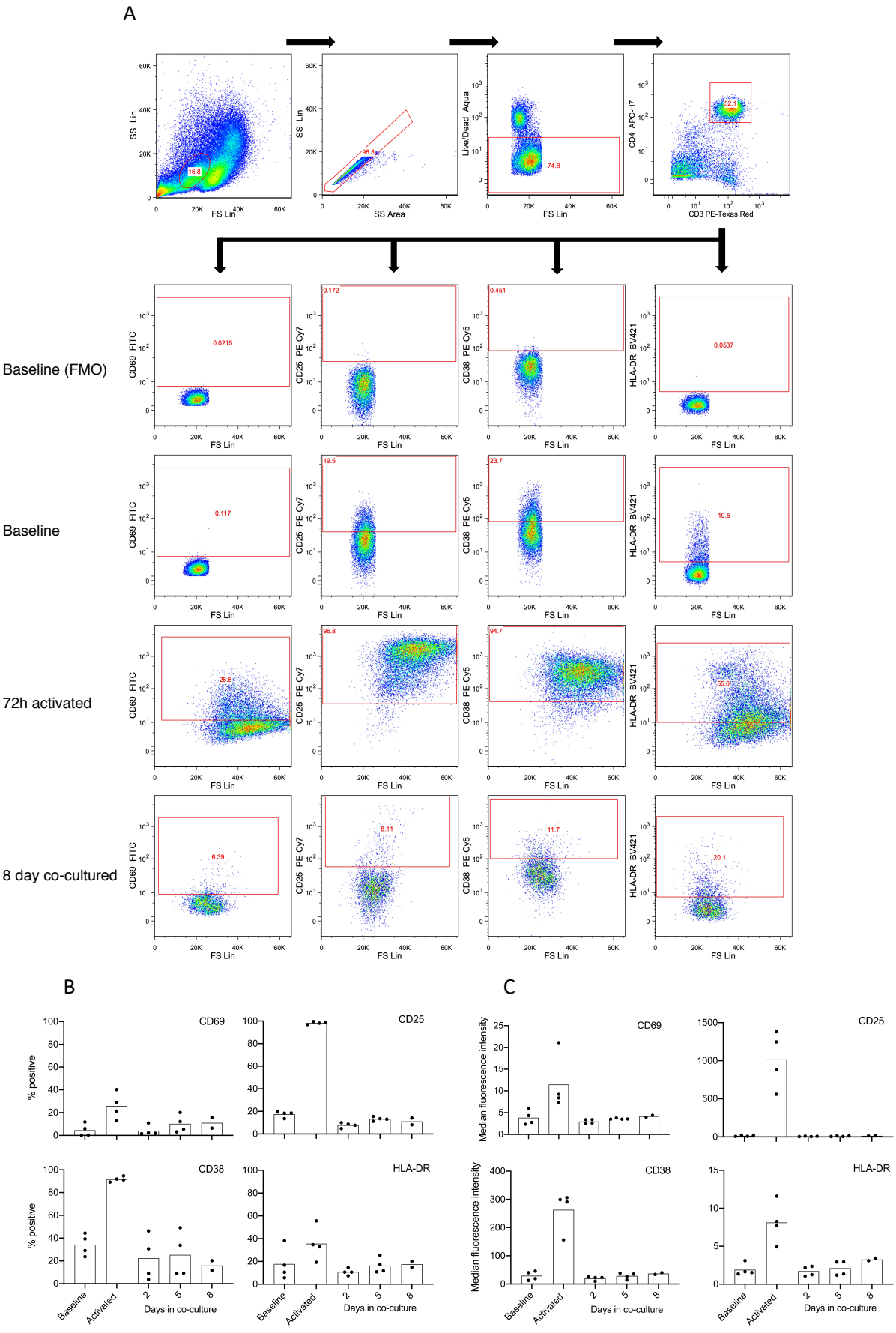

A
SS Lin
FS Lin
SS Area
Live/Dead Aqua
CD4 APC-H7
CD3 PE-Texas Red
Baseline (FMO)
Baseline
72h activated
8 day co-cultured
CD69 FITC
CD25 PE-Cy7
CD38 PE-Cy5
HLA-DR BV421
B
C
% positive
Median fluorescence intensity
CD69
CD25
CD38
HLA-DR
Baseline
Activated
Days in co-culture

Figure 4.12 Flow cytometric analysis of activation marker expression in CD4+ T cells in a less highly activated viral replication assay compared to the standard HIV-1 replication assay
CD8-depleted PBMCs that had not been pre-activated were co-cultured with allogeneic MDDCs (both from HIV-seronegative donors) that had been pre-pulsed with HIV-1 NL4-3 BaL. Expression of activation markers CD69, CD25, CD38 and HLA-DR in the CD4+ T cells was analysed by flow cytometry, using "flow cytometry panel 2" (Chapter 2). **A.** First row: gating strategy for live, single, CD4+CD3+ T cells within the baseline sample from one donor (before CD8+ T cell depletion or any co-culture or activation). Arrows indicate serial gates. All subsequent data in this figure is from the CD4+ T cell compartment. Second row: FMO samples for the activation markers at baseline. Third row: activation markers at baseline identified using the FMO gates. Fourth row: activation markers after 72 hours of activation with stimuli used in the standard HIV-1 replication assay. Fifth row: activation markers in cells co-cultured with allogeneic MDDCs for eight days. The gates for activation markers in rows four and five were also set using FMOs (not shown) which were stained at those same time points. All the data in this subfigure are taken from the same donor. **B.** The percentage of CD4+ T cells positive for the activation markers at baseline, after 72-hour activation with stimuli used in the standard HIV-1 replication assay, or after co-culture for two, five or eight days with virus-pulsed MDDCs. Data are from n=4 experiments that employed MDDCs from n=2 donors and CD8-depleted PBMCs from n=3 donors in n=4 unique combinations, with the exception of the day eight timepoint, for which available data comprised n=2 unique donor combinations. Bars represent the group means. **C.** The MFI of CD69, CD25, CD38 and HLA-DR values from (B), within CD4+ T cells. Bars represent the group means.

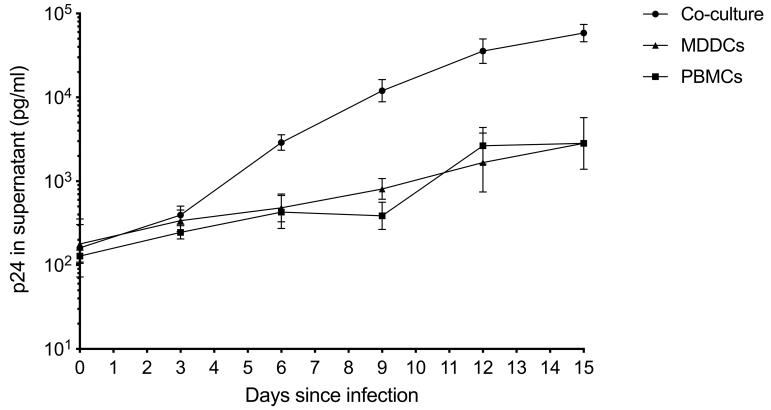


Figure 4.13 Analysis of viral growth in a less highly activated CD4+ T cell HIV-1 replication assay
CD8-depleted PBMCs that had not been pre-activated were co-cultured with allogeneic MDDCs (both from HIV-seronegative donors) that had been pre-pulsed with HIV-1 NL4-3 BaL. Representative viral growth curve from one of n=8 MDDC-PBMC donor combinations (from experiments employing n=3 MDDC donors and n=6 PBMC donors in eight unique combinations). Error bars represent the geometric SD of triplicate wells. Virus replication in CD8-depleted PBMCs or MDDCs pulsed with virus and cultured alone is also shown.

4.2.8 No effect of TGF-β superfamily cytokines on HIV-1 replication in phenotypically less activated cells

To assess the effects of TGF-β superfamily cytokines on HIV-1 replication in the less activated cell system, non-pre-activated CD8-depleted PBMCs were treated with these cytokines for 24 hours prior to co-culture with virus-pulsed MDDCs. In contrast to its effects on HIV-1 replication in highly activated cells, TGF-β_1 had no significant effect on viral replication in this setting (Fig. 4.14A, B). Interestingly, however, IFN-α induced a very profound inhibition of viral replication

in the co-culture system (Fig. 4.14A, B). When CD8-depleted PBMCs were pre-treated with IFN-α for 24 hours and then co-cultured with MDDCs without IFN-α being present during the co-culture (so that the MDDCs were not exposed to IFN-α), viral replication was also markedly reduced, although the reduction was less profound than when IFN-α was also included during the co-culture period, suggesting that IFN-α acts on both T cells and MDDCs to reduce HIV-1 replication in this system (Figs. 4.14A, B). BMP-2 and activin A also had no effect on HIV-1 replication in the co-culture system (Fig. 4.14B). The responsiveness of non-pre-activated $CD4^+$ T cells to TGF-β_1 and BMP-2 was confirmed by western blot analysis of SMAD signalling (Figs. 4.14C, D). The responsiveness of non-pre-activated PBMCs to activin A was not successfully demonstrated but has been demonstrated in a prior study by others[394].

To address whether the lack of HIV-1 inhibition by TGF-β_1 in less activated $CD4^+$ T cells is a phenomenon unique to DC-mediated transmission, the standard HIV-1 replication assay using anti-CD3/anti-CD28 antibody-mediated activation was repeated, and viral replication in CD8-depleted PBMCs pre-activated using a five-fold lower concentration of the anti-CD3/anti-CD28 antibodies was assessed in parallel. Prior work by other members of the lab has demonstrated this concentration to yield a modest reduction in the percentage of $CD4^+$ T cells expressing CD69, CD25 and HLA-DR compared to the higher concentration (not shown). Using these activation conditions, HIV-1 replication was still achieved, but at a slightly slower kinetic than at the higher concentration (Fig. 4.15A). TGF-β_1 inhibited HIV-1 replication to a lesser degree in more weakly activated cells (Fig. 4.15A, B). Time constraints precluded performance of a sufficiently large number of biological repeats to enable robust statistical analysis of the data, but the results obtained in n=3 donor trios suggest that TGF-β_1-mediated inhibition is contingent on T cell activation status, regardless of whether infection is mediated by transfer of virus from DCs or is initiated by cell-free virus.

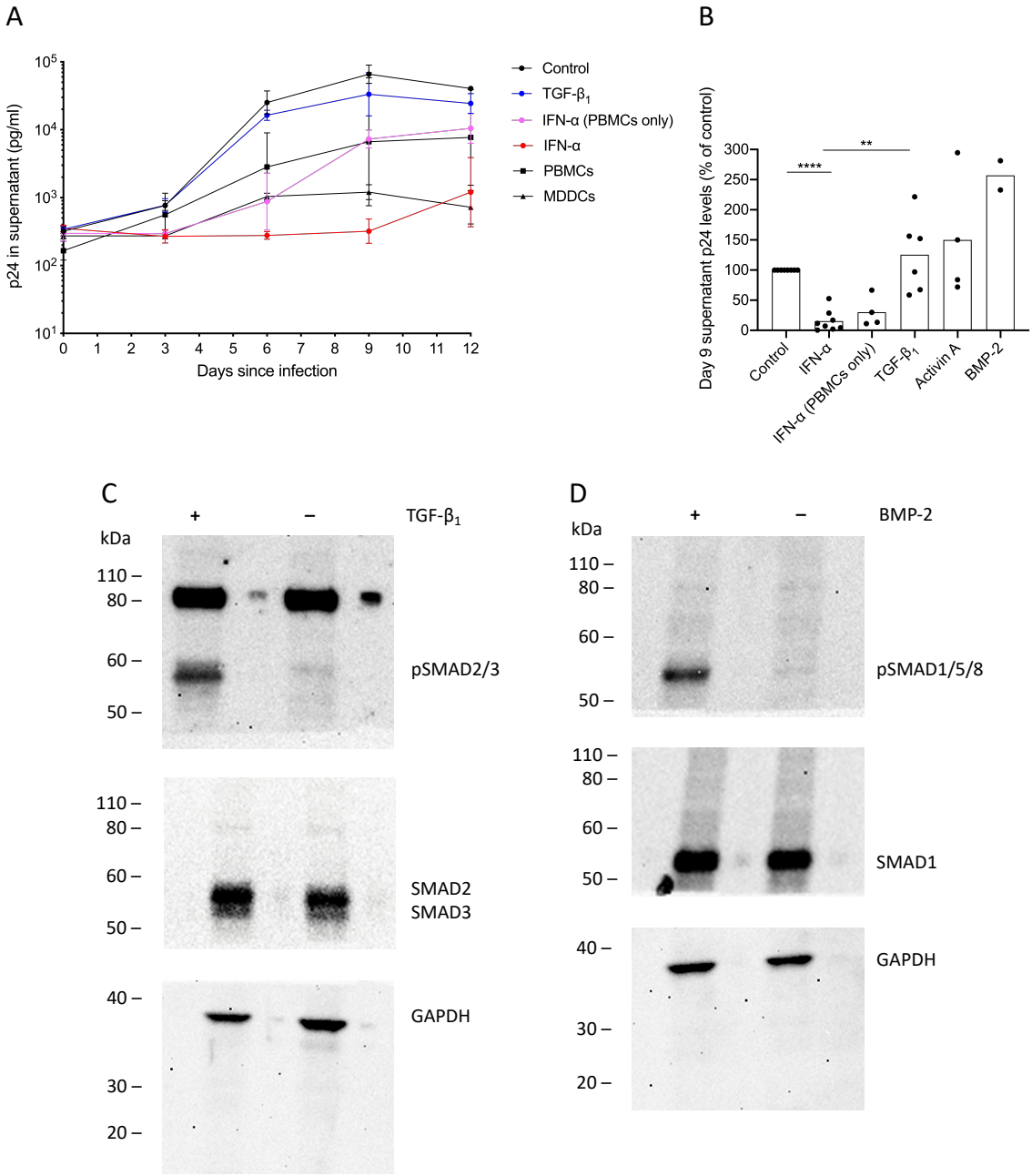


Figure 4.14 Analysis of the effects of TGF-β superfamily cytokines on HIV-1 replication in an MDDC-CD4⁺ T cell co-culture HIV-1 replication assay

Non-pre-activated CD8-depleted PBMCs from HIV-seronegative donors were treated for 24 hours with TGF-β superfamily cytokines and then co-cultured in the continued presence of the same cytokine with allogeneic MDDCs (also from HIV-seronegative donors) that had been pre-pulsed with HIV-1 NL4-3 BaL. **A.** Viral growth curves from one representative MDDC-PBMC donor combination showing the effects of TGF-β_1 (50ng/ml) and IFN-α (1000IU/ml) on viral replication in the co-culture system. Viral replication was also assessed in conditions where IFN-α has been applied for 24 hours to the CD8-depleted PBMCs before they were added to the MDDCs, but was not present in the co-culture (IFN-α (PBMCs only)). HIV-1 replication in non-cytokine treated virus-pulsed PBMCs or MDDCs alone is also shown. Error bars represent the geometric SD of triplicate wells. **B.** The effects of TGF-β_1, IFN-α, activin A (5nM) or BMP-2 (25nM) on virus replication in co-cultures (supernatant p24 values at day nine as a percentage of untreated control) performed with n=8 (IFN-α), n=6 (TGF-β_1), n=4 (IFN-α PBMCs only and activin A) and n=2 (BMP-2) MDDC-PBMC donor combinations from n=3 MDDC donors and n=6 PBMC donors in unique combinations. Bars represent group means. Mixed-effects analysis with Tukey's post-test (only on conditions with n=5 or greater). **P<0.01, ****P<0.0001. **C.** Non-pre-activated CD4⁺ T cells from HIV-seronegative donors were treated with TGF-β_1 (50ng/ml) for two hours before western blot analysis of SMAD2/3 signalling. One representative result of experiments performed with cells from n=2 donors. **D.** Non-pre-activated CD4⁺ T cells from HIV-seronegative donors were treated with BMP-2 (25nM) for ten hours before western blot analysis of SMAD1/5/8 signalling. One representative result of experiments performed with cells from of n=2 donors.

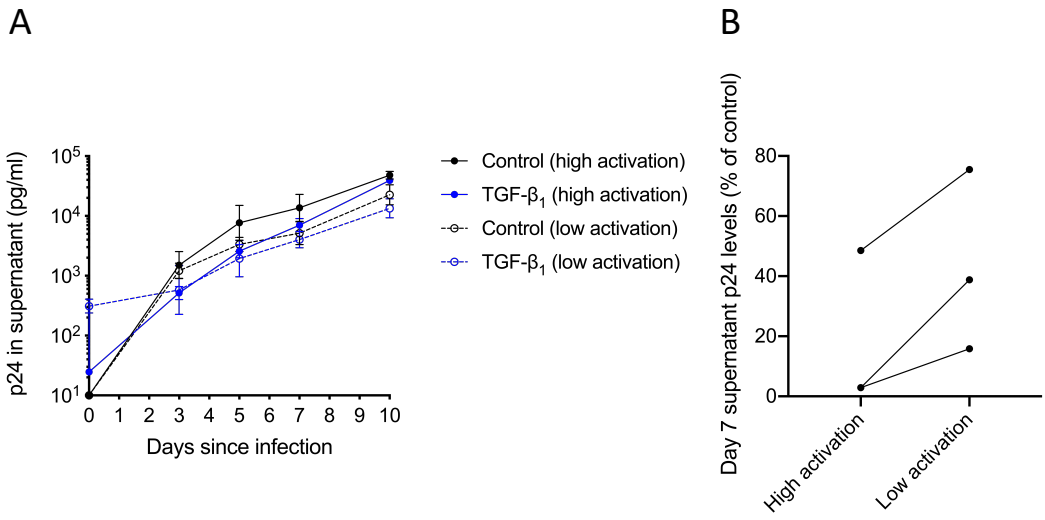


Figure 4.15 Differential TGF-β₁-mediated inhibition of HIV-1 replication in CD8-depleted PBMCs pre-activated with high or low concentrations of antibodies to CD3 and CD28
CD8-depleted PBMCs pooled from three HIV-seronegative donors were pre-activated with the standard, strong T cell activation stimulus (50ng/ml anti-CD3, 100ng/ml anti-CD28, 50IU/ml IL-2) or a weaker stimulus (10ng/ml anti-CD3, 20ng/ml anti-CD28, with the same amount of IL-2) for 72 hours, adding TGF-β_1 (50ng/ml) for the last 24 hours before infecting with HIV-1 CH058 6M and culturing in the continued presence of TGF-β_1. **A.** Viral replication curves from one representative experiment to illustrate levels of viral replication in CD8-depleted PBMCs exposed to the two different activation stimuli (with and without TGF-β_1). Error bars represent the geometric SD of triplicate wells. **B.** TGF-β_1-mediated inhibition of viral replication (supernatant p24 values at day seven (when substantial virus replication had occurred in control cells exposed to the lower as well as the higher activation stimulus) as a percentage of untreated controls) in cells from n=3 donor trios.

4.2.9 No effect of TGF-β superfamily cytokines on HIV-1 replication in 293FT cells

TGF-β superfamily cytokines upregulate canonical antiviral genes in Huh hepatoma cells, and restrict replication of hepatotropic viruses in these cells, as well as the replication of Zika virus in epithelial cells[363]. But for most members of the TGF-β superfamily, with the exception of TGF-β_1, data presented in this chapter thus far reveal no effect on HIV-1 replication in $CD4^+$ T cells and macrophages. It was next questioned whether TGF-β superfamily cytokines exert antiviral activity against HIV-1 in a non-haematopoietic cell type.

293FT cells are of embryonic kidney origin and have a mixed epithelial and mesenchymal phenotype[583]. These cells can be readily transfected with plasmids encoding full-length HIV-1 genomes, which are then transcribed, leading to production of viral proteins and virion assembly and release, although no further spread of infection occurs, as the newly produced virions cannot infect the 293FT cells, which are $CD4^-$[584]. Using this system, in which all the

later stages of the HIV-1 replication cycle occur, the effects of TGF-β superfamily cytokines on HIV-1 production in 293FT cells were assessed. 293T cells are reported to be responsive to TGF-β_1[585], BMP-2[586] and activin A[587].

In an initial experiment, IFN-α, which was tested in parallel, very modestly reduced HIV-1 replication in 293FT cells, consistent with published data indicating that 293T cells are responsive to type I IFNs, but upregulate expression of many ISGs less well than primary cells[576]. However, no effect of TGF-β_1, activin A, or BMP-2 on virus production was observed (Fig. 4.16). Likewise when a further experiment was performed with half as much HIV-1 NL4-3 DNA (0.15µg), and supernatant p24 release was assessed at 6, 12, 24, and 48 hours post-transfection to give greater insight into the kinetics of virus production before the plateau in p24 values was reached, a lack of any effect of TGF-β superfamily cytokines was again observed (data not shown). Here too, further experiments could have been performed to generate data amenable to robust statistical analysis had time permitted; the results presented do however suggest that TGF-β superfamily cytokines do not inhibit the later stages of the HIV-1 replication cycle in 293FT cells.

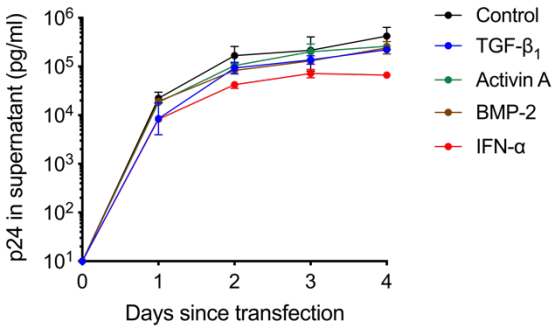


Figure 4.16 Analysis of the effects of TGF-β superfamily cytokines on HIV-1 replication in 293FT cells
293FT cells were treated with TGF-β_1 (50ng/ml), activin A (5nM), BMP-2 (25nM) or IFN-α (1000IU/ml) for 24 hours before (and continuously after) lipotransfection with 0.3µg HIV-1 NL4-3 DNA. Supernatant p24 was analysed at serial timepoints after transfection. Error bars represent the geometric SD of triplicate wells.

4.3 Discussion

This chapter addressed the potential role of TGF-β superfamily cytokines in controlling HIV-1 replication in several different *in vitro* replication systems. In $CD4^+$ T cells and macrophages, the two major target cells of HIV-1, SMAD signalling in response to TGF-β superfamily ligands was robustly demonstrated.

In macrophages, TGF-β_1 had no effect on viral replication. This is at odds with published data that apparently collectively show TGF-β, either applied prior to or at the time of infection, enhances HIV-1 replication in MDMs. These studies used a range of TGF-β concentrations from the pg/ml range[546] to the low ng/ml[549,551] and higher ng/ml[550] ranges. However, all of these studies analysed relatively late time points, taking readouts 10-14 days post-infection. And in fact, in one study, although TGF-β increased the amount of virus present from day 12 onwards in a multiple-round infection assay, prior to this time point, the inverse outcome was actually observed[546]. In another, earlier time points were taken but no effect was seen prior to day 12[551]. This chapter examined MDMs principally at seven days post-infection, as it was by which point in the assay by which viral growth curves plateaued. One way by which TGF-β may mediate increased susceptibility of macrophages to HIV-1 infection is through promoting maturation[588,589]. TGF-β is involved in the differentiation of some types of macrophage, namely alveolar macrophages[590] and microglia[591]. Another mechanism by which TGF-β can enhance macrophage susceptibility to X4-tropic HIV-1 is through increasing expression of this coreceptor[548]. The present study in this chapter used the R5-tropic NL4-3 BaL, perhaps decreasing the likelihood of observing viral enhancement.

By contrast to all of the above, there are a small number of published pieces of work showing TGF-β inhibits HIV-1 replication in MDMs[545,551,552]. In two of these studies, TGF-β exerted its action when applied to cells between 7-16 days post-infection onwards. However, another

study also employed this methodology and still found enhancement of replication[549]. Taking all of these findings together, it appears that TGF-β has no effect on HIV-1 replication in MDMs within the first 7-10 days post-infection but may either positively or negatively regulate HIV-1 replication at later timepoints depending on the timing of cytokine exposure. *In vivo*, it could be speculated that TGF-β may have no effect on HIV-1 replication in macrophages that have recently differentiated from monocytes recently recruited to early sites of viral replication, but in longer-lived tissue-resident macrophages that have been infected for a longer time period, the cytokine may have an effect on viral replication.

The effects of activins and BMPs on HIV-1 replication in macrophages were also analysed; and activins/BMPs, as well as other non-TGF-β members of the superfamily, were also studied in PBMCs. Activin A and BMP-2 did not modulate HIV-1 replication in macrophages, and activin A did not boost IFN-α-mediated inhibition of virus replication in these cells. Similarly, in PBMCs, activins A and B, BMPs 2 and 6, GDF-15 and inhibin A had no effect on the virus, either alone or in combination with IFN-α. Furthermore, activin A and BMP-2 treatment of cells 24 hours before or after addition of IFN-α did not affect IFN-α action. These findings are in stark contrast to results from studies performed with a range of other viruses such as HBV, HCV, Zika virus[363,413] and a murine gammaherpesvirus[414], which have been shown to be sensitive to restriction by some of these cytokines, particularly BMPs. The lack of effect of activins and BMPs on HIV-1 inhibition by IFN-α are also interesting given data published by others. In hepatocytes, Eddowes and colleagues have shown BMP-6-treated cells have enhanced STAT1 signalling in response to IFN-α, and BMP-6 boosts IFN-α-mediated expression of many ISGs[363], some of which are known to repress HIV-1, including *ISG15*, IFN-induced protein with tetratricopeptide repeats 3 (*IFIT3*), and *IFITM1*[569]. ISG15 prevents HIV-1 virion release[191]. IFIT3 has activity against HIV-1[592] and the mechanism for this is unknown,

but against influenza A virus, IFIT3 complexes with other IFIT members to bind and sequester viral RNA containing a 5' triphosphate group[593].

The lack of effects of BMPs and activins on HIV-1 replication in leukocytes observed in this chapter might be due to cell type-related effects, as studies reporting effects on the replication of other viruses focused on hepatoma or epithelial cell lines[363,413]. Other studies also confirm an IFN-like gene signature after BMP treatment in endothelial and mesenchymal cells[415,416]. It may be the case that although they trigger SMAD phosphorylation in cells of myeloid or lymphoid origin, activins and BMPs elicit a different transcriptional signature in these cells, and this signature lacks genes involved in cellular responsiveness to type I IFNs and antiviral genes that control HIV-1. Another possibility is that in CD8-depleted PBMC experiments, the degree of activation of $CD4^+$ T cells may already have raised transcription of antiviral genes that control HIV-1 replication to the level at which they exert their maximal activity against the virus, as $CD4^+$ T cell activation upregulates many ISGs[573–576]. To investigate this further, it could be examined whether the treatment of $CD4^+$ T cells activated under conditions in this chapter, and treated with activin A or BMP-2, upregulate canonical ISGs. This was further explored in Chapter 5.

The only member of the TGF-β superfamily analysed that was found to impact HIV-1 replication was TGF-β_1, which inhibited virus replication in activated $CD4^+$ T cells and CD8-depleted PBMCs. TGF-β_1 was found to inhibit R5- and X4-tropic virus; and both patient sequence-matched and lab-adapted strains. This is in general agreement with a small amount of published work in T cells/PBMCs studied under similar conditions, but this chapter provides a much more conclusive set of data. Wang and colleagues showed inhibition of the replication of a range of R5-, X4 and dual-tropic viruses in PBMCs by 20ng/ml TGF-β[543]. However, it is unclear in this paper how much productive viral replication occurred in non-cytokine treated

cells. A snapshot of supernatant p24 levels at 10 days post-infection is reported, though no baseline values or consecutive measurements made across a time course are shown. Viral DNA levels are recorded, indicating some reverse transcription, but this does not necessarily equate to significant productive infection. Furthermore, this study used no mitogen activation stimulus to try and elicit T cell activation. An initial figure in this study details low activation marker expression under these conditions. It is generally accepted that HIV-1 does not productively infect resting $CD4^+$ T cells *in vitro* without some form of modification of the intracellular environment[578,579] or the use of allogeneic DC-mediated infection[582], raising further questions about productive replication in this study.

More convincingly, Peterson and colleagues demonstrated inhibition of HIV-1 replication in PHA-stimulated PBMCs after three days of infection at TGF-β concentrations similar to those routinely employed in this chapter (1-10ng/ml) but noted the opposite effect at pg/ml concentrations[544]. Data presented in this chapter indicate a dose-dependent inhibition which is most pronounced at 50ng/ml, with no such enhancement of viral replication in the pg/ml concentrations.

Three studies observed no impact of TGF-β on HIV-1 replication in primary $CD4^+$ T cells, though these discrepancies can be reconciled with data in this chapter. In the first, researchers found no effect of 0.2ng/ml TGF-β on HIV-1 replication in T cells. However, this study used a single-round reporter virus in non-mitogen-stimulated cells[546], which is very different to the multiple-round spreading replication in activated cells in this chapter. Another study reported no effect of TGF-β on HIV-1 replication in a T cell line[545], though primary cells would be considered a better example of the real physiological picture. Many HIV-permissive T cell lines have innate immune defects[576], which may confound results if TGF-β mediates its activity via these mechanisms. Unsurprisingly, IFN-α also only minimally inhibits HIV-1 in many T cell

lines[594]. Finally, a third study showed no effect of TGF-β on HIV-1 NL4-3 replication three and five days post-infection in primary T cells[547]. However, this study used 15μM TGF-β, equivalent to approximately 375μg/ml (25kDa of dimeric recombinant protein from the manufacturer used in this study, equivalent to approximately 25kg/mol), equating to over 7000-fold greater than the concentration used in the *in vitro* assays in this chapter, and over 400-fold greater than the highest circulating concentrations in HIV-1 infection *in vivo* seen in Chapter 3. Although not all batches of recombinant cytokines have equivalent functional activity, the physiological relevance of concentrations that differ by this order of magnitude should be questioned.

Overall, this chapter provides a robust body of evidence that TGF-β_1 inhibits HIV-1 replication in activated primary $CD4^+$ T cells. TGF-β_1-mediated modulation of HIV-1 replication was not as profound as that elicited by IFN-α, but the two combined outperformed TGF-β_1 alone in an additive fashion, suggesting non-overlapping mechanisms of action. The abrogation of signalling by either TGF-β_1 or IFN-α had no effect on the viral inhibition mediated by the other. This makes it unlikely that one restricts the virus by causing secretion and autocrine action of the other, for example. It cannot be said from these data whether either of these cytokines modulate signalling machinery components of the other, but it can be concluded that even if one does, the absence of this modulation does not affect inhibition mediated by the other. However, these data were gathered using relatively high concentrations of TGF-β_1 and IFN-α. It may be that an abundance of ligand renders the impact of TGF-β_1 signalling on IFN-α function expendable, and vice versa. Further work could examine a range of cytokine concentrations in similar experiments.

This chapter found TF viruses to be relatively more resistant to the effects of TGF-β_1 than 6M viruses derived from the same patients, which is likely explained by the fact that TF viruses had a lower replicative efficiency, rather than any TGF-β_1-specific resistance. At least one

other study has also found TF viruses to have a lower replicative efficiency than viruses in chronic infection[595], and another found no statistically significant difference between the two[56]. TF viruses were also more resistant to IFN-α than 6M viruses as reported by others[56,57,595]. However, IFN-α resistance is specifically selected for in TF viruses, and consequently, these viruses did not show any correlation between replicative efficiency and IFN-α resistance, whereas both TF and all viruses (TF and 6M) showed good inverse correlation between replicative efficiency and TGF-β_1 resistance. Therefore, viruses that replicate to the greatest degree with the most rounds of replication are most sensitive to the inhibitory effect of TGF-β_1 (as is known for type I IFNs[566]), but unlike with IFN-α, TF viruses are likely not selected for TGF-β_1 resistance.

These findings could have implications *in vivo*. Despite the absence of evidence for a selection pressure on TF viruses for TGF-β_1 resistance, data in this chapter have nonetheless revealed inhibition of the replication of both TF and 6M viruses by TGF-β_1 *in vitro*, at a concentration (50ng/ml) that was observed (or exceeded) in the plasma of individuals in the subacute and chronic stages of HIV-1 infection *in vivo* in Chapter 3. Although in AHI, plasma TGF-β_1 did not reach this concentration, cytokine concentrations in tissue microenvironments may be different from those seen in plasma, so this does not rule out the possibility of TGF-β_1-mediated restriction of TF virus replication at mucosal sites *in vivo*. The restrictive activity of TGF-β_1 could therefore potentially be harnessed for therapeutic value; discussed in Chapter 6.

In order to study the effects of TGF-β_1 on HIV-1 replication in a less activated cell system, a MDDC-CD4$^+$ T cell transmission infection assay was developed. In this assay CD4$^+$ T cells showed no upregulation of phenotypic activation markers, yet viral replication was well supported. The viral growth kinetics were slower than those in the standard HIV-1 replication assay, taking 9-12 days for the virus to peak. Under these conditions, TGF-β_1 had no effect on

HIV-1 replication. In addition, in the standard HIV-1 replication assay, TGF-β_1 stemmed viral replication to a lesser extent in cells activated with a weaker anti-CD3/CD28 stimulus. However, one weakness of the latter experiments is that the lower activation stimulus resulted in a reduced viral replicative efficiency (as measured by p24 in supernatant), which may have been due to the virus undergoing fewer rounds of replication. This could explain the reduced effect of TGF-β_1 in inhibiting HIV-1 replication under these conditions, rather than due to the reduced cell activation status. To address this, future work could utilise an HIV-1 entry inhibitor to analyse the extent to which supernatant p24 is reduced by TGF-β_1 after a single round of viral replication. It may also be the case that TGF-β_1 mediates some inhibitory effect on HIV-1 replication through a reduction in cell activation, as activation status is known to correlate with permissiveness to, and productiveness of HIV-1 infection[77,570]. This could explain why the cytokine has no effect on viral replication in cells with a less activated immunophenotype, or in macrophages. The effects of TGF-β_1 on $CD4^+$ T cell activation status under high activation conditions used in the standard HIV-1 replication assay, as well as other possible mechanisms by which the cytokine may inhibit HIV-1 replication, were addressed in Chapter 5.

As previously mentioned, TCR ligation and $CD4^+$ T cell activation upregulates the expression of many ISGs, which makes it possible for the strong activation seen in the standard HIV-1 replication assay system to pre-raise potential HIV-controlling genes to maximal effective levels, rendering additionally increased expression by recombinant activin A and BMP-2 redundant, if these cytokines do induce this transcriptional profile in $CD4^+$ T cells. That activin A and BMP-2 also had no effect in phenotypically less activated cells makes it less likely that these cytokines induce any HIV-restrictive genes in $CD4^+$ T cells at all. However, there may still be some degree of $CD4^+$ T cell activation in the MDDC assay system, evidenced by the ability of these cells to support productive viral replication, despite the outwardly “resting” phenotype, as is seen *in vivo*[78,79], so the same redundancy may be occurring. Given published

literature on the induction of antiviral genes by activins and BMPs in other cell types, there remains a strong case for further work to establish whether this is the case in HIV-permissive cell types. If these cytokines do upregulate antiviral genes in common with IFN-α in $CD4^+$ T cells yet, unlike IFN-α, have no inhibitory activity on HIV-1, this may provide valuable insight into ruling out certain ISGs for having HIV-controlling activity, as the type I IFN transcriptome is vast, and the relative contributions of each ISG to HIV-1 control are not well-defined.

To analyse the effects of TGF-β_1 (as well as BMP-2, activin A and IFN-α) on HIV-1 replication in a more epithelial-like cell type, human embryonic 293FT cells were transfected with HIV-1 DNA. No effect was seen on HIV-1 replication. Interestingly, a prior study has documented inhibition of a murine gammaherpesvirus in these cells by BMP-2 overexpression[414]. However, the same study found no effect of BMP-2 on the replication of VSV, indicating that this phenomenon may be virus-specific, likely due to the repertoire of antiviral genes induced and the relative sensitivity of the virus in question to those genes. Although IFN-α was optimistically selected as a positive control of HIV-1 inhibition in 293FT cells, it only modestly inhibited the virus. This was not entirely unexpected, given reports by others of these cells being poorly responsive to IFN-α[576], concluded either due to failing to upregulate genes with anti-HIV-1 activity such as APOBEC3G[596], or failing to inhibit VSV replication[597]. In light of these findings, it may be prudent in future work to investigate whether 293FT cells upregulate key antiviral genes in response to TGF-β_1, BMP-2, activin A and IFN-α.

In conclusion, this chapter has demonstrated TGF-β_1-mediated control of HIV-1 replication in activated $CD4^+$ T cells that operates independently of IFN-α, and no inhibition in macrophages. The action of TGF-β_1 is contingent on T cell activation status, which may also explain the absence of an effect in macrophages. Activins and BMPs completely lacked any effect on HIV-1 replication in both macrophages and $CD4^+$ T cells. Further work is now needed to elucidate

the mechanism(s) by which TGF-β_1 exerts this activity, as well as probing why activin A and BMP-2 fail to do the same despite a strong precedent for these cytokines to induce an IFN-like gene signature in other cell types that is capable of controlling other viruses. Chapter 5 of this thesis addressed these questions.

Chapter 5

Exploration of the mechanisms of TGF-β_1-mediated inhibition of HIV-1 replication

5.1 Introduction

In the previous chapter, TGF-β_1 inhibited both primary R5-tropic and lab-adapted X4-tropic HIV-1 strains in activated CD4$^+$ T cells, but had no effect on HIV-1 replication in macrophages or less highly activated CD4$^+$ T cells, showing that its inhibitory activity is cell type- and activation state-dependent. TGF-β_1 has also been reported to inhibit or conversely enhance HIV-1 replication in a number of prior studies performed principally with lab-adapted viruses in different *in vitro* infection systems, with relatively few studies offering mechanistic insights into how the cytokine may be exerting its effects on the virus. TGF-β_1 has pleiotropic effects on T cells, influencing differentiation, homeostasis, cell cycle activity, activation and proliferation[254]; raising a number of hypotheses as to how it may influence HIV-1 replication. Addressing these hypotheses was the focus of this chapter.

Type I IFNs inhibit HIV-1 replication principally via upregulation of expression of genes encoding proteins that have direct antiviral activity against HIV-1[191,554,569,592]. Given the precedent set for other TGF-β superfamily cytokines to induce the expression of ISGs, many of which are antiviral, in other cell types[363,415,416], whether this transcriptional signature is induced in activated CD4$^+$ T cells by the TGF-β superfamily cytokines studied in this thesis thusfar (TGF-β_1, activin A, BMP-2) warranted investigation.

Contrasting with the inhibitory effects observed on HIV-1 replication in activated CD4$^+$ T cells in Chapter 4, TGF-β has been reported to increase expression of HIV-1 coreceptors CCR5 and CXCR4 in CD4$^+$ T cells[543] (although, cells in this study were non-mitogen-stimulated),

which can render cells more susceptible to infection. Similarly, TGF-β orchestrates Th cell differentiation and plays roles in Tfh[318], Th17 and Treg[138] differentiation, whilst inhibiting Th1[320] and Th2 differentiation[321]. Given the differential susceptibility of these Th subsets to HIV-1 infection[243,245–247,598] or HIV-1-induced apoptosis[599], the impact of TGF-β_1 on subset differentiation bias under the culture conditions of Chapter 4 was of interest to explore.

There is a body of literature examining the effects of TGF-β on transcription from the HIV-1 LTR. The HIV-1 5' LTR serves as the viral promoter, containing U3, R and U5 regions. The U3 region contains a "CATA box" sequence approximately 25 base pairs upstream of the transcription start site, and like the similar TATA box in eukaryotic genes, is bound by host cell RNA polymerase II[600]. The U3 region also contains binding sites for host transcription factors NF-κB[38], NFAT and SP1[39] (Fig. 5.1). Studies describing an impact of TGF-β on transcription from the HIV-1 LTR activity have yielded conflicting results: the effects mediated may be cell type-dependent[546,601–603].

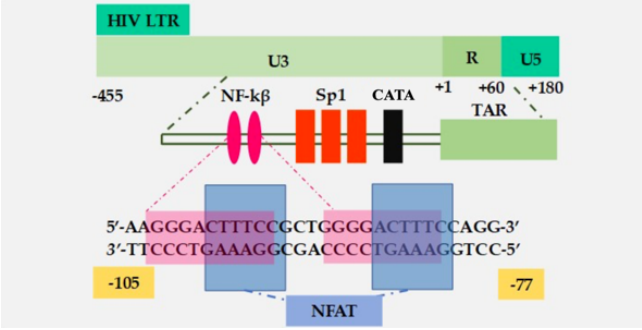


Figure 5.1 The structure of the HIV-1 LTR
The HIV-1 LTR, which comprises U3, R and U5 regions. The U3 region contains two NF-κB binding sites (pink), which overlap with two NFAT binding sites (blue), and three SP1 binding sites. Numbers denote position relative to the 5' transcription start site (+1). TAR=trans-activation response element, which is bound by Tat[31], stimulating transcription from the LTR. Figure adapted from[604].

FOXP3, the expression of which is induced in the differentiation of pTregs from TGF-β-exposed naïve $CD4^+$ T cells, also modulates activity from the HIV-1 LTR, although as with TGF-β, results from different studies are also conflicting. In overexpression experiments,

FOXP3 has been seen to both diminish[605,606] and enhance[607] HIV-1 LTR activity in primary $CD4^+$ T cells. Inhibition has also been seen in 293T cells transfected with FOXP3[605,607].

Regardless of the discordant effects observed of TGF-β (or FOXP3) on the HIV-1 LTR, almost all studies report a dependence on U3 region proximal NF-κB binding sites[546,603,605–607]. The deletion of these sites (located around -105 to -77 to the 5' transcription start site (Fig. 5.1)) abrogates the effect, implying TGF-β/FOXP3-mediated modulation of NF-κB biology.

The NF-κB transcription factor family comprises five members in eukaryotes; p50, p52, p65 (RelA), RelB and c-Rel, which form homo- or heterodimers, the most abundant of which are p50/p65 heterodimers[608]. The NF-κB pathway is activated in leukocytes through stimulation of a breadth of receptors including pro-inflammatory cytokine receptors, PRRs and the TCR; and initiates transcription of hundreds of target genes involved in immune responses, inflammation and cellular proliferation, chemotaxis, adhesion, apoptosis and differentiation[609]. NF-κB is sequestered in inactive form in the cytoplasm bound to inhibitor of kappa B (IκB) family proteins. IκB is phosphorylated by the IκB kinase (IKK) complex of proteins (made up of IKK1, IKK2 and IKKγ), leading to IκB proteasomal degradation, liberating NF-κB and allowing its nuclear entry, where it can directly bind DNA[608] (Fig. 5.2). Inside the nucleus, post-translational NF-κB subunit modifications including phosphorylation and acetylation greatly increase the potency and duration of the transcriptional response[610].

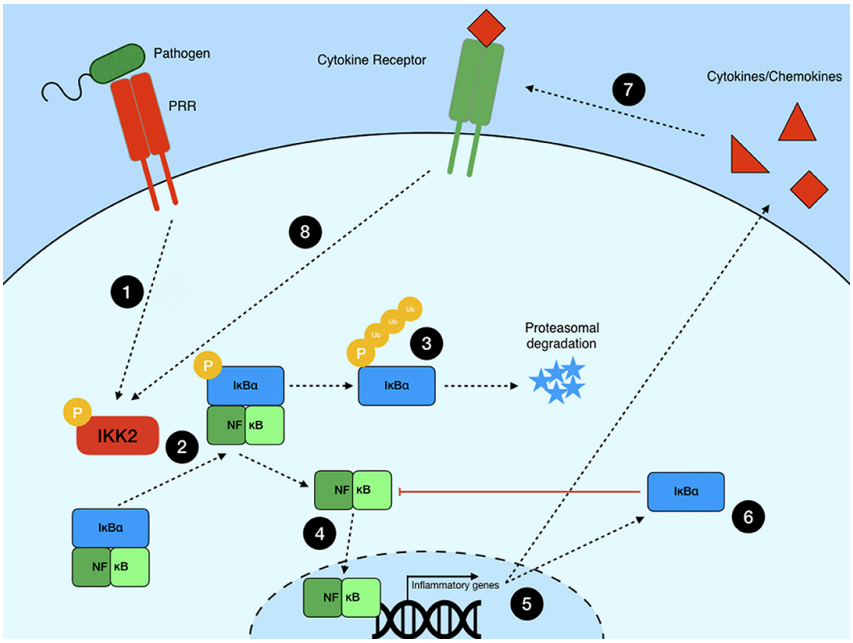


Figure 5.2 Canonical NF-κB pathway activation
(1) PRR, cytokine receptor or other receptor (e.g. TCR) stimulation leads to phosphorylation and activation of IKK2. (2) IKK2 phosphorylates IκBα, (3) resulting in its ubiquitination and proteasome-mediated destruction. (4) This relinquishes NF-κB from its complex with IκBα, allowing its nuclear entry. (5) NF-κB binds DNA, initiating transcription of target genes. (6) These include IκBα, which negatively feeds back to limit excessive activation of the pathway. (7) Other products include cytokines and chemokines (e.g. TNF), (8) which may further positively stimulate the pathway in an autocrine manner. Figure taken from[611].

When measuring NF-κB activation in the laboratory setting, it is common practice to analyse multiple parts of the pathway to draw robust conclusions. Popular choices indicating pathway activation include the detection of p65 phosphorylation, IκB phosphorylation or a reduction in total IκB, assessed by western blot on whole cell extracts[612]. An increase in the nuclear to cytoplasmic ratio of p65 by fractionation western blot or image-based tracking can also be employed[612]. The binding of NF-κB to DNA can be measured on nuclear extracts using electrophoretic mobility shift assay[613]. The use of NF-κB-responsive reporter constructs has also been reported[614].

The NF-κB pathway is mostly considered to be stimulated by TGF-β[615], but only within a few hours *in vitro*, after which the opposite is seen due to negative feedback loops. TAK1 activates IKK leading to NF-κB activation in squamous cell carcinoma cells within a few hours of *in vitro* TGF-β treatment[616]. The same findings have been noted in chondrosarcoma cells[617]. One

study showed TGF-β to induce TAK1-mediated NF-κB activation after three hours, sequentially followed by IκB-mediated suppression at a 24-hour timepoint in epithelial cells, hepatocytes and fibroblasts[618]. Accordingly, other studies using salivary gland cells[613] and a breast cancer carcinoma cell line[619], showed TGF-β inhibits the NF-κB pathway at 48 hours post-treatment through induction of IκBα mRNA or prolongation of IκBα protein half-life. However, in intestinal mononuclear cells, TGF-β upregulates IκBα protein expression within only 7 hours of treatment[620], indicating that the effects of TGF-β on the NF-κB pathway may be cell type dependent.

Given the findings in Chapter 4, in which TGF-β_1 was shown to inhibit HIV-1 replication in activated $CD4^+$ T cells but not those with a less activated phenotype, another possible mechanism by which TGF-β may suppress HIV-1 replication is through modulation of cell activation status. TGF-β is generally considered to impede T cell activation and proliferation[323,325]. However, the degree to which TGF-β affects T cell activation may depend on the initial T cell activation status. Whilst both resting and activated T cells are responsive to TGF-β, strong TCR stimulation downregulates surface expression of TGFBR1 (ALK5) and TGFBR2 rendering T cells less TGF-β-responsive[563]. This could explain why TGF-β inhibits proliferation of naïve T cells at first activation, but not re-stimulated effector cells[621]. The same phenomenon is seen when comparing iTreg-mediated suppression of proliferation following activation of naïve versus effector T cells[622]; and Tregs utilise TGF-β as one major mechanism to exert their immunosuppressive effects.

In addition, in activated cells, TGF-β has been seen to downregulate the activation marker CD25, but upregulate early activation marker CD69[623], indicating TGF-β action on activation marker expression is not always unidirectional, which may again be contingent on cell activation status at the time of cytokine stimulation. Thus, examining the effects of TGF-β on

T cell activation and proliferation in the context of the conditions used in this thesis was important to explore.

One mechanistic study appeared to show TGF-β-mediated inhibition of R5-, X4- and dual-tropic HIV-1 strains in $CD4^+$ T cells that the authors proposed to be due to apoptosis driven by the TGF-β/infection combination (with no apoptosis detected in TGF-β-treated, uninfected cells), which was most pronounced with a R5 virus (HIV-1 BaL)[543]. However, in the single virus strain that appeared most appreciably sensitive to TGF-β (HIV-1 89.6, 10-fold reduction in amount of virus), the degree of apoptosis appeared modest compared to control (5% more apoptosis). In addition, apoptosis of $CD4^+$ T cells was not shown for this virus, instead only apoptosis of all PBMCs. In contrast, the strain of virus in which $CD4^+$ T cell apoptosis appeared most marked (HIV-1 BaL, 4-fold more apoptosis compared to control), was only inhibited mildly by TGF-β (2-fold reduction in amount of virus). Thus, this mechanism does not entirely provide a satisfactory explanation for TGF-β-mediated viral inhibition. In addition, it also remains questionable whether there was productive viral replication in this study as baseline supernatant p24 levels following infection and washing of cells were not measured[543]. Regardless, whether TGF-β_1 mediates anti-HIV-1 activity through a reduction in cell viability was another a pertinent question to be addressed.

In this chapter I thus aimed to explore:

- The effects of TGF-β superfamily cytokines on the $CD4^+$ T cell transcriptome.
- Whether TGF-β_1 impacts Th phenotype and FOXP3 expression
- Whether TGF-β_1 impacts CCR5 and CXCR4 expression
- The effects of TGF-β_1 on HIV-1 LTR transcriptional activity and NF-κB activation in $CD4^+$ T cells.
- The effects of TGF-β_1 on $CD4^+$ T cell activation status, proliferation and viability.

5.2 Results

5.2.1 TGF-β_1 modulates the expression of a distinct set of genes to IFN-α in activated $CD4^+$ T cells, with no upregulation of canonical antiviral genes

To understand more about what TGF-β_1 does to the cells in the assay conditions used in this thesis, as well as to address the antiviral gene upregulation hypothesis and to gain insight into potential crosstalk between TGF-β_1 and IFN-α pathways, transcriptional analysis of $CD4^+$ T cells was carried out. $CD4^+$ T cells from HIV-seronegative donors were activated for 48 hours in the same way as in the standard HIV-1 replication assay system, and treated with these cytokines for 24 hours, before RNA extraction and RNAseq. RNA was also extracted from an aliquot of the same cells before activation. mRNA was sequenced using an Illumina HiSeq platform. FASTQ files were analysed by mapping of reads to the reference genome GRCh38/hg38 using aligner STAR, and DEGs calculated using the Bioconductor package *edgeR*, all conducted by Nicki Gray (University of Oxford, UK).

Activated cells exhibited differential expression of 8993 genes (false discovery rate or adjusted P value <0.05) relative to non-activated cells (Fig. 5.3A and Appendix I). Pathway analysis revealed differential expression of gene sets involved in diverse processes such as TCR signalling, mammalian target of rapamycin signalling, ubiquitination, translation and protein synthesis (Fig. 5.3B), consistent with T cell activation.

IFN-α treatment of activated cells for 24 hours resulted in differential expression of 766 genes (adjusted P <0.05) relative to activated, non-cytokine treated control cells (Fig. 5.4A and Appendix II). Pathway analysis showed downregulation of eukaryotic initiation factor 2 signalling (a major mechanism by which type I IFNs shut down protein synthesis, through activation of protein kinase R^{624}); upregulation of PRRs and downstream signalling pathways plus IFN signalling; and modulation of genes involved in antigen presentation (Fig. 5.4B).

Examples of specific genes that were upregulated included HIV-1 restriction factors such as *BST2*, *SAMHD1*, *MX2*, *OAS1, TRIM5* and *IFITM3* (but not *APOBEC3G*); as well as other canonical ISGs that had also been identified as upregulated by TGF-β superfamily cytokines in hepatocytes in a prior report[363], such as *STAT2*, *IRF9, IFI6*, *ISG15*, although not *JAK1*, which was upregulated in that study.

TGF-β_1 treatment of activated cells resulted in differential expression of 263 genes (adjusted P<0.05) relative to untreated controls (Fig. 5.5A and Appendix III). These included *TGFBR2* (1.3-fold upregulation, adjusted P=0.005), *SMAD7* (2.8-fold upregulation, adjusted P=1.62e-6), and *PMEPA1* (6.8-fold upregulation, adjusted P=1.57e-5) canonical TGF-β target genes[625,626] that are useful indicators of a cellular response to this cytokine. Of the 263 genes whose expression was significantly modulated by TGF-β_1, 21 were also differentially expressed in IFN-α treated cells relative to the control condition (Fig. 5.5B). These overlapping DEGs are detailed in Table 5.1. They had diverse functions but did not include any of the well-characterised HIV-1 restriction factors mentioned above.

One of the 21 genes, the gene encoding chemokine XCL1, has documented inhibitory activity against HIV-1[627]. XCL1, also known as lymphotactin, is particularly expressed by $CD8^+$ T cells but is also produced by Th1 cells[628], and was appreciably expressed in activated $CD4^+$ T cells in the RNAseq dataset ($\log_2$ counts per million (CPM) 1.90). However, TGF-β_1 treatment downregulated, rather than upregulated *XCL1* by a fold-change of 0.57 (adjusted P=0.0057), as did IFN-α by a fold-change of 0.66 (adjusted P=0.032) (Appendix III). Overall, it was concluded that the TGF-β_1-induced transcriptome is distinct from that of IFN-α in activated $CD4^+$ T cells, with no upregulation of canonical antiviral genes by the former.

To confirm the upregulation of canonical TGF-β target genes *TGFBR2* and *SMAD7* and downregulation of *XCL1* by TGF-β_1, expression of these genes in the same cells as those employed for the RNAseq analysis was determined by qRT-PCR. These data are shown in Fig. 5.6, along with analysis of expression of the same genes in IFN-α-treated cells for comparison. This figure also shows qRT-PCR validation of other genes differentially regulated by TGF-β_1 that are considered later in this chapter. For all genes validated in this way, qRT-PCR corroborated the RNAseq findings in terms of directionality (though not always quite reaching statistical significance in the qRT-PCR analysis), giving further support that these selected genes were differentially regulated by TGF-β_1 (and not by IFN-α). One exception to this was *TGFBR2,* which was slightly but nonetheless statistically significantly upregulated in IFN-α-treated as compared to control cells in the qRT-PCR analysis but not in the RNAseq analysis (Fig. 5.6, Appendix II).

Table 5.1
Genes differentially regulated by both TGF-β_1 and IFN-α in activated $CD4^+$ T cells

Gene	Protein encoded	Description	TGF-β_1 [A]		IFN-α [B]	
			Log_2FC	Adj P	Log_2FC	Adj P
ARID5A	AT-rich interaction domain 5A	Cell growth regulator[629], stabilises IL-6 mRNA[630]	0.36	0.009	0.36	0.003
ATP1B1	ATPase Na+/K+ transporting subunit beta 1	Na+ K+ ATPase subunit protein[629]	1.09	0.002	-0.74	0.037
CD38	CD38	T cell activation marker. Modulator of cellular NAD availability[631]	-0.65	0.017	1.35	1.17 e-07
CERK	Ceramide kinase	Involved in sphingolipid metabolism[629]	0.44	0.014	-0.47	0.003
CHI3L2	Chitinase 3-like 2	Lacks chitinase activity. Involved in cartilage generation in chondrocytes[629]	0.88	0.003	0.10	2e-04
COL6A3	Collagen type VI alpha 3 chain	An alpha chain of type VI collagen[629]	1.20	0.003	-0.97	0.015
CSF2	GM-CSF	Stimulates granulocyte and	-1.42	1e-04	-0.94	0.006

		macrophage production/activity[632]				
FHL3	Four and a half LIM domains 3	Actin-binding protein. Interacts with SMADs 2, 3 and 4, and induce TGF-β-like effects[633]	0.89	0.004	0.70	0.016
FLJ32255	FLJ32255	Uncharacterised	0.46	0.048	0.81	2.24 e-05
HOPX	HOP homeobox	Modulates cardiac development[629]	-0.78	0.047	-0.93	0.005
IRS1	Insulin receptor substrate 1	Signal transduction from the insulin receptor and the insulin-like growth factor-1 receptor[629]	0.78	0.021	1.82	1.75 e-08
ITGAE	Integrin subunit alpha E	Integrin protein	0.85	0.001	-0.57	0.023
KIAA1671	KIAA1671	Uncharacterised	1.20	4.89 e-06	0.55	0.026
PPARG	Peroxisome proliferator activated receptor gamma	Regulator of lipid and glucose metabolism[629]	0.75	0.013	-0.68	0.020
PRF1	Perforin 1	Forms pores in membranes to enable granzyme entry during NK and $CD8^+$ T cell cytolysis[629]	-0.45	0.042	0.49	0.010
REEP2	Receptor accessory protein 2	Endoplasmic reticulum-shaping protein[629]	0.92	0.018	-0.82	0.034
RGS1	Regulator of G protein signalling 1	Reduces G protein signalling	0.65	0.004	0.67	0.001
SARDH	Sarcosine dehydrogenase	Mitochondrial enzyme catalysing sarcosine to glycine	1.46	1.48 e-10	-0.62	2e-04
TMEM-200A	Transmembrane protein 200A	Uncharacterised	0.72	0.028	-0.72	0.018
VASH1	Vasohibin 1	Inhibitor of angiogenesis[634]	1.65	1.01 e-07	-0.69	0.012
XCL1	X-C motif chemokine ligand 1	Lymphocyte-attracting chemokine with antiviral inhibitory activity against HIV-1[627]	-0.82	0.006	-0.61	0.032

[A] Log_2 fold change and adjusted P values for DEGs in TGF-β_1-treated activated $CD4^+$ T cells relative to untreated control cells.

[B] Log_2 fold change and adjusted P values for DEGs in IFN-α-treated activated $CD4^+$ T cells relative to untreated control cells.

FC=fold change, Adj P= adjusted P value.

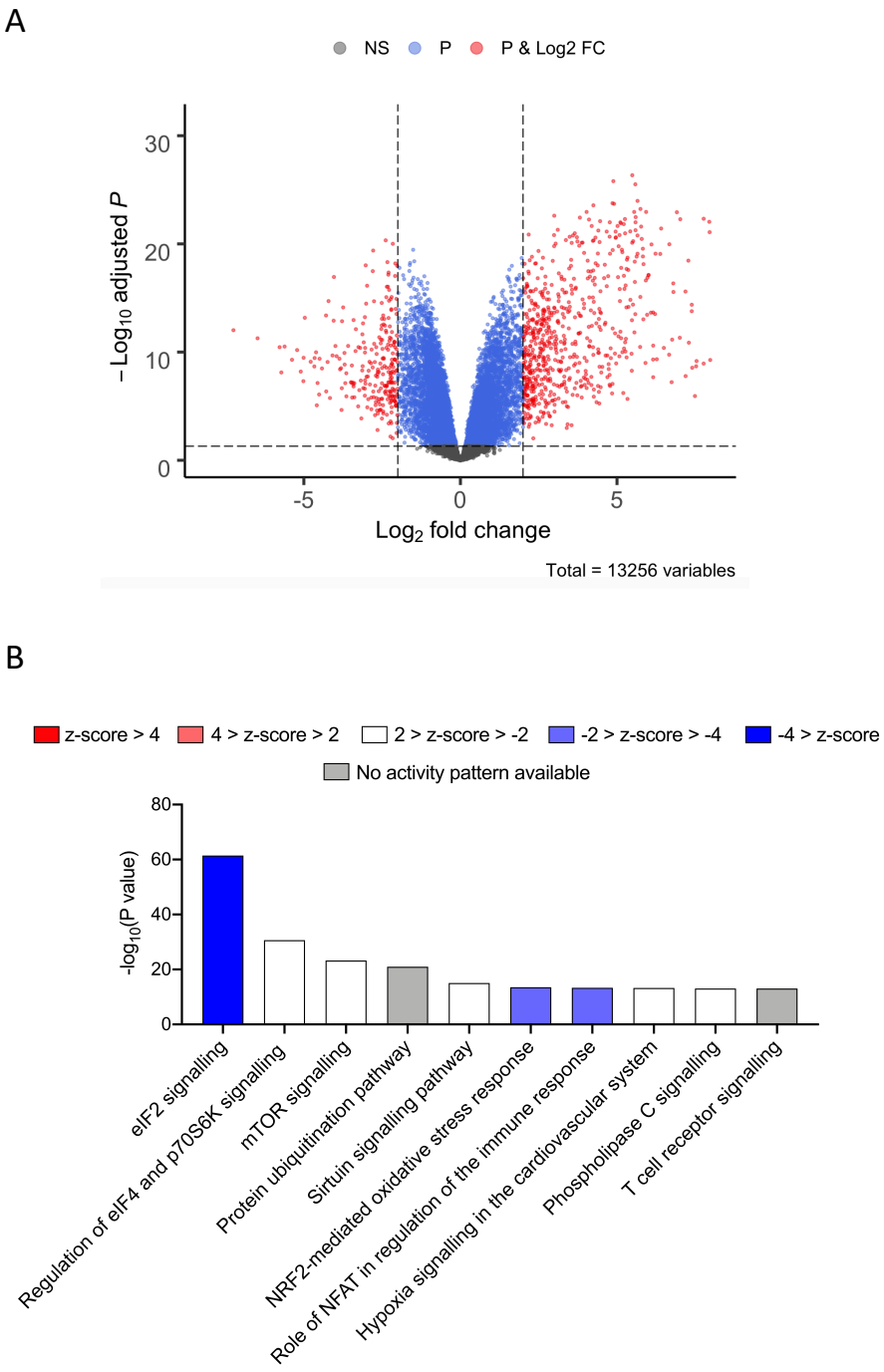


Figure 5.3 Comparative analysis of gene expression in CD4+ T cells directly *ex vivo* and after activation for 72 hours with antibodies to CD3 and CD28

CD4+ T cells from n=5 HIV-seronegative donors were activated by stimulation for 72 hours with 50ng/ml anti-CD3, 100ng/ml anti-CD28 and 50IU/ml IL-2 before RNA extraction and RNAseq. **A.** Volcano plot illustrating genes differentially expressed in 72-hour activated cells relative to non-activated cells. NS=not significant. Blue dots indicate an adjusted P value <0.05. Red dots indicate both an adjusted P value <0.05 and a $\log_2$ fold change of >2 (>4-fold). **B.** DEGs with an adjusted P value <0.05 and a $\log_2$ CPM value of >6 (>64 CPM) and a fold change of any magnitude were subjected to Ingenuity pathway analysis. The top ten pathways are displayed, from left to right starting with the most statistically significantly differentially regulated pathways, as defined by pathway analysis P value. Z-scores indicate the directionality and magnitude of differential expression of genes within a pathway, and bars are coloured according to their Z-score.

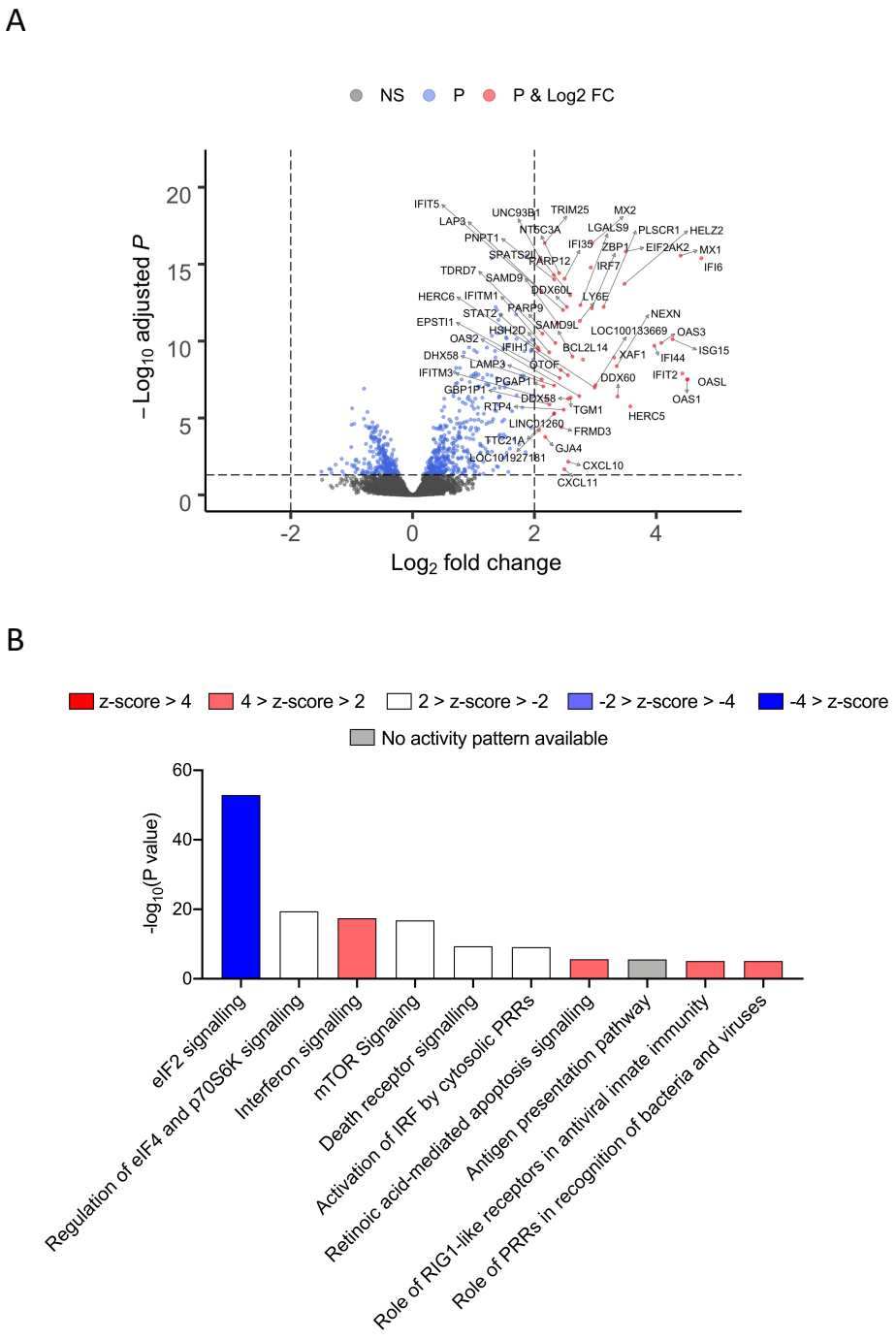


Figure 5.4 The effects of IFN-α on the transcriptome of activated CD4⁺ T cells
CD4⁺ T cells from n=5 HIV-seronegative donors were activated by stimulation for 48 hours with 50ng/ml anti-CD3, 100ng/ml anti-CD28 and 50IU/ml IL-2 before treatment with IFN-α (1000IU/ml) for 24 hours followed by RNA extraction and RNAseq. **A.** Volcano plot illustrating genes differentially expressed in IFN-α-treated cells relative to untreated control cells. NS=not significant. Blue dots indicate an adjusted P value <0.05. Red dots indicate both an adjusted P value <0.05 and a $\log_2$ fold change of >2 (>4-fold). **B.** DEGs with an adjusted P value <0.05 and a $\log_2$ CPM of >1 (>2 CPM) and a fold change of any magnitude were subjected to Ingenuity pathway analysis. The top ten pathways are displayed, from left to right starting with the most statistically significantly differentially regulated pathways, as defined by pathway analysis P value. Z-scores indicate the directionality and magnitude of differential expression of genes within a pathway, and bars are coloured according to their Z-score.

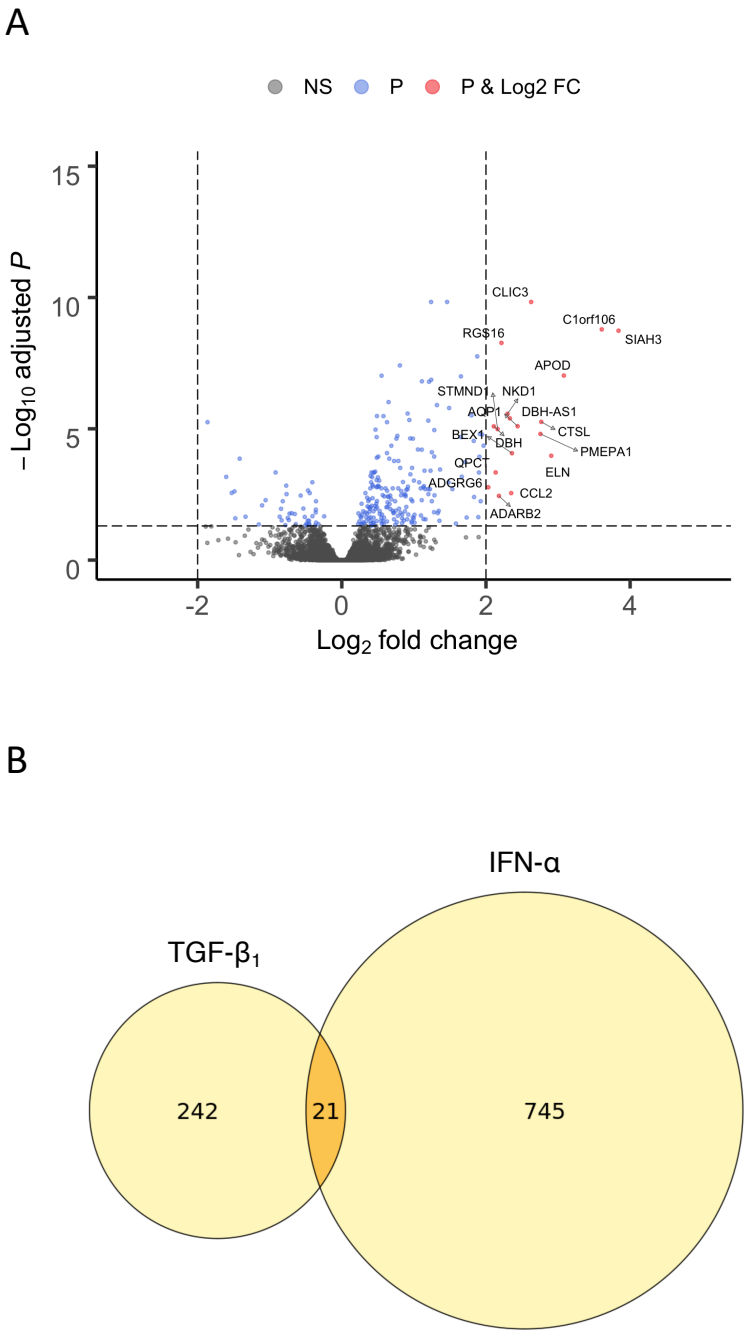


Figure 5.5 The effects of TGF-β$_1$ on the transcriptome of activated CD4$^+$ T cells
CD4$^+$ T cells from n=5 HIV-seronegative donors were activated by stimulation for 48 hours with 50ng/ml anti-CD3, 100ng/ml anti-CD28 and 50IU/ml IL-2 before treatment with TGF-β$_1$ (50ng/ml) for 24 hours followed by RNA extraction and RNAseq. **A.** Volcano plot illustrating genes differentially expressed in TGF-β$_1$-treated cells relative to untreated control cells. NS=not significant. Blue dots indicate an adjusted P value <0.05. Red dots indicate both an adjusted P value <0.05 and a log$_2$ fold change of >2 (>4-fold). **B.** Area proportional Venn diagram illustrating the extent of overlap of genes differentially expressed (adjusted P<0.05) relative to untreated control cells in TGF-β$_1$ and IFN-α treated cells with a log$_2$ CPM of >1 (>2 CPM) and a fold change of any magnitude.

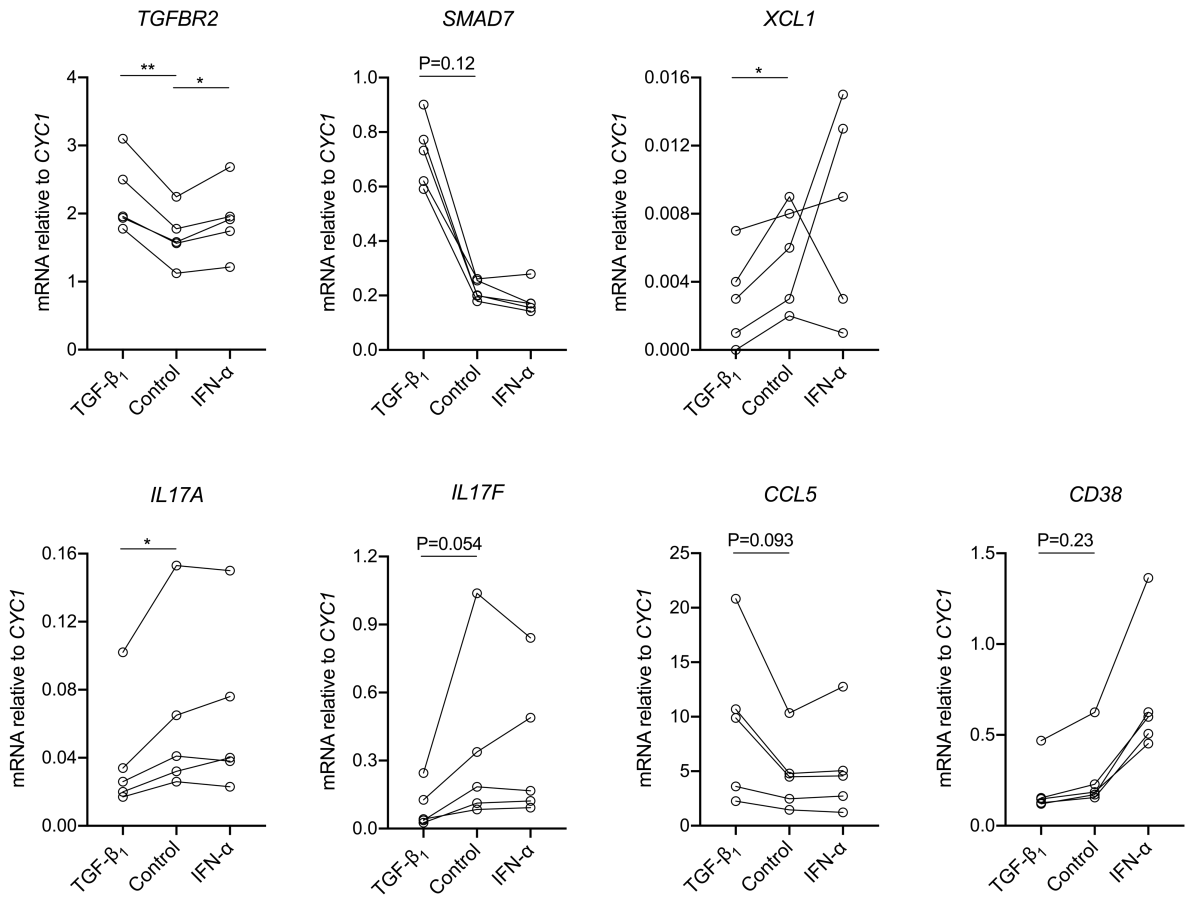


Figure 5.6 qRT-PCR analysis of selected genes in TGF-β$_1$- and IFN-α-treated activated CD4$^+$ T cells identified from the RNA sequencing dataset
CD4$^+$ T cells from n=5 HIV-seronegative donors were activated for 48 hours with 50ng/ml anti-CD3, 100ng/ml anti-CD28 and 50IU/ml IL-2 before treatment with TGF-β$_1$ (50ng/ml) or IFN-α (1000IU/ml) for 24 hours followed by RNA extraction and sequencing to determine gene expression levels. The expression of selected genes identified on the basis of RNAseq analysis as being differentially regulated by TGF-β$_1$ in the same cell lysates was then re-analysed by qRT-PCR. Gene expression is shown relative to the expression of the stably expressed reference gene, *CYC1*. Expression of each gene in cytokine-treated cells was compared to that in control condition (cells activated for 72 hours with no cytokine treatment for the last 24 hours), using a Friedman test with Dunn's post-test comparing to control (*SMAD7*, *IL17A*, *IL17F*, *CD38*) or one-way ANOVA with Dunnett's post-test comparing to control (*TGFBR2*, *XCL1*, *CCL5*), *P<0.05, **P<0.01.

5.2.2 TGF-β$_1$ and IFN-α do not modulate the transcription of genes involved in one-another's signalling pathways

Work by others has demonstrated the upregulation of IRFs in hepatoma cells, DCs and CD4$^+$ T cells by TGF-β superfamily cytokines[363,410,421]. Given this precedent, it was investigated whether TGF-β$_1$ or IFN-α regulate the expression of genes involved in each other's signalling pathways in CD4$^+$ T cells, using the RNAseq datasets.

The effects of TGF-β_1 on genes involved in type I IFN transcription (IRF genes) and involved in type I IFN signalling and ISG expression (IFN receptor genes, JAK/STAT genes and IRF9[106]) were examined. STAT3, a negative regulator of type I IFN signalling[427] was also examined. In cells activated for 48 hours and treated with TGF-β_1 for 24 hours, no differential expression (relative to untreated cells) of any type I IFN pathway genes was observed (Table 5.2).

Table 5.2 Analysis of the effects of TGF-β_1 on expression of IFN-α signalling pathway genes in activated CD4$^+$ T cells

Gene	Protein encoded	Log_2 fold change [A]	Adjusted P value [A]
IFNAR1	IFNAR alpha chain	0.024	0.9996
IFNAR2	IFNAR beta chain	0.205	0.6401
IRF1	IRF1	0.097	0.9996
IRF3	IRF3	-0.078	0.9996
IRF5	IRF5	-0.216	0.9047
IRF7	IRF7	0.007	0.9996
IRF8	IRF8	-0.142	0.9551
IRF9	IRF9	0.050	0.9996
JAK1	JAK1	0.003	0.9996
STAT1	STAT1	-0.044	0.9996
STAT2	STAT2	-0.038	0.9996
STAT3	STAT3	0.041	0.9996
TYK2	Tyrosine kinase 2 [B]	-0.093	0.9261

[A] Log_2 fold change and adjusted P values for genes differentially expressed in TGF-β_1 (50ng/ml)-treated activated CD4$^+$ T cells relative to untreated control cells.
[B] Member of the JAK family involved in type I IFN signalling

The effects of IFN-α on TGF-β superfamily receptor and SMAD genes were also analysed by comparing expression levels in cells activated for 48 hours and treated with IFN-α for 24 hours to those in activated cells not treated with IFN-α. As noted previously, IFN-α upregulated *FHL3* (Table 5.1), an actin-binding protein that binds with SMADs 2, 3 and 4, and induces TGF-β-like effects in a TGF-β-independent manner[633]. However, overall no differential expression (relative to untreated cells) of any major TGF-β superfamily signalling pathway genes was observed by RNAseq (Table 5.3); although as previously mentioned *TGFBR2,* expression of which was also assessed by qRT-PCR owing to the fact it is a common TGF-β_1 target gene, was found to be marginally upregulated by IFN-α when analysed by this method (Fig. 5.6).

Table 5.3 Analysis of the effects of IFN-α on expression of TGF-β superfamily signalling pathway genes in activated CD4+ T cells			
Gene	**Protein encoded**	**Log_2 fold change [A]**	**Adjusted P value [A]**
ACVR1	ALK2	-0.025	0.9691
ACVR1B	ALK4	-0.025	0.9691
ACVR1C	ALK7	-0.069	0.9130
ACVR2A	ACVR2A	0.056	0.9386
ACVR2B	ACVR2B	-0.046	0.9575
ACVRL1	ALK1	0.099	0.9632
BMPR1A	ALK3	-0.053	0.9386
BMPR1B	ALK6	ND[B]	
BMPR2	BMPR2	0.443	0.0945
SMAD1	SMAD1	0.028	0.9879
SMAD2	SMAD2	-0.077	0.7517
SMAD3	SMAD3	0.086	0.8800
SMAD4	SMAD4	0.140	0.5886
SMAD5	SMAD5	-0.156	0.6516
SMAD6	SMAD6	ND	
SMAD7	SMAD7	-0.461	0.1665
SMAD9	SMAD8	ND	
TGFBR1	ALK5	-0.331	0.1028
TGFBR2	TGFBR2	0.017	0.9799

[A] Log_2 fold change and adjusted P values for genes differentially expressed in IFN-α (1000IU/ml)-treated activated CD4+ T cells relative to untreated control cells.
[B] No data. No reads were mapped to these genes.

5.2.3 Activin A and BMP-2 minimally alter the transcriptome of activated CD4+ T cells and do not induce the expression of antiviral genes

In hepatoma[363], epithelial[363], endothelial[416] and mesenchymal[415] cell lines, activins and BMPs are documented to upregulate canonical ISGs including some antiviral genes. To analyse the transcriptional changes induced by activin A and BMP-2 in CD4+ T cells activated under the same activation conditions as in the standard HIV-1 replication assays, 48-hour activated cells were treated with these cytokines for 24 hours, and gene expression was profiled as part of the same RNAseq experiment as detailed previously.

Activin A treatment of activated CD4+ T cells for 24 hours resulted in no significant changes in gene expression (i.e. no DEGs were identified with adjusted P <0.05) relative to untreated control cells. When considering unadjusted P values, activin A differentially regulated 186 genes (unadjusted P<0.05) (Appendix IV), one of which was *MMP2*, an activin A target gene[635],

with a 1.65-fold upregulation, unadjusted P=0.035. This indicated that the cells likely had responded to activin A treatment, but overall, relatively little differential gene expression was induced. The trend for upregulation of *MMP2* was verified by qRT-PCR, although the difference in expression observed in activin A-treated versus control cells did not quite reach statistical significance (Fig. 5.7).

BMP-2 treatment of activated cells for 24 hours also resulted in identification of no DEGs (adjusted P <0.05) relative to untreated controls. Similar to with activin A, when considering unadjusted P values, the canonical BMP target gene *ID3*[636] was the second most differentially expressed of 76 genes (unadjusted P<0.05) (Appendix V), with a 1.4-fold upregulation, unadjusted P=0.006. The trend for upregulation of *ID3* was verified by qRT-PCR, although the change did not quite reach statistical significance (Fig. 5.7).

Given the lack of upregulation of genes encoding HIV-1 restriction factors (e.g. *MX2*, *OAS1*, *TRIM5*, *IFITM3* and *APOBEC3G*) in activated $CD4^+$ T cells by the TGF-β superfamily cytokines examined here detected by RNAseq analysis, a full qRT-PCR analysis was carried out to verify the expression of these genes in all the samples from this experiment (i.e. the starting $CD4^+$ T cells from each donor prior to activation, and cells pre-activated for 48 hours then incubated for a further 24 hours with TGF-β_1, IFN-α, activin A and BMP-2 or no cytokine addition. qRT-PCR analysis confirmed statistically significant upregulation of *MX2*, *OAS1* and *IFITM3* and a strong trend for upregulation of *TRIM5* (but not *APOBEC3G*) in IFN-α-treated cells (Fig. 5.8), but no upregulation of these genes by TGF-β superfamily cytokines, paralleling findings from the RNAseq data.

Similarly, given the upregulation of several ISGs (*JAK1*, *STAT2*, *IRF9, IFI6* and *ISG15*), the first three of which are involved in type I IFN signalling, by BMP-6 in hepatocytes observed in

a prior study[363], but the lack of upregulation of these genes in activated CD4+ T cells by the TGF-β superfamily cytokines tested here, the expression of these genes was also verified by qRT-PCR in all samples from the RNAseq experiment. qRT-PCR analysis confirmed significantly higher expression of all these genes (except *JAK1*, which showed a trend for higher levels) in IFN-α-treated versus control cells (Fig. 5.9), but no upregulation of these genes by TGF-β superfamily cytokines, consistent with the RNAseq data.

Overall, these data reveal that in activated CD4+ T cells, activin A and BMP-2 do not appreciably perturb the cellular transcriptome, including not differentially regulating known HIV-1 restriction factors or type I IFN signalling genes/antiviral genes shown to be upregulated by activins and BMPs in hepatocytes by other studies.

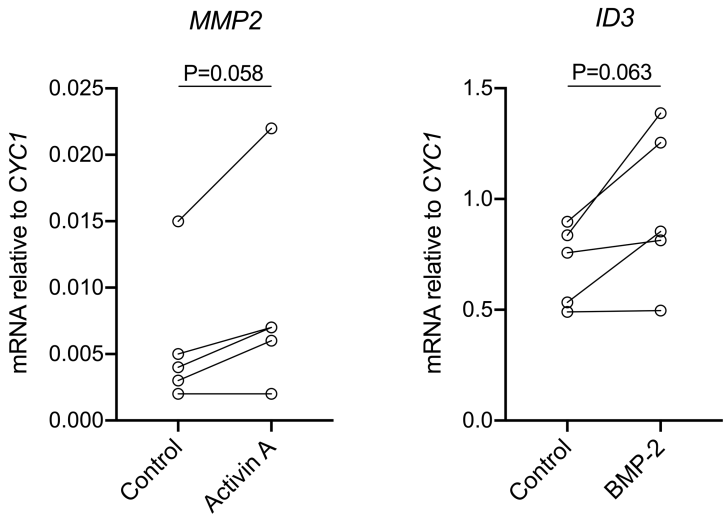


Figure 5.7 qRT-PCR analysis of the expression of selected target genes in activin A- and BMP-2-treated activated CD4+ T cells
CD4+ T cells from n=5 HIV-seronegative donors were activated for 48 hours with 50ng/ml anti-CD3, 100ng/ml anti-CD28 and 50IU/ml IL-2 before treatment with activin A (5nM) or BMP-2 (25nM) for 24 hours followed by RNA extraction and sequencing to determine gene expression levels. The expression of selected genes identified on the basis of RNAseq analysis as being differentially regulated by activin A or BMP-2 (but only on the basis of unadjusted P values) in the same cell lysates was then re-analysed by qRT-PCR. Gene expression is shown relative to the expression of the stably expressed reference gene, *CYC1*. Expression of each gene in cytokine-treated cells was compared to that in control condition (cells activated for 72 hours with no cytokine treatment for the last 24 hours), using a paired t-test.

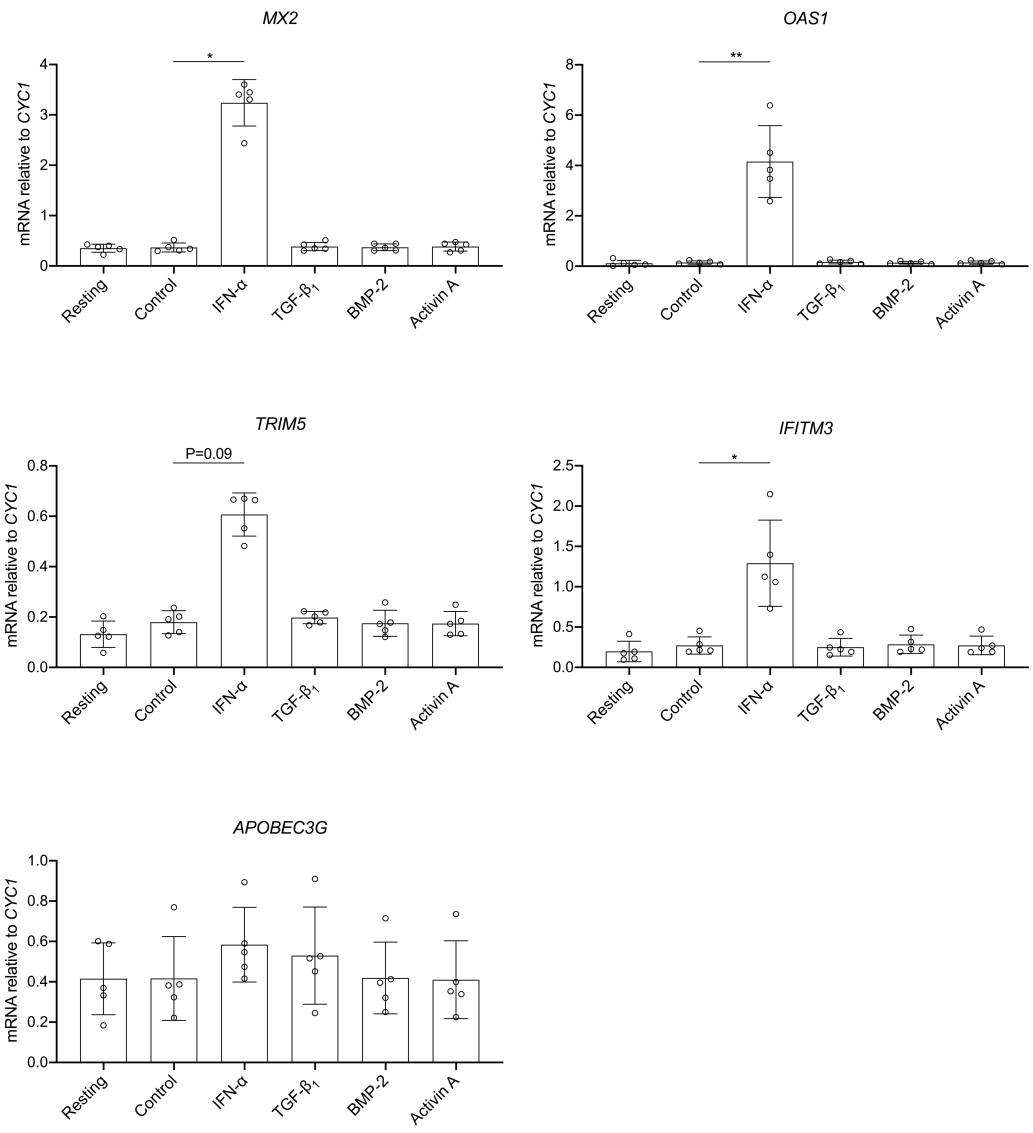


Figure 5.8 qRT-PCR analysis of the expression of genes encoding selected HIV-1 restriction factors in TGF-β superfamily and IFN-α-treated activated CD4⁺ T cells

CD4⁺ T cells from n=5 HIV-seronegative donors were activated for 48 hours with 50ng/ml anti-CD3, 100ng/ml anti-CD28 and 50IU/ml IL-2 before treatment with IFN-α (1000IU/ml), TGF-β_1 (50ng/ml), activin A (5nM) or BMP-2 (25nM) for 24 hours followed by RNA extraction and sequencing to determine gene expression levels. The expression of genes encoding selected HIV-1 restriction factors in the same cell lysates was then re-analysed by qRT-PCR. Gene expression is shown relative to the expression of the stably expressed reference gene, *CYC1*. Bars represent the group mean, error bars denote the SD. Expression of each gene in cytokine-treated cells was compared to that in control condition (cells activated for 72 hours with no cytokine treatment for the last 24 hours), using a Friedman test with Dunn's post-test comparing to control (*MX2*, *TRIM5*, *APOBEC3G*) or one-way ANOVA with Dunnett's post-test comparing to control (*OAS1*, *IFITM3*), *P<0.05, **P<0.01.

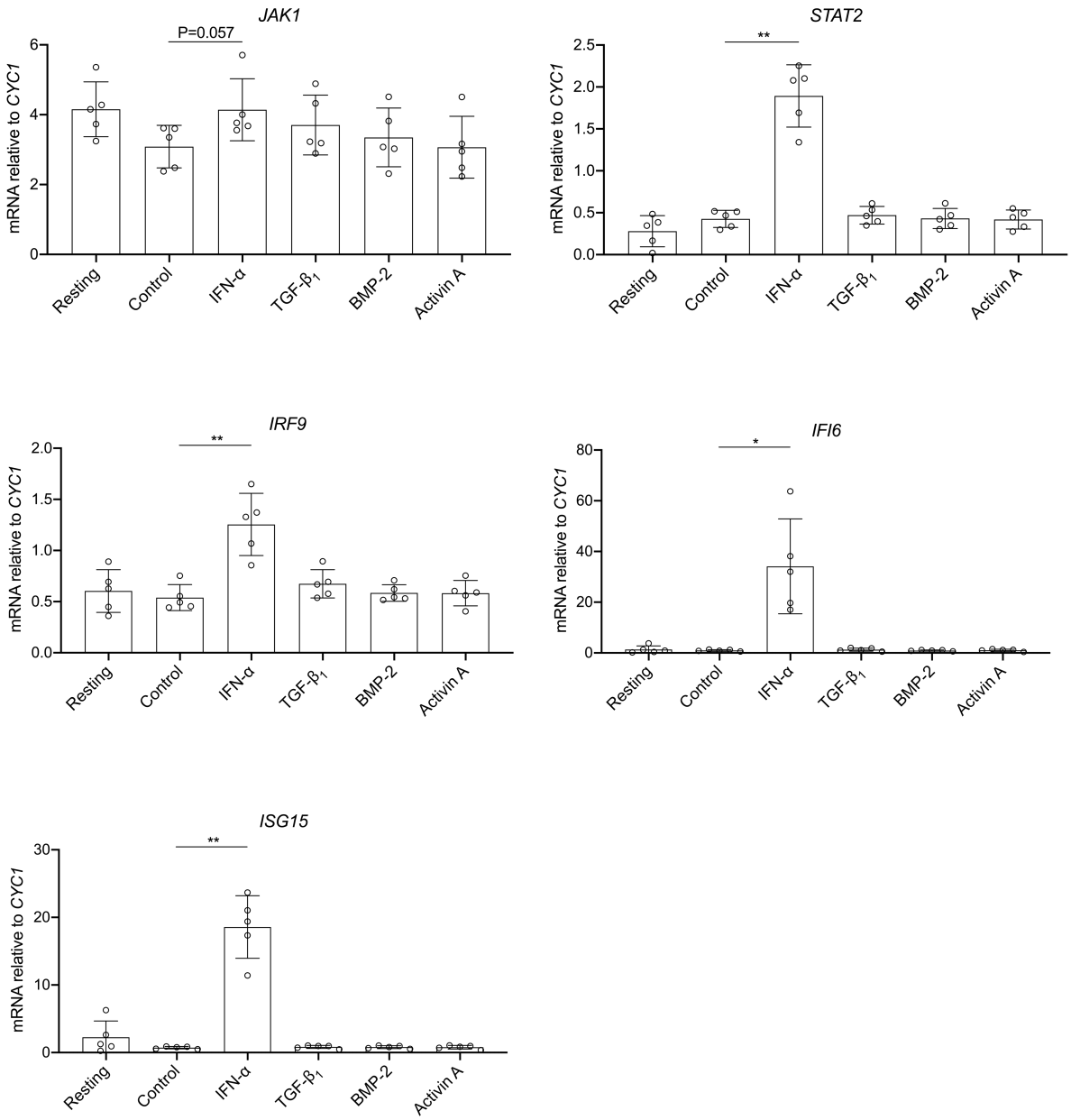


Figure 5.9 qRT-PCR analysis of the expression of selected ISGs previously shown to be upregulated in BMP-treated hepatocytes, in TGF-β superfamily and IFN-α-treated activated CD4+ T cells

CD4+ T cells from n=5 HIV-seronegative donors were activated for 48 hours with 50ng/ml anti-CD3, 100ng/ml anti-CD28 and 50IU/ml IL-2 before treatment with IFN-α (1000IU/ml), TGF-β_1 (50ng/ml), activin A (5nM) or BMP-2 (25nM) for 24 hours followed by RNA extraction and sequencing to determine gene expression levels. The expression of selected genes previously identified as upregulated in BMP-treated hepatocytes[363] in the same cell lysates was then re-analysed by qRT-PCR. Gene expression is shown relative to the expression of the stably expressed reference gene, *CYC1*. Bars represent the group mean, error bars denote the SD. Expression of each gene in cytokine-treated cells was compared to that in control condition (cells activated for 72 hours with no cytokine treatment for the last 24 hours), using a Friedman test with Dunn's post-test comparing to control (*JAK1*) or one-way ANOVA with Dunnett's post-test comparing to control (*STAT2*, *IRF9*, *IFI6, ISG15*), *P<0.05, **P<0.01.

5.2.4 TGF-β_1 downregulates *IL17* expression and upregulates *CCL5* in activated CD4$^+$ T cells

To gain more insight into the overall transcriptional changes in activated CD4$^+$ T cells treated with TGF-β_1, pathway analysis was performed on the RNAseq data. Differential expression of genes associated with TGF-β signalling was marked enough to make this the third most statistically significant pathway. Among the top 10 pathways, four involved IL-17 or IL-23 signalling, key components of Th17 cell biology (Fig. 5.10A). A more detailed view of the DEGs in these pathways and the directionality of differential expression of each gene in the pathways is provided in Fig. 5.10B.

Notably, *IL17A* and *IL17F*, subtypes of IL-17, were both downregulated by TGF-β_1 (Fig. 5.10B). This was confirmed with qRT-PCR, where *IL17A* was statistically significantly downregulated by TGF-β_1, and *IL17F* was also downregulated almost with statistical significance (Fig. 5.6). Additionally, TGF-β_1 also upregulated *CCL5* (Fig. 5.10B), a trend which was verified by qRT-PCR, although the difference did not reach statistical significance (Fig. 5.6).

The downregulation of IL-17 genes could represent a mechanism by which TGF-β_1 inhibits HIV-1 replication, given the inherent pro-inflammatory nature of this cytokine. IL-17 activates NF-κB and also synergises with other pro-inflammatory cytokines such as TNF and IL-6[637], which are drivers of T cell activation. The upregulation of CCL5 could also represent an HIV-1-restrictive mechanism. CCL5 inhibits the replication of R5-tropic HIV-1 strains by ligation and subsequent downregulation of the viral coreceptor CCR5[638].

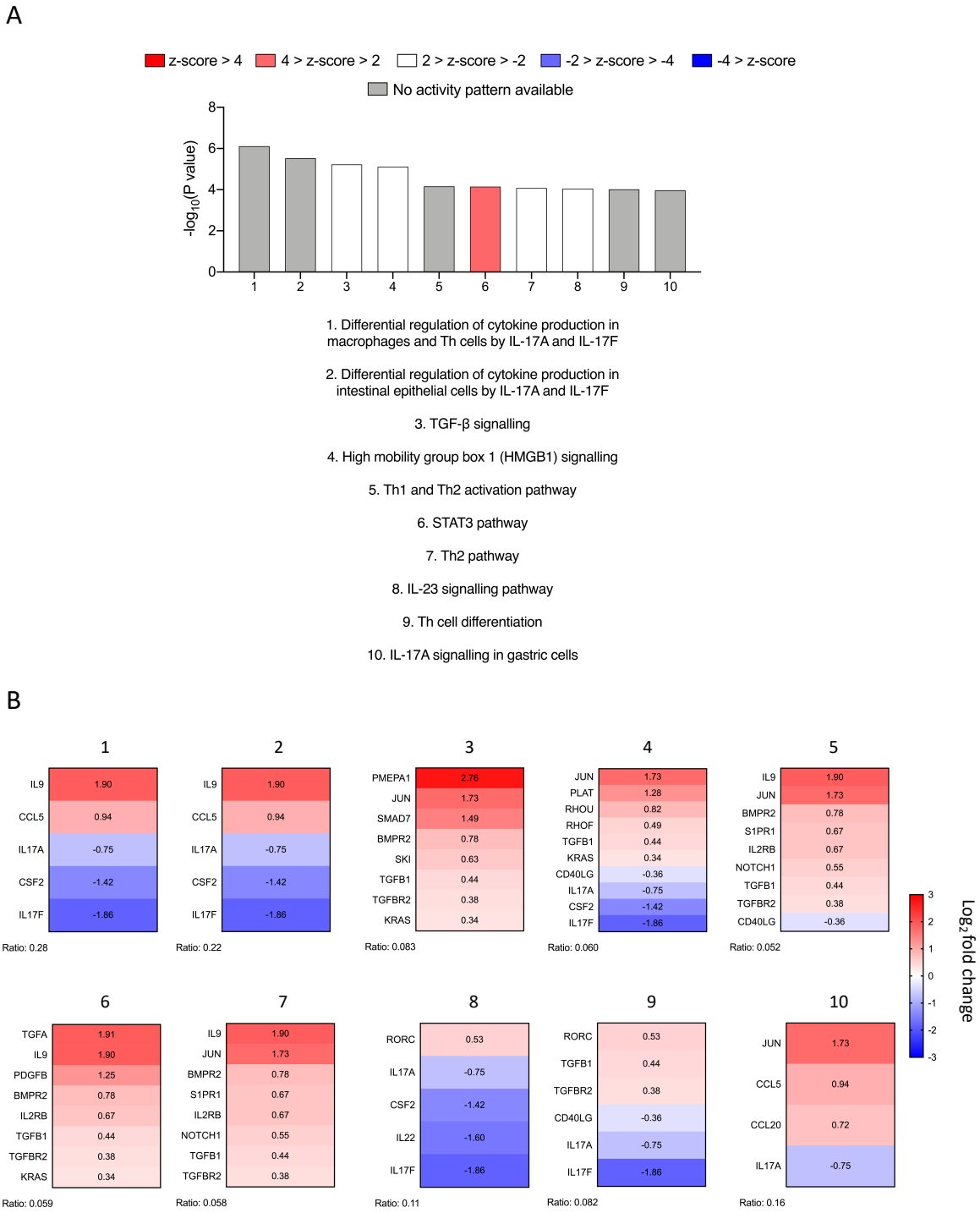


Figure 5.10 Pathway analysis of genes differentially expressed in TGF-β$_1$-treated versus non-cytokine-treated activated CD4$^+$ T cells

Ingenuity pathway analysis was performed on the genes differentially expressed in TGF-β$_1$-treated versus untreated activated CD4$^+$ T cells identified by RNAseq analysis (DEGs with adjusted P value <0.05 and a log$_2$ CPM of >1 (>2 CPM) with no fold change exclusions). **A.** The top ten pathways, from left to right starting with the most statistically significantly differentially regulated pathways, as defined by pathway analysis P value. Z-scores indicate directionality of differential expression of genes within a pathway and are denoted by the colours shown. **B.** Heat maps of the top ten pathways showing log$_2$ fold changes of each DEG within that pathway, using the same key for the ten pathways as in (A). Ratio=the number of genes that map to a pathway to the total number of genes within that pathway.

5.2.5 Recombinant IL-17 does not reverse TGF-β_1-mediated inhibition of HIV-1 replication

Given that TGF-β_1 downregulated *IL17A* and *IL17F*, it was questioned whether IL-17 protein inherently promotes HIV-1 replication, and whether its downregulation could be an explanation for TGF-β_1-mediated viral inhibition. Activated CD8-depleted PBMCs were treated with TGF-β_1 along with recombinant IL-17 before and continuously after infection with HIV-1 CH058 6M. IL-17 did not reverse TGF-β_1-mediated inhibition of viral replication, nor did IL-17 treatment alone enhance viral replication (Fig. 5.11).

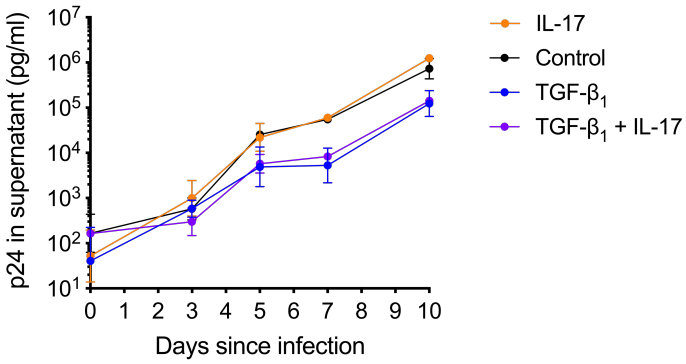


Figure 5.11 Analysis of the effects of IL-17 on TGF-β_1-mediated inhibition of HIV-1 replication
CD8-depleted PBMCs pooled from a trio of donors were activated for 48 hours then treated with no added cytokines (control), TGF-β_1 (50ng/ml), IL-17 (50ng/ml) or both cytokines together for 24 hours before (and continuously after) infecting with HIV-1 CH058 6M. Error bars represent the geometric SD of triplicate wells. Data from one representative experiment of n=2 performed with cells from different donor trios.

5.2.6 Blocking the IL-17 receptor does not inhibit HIV-1 replication

Similarly, it was examined whether blocking IL-17 activity imitated the inhibition of HIV-1 replication seen with TGF-β_1. Activated PBMCs were treated with an IL-17 receptor A (IL-17RA)/IL-17 receptor (IL-17R)-blocking antibody before and during infection with HIV-1 CH058 6M. IL-17RA is the major IL-17R subtype with which other IL-17R subtypes complex[637].

As it is documented that blocking IL-17RA signalling can lead to upregulation of TGF-β_1 in human PBMCs[639], endogenous TGF-β_1 production in these circumstances was controlled for by using the small molecule ALK4, 5 and 7 blocker SB431542. IL-17RA/IL-17R neutralisation had no effect on HIV-1 replication (Fig. 5.12).

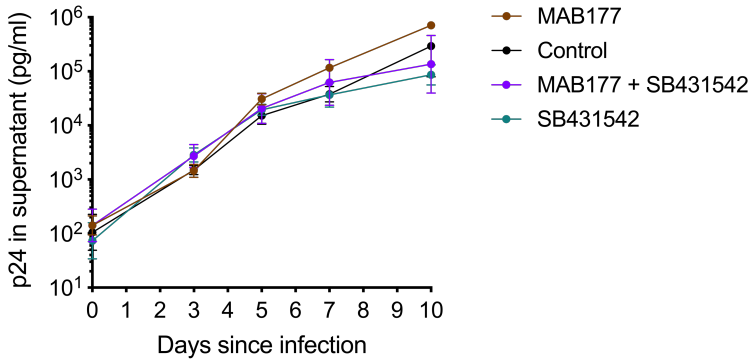


Figure 5.12 Analysis of the effects of blocking IL-17 signalling on HIV-1 replication
CD8-depleted PBMCs pooled from a trio of donors were activated for 48 hours then treated with no added cytokines (control), IL-17RA/IL-17R neutralising antibody MAB177 (10µg/ml), ALK4, 5 7 inhibitor SB431542 (10µM) or both treatments together for 24 hours before (and continuously after) infecting with HIV-1 CH058 6M. Error bars represent the geometric SD of triplicate wells. Data from one representative experiment of n=2 performed with cells from different donor trios.

5.2.7 TGF-β_1 and IFN-α do not inhibit HIV-1 replication via a mechanism involving the chemokine XCL1

Gene expression analysis demonstrated downregulation of the chemokine XCL1 (previously shown to mediate inhibition of HIV-1 replication[627]) in activated $CD4^+$ T cells after 24 hours of TGF-β_1 and IFN-α treatment. However, other studies have observed upregulation of expression of this gene in activated murine $CD8^+$ T cells at 40 hours post-TGF-β treatment[640], indicating that TGF-β-induced XCL1 expression may be dynamic and timepoint-sensitive (and/or be cell type-dependent). Furthermore, HIV-1 Tat induces *XCL1* gene expression and XCL1 protein synthesis in the brains of mice, through direct Tat-mediated activation of the *XCL1* promoter[641]. Given these data, whether TGF-β_1 and IFN-α mediate HIV-1 inhibitory activity via induction of this chemokine was investigated.

Activated CD8-depleted PBMCs were treated with TGF-β_1 or IFN-α along with an anti-XCL1 neutralising antibody at a neutralising dose recommended by the manufacturer and employed in a prior study[627] both before and during infection with HIV-1 CH058 6M. Inhibiting XCL1 in TGF-β_1- (Fig. 5.13A) and IFN-α-treated (Fig. 5.13B) cultures had no effect on TGF-β_1 or IFN-α activity, nor did the neutralising antibody alone have any effect on HIV-1 replication, indicating that HIV-1 inhibition by these cytokines is not mediated through XCL1. In the same assay, the HIV-1 inhibitory activity of recombinant XCL1 was also assessed. In contrast to the observations made in a prior study in which XCL1 inhibited both R5-tropic and X4-tropic HIV-1 strains[627], XCL1 was not found to substantially inhibit CH058 6M replication in the assay system employed here (Fig. 5.13C).

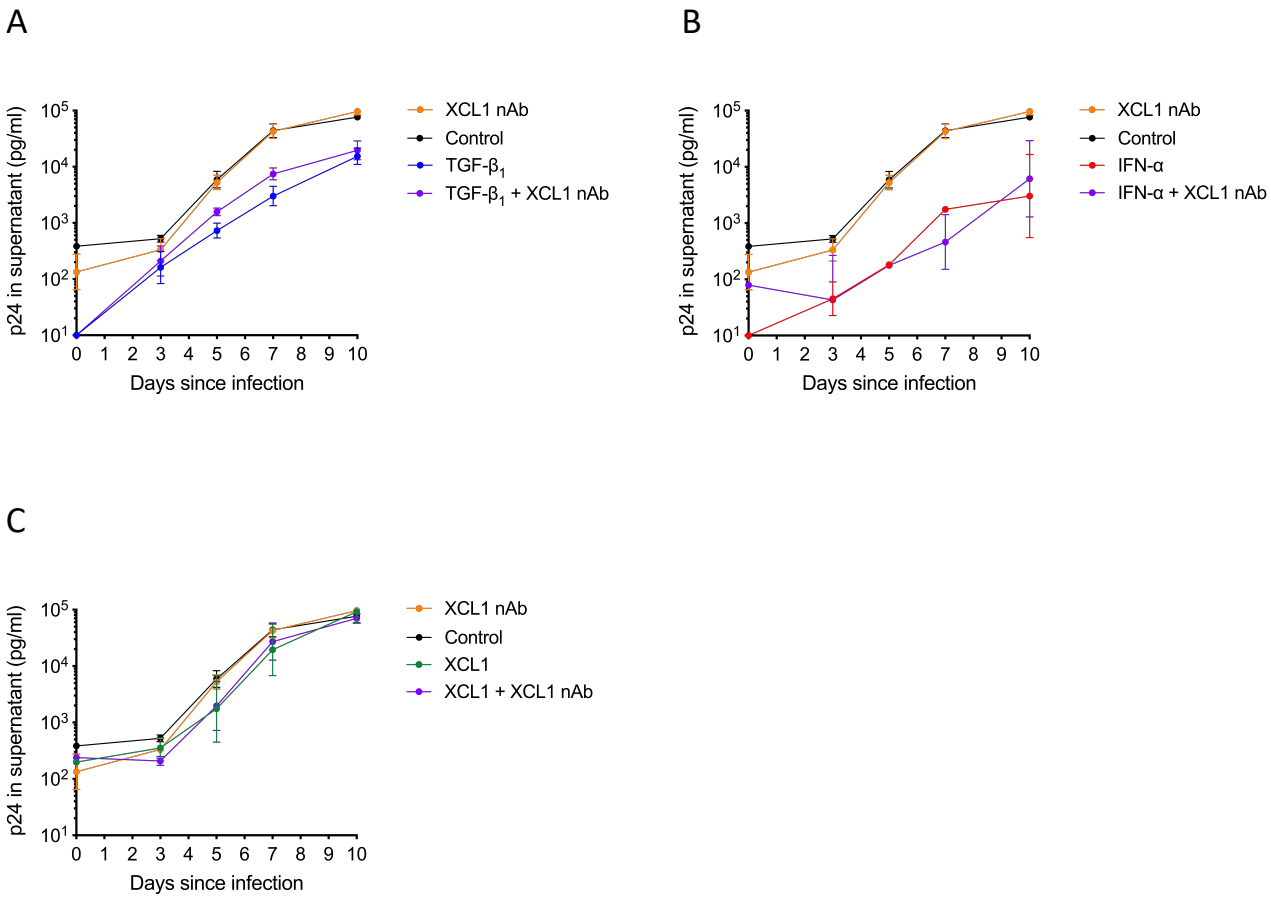


Figure 5.13 Analysis of the effects of inhibiting XCL1 on TGF-β$_1$- and IFN-α-mediated inhibition of HIV-1 replication
CD8-depleted PBMCs pooled from a trio of donors were activated for 48 hours then treated with no added cytokines (control), a XCL1-neutralising antibody (nAb) (10µg/ml) and **A.** TGF-β$_1$ (50ng/ml), **B.** IFN-α (1000IU/ml) or **C.** XCL1 (0.4µM) for 24 hours before (and continuously after) infecting with HIV-1 CH058 6M. Error bars represent the geometric SD of triplicate wells. Data from one representative experiment of n=2 performed with cells from different donor trios.

5.2.8 Analysis of the effects of TGF-β$_1$ on the T helper subset composition within activated CD4$^+$ T cell cultures

Transcriptional profiling data shown earlier in this chapter indicated modulation of Th pathways, including downregulation of IL-17 expression, in TGF-β$_1$-treated activated CD4$^+$ T cells. However, recombinant IL-17 did not perturb the effects of TGF-β$_1$ on HIV-1 replication, nor did the blocking of IL-17 activity. The downregulation of IL-17 genes observed in TGF-β$_1$-treated cells may have been indicative of a reduced proportion of Th17 cells (the primary Th subset capable of producing IL-17[642]) in the activated CD4$^+$ T cell cultures. Th17 cells are

relatively more susceptible to HIV-1 infection than many other Th subsets, and Th cells under Th17-polarising conditions are more susceptible to infection[247], so the hypothesis that TGF-β_1 may inhibit HIV-1 replication by altering the $CD4^+$ Th subset composition in the assay system employed here was investigated.

To address this, $CD4^+$ T cells activated for 48 hours under the same conditions as in the standard HIV-1 replication assays (but not infected) were treated with TGF-β_1 for a further four days before analysis of the Th subset composition by flow cytometry. The proportions of naïve and various memory T cell populations (T central memory (Tcm), T effector memory (Tem) and $CD45RA^+$ Tem (Temra) cells) were also analysed, as naïve and memory cell subsets have also been reported to exhibit differential abilities to support HIV-1 replication and/or transmission[643].

The gating strategy used to identify different cell subsets in non-activated and 48-hour activated $CD4^+$ cells (just prior to TGF-β_1 treatment) is shown in Fig. 5.14. Within $CD4^+$ T cells, naïve/memory T cell compartments were distinguished using CCR5 and CD45RA[644,645]; and Th1, Th2, Th1/17 and Th17 cells using CCR6 and CXCR3[645,646]. $CXCR5^+$ cells were described as "follicular", and were then further subdivided into either T follicular regulatory (Tfr) cells ($CXCR5^+CD25^+FOXP3^+$), Tfh ($CXCR5^+CD25^-FOXP3^-$) cells[647]; and into Th1-like ($CXCR5^+CCR6^-CXCR3^+$), Th2-like ($CXCR5^+CCR6^-CXCR3^-$), Th17-like ($CXCR5^+CCR6^+CXCR3^-$) or Th1/17-like ($CXCR5^+CCR6^+CXCR3^+$) follicular cells[648].

Following 48 hours of activation, the naïve, Tcm and Temra compartments were largely unchanged, and the percentage of Tem cells slightly decreased. After a further four days, the percentage of naïve T cells sharply decreased (an expected finding, due to differentiation of these cells into effector subsets after activation) as did Temra cells, while the proportion of

Tems and Tcms slightly increased, although the increase in Tems was not seen in TGF-β_1-treated cells (Fig. 5.15A), likely due to the immunosuppressive activity of the cytokine.

Following 48 hours of activation, $CD4^+$ T cells highly expressed CD25 and CD38, indicating robust activation, and expression of these activation markers remained largely unchanged after a further four days of TGF-β_1 treatment in the two donors studied, though expression of CD38 was marginally lower in TGF-β_1-treated cells (Fig. 5.15B). As well as analysing activation marker expression on total $CD4^+$ T cells, this was also analysed in the Tcm and Tem compartments separately, where the findings were the same as those in total $CD4^+$ T cells (data not shown).

The proportions of $CD25^+FOXP3^+$ $CD4^+$ T cells (many of which are Treg cells, but some increase in FOXP3 expression also occurs in non-Treg cells following activation[649]) and $CD25^+FOXP3^{hi}$ Treg cells (which are more likely to be effector Tregs with great suppressive capacity[650]) greatly increased after cell activation from around 1% and 0% to 40% and 7% respectively. After a further four days, both populations declined in frequency (to around 20% and 0.5% respectively), although in TGF-β_1-treated cells, a trend was seen for retention of a slightly greater percentage of these populations, at around 30% and 1% respectively (Fig. 5.15C).

The effects of TGF-β_1 on Th1, Th2 and Th1/17 populations were unremarkable. Following 48 hours of activation, the proportions of Th1 and Th2 cells roughly doubled and halved respectively (consistent with data from others, finding that stimulation of T cells through ligation of CD3/CD28 *in vitro* tends to skew cells towards a Th1 phenotype[651]), remaining so after a further four days, regardless of the presence of TGF-β_1. Th1/17 cell percentages remained unaffected by activation or subsequent TGF-β_1 treatment. The proportion of $CXCR5^+$ (follicular)

cells quadrupled from around 10% to 40% of total CD4+ T cells after 48 hours of activation, which then halved after a further four days, with the presence of TGF-β_1 having no effect (Fig. 5.15D). This is in contrast to in CD8+ T cells, where just over three days of culture with TGF-β_1 has been found to increase CXCR5 expression[357], although in that study, TGF-β_1 was added to cultures at the same time as the cell activation stimulus, rather than after 48 hours as in this chapter.

Within the follicular compartment, Th1-like, Th2-like and Th1/17-like cells showed similar patterns to their canonical (Th1, Th2, Th1/17) counterparts. Also within the follicular compartment, percentages of Tfh and Tfr cells, though perturbed by activation (decreasing and increasing respectively), were unaffected by TGF-β_1 (Fig. 5.15E). As well as analysing total CD4+ T cells, percentages of all the aforementioned Th subsets were also analysed in the Tcm and Tem compartments separately, where the findings were the same as in total CD4+ T cells (data not shown). TGF-β_1 had no effect on the percentage of Th17 and Th17-like follicular cells within total CD4+ T cells or the Tcm compartment. However, in the Tem compartment TGF-β_1 appeared to roughly halve the proportions of these cells relative to controls (Fig. 5.16).

In summary, these data indicate that in activated CD4+ T cells, TGF-β_1 reduces the proportion of Tem cells, and may reduce the percentage of Th17 and Th17-like follicular cells within the Tem compartment. The latter could represent a mechanism that reduces HIV-1 replication, although as this analysis was only conducted using cells from n=2 donors due to time constraints and no statistical analysis of the data was possible, these are preliminary findings. In total CD4+, Tcm and Tem compartments, TGF-β_1 may induce a Treg cell phenotype. This could also represent a mechanism of HIV-1 restriction, given that FOXP3 is documented by other studies to inhibit HIV-1[605,606], and warrants further experimental investigation. However again, these findings require follow-up with a greater number of donors.

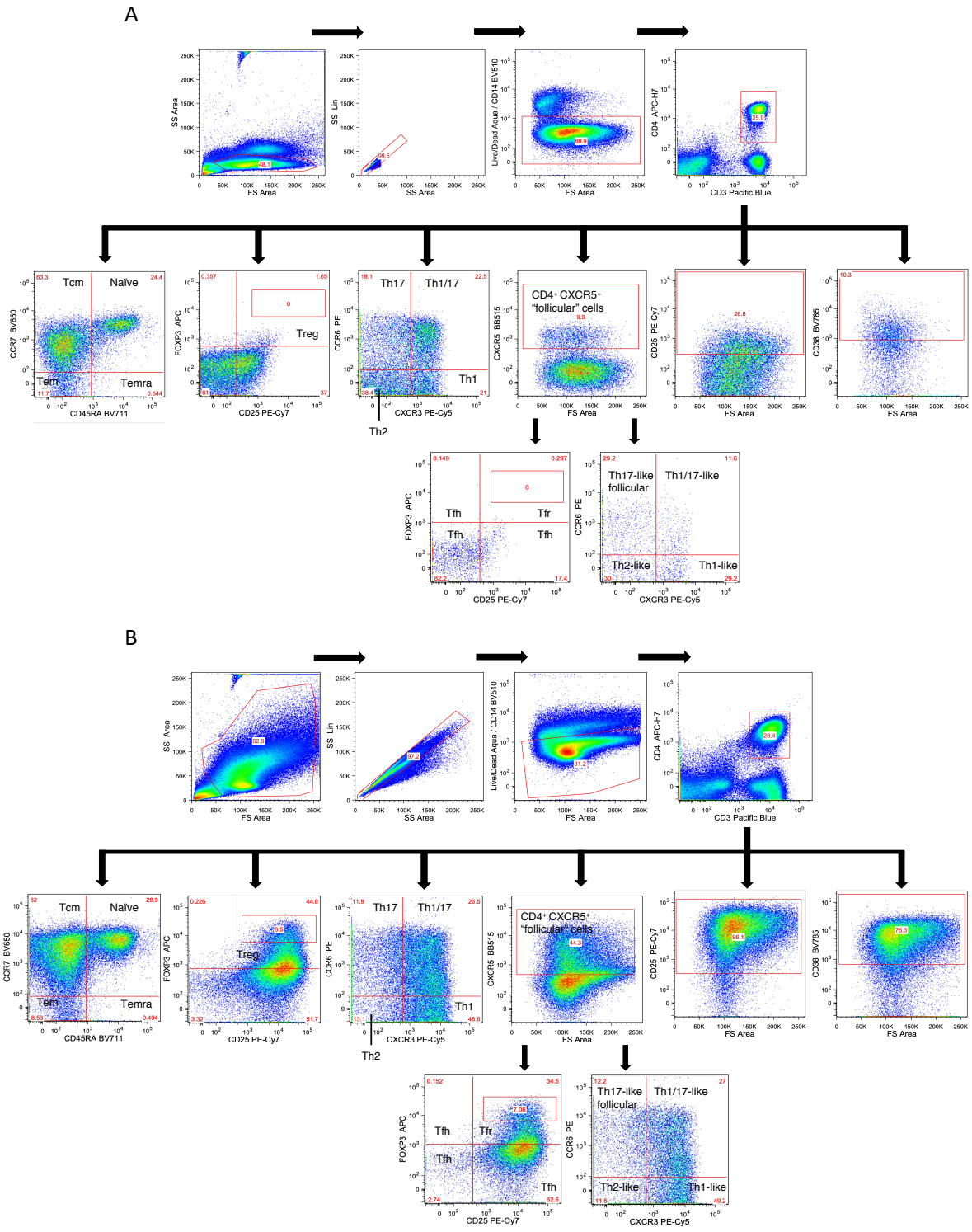


Figure 5.14 Gating strategy for T helper subset analysis in CD4⁺ T cells
Gating strategy for flow cytometric analysis of PBMCs for naïve/memory markers, activation markers and Th phenotypic markers in CD4⁺ T cells using "flow cytometry panel 3" (Chapter 2). **A.** Non-activated cells from one representative donor. **B** 48-hour activated cells from the same representative donor. In (B), a wide initial gate was used to allow for the heterogeneity of lymphocyte size during activation. In both (A) and (B), cells were sequentially gated on single, live, CD4⁺ T cells (top row). Arrows indicate serial gates. CD14⁺ cells were gated out in the dump channel along with dead cells staining positive for the amine-reactive dye. Within the live, CD4⁺ T cell population; naïve and memory CD4⁺ T cell subsets, Treg cells, Th subsets, follicular cells, CD25⁺ and CD38⁺ cells were identified as indicated (middle row). Gates for analysis of CD25 and CD38 expression on total CD4⁺ T cells were drawn using FMOs. Tfh/Tfr and Th subsets within the follicular population were further defined as shown (bottom row).

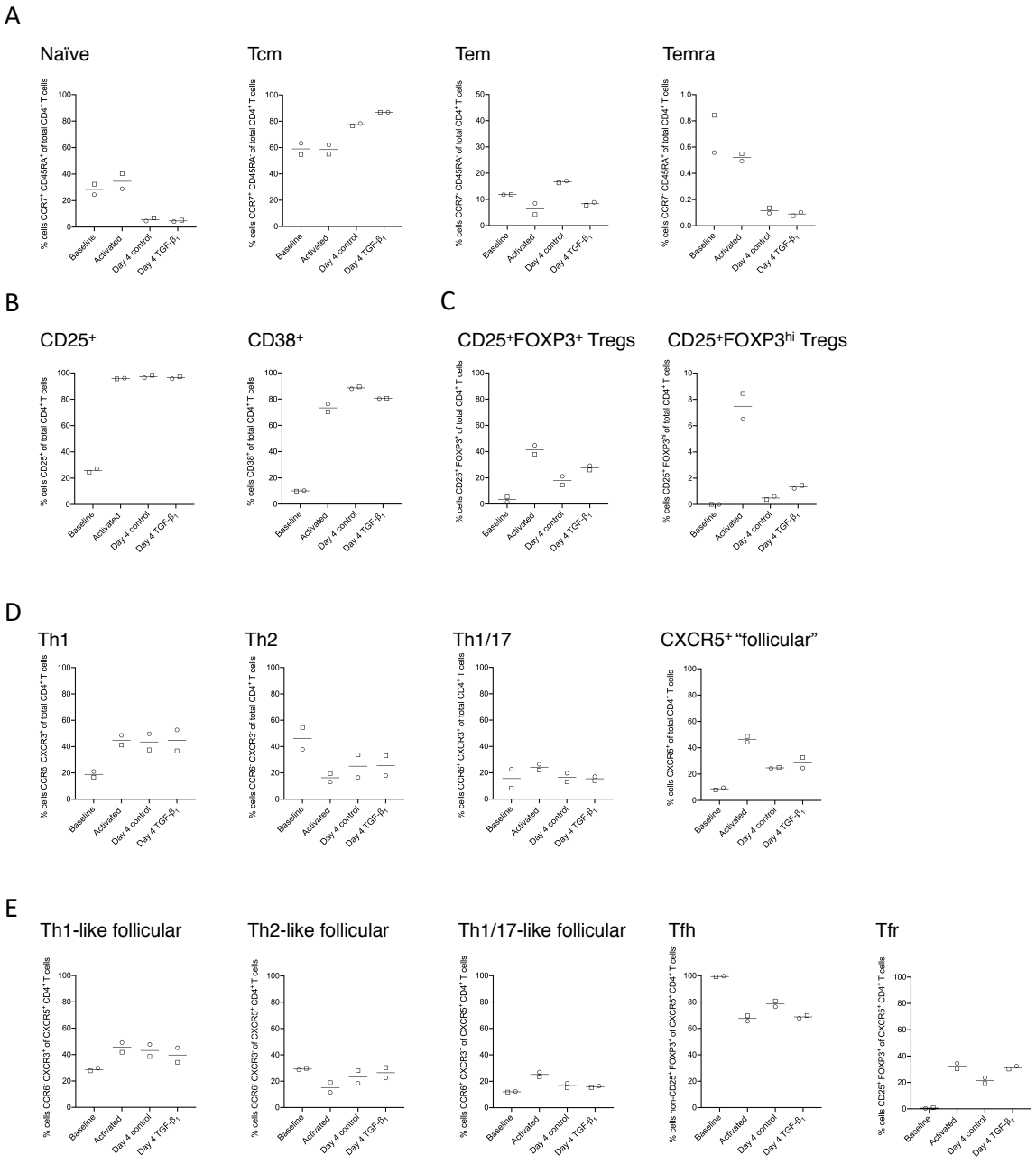


Figure 5.15 Analysis of the effects of TGF-β_1 on proportions of T helper subsets in total activated CD4+ T cells

PBMCs from n=2 HIV-seronegative donors were analysed at baseline, after activation for 48 hours with 50ng/ml anti-CD3, 100ng/ml anti-CD28 and 50IU/ml IL-2, and after incubation for a further four days without ("day 4 control") or with TGF-β_1 (50ng/ml) ("day 4 TGF-β_1"). The activation stimulus was removed 24 hours post-TGF-β_1 treatment. Expression of naïve/memory markers, activation markers and Th phenotypic markers was assessed on live CD4+ T cells by flow cytometry using the gating strategy shown in Figure 5.14. Each shape represents a donor, lines represent the group means. **A.** The percentage of naïve, Tcm, Tem and Temra cells in total CD4+ T cells. **B.** The percentage of cells expressing CD25 and CD38 in total CD4+ T cells. **C.** The percentage of CD25+FOXP3+ cells and CD25+FOXP3hi Tregs in total CD4+ T cells. **D.** The percentage of Th1, Th2, Th1/17 and CXCR5+ follicular cells in total CD4+ T cells. **E.** The percentage of Th1-like, Th2-like, Th1/17-like, Tfh and Tfr cells in the CXCR5+ population of total CD4+ T cells.

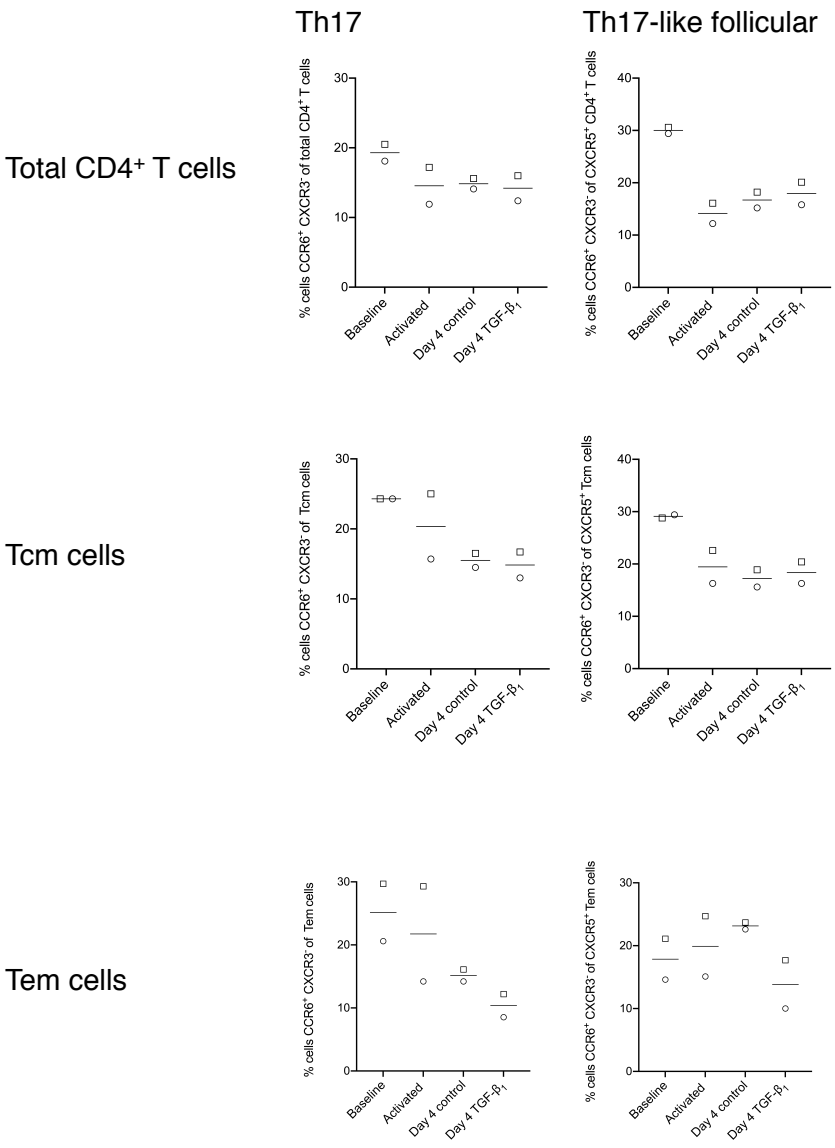


Figure 5.16 Analysis of the effects of TGF-β_1 treatment of activated CD4+ T cells on proportions of Th17 and Th17-like follicular cells in total CD4+ T cell, Tcm and Tem compartments
The percentage of Th17 and Th17-like follicular cells within the total CD4+ T cell, Tcm and Tem compartments at baseline, after 48 hours of activation, and after 48 hours of activation followed by a further four days of incubation -/+ TGF-β_1 (50ng/ml). Data shown are from n=2 donors studied, assessed as part of the same experiment as shown in Fig. 5.14. Each shape represents a donor, lines represent the group means.

5.2.9 Analysis of the effects of TGF-β_1 on CCR5 and CXCR4 expression

The expression of HIV-1 coreceptors CCR5 and CXCR4 determines the susceptibility of cells to infection with R5- and X4-tropic viruses, respectively. It has important clinical significance, as exemplified by the 1996 discovery that considerable resistance to HIV-1 infection is conferred on individuals with homozygous for a 32bp deletion in the *CCR5* gene[652], although they can still become infected with X4-utilising viruses. These are more pathogenic, and coreceptor switch of the virus from R5-tropic to X4- or dual-tropic generally results in accelerated disease progression[59]. Thus, the effects of TGF-β_1 on CCR5 and CXCR4 expression in $CD4^+$ T cells were analysed.

As with the experiment looking at Th subsets, PBMCs were activated for 48 hours before treating with TGF-β_1 for four days, and CCR5 and CXCR4 expression in $CD4^+$ T cells was assessed by flow cytometry. Representative data from one donor is shown in Fig. 5.17A. After 48 hours of activation, cells upregulated CXCR4 but not CCR5. However, the latter was upregulated after a further four days. CCR5 expression was unchanged by TGF-β_1. However, whereas CXCR4 expression decreased from almost 100% of cells to 80% four days after the initial 48-hour activation, this decrease did not occur in TGF-β_1-treated cells, in which expression remained at almost 100%. These findings were also paralleled in the Tcm and Tem compartments (Fig. 5.17B).

The MFIs of CCR5 and CXCR4 were also considered. Here, a less valid comparison can be made between baseline and activated cells owing to the fact that activated cells increase in size, which may elevate the MFI. However, a fair comparison can still be made between four-day TGF-β_1 and four-day untreated control cells. When considering the CCR5 and CXCR4 MFIs in total $CD4^+$ cells, Tcm and Tem compartments, the same patterns were seen as with proportion of positive cells, with one exception: the MFI of CCR5 was approximately doubled

in cells treated for four days TGF-β_1, compared to control untreated cells, indicating an increase in the level of expression of this marker (Fig. 5.17B).

All together, these results indicate that TGF-β_1 likely does not mediate its inhibitory activity on HIV-1 replication in activated $CD4^+$ T cells through modulation of CCR5 or CXCR4 expression.

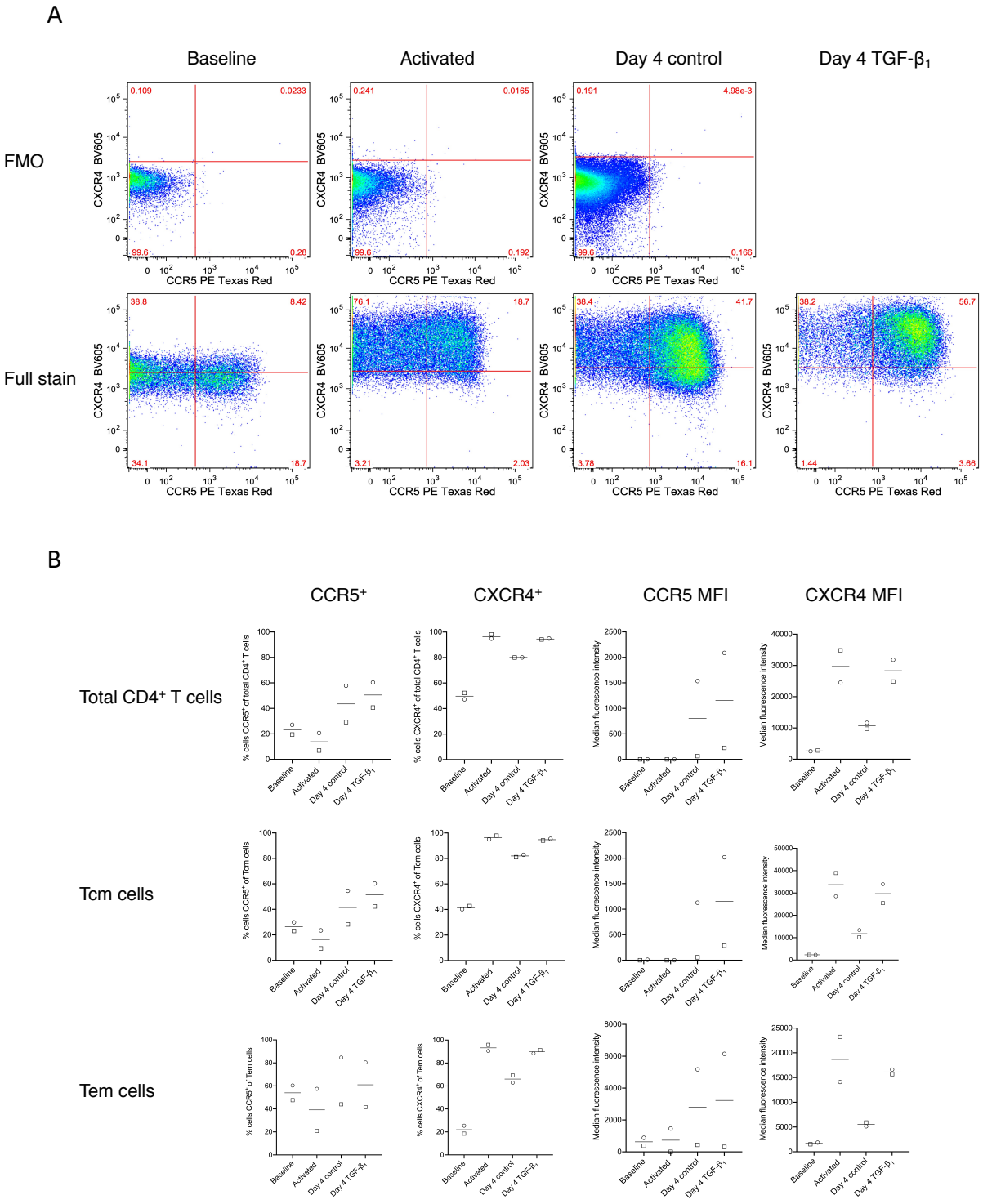


Figure 5.17 Analysis of the effects of TGF-β$_1$ treatment of activated CD4$^+$ T cells on expression of CCR5 and CXCR4 in total CD4$^+$ T cell, Tcm and Tem compartments

A. The expression of CCR5 and CXCR4 within the total CD4$^+$ T cell, Tcm and Tem compartments at baseline, after 48 hours of activation, and after 48 hours of activation followed by a further four days of incubation -/+ TGF-β$_1$ (50ng/ml), were assessed as part of the same experiment as shown in Fig. 5.14. Sample gating within the total CD4$^+$ T cell population is shown in one representative donor. Initial gating on single, live, CD4$^+$ T cells was done as in Fig. 5.14. An FMO (more correctly, a FM-two, lacking antibodies against both CCR5 and CXCR4) was stained at each time point studied, in order to draw the gates for these markers. At the day four timepoint, the same FMO sample was used to gate both the TGF-β$_1$ and control samples. **B.** The percentages of cells expressing CCR5 and CXCR4, and MFI values for these markers in total CD4$^+$ T cells, Tcm and Tem compartments from n=2 donors studied. Each shape represents a donor, lines represent the group means. A small number of MFI values were negative numbers. These were assigned a value of 0.

5.2.10 TGF-β_1 does not induce a Treg phenotype or induce FOXP3 expression in activated CD4$^+$ T cells

TGF-β induces FOXP3 expression and Treg lineage commitment in naïve T cells[138] and FOXP3 has been shown to exert effects on transcription from the HIV-1 LTR, albeit conflicting ones[605–607]. Given these prior studies, and given the preliminary results earlier in this chapter showing a trend for TGF-β_1 to induce a Treg phenotype and FOXP3 expression in activated CD4$^+$ T cells in cells from n=2 HIV-seronegative donors, whether TGF-β induced a Treg phenotype or FOXP3 expression in activated CD4$^+$ T cells was investigated in a more robust experiment using cells from a greater number of donors.

PBMCs from HIV-seronegative donors were activated for 48 hours and treated with TGF-β_1 before analysing CD4$^+$ T cell expression of CD25 and FOXP3 at two and five days post-treatment (Fig. 5.18A). Both the percentage of CD4$^+$ T cells with a Treg phenotype (CD25$^+$FOXP3$^+$ and CD25$^+$FOXP3^{hi}) and the intensity of FOXP3 expression in CD4$^+$ T cells were evaluated. TGF-β_1 was not seen to affect the proportion of Treg cells (Fig. 5.18B) or FOXP3 expression within the CD4$^+$ T cell population (Fig. 5.18C) at either timepoint.

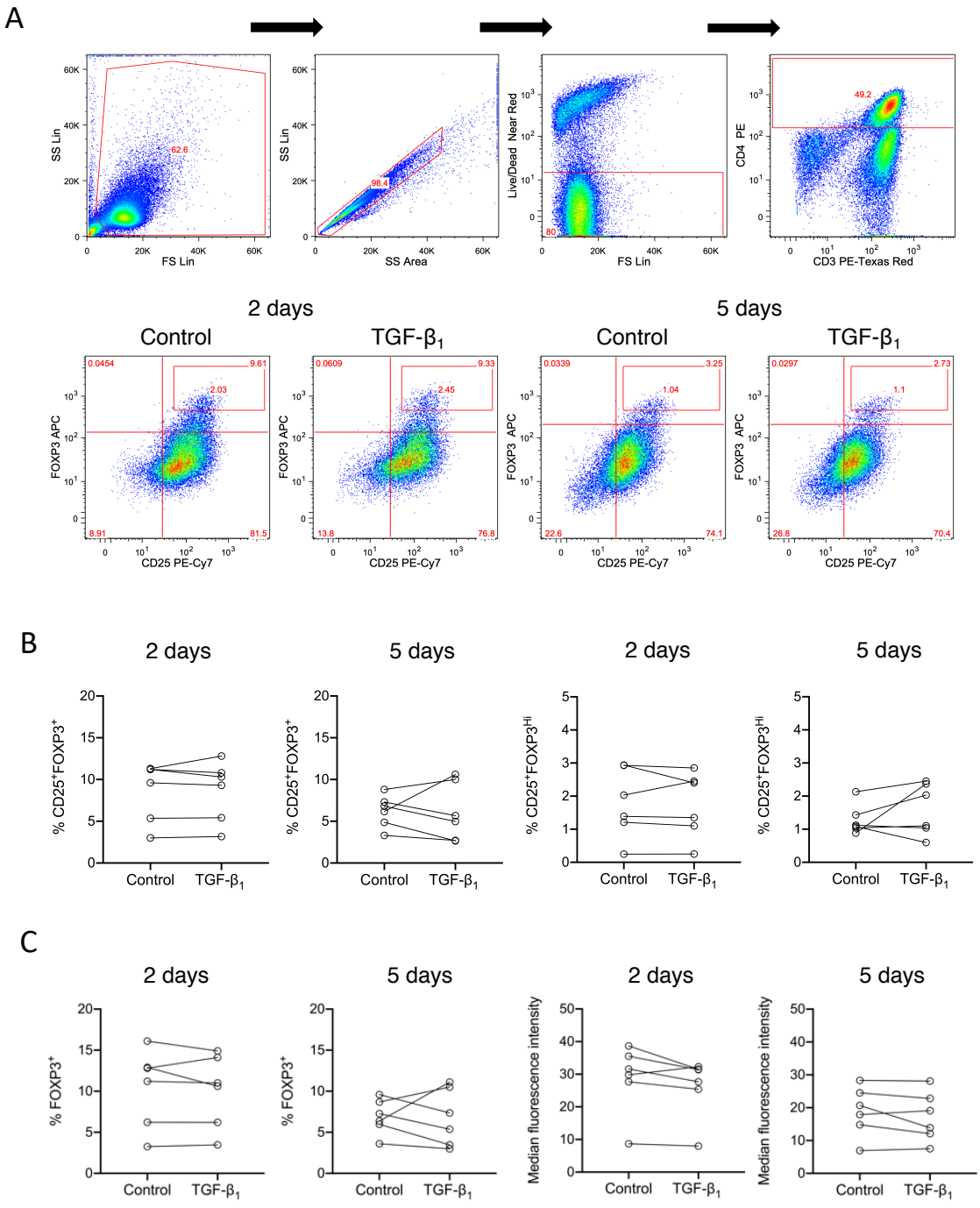


Figure 5.18 Analysis of the effects of TGF-β$_1$ on Treg markers in activated CD4$^+$ T cells
PBMCs from n=6 HIV-seronegative donors were activated for 48 hours with 50ng/ml anti-CD3, 100ng/ml anti-CD28 and 50IU/ml IL-2, then were treated with TGF-β$_1$ (50ng/ml) for a further two or five days before flow cytometric analysis for Treg phenotypic markers using "flow cytometry panel 4" (Chapter 2). The activation stimulus was removed 24 hours post-TGF-β$_1$. **A.** Top row: gating strategy used to identify CD4$^+$ T cells (plots shown are from a day two untreated control sample). A wide initial gate was used to allow for the heterogeneity of lymphocyte size during activation, followed by sequential gating on single, live, CD4$^+$ T cells. Arrows indicate serial gating. Lower row: expression of CD25 and FOXP3 in CD4$^+$ T cells from one representative donor at two and five days post-TGF-β$_1$. CD25$^+$FOXP3^{hi} CD4$^+$ T cells are shown within an additional gate drawn within the upper right quadrant. The CD25 gate was drawn using an FMO control, and the same quadrant gate drawn on control cells was applied to TGF-β$_1$-treated cells. **B.** The percentage of Tregs (CD25$^+$FOXP3$^+$ (left-hand side) and CD25$^+$FOXP3^{hi} (right-hand side)) within CD4$^+$ T cells in n=6 donors at two and five days post-TGF-β$_1$. Groups were compared with a paired t-test, P>0.05 at both timepoints. **C.** The percentage of CD4$^+$ T cells positive for FOXP3 (left-hand side), and the FOXP3 MFI (right-hand side), in n=6 donors at two and five days post-TGF-β$_1$. Groups were compared with a paired t-test, P>0.05 at both timepoints.

5.2.11 TGF-β_1 attenuates transcription from the HIV-1 LTR in activated CD4$^+$ T cells

In order to interrogate the effect of TGF-β_1 on transcriptional activity from the HIV-1 LTR, immortalised T cell lines or activated CD4$^+$ T cells from HIV-seronegative donors were infected with an HIV-1 NL4-3 luciferase reporter virus pseudotyped with the VSV envelope glycoprotein, incubated for 72 hours to allow entry, integration and initial gene expression to occur, then treated with TGF-β_1 for 24 hours, after which luciferase signal intensity was read out as a measure of LTR activity.

Data from preliminary experiments with immortalised T cell lines were equivocal. There was a trend for TGF-β_1 to slightly increase transcriptional activity from the HIV-1 LTR in Jurkat.CCR5 (Fig. 5.19A) and MOLT-4.CCR5 cells (Fig. 5.19B), whilst in CEM.NKR.CCR5 cells an opposite trend was seen (Fig. 5.19C).

In primary cells, TGF-β_1 statistically significantly attenuated the LTR-driven luciferase signal in activated CD4$^+$ T cells (Fig. 5.20A). As the luciferase signal showed a large range in relative light unit signal across donors, data were normalised relative to the untreated control for visual purposes to better observe the overall trend (Fig. 5.20B). To assess whether TGF-β_1 significantly impacted cell numbers (which could explain a reduction in signal not intrinsic to the viral LTR), in n=8 of the n=16 donors, cells were counted after 24 hours of TGF-β_1 treatment, just prior to lysis. No statistically significant difference was observed in cell numbers ($P=0.42$) (Fig. 5.20C). From these findings, it was concluded that TGF-β_1 reduces transcription from the HIV-1 promoter in activated CD4$^+$ T cells, which likely represents a mechanism by which the cytokine inhibits HIV-1 replication in these cells.

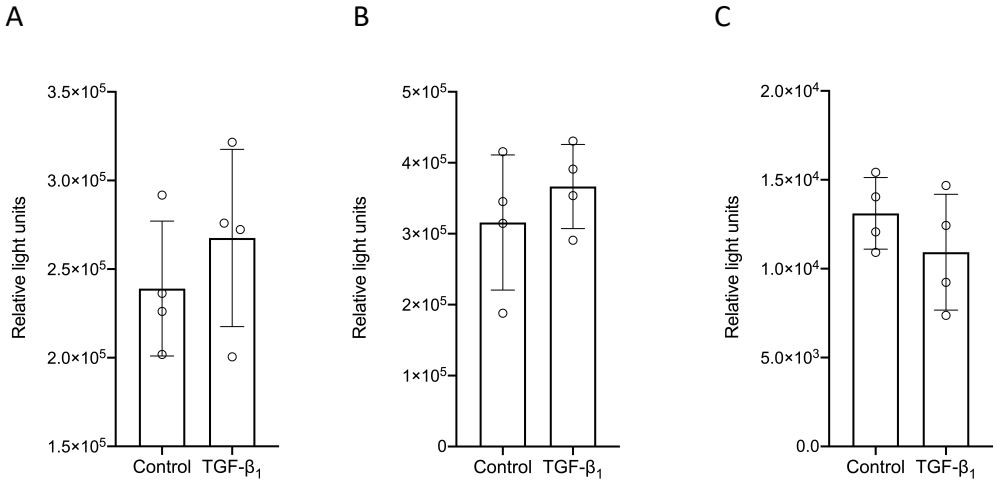


Figure 5.19 Analysis of the effects of TGF-β_1 on transcriptional activity from the HIV-1 LTR in immortalised T cell lines

A. Jurkat.CCR5, **B.** MOLT-4.CCR5 and **C.** CEM.NKR.CCR5 T cell lines were infected with VSV G HIV-1 NL4-3 Luc for 72 hours to allow integration and expression of the viral genome. Cells were then treated with TGF-β_1 (50ng/ml) for 24 hours before lysing and reading the luciferase signal. The datapoints shown are replicate wells from a single experiment; bars represent the mean of the n=4 wells tested, error bars represent the SD.

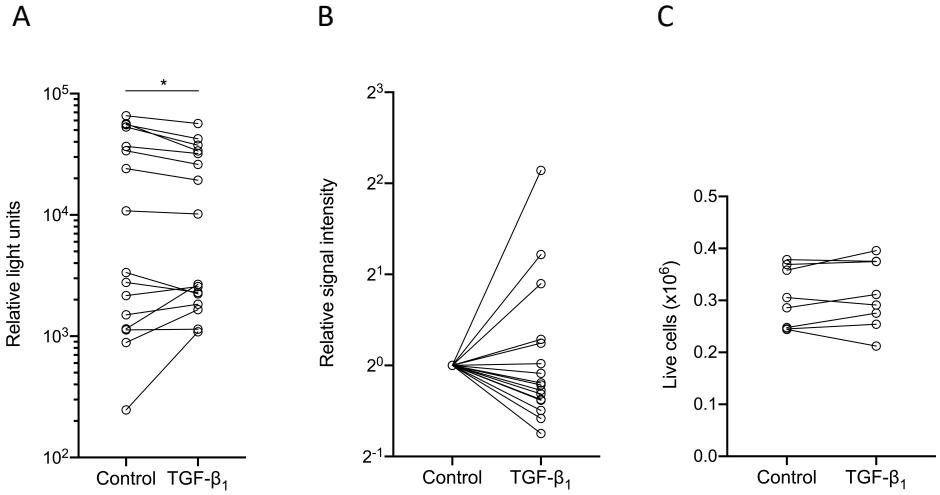


Figure 5.20 The effects of TGF-β_1 on transcriptional activity from the HIV-1 LTR in activated primary CD4$^+$ T cells

A. Purified CD4$^+$ T cells from n=16 HIV-seronegative donors were activated by stimulation for 72 hours with 50ng/ml anti-CD3, 100ng/ml anti-CD28 and 50IU/ml IL-2, then infected with VSV-G pseudotyped HIV-1 NL4-3 Luc for 72 hours. Cells were then treated with TGF-β_1 (50ng/ml) for 24 hours before lysing and reading the luciferase signal. Wilcoxon signed-rank test, *P<0.05. **B.** Data from (A), normalised relative to controls. **C.** In n=8 of the n=16 donors, the effect of TGF-β_1 on live cell count was examined after 24 hours. Paired t-test, P=0.42.

5.2.12 The effects of TGF-β_1 on the NF-kB pathway in activated CD4$^+$ T cells

To investigate whether TGF-β_1 affects NF-kB pathway activation, CD4$^+$ T cells from three HIV-seronegative donors were activated and lysed directly or after treatment with TGF-β_1 for variable time periods up to 24 hours. Indicators of NF-kB activation were measured by western blot, including p-p65, total p65, and IκBα, which revealed some inter-donor variability (Fig. 5.21A). When considering all donors together, there was a slight trend for an increase in phosphorylated p65 by 6 hours post-TGF-β_1, but no obvious reduction in the amount of IκBα at the same timepoint, which would provide more conclusive proof of NF-kB activation. There were no other obvious differences between TGF-β_1 and control at other timepoints (Fig. 5.21B). Overall, no marked effect of TGF-β_1 on NF-kB activation was observed in this analysis. However, these experiments lacked a positive control to confirm the utility of this approach to demonstrate changes in NF-kB activity in activated primary CD4$^+$ T cells, and the sensitivity of the readouts employed was unclear, so it cannot be precluded that TGF-β_1 does impact on NF-kB activity in activated CD4$^+$ T cells.

The RNAseq dataset discussed in previous sections was also interrogated to ask whether TGF-β_1 has any effects on the expression of genes involved in the NF-κB pathway. 24 hours of TGF-β_1 treatment of 48-hour activated CD4$^+$ T cells did not differentially regulate expression (relative to untreated cells) of any NF-κB subunit genes, IκB inhibitory regulatory genes, IKK complex genes or the gene encoding TAK1 (Table 5.4).

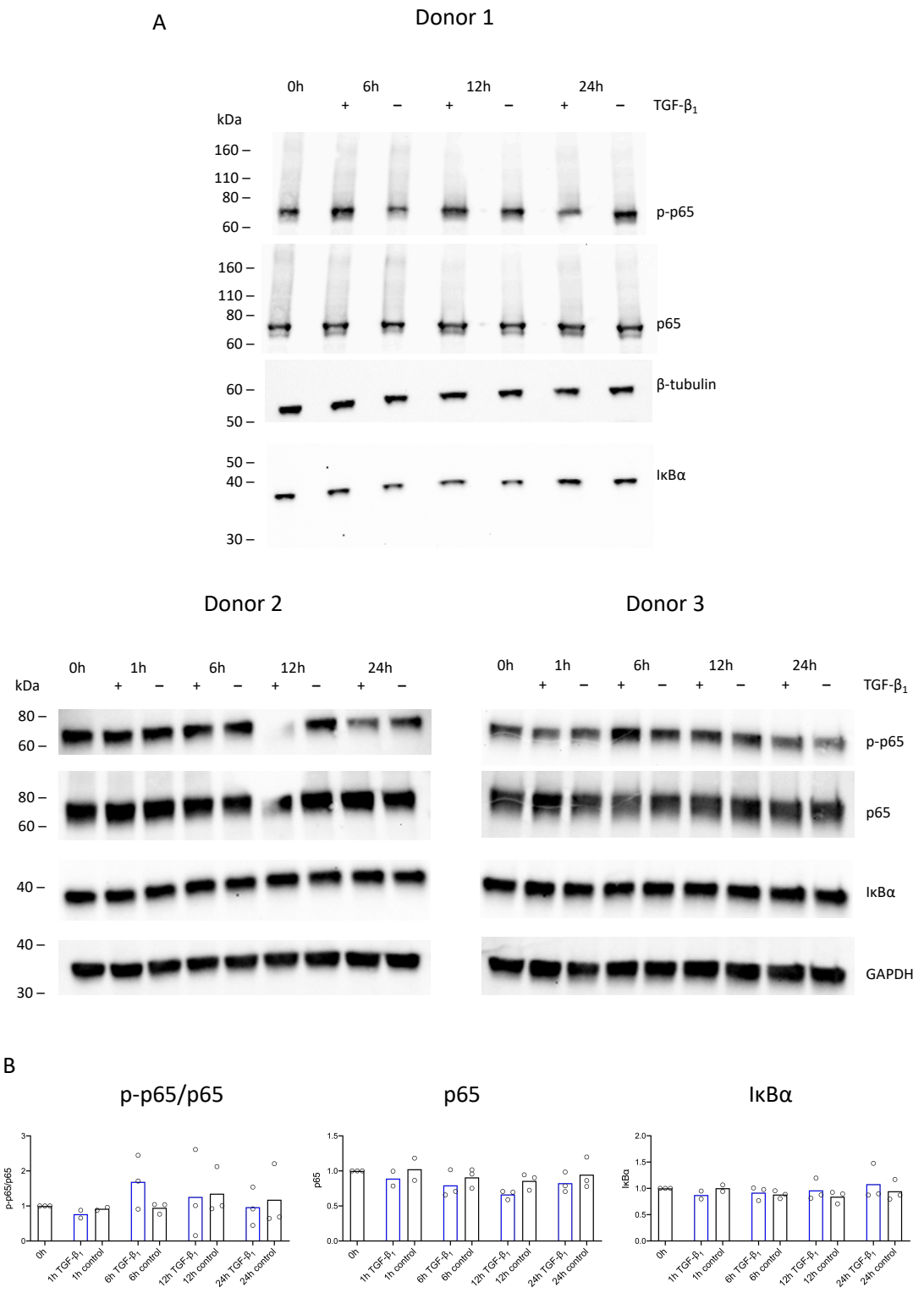


Figure 5.21 Analysis of the effects of TGF-β1 on the NF-κB signalling pathway in activated CD4+ T cells
Purified CD4+ T cells from n=3 HIV-seronegative donors were activated for 48 hours with 50ng/ml anti-CD3, 100ng/ml anti-CD28 and 50IU/ml IL-2 then lysed before (n=3 donors) or after treatment with TGF-β1 (50ng/ml) for one (n=2 donors); six, 12 or 24 hours (n=3 donors). Western blot for p-p65, total p65 (p65), or IκBα was performed on whole cell lysates. **A**. Blots from time courses from each donor. **B.** Summary of data from all 3 donors showing densitometric analysis (normalised to the relative housekeeping protein) of p-p65 as a factor of total p65 (left), total p65 (centre), and IκBα (right). Values are plotted relative to the baseline band ("0 hours").

Table 5.4 Analysis of the effects of TGF-β_1 on expression of NF-κB pathway genes in activated CD4$^+$ T cells			
Gene	**Protein encoded**	**Log_2 fold change [A]**	**Adjusted P value [A]**
CHUK	IKK1	-0.137	0.9996
IKBKB	IKK2	-0.110	0.9237
IKBKG	IKKγ	-0.189	0.7994
MAP3K7	TAK1	0.047	0.9996
NFKB1	p50	-0.006	0.9996
NFKB2	p52	-0.258	0.9122
NFKBIA	IκBα	0.122	0.9539
NFKBIB	IκBβ	-0.083	0.9996
REL	c-Rel	-0.027	0.9996
RELA	p65	0.031	0.9996
RELB	RelB	-0.068	0.9996

[A] Log_2 fold change and adjusted P values for genes differentially expressed in TGF-β_1-treated activated CD4$^+$ T cells relative to untreated control cells.

5.2.13 TGF-β_1 decreases the phenotypic activation status of highly activated CD4$^+$ T cells

To ascertain whether TGF-β_1 exerts any effect on the activation status of CD4$^+$ T cells under the conditions used in the HIV-1 replication assays, the aforementioned RNAseq dataset was interrogated for potential differential expression of genes encoding T cell activation markers. These included CD69, CD25, CD38, HLA-DR, CD71[653], Ki-67[653], CD44[654], CD137[655], CD154[656], CD122 (the beta subunit of the IL-2 receptor) and CD134 (OX40)[657].

In CD4$^+$ T cells that had been activated for 48 hours, 24 hours of TGF-β_1 treatment resulted in statistically significant downregulation of *CD38* (0.6-fold) and the gene encoding CD154 (0.78-fold); statistically significant upregulation of the gene encoding CD122 1.6-fold, and gene expression of other markers was unaltered (Table 5.5). *CD38* was further examined by qRT-PCR, and although the same subtle trend for downregulation was observed, the difference did not reach statistical significance in the n=5 donors tested (Fig. 5.6).

To gain more insight into changes in the phenotypic activation status of CD4$^+$ T cells over time, CD8-depleted PBMCs from three more HIV-seronegative donors were activated for 48 hours and then treated with TGF-β_1 and subsequently stained to evaluate activation marker expression on CD4$^+$ T cells and analysed by flow cytometry.

At 24 hours post-TGF-β_1 addition, expression of early activation markers CD69 and CD38, late marker CD25 and very late marker HLA-DR were analysed (Fig. 5.22A). When considering n=3 donors together, TGF-β_1 had no obvious effect on the percentage of $CD4^+$ T cells expressing these markers (Fig. 5.22B) and largely no effect on the MFI of these markers at this timepoint, although the intensity of expression of CD38 showed a slight trend to be decreased in TGF-β_1-treated cells (Fig. 5.22C).

Cell surface expression of CD38 and CD25 in $CD4^+$ T cells was also analysed by flow cytometry at two and five days post-TGF-β_1 in n=5 donors (Fig. 5.23A). Overall, TGF-β_1 showed a trend to decrease the percentage of cells expressing CD38 at day two, and statistically significantly decreased expression of CD25 at day five (Fig. 5.23B). When considering MFIs, TGF-β_1 statistically significantly decreased the intensity of expression of CD38 at both days two and five post-treatment, and of CD25 at day five (Fig. 5.23C).

Next, a comparison was made with less activated cells co-cultured with HIV-1-pulsed allogeneic MDDCs, a viral replication assay system in which TGF-β_1 had no effect on viral replication. Under these conditions, TGF-β_1 had no effect on the percentage of $CD4^+$ T cells expressing CD69, CD38, CD25 or HLA-DR at two, five or eight days post-co-culture (Fig. 5.24A), nor on the MFI of those markers (Fig. 5.24B).

In summary, it was concluded that TGF-β_1 reduces the phenotypic activation status of $CD4^+$ that are already highly activated prior to cytokine treatment (and this effect was observed as most pronounced between two and five days post-TGF-β_1 treatment), but not that of less activated cells. As shown in Chapter 4, HIV-1 can replicate in cells in both of these states, but TGF-β_1 restricted replication of the virus only in the former, indicating that reduction of cell

activation state likely represents a key mechanism of TGF-β_1-mediated inhibition of HIV-1 replication.

Table 5.5 The effects of 24 hours of TGF-β_1 treatment of pre-activated CD4$^+$ T cells on expression of T cell activation marker-encoding genes

Gene	Protein encoded	Log_2 fold change [A]	Adjusted P value [A]
CD38	CD38	-0.652	0.0176 *
CD40LG	CD154	-0.362	0.0154 *
CD44	CD44	0.219	0.8565
CD69	CD69	0.103	0.9996
HLA-DRA	HLA-DR alpha chain	-0.020	0.9996
IL2RA	CD25 (IL-2 receptor subunit alpha)	-0.212	0.7172
IL2RB	CD122 (IL-2 receptor subunit beta)	0.672	0.0035*
MKI67	Ki-67	-0.868	0.1407
TFRC	CD71	-0.270	0.7819
TNFRSF4	CD134 (OX40)	-0.444	0.3003
TNFRSF9	CD137	0.308	0.7413

[A] Log_2 fold change and adjusted P values for genes differentially expressed in TGF-β_1-treated activated CD4$^+$ T cells relative to untreated control cells.
* Adjusted P value<0.05

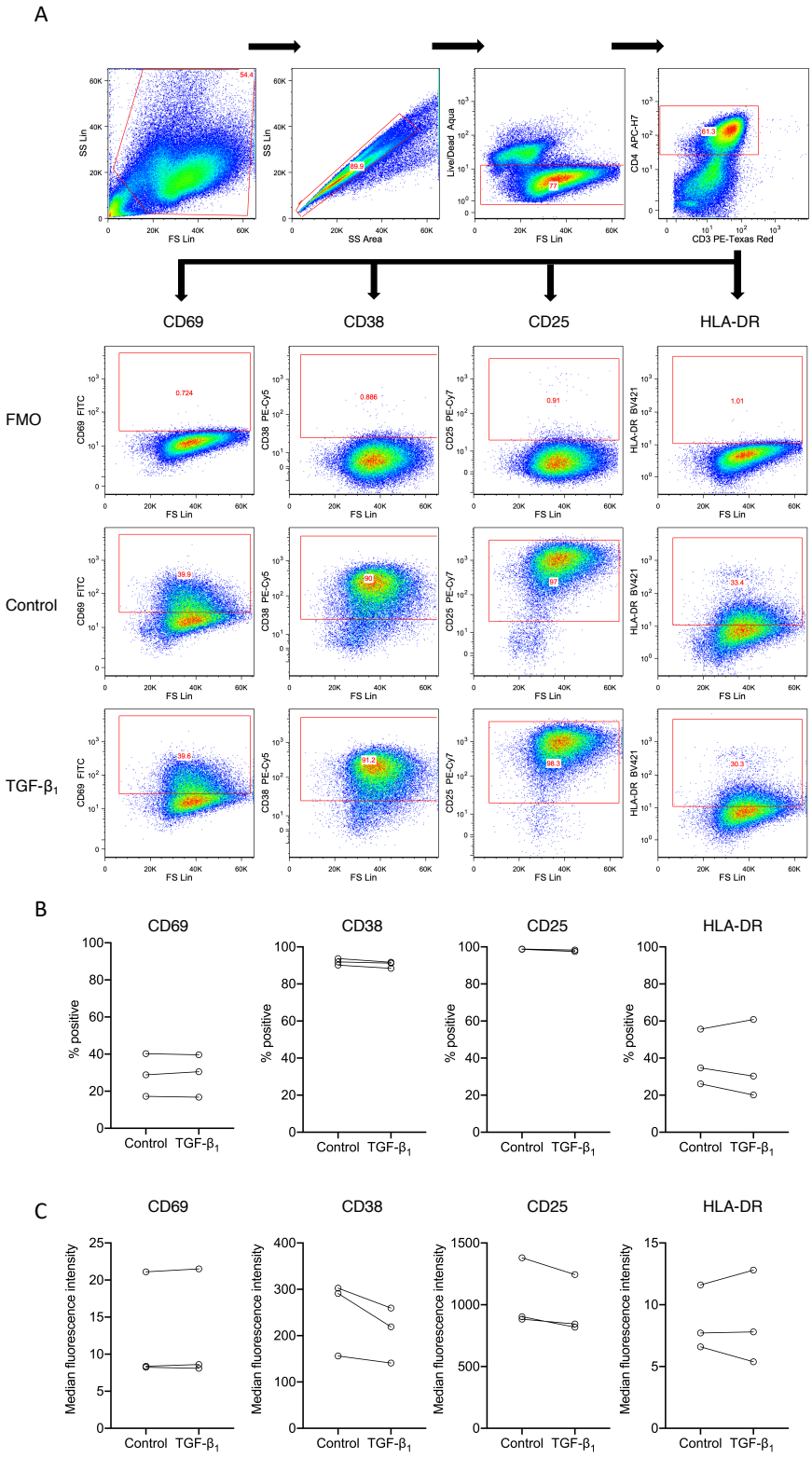


Figure 5.22 Analysis of the effects of treatment of pre-activated CD4⁺ T cells with TGF-β$_1$ for 24 hours on expression of cellular activation markers

CD8-depleted PBMCs from n=3 HIV-seronegative donors were activated for 48 hours with 50ng/ml anti-CD3, 100ng/ml anti-CD28 and 50IU/ml IL-2 before treatment with TGF-β$_1$ (50ng/ml) for 24 hours, then expression of T cell activation markers was assessed by flow cytometry using "flow cytometry panel 2" (Chapter 2). **A.** Gating strategy and expression of CD69, CD38, CD25 and HLA-DR in CD4⁺ T cells in one representative donor. A wide initial gate was used to allow for the heterogeneity of lymphocyte size during activation, followed by sequential gating on single, live, CD4⁺ T cells. Arrows denote sequential gates on the same sample. **B.** The percentage of CD4⁺ T cells positive for the activation markers. **C.** The MFIs of the same markers in CD4⁺ T cells.

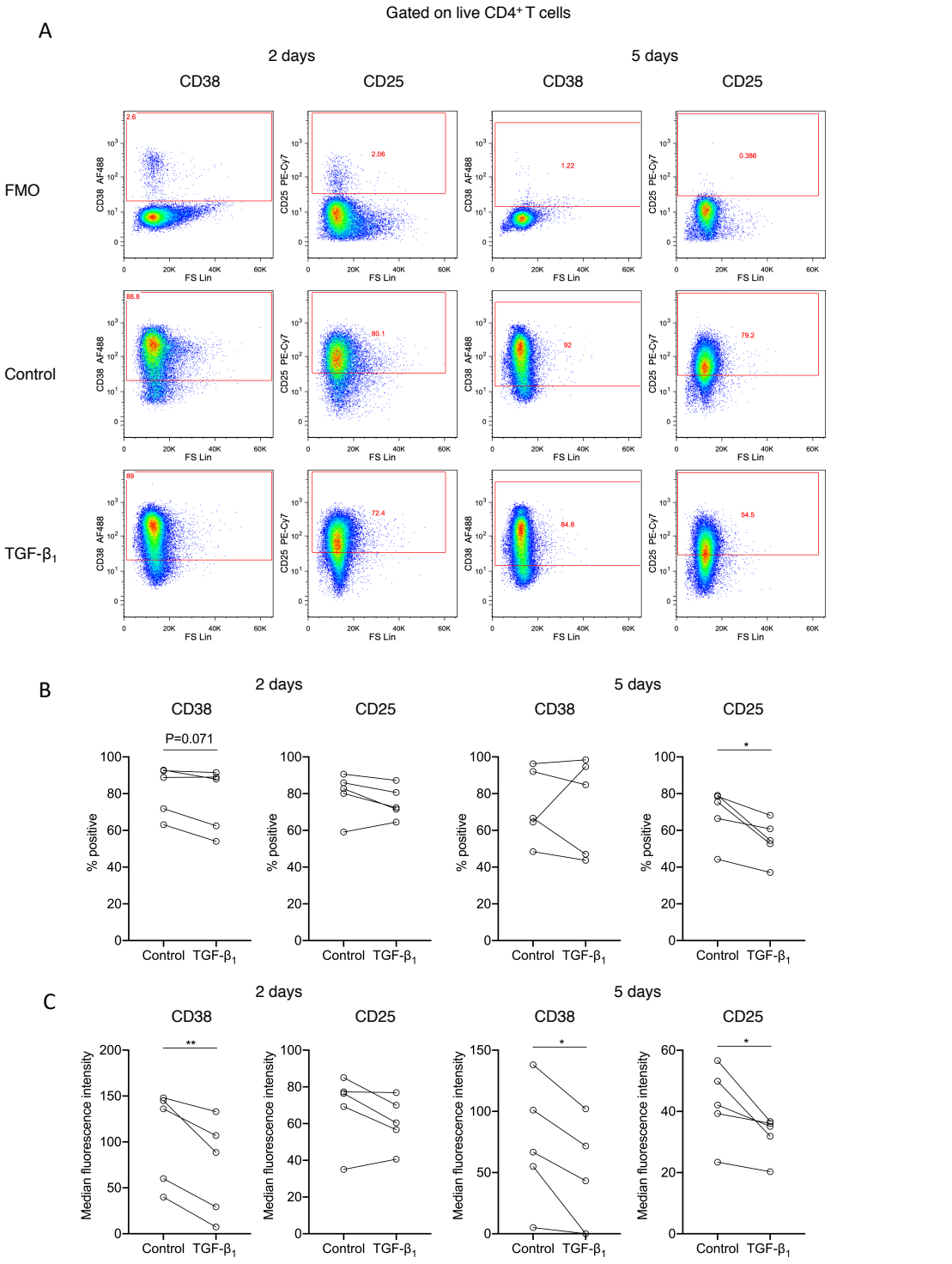


Figure 5.23 The effects of TGF-β$_1$ on activation marker expression in activated CD4$^+$ T cells after two and five days

PBMCs from n=5 HIV-seronegative donors were activated for 48 hours with 50ng/ml anti-CD3, 100ng/ml anti-CD28 and 50IU/ml IL-2 before treatment with TGF-β$_1$ (50ng/ml) for two and five days, then expression of T cell activation markers was assessed by flow cytometry using "flow cytometry panel 4" (Chapter 2). The activation stimulus was removed 24 hours post-TGF-β$_1$. **A.** Expression of CD38 and CD25 in CD4$^+$ T cells in one representative donor. Initial gating on live CD4$^+$ T cells was done as in Fig. 5.18, which used the same panel. **B.** The percentage of CD4$^+$ T cells positive for CD38 and CD25 in n=5 donors. Paired t-test, *P<0.05. Similar results were obtained with donor trios comprising some single donors used in this figure (data not shown). **C.** The MFIs of the same markers in CD4$^+$ T cells. A small number of MFI values were negative numbers. These were assigned a value of 0. Paired t-test, *P<0.05, **P<0.01.

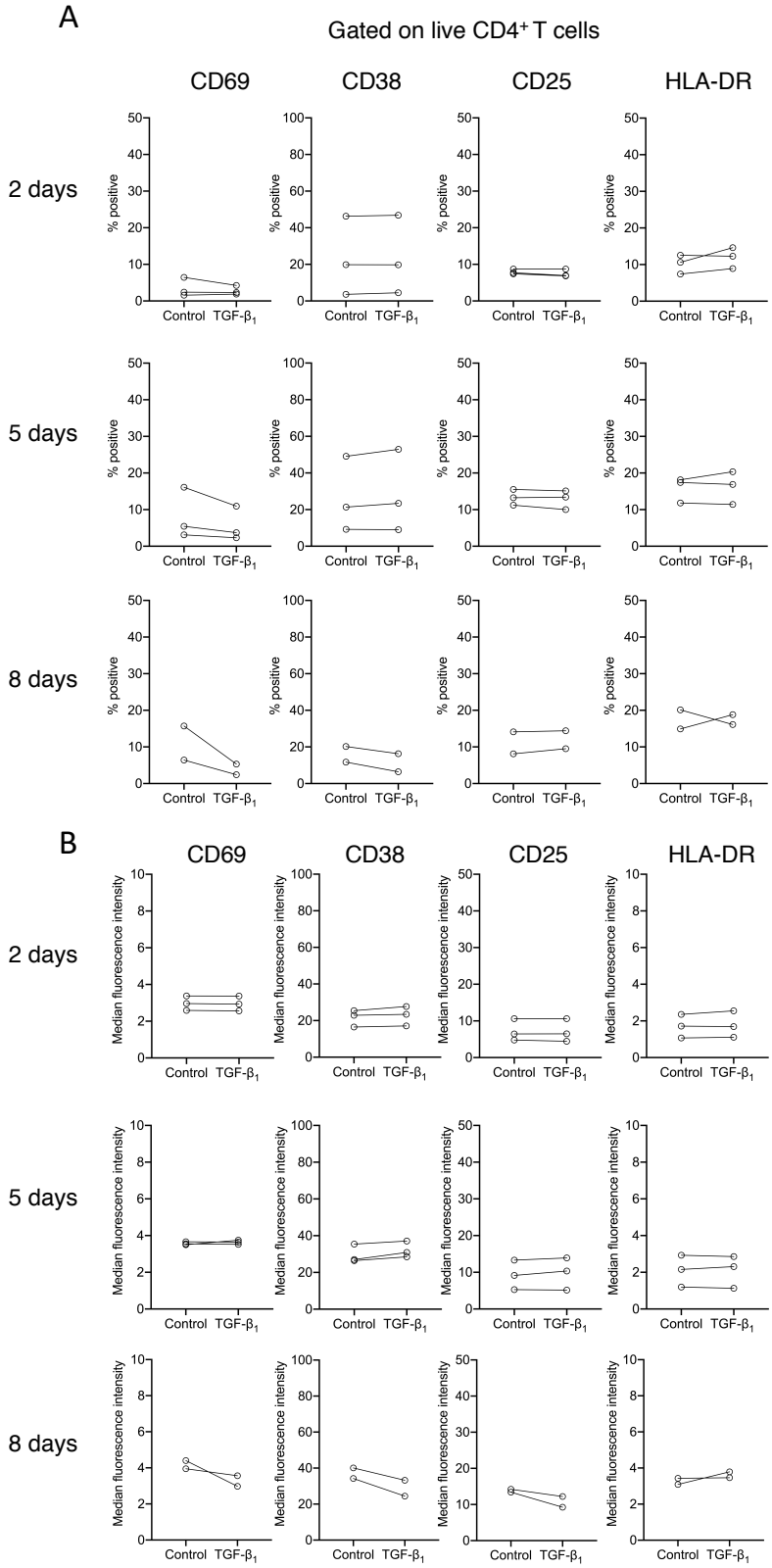


Figure 5.24 Analysis of the effects of TGF-β$_1$ on activation marker expression in CD4$^+$ T cells co-cultured with allogeneic MDDCs

CD8-depleted PBMCs from n=3 HIV-seronegative donors were treated with TGF-β$_1$ (50ng/ml) for 24 hours before co-culture with HIV-1 NL4-3 BaL-pulsed allogeneic MDDCs for a further two, five and eight days (with TGF-β$_1$ remaining in the culture), then expression of T cell activation markers was assessed by flow cytometry using "flow cytometry panel 2" (Chapter 2). Initial gating on live CD4$^+$ T cells was done as in Fig. 5.22, which used the same panel. **A.** The percentage of CD4$^+$ T cells positive for CD69, CD38, CD25 and HLA-DR in n=3 (timepoints days two and five) or n=2 (day eight) donors. **B.** The MFIs of the same markers in CD4$^+$ T cells.

5.2.14 TGF-β_1 negatively affects activated CD4$^+$ T cell proliferation

Given the finding that TGF-β_1 decreases the phenotypic activation state of CD4$^+$ T cells, it was next assessed whether TGF-β_1 has any impact on activation-induced T cell proliferation. Although it is generally accepted that TGF-β_1 is an overall suppressive cytokine, it is also responsible for some homeostatic proliferation and maintenance of CD4$^+$ T cells under certain circumstances[314]. It was therefore important to determine whether, in cultures under specific assay conditions used in this thesis thusfar, TGF-β_1 had any impact on T cell proliferation.

PBMCs from HIV-seronegative donors were stained with a proliferation-tracking dye, CTV, before activating under the same conditions as in the standard HIV-1 replication assay (although cells were not infected) and treating with TGF-β_1. Proliferation was assessed two and five days post-TGF-β_1 treatment. At both timepoints, TGF-β_1 reduced CD4$^+$ T cell proliferation (Fig. 5.25A). TGF-β_1 statistically significantly reduced the percentage of cells that divided at day two and trended towards the same effect at day five (Fig. 5.25B) as well as reducing several indices used to quantify cell division (Fig. 5.25C).

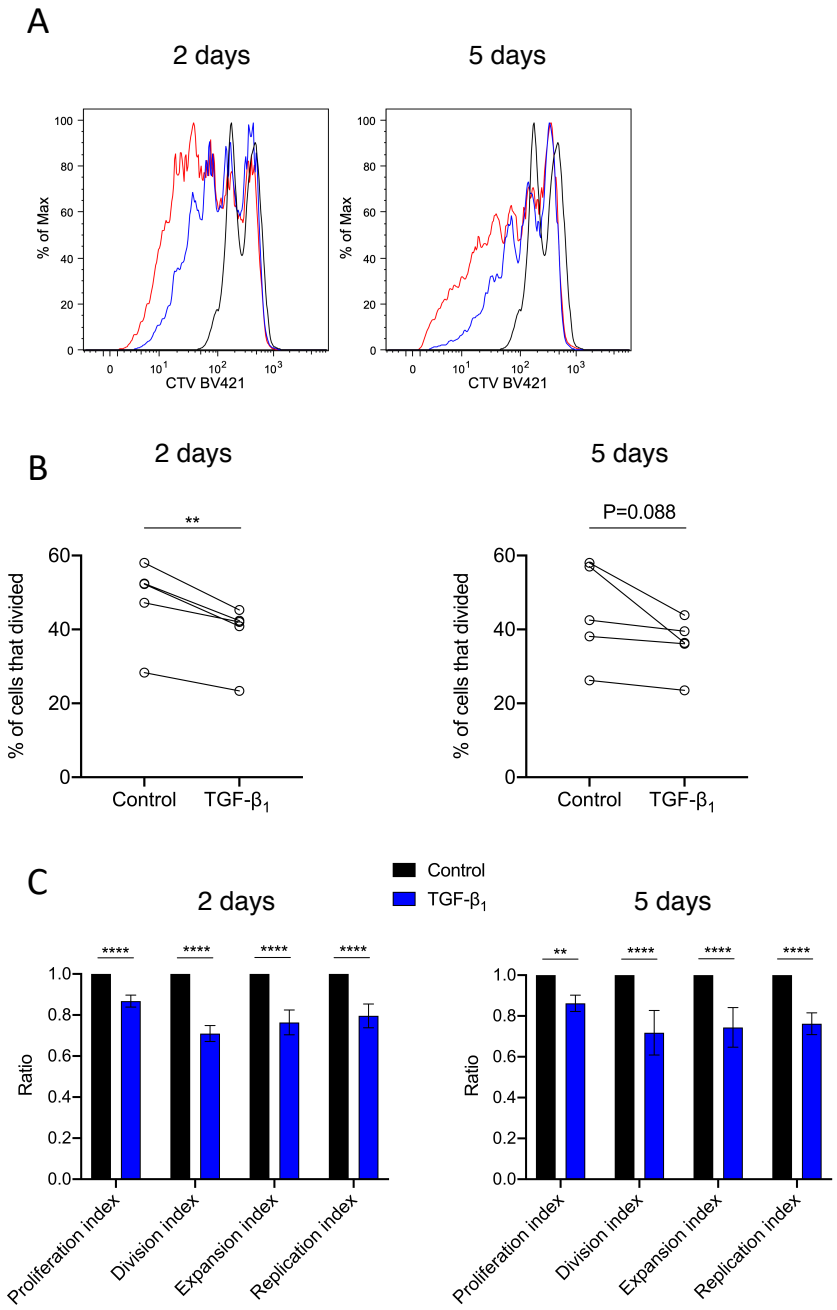


Figure 5.25 The effects of TGF-β$_1$ on activated CD4$^+$ T cell proliferation
PBMCs from n=5 HIV-seronegative donors were stained with CTV before activating for 48 hours with 50ng/ml anti-CD3, 100ng/ml anti-CD28 and 50IU/ml IL-2. Cells were then treated with TGF-β$_1$ (50ng/ml) for two and five days, then CD4$^+$ T cell proliferation was assessed by flow cytometry using "flow cytometry panel 4" (Chapter 2). The activation stimulus was removed 24 hours post-TGF-β$_1$. **A.** Histograms showing the signal intensity of CTV in CD4$^+$ T cells in one representative donor at days two and five post TGF-β$_1$ addition, with each peak representing a division. Initial gating on CD4$^+$ T cells was done as in Fig. 5.18, which used the same panel. Black=cells after 48 hours of activation, just prior to TGF-β$_1$ addition, blue=TGF-β$_1$, red=control. **B.** The percentage of CD4$^+$ T cells from n=5 donors that divided by days two and five post TGF-β$_1$ addition, as calculated by the proliferation function on FlowJo 9. Paired t-test, **P<0.01. **C.** Indices of cell division in CD4$^+$ T cells from n=5 donors two and five days post-TGF-β$_1$ treatment, as calculated using the proliferation function on FlowJo 9, shown relative to the untreated control condition. Proliferation index=the total number of divisions divided by the number of cells that underwent division (only considers responsive cells). Division index=the average number of divisions that any given cell in the original population underwent (considers all cells). Expansion index=fold expansion of the whole culture overall. Replication index=fold expansion of only the cells that proliferated. Bars represent the group mean, error bars represent the SD. TGF-β$_1$ was compared to control for each index using two-way ANOVA with Sidak's post-test, as four comparisons were made. **P<0.01, ****P<0.0001. Results similar to those in (B) and (C) were also obtained with donor trios comprising some donors used in this figure (data not shown).

5.2.15 TGF-β_1 does not affect the viability of activated CD4$^+$ T cells

Next, the influence of TGF-β_1 on cell survival and cell numbers was considered. It was assessed whether TGF-β_1 affects the viability of CD4$^+$ T cells activated under the same strong stimulation conditions as used in the standard HIV-1 replication assays (but cells were not infected). Activated CD8-depleted PBMCs from HIV-seronegative donors were treated with TGF-β_1 for two or five days, then stained with an amine-reactive viability dye and the percentage of live cells within the CD4$^+$ T cell population was analysed by flow cytometry (Fig. 5.26A). At two and five days post-TGF-β_1 treatment there was no statistically significant difference in viability between control and TGF-β_1-treated cells (Fig. 5.26B). At four days post TGF-β_1, CD4$^+$ T cell numbers were assessed, and were found to be substantially reduced compared to controls (Fig. 5.26C).

In a prior study, it has been reported that CD4$^+$ T cells infected with a R5-tropic HIV-1 isolate that are also treated with TGF-β_1 undergo increased apoptosis after a 10-day infection as compared to non-TGF-β_1-treated infected cells[543]. Viability was thus also assessed in CD8-depleted PBMCs cells that had been infected with R5-tropic HIV-1 CH058 6M for 10 days and had also been treated with TGF-β_1 for 24 hours before (and continuously throughout) infection, in the standard HIV-1 replication assay. At day 10, TGF-β_1 had no effect on viability (Fig. 5.26D). However, there was a statistically significant reduction in total cell numbers with TGF-β_1 treatment (Fig. 5.26E).

Taken together, these findings in both single donors and donor trios uninfected and infected with HIV-1 respectively all indicate that TGF-β_1-mediated reduction in T cell activation and proliferation leads overall to decreased cell numbers, with no effect on viability or cell survival.

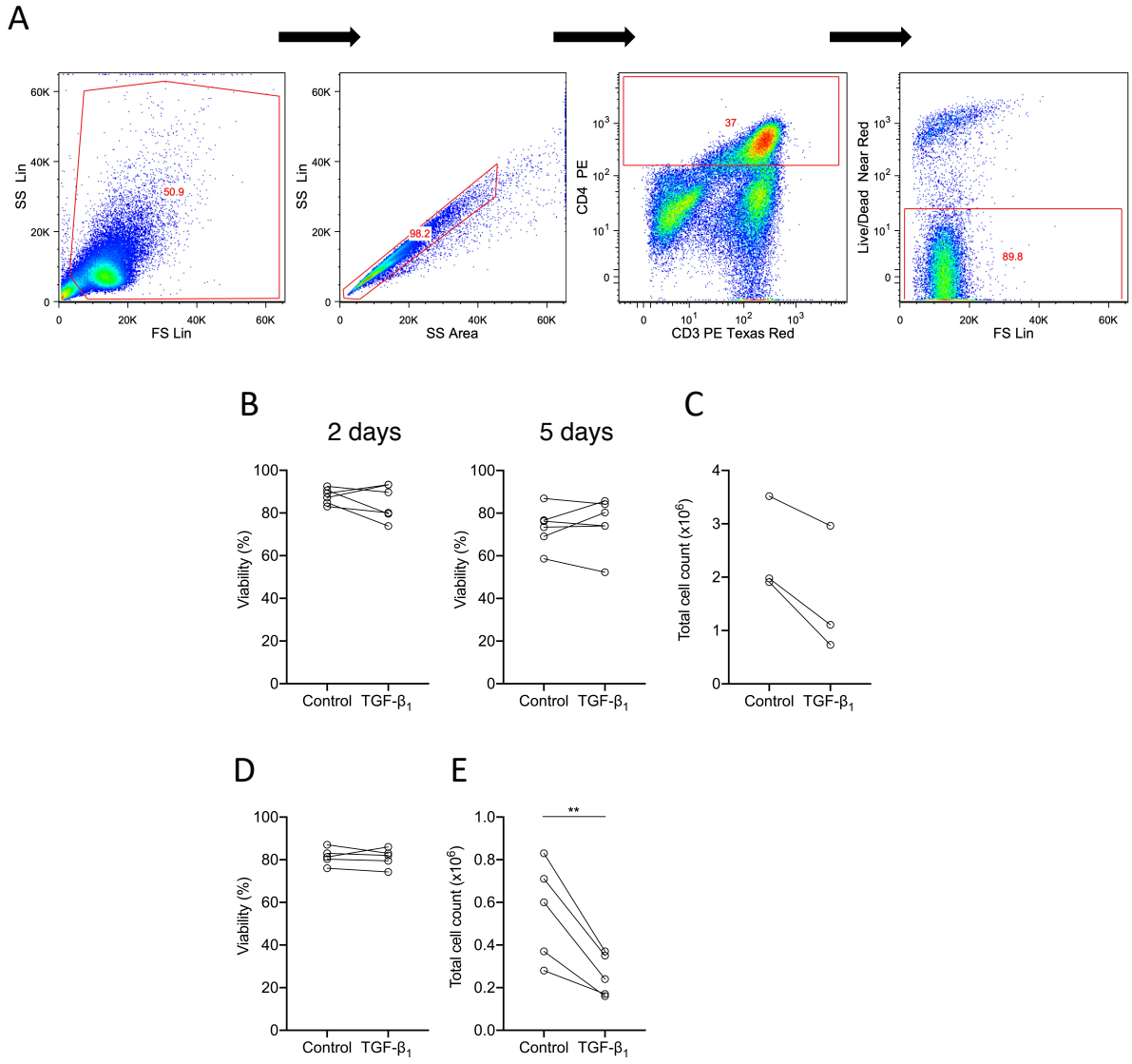


Figure 5.26 Analysis of the effects of TGF-β_1 on viability and cell numbers of activated CD4⁺ T cells
A. PBMCs from HIV-seronegative donors were activated for 48 hours with 50ng/ml anti-CD3, 100ng/ml anti-CD28 and 50IU/ml IL-2. Cells were then treated with TGF-β_1 (50ng/ml) for two or five days, then CD4⁺ T cell viability was assessed by flow cytometry using the amine-reactive dye Live/Dead Near Red, as part of "flow cytometry panel 4" (Chapter 2). The activation stimulus was removed 24 hours post-TGF-β_1. A wide initial gate was used to allow for the heterogeneity of lymphocyte size during activation. CD4⁺ T cells negative for the dye were considered viable. **B.** Data from (A) in n=6 donors. Groups were compared with a paired t-test, P>0.05 at both timepoints. **C.** In n=3 donors, CD4⁺ cell (both live and dead combined) numbers in equal sample volumes were assessed using CountBright flow cytometry counting beads. **D.** Under standard high HIV-1 replication assay conditions, activated CD8-depleted PBMCs from n=5 HIV-seronegative donor trios were treated with TGF-β_1 (50ng/ml) for 24 hours before (and continuously after) infection with HIV-1 CH058 6M. Exponential viral growth was confirmed by measuring p24 in supernatant (data not shown). At 10 days post-infection, CD8-depleted PBMC viabilities were compared with control cells, as measured by Trypan Blue exclusion using a TC-20™ cell counter. **E.** In the same experiment, cell counter was used to count total (live and dead) cells in wells. The mean counts of triplicate wells are displayed. Paired t-test, **P<0.01.

5.2.16 TGF-β_1-mediated inhibition of HIV-1 replication in activated CD4$^+$ T cells may not be contingent upon its effects on T cell proliferation

Data in this thesis so far has shown TGF-β_1 to reduce cell activation status, reduce cellular proliferation and inhibit HIV-1 replication, in highly pre-activated CD4$^+$ T cells. To try to disentangle whether the effects of TGF-β_1 on HIV-1 replication are predominantly mediated by affecting the cellular activation state and the intracellular environment, or through a reduction in cell proliferation and cell numbers, an experiment was devised. In this experiment, cells were activated with a reduced (2.5-fold weaker) anti-CD3, anti-CD28 activation stimulus (but not exposed to TGF-β_1), in parallel with cells activated under standard high activation conditions and treated with TGF-β_1, before measuring CD4$^+$ T cell activation status (as determined by CD38 and CD25 expression) and proliferation (Fig. 5.27A). The aim of this was to achieve a reduction of cell activation status in the former condition similar to that seen in the latter condition, but without affecting proliferation of cells in the former condition. The impact of these on HIV-1 replication was then assessed.

Owing to time constraints, only n=1 donor trio was assessed. Although neither TGF-β_1 treatment nor the reduced anti-CD3/CD28 activation stimulus impacted the percentage of cells expressing CD38 and CD25 (Fig. 5.27B), both conditions reduced the MFIs of these markers in CD4$^+$ T cells (Fig. 5.27C). To check whether TGF-β_1 treatment and the reduced activation stimulus appreciably changed the size of the cells (which could affect fluorescence intensity of activation markers), the FS and SS of the CD4$^+$ T cells for these conditions were compared and revealed no obvious difference (Fig. 5.27D). When assessing proliferation, as determined by the percentage of cells that divided five days after the time of TGF-β_1 treatment, the TGF-β_1-treated cells had a reduced level of proliferation, but the reduced activation stimulus had no effect (Fig. 5.27E). In the HIV-1 replication assay run in parallel, both conditions reduced supernatant p24 levels to the same degree (one log) (Fig. 5.27F).

These findings, though extremely preliminary and in need of expansion with a greater number of donor trios, indicate that the inhibitory effects of TGF-β_1 on HIV-1 replication are more contingent on its effects on T cell activation status than its effects on cellular proliferation, the latter inducing no additional reduction in supernatant p24.

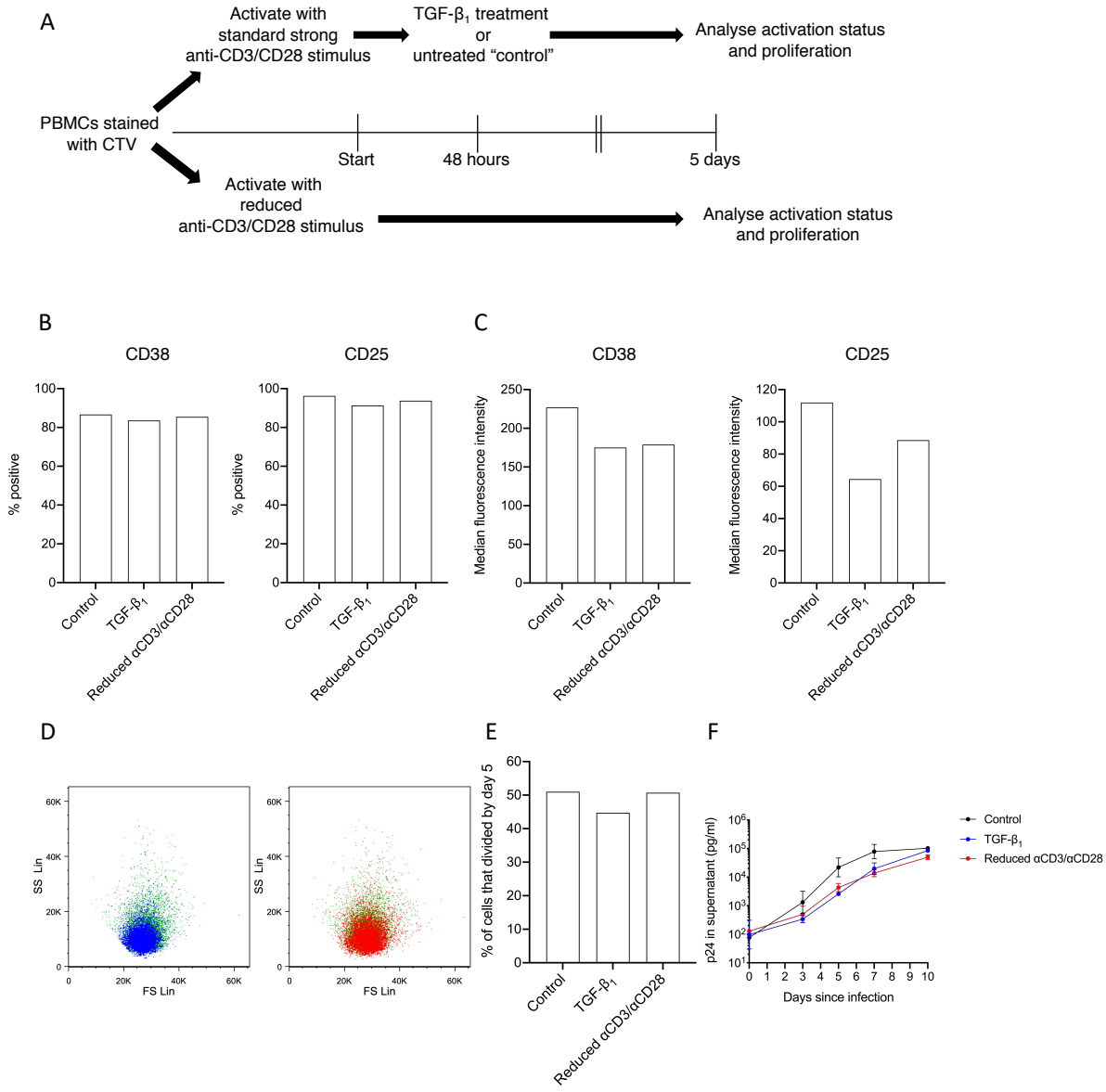


Figure 5.27 Analysis of the effects of TGF-β$_1$ and a reduced cell activation stimulus on CD4$^+$ T cell activation status, proliferation and on HIV-1 replication
PBMCs from n=1 donor trio were stained with CTV and activated for 48 hours with 50ng/ml anti-CD3, 100ng/ml anti-CD28 and 50IU/ml IL-2 before treatment with TGF-β$_1$ (50ng/ml) or no cytokine added ("control") for five days. In parallel, an aliquot of the same cells was activated with a 2.5-fold lower anti-CD3/CD28 stimulus with the same concentration of IL-2, and not treated with TGF-β$_1$. The activation stimulus was removed 24 hours post-TGF-β$_1$ treatment in all samples. At five days post-TGF-β$_1$ treatment, CD4$^+$ T cell activation status and proliferation were assessed in all three conditions by flow cytometry using "flow cytometry panel 5" (Chapter 2). Initial gating on CD4$^+$ T cells was done as in Fig. 5.18, which used a very similar panel. **A.** Schematic of the experimental timeline. **B.** The percentage of CD4$^+$ T cells positive for CD38 and CD25, gated using an FMO stain. **C.** The MFIs of CD38 and CD25 in CD4$^+$ T cells. **D.** FS and SS of CD4$^+$ T cells from the TGF-β$_1$-treated condition (left) and of the reduced anti-CD3/CD28 condition (right), each compared to control. Green=control, blue=TGF-β$_1$, red=reduced anti-CD3/CD28 stimulus. **E.** The percentage of cells that divided for each condition, as calculated by the proliferation function on FlowJo 9. **F.** In parallel, CD8-depleted PBMCs from the same donor trio were subjected to the same conditions. 24 hours after TGF-β$_1$ treatment, cells were infected with HIV-1 CH058 6M using the standard HIV-1 replication assay protocol, and supernatant p24 concentrations were assessed at different times post-infection. Error bars represent the geometric SD of triplicate wells.

5.3 Discussion

This chapter dissected possible mechanisms of TGF-β_1-mediated inhibition of HIV-1 replication in $CD4^+$ T cells. Using RNAseq, it was elucidated that TGF-β_1 induces a transcriptional signature in activated $CD4^+$ T cells distinct to that elicited by IFN-α, with the former not upregulating any known antiviral genes. Unlike TGF-β_1 and IFN-α, activin A and BMP-2 did not appreciably transcriptionally perturb $CD4^+$ T cells. This may explain why these cytokines were not found to have any effect on HIV-1 replication in the prior results chapter. Although key hits from the RNAseq dataset were validated by qRT-PCR using the same lysates from the same donors, these findings could in future be reaffirmed in a follow-up qRT-PCR experiment with an additional set of unique donors.

TGF-β_1 differentially regulated one gene with documented HIV-1-restrictive activity, the gene encoding the chemokine XCL1 (the HIV-inhibitory activity of which is likely due to interaction with gp120[627]). Notably, recombinant XCL1 failed to inhibit HIV-1 replication in the assays performed here using the R5-tropic HIV-1 strain CH058 6M. Although in a prior study, XCL1 was found to inhibit both R5- and X4-tropic lab-adapted strains and also a range of primary virus isolates, the same study found two R5-tropic isolates to be completely XCL1 resistant[627], suggesting that its inhibitory activity may be Env sequence-dependent. This could be explored further in future by performing additional experiments with a selection of both R5- and X4-tropic strains. Importantly however, as TGF-β_1 effectively inhibited the replication of HIV-1 strain CH058 6M, and neutralisation of XCL1 protein in HIV-1 replication assays had no impact on TGF-β_1- or IFN-α-mediated inhibition, it can be concluded that TGF-β_1-mediated inhibition of HIV-1 replication is not dependent on modulation of *XCL1* transcription.

Through pathway analysis, TGF-β_1 was found to downregulate expression of IL-17 isoform genes. However, addition of recombinant IL-17 to TGF-β_1-treated cultures, as well as inhibition

of IL-17 activity with a neutralising antibody, revealed no role of this cytokine in TGF-β_1 inhibition of HIV-1. TGF-β_1 was also found to upregulate the *CCL5* gene, a chemokine with known HIV-1-restrictive activity, but given that TGF-β_1 inhibits both R5- and X4-tropic viruses, the latter of which are not inhibited by CCL5[658,659], CCL5 upregulation also cannot be a complete mechanistic explanation, even if this mechanism could play a part against R5-tropic strains. Further investigation of this could entail blocking CCL5 activity with a neutralising monoclonal antibody in TGF-β_1-treated HIV-1 replication assays.

This chapter confirmed a lack of induction of both HIV-1 restriction factor genes as well as genes involved in type I IFN signalling by TGF-β_1, activin A and BMP-2 in $CD4^+$ T cells, verified by both RNAseq and qRT-PCR. These findings are interesting, given observations by others that this occurs in many other cell types including hepatocytes, epithelial cells, endothelial cells and mesenchymal cells in experiments performed with the latter two cytokines[363,415,416]. TGF-β_1 has more limited evidence but has been observed to upregulate *IFITM3* in glioma cells[485] and many ISGs indirectly through type I IFN induction in HPV-infected keratinocytes[486]. Interestingly, work in Chapter 4 showed no effect of TGF-β_1, activin A and BMP-2 on HIV-1 replication in 293FT cells, despite the fact that these cells have an epithelial/mesenchymal-like phenotype[583].

Future work in this area could entail taking a cell line that is known to robustly upregulate some of these genes, such as Huh7 or Huh7.5 cells, and attempting to transfect with the HIV-1 genome to achieve virus production, and examining the effects of treatment of the cells with TGF-β superfamily cytokines on virus output. This would address whether HIV-1 is inherently resistant to the intracellular environment created by these cytokines that restricts other viruses in hepatoma cells[363], or whether they may putatively contribute to restriction of HIV-1 replication in any non-haematopoietic cells that become infected by the virus *in vivo*[660].

Regardless of this, however, the observations made here have broader relevance by highlighting the fact that the antiviral activity of TGF-β superfamily cytokines is not as cell-type independent as that of type I IFNs, but instead is more akin to that of type III IFNs, which act in a tissue-specific manner[114].

This chapter also examined the impact of TGF-β_1 on the Th cell makeup of $CD4^+$ T cells after activation under the same activation conditions as used throughout this thesis in standard HIV-1 replication assays, under which TGF-β_1 inhibits HIV-1 replication. Although this was only addressed in a preliminary experiment from which limited conclusions can be drawn, TGF-β_1 appeared to have no effect on naïve or Tcm percentages, at odds with a prior study showing that TGF-β signalling inhibits Tcm differentiation[661], though others have shown TGF-β maintains memory T cell populations[662]. However, studies vary on the choice of markers to define memory populations, and in studies in which T cells are activated[661], variation in results could be explained by differences in activation stimuli used. TGF-β_1 did appear to prevent a rise in the percentage of $CCR7^-CD45RA^-$ Tem cells, in line with other studies demonstrating an inhibition of effector cell differentiation by TGF-β[321]. One study has shown Tems to have increased susceptibility to R5-tropic strains relative to naïve cells. However, the same study also showed that Tems are relatively more resistant to X4-tropic strains compared to naïve cells[663]. Given that work in the previous chapter demonstrated TGF-β_1 to inhibit the replication of both R5- and X4-tropic strains equally, a reduction in the percentage of Tems by the cytokine likely does not constitute a major mechanism by which TGF-β_1 exerts its antiviral activity.

Within the Tem compartment, TGF-β_1 appeared to reduce the percentage of $CCR6^+CXCR3^-$ Th17 and $CXCR5^+CCR6^+CXCR3^-$ Th17-like follicular-phenotype cells. Further work is needed to expand these data with a greater number of HIV-seronegative donors, and at a range of serial timepoints to draw more robust conclusions, rather than only on the fourth day post-

TGF-β_1. In addition, an alternative flow cytometry panel utilising intracellular staining for Th subset-specific transcription factors or including intracellular staining for cytokines such as IL-17 and IFN-γ would strengthen the conclusions drawn, as there may be some surface chemokine expression overlap between some Th subsets. For example, FOXP3$^+$ Treg cells have been reported to be CCR6$^+$CXCR3$^-$, making this phenotype potentially not unique to Th17 cells; and there is also some overlap in expression of CXCR3 between Th1 and Treg cells[664].

If the findings of the preliminary experiment performed here can be replicated, a decrease in the proportion of Th17 and Th17-like cells may help to provide an explanation for the antiviral activity of TGF-β_1, given that Th17 cells are more susceptible to HIV-1 infection than many other Th subsets, and Th cells show increased susceptibility to both R5- and X4-tropic strains under Th17-polarising conditions[247]. However, TGF-β_1-mediated effects on supernatant p24 levels were noted as early as day three post-infection in HIV-1 replication assays, indicative of an effect before marked changes in Th subset composition are likely to have occurred. Therefore, although this is a credible mechanism, it is likely not one that acts in the earliest stages of infection. To further explore this mechanism, Th cells could be sorted based on chemokine receptor expression, maintained in cultures with Th subset-polarising cytokines, and again the effects of TGF-β_1 on numbers of those subsets analysed. Working with monocultures with higher cell numbers of each Th subset may enhance any effects seen, making differences after TGF-β_1 treatment more obvious.

Within the same set of experiments, it initially seemed that TGF-β_1 increased the percentages of CD25$^+$FOXP3$^+$ and CD25$^+$FOXP3^{hi} Treg cells present in the CD4$^+$ T cell population. However, a follow-up experiment with a greater number of HIV-seronegative donors found TGF-β_1 to have no impact on the proportion of these cells.

The impact of TGF-β_1 on the expression of viral coreceptors CCR5 and CXCR4 in activated $CD4^+$ T cells was also examined. Despite the findings by others[543], TGF-β_1 did not affect the percentage of $CD4^+$ T cells expressing CCR5. However, the cytokine did appear to slightly increase the intensity of CCR5 expression in the n=2 donors studied. TGF-β_1 also showed a trend to maintain high levels of expression of CXCR4 on activated $CD4^+$ T cells, which decreased in control cells. Other studies have documented TGF-β_1 to increased expression of CXCR4 in MDMs[548] and a mammary epithelial cell line[665]. Such an observation probably has no net effect on HIV-1 replication, given that data in Chapter 4 revealed TGF-β_1 to restrict replication of R5- and X4-tropic strains equally. Though again, as with the conclusions on Th cell subsets, the very low n of this experiment should be expanded, and a kinetic analysis performed before stronger conclusions can be drawn.

This chapter found TGF-β_1 to reduce transcriptional activity from the HIV-1 LTR in primary $CD4^+$ T cells. Cells were infected with the pseudotyped reporter virus for 72 hours before the application of TGF-β_1, resulting in a modest but statistically significant effect. Future work expanding on this could apply TGF-β_1 after a shorter timeframe, given that HIV-1 transcripts can appear in the cytoplasm in under 24 hours[666]. It may be that with a shorter experiment, there is less time for the luciferase signal to build up, and a more pronounced effect of TGF-β_1 may be observed. The findings in this section were important to clarify as this is an issue for which no previous consensus has been observed in experiments performed in other cell types. TGF-β was found to inhibit HIV-1 LTR activity in a mammary epithelial cell line[546], but stimulated it in MDMs[546], an immortalised keratinocyte cell line[603] and a murine pre-B cell lymphoma cell line[603]. TGF-β also stimulated the LTR in primary human mesangial cells but only in the pg/ml dose range; with no effect noted in the ng/ml range[601]. In an astrocytic cell

line, transcription from the HIV-1 LTR was stimulated by SMAD3 but inhibited by SMAD4[602], both of which accumulate in the nucleus following cellular TGF-β stimulation[288].

Data from Chapter 4 demonstrated differential sensitivity of TF and 6-month consensus sequence paired viruses. However, in most of the paired viruses studied, only minimal differences exist between the TF and 6M LTR sequences[57]. Inspection of the LTR regions in these viruses (not shown in this thesis) has revealed that in six of the seven pairs studied, there were no nucleotide changes at all within the LTR regions containing NF-κB/NFAT binding sites; and in the single discrepant pair of viruses, CH058 TF and CH058 6M, this was due to a single nucleotide change. This highlights that although, as shown in this chapter, TGF-β_1 reduces transcription from the LTR, this does not underlie the differential sensitivity of TF and 6M viruses to inhibition by the cytokine in Chapter 4, supporting the previous conclusion in that chapter that this phenomenon was likely due to differences in viral fitness.

To further dissect the inhibition of the HIV-1 LTR by TGF-β_1, the effects of the cytokine on the activation of the NF-κB pathway were examined. In work by others, one study that found TGF-β to inhibit HIV-1 LTR activity indicated the phenomenon may be due to downregulation of transcription of an IKK gene in mammary epithelial cells. However, in the same study, in which TGF-β was also seen to stimulate HIV-1 LTR activity in MDMs, transcription of the same gene was unaffected[546]. Similarly, in another study in which TGF-β was found to stimulate HIV-1 LTR activity, the authors found the phenomenon not to be mediated through changes in the levels of IκB proteins, nor also through changes in the nuclear:cytoplasmic ratio of p50 or p65 subunits or DNA binding ability of NF-κB subunits[603]. Similarly, in a third study finding TGF-β_1 stimulation of the LTR in human mesangial cells, no effect was noted on DNA binding of NF-κB[601]. Taken together, these studies indicate that in cell types in which TGF-β_1 inhibits transcription from the HIV-1 LTR, this may be mediated through downregulation of the IKK

pathway, but that in cell types in which TGF-β-mediated LTR stimulation is seen, obvious modulation of various components of the NF-κB pathway is not observed, even if in both cases, intact NF-κB binding sites in the LTR are required[546,603].

Data in this chapter found no evidence of an effect of TGF-β_1 on activation of the NF-κB pathway in CD4$^+$ T cells, either at the protein level or the transcriptional level of NF-κB genes, including IKK genes. However, when immunoblotting for NF-κB and IκB proteins, relatively strong bands were detected at baseline, probably due to the fact the cells were highly activated for 48 hours prior to TGF-β_1 treatment. It may be that under high cellular activation conditions, if TGF-β_1 exerts relatively subtle effects on NF-κB activation, these may be missed, particularly with the western blot, which is only a semi-quantitative technique. Further experiments addressing this point should utilise an NF-κB-responsive reporter construct, which may be relatively more sensitive.

A number of studies have also found FOXP3 to exert various effects on the HIV-1 LTR in CD4$^+$ T cells. These include reduction of transcription from the LTR[605,606] which may at least in part be mediated by a reduction of NFAT2 binding to dual NF-κB/NFAT binding sites[606]; and stimulation of the LTR which may in part be due to increased DNA binding of p65[607]. High expression of FOXP3 is a hallmark of Tregs, which can be induced from naïve cells by TGF-β. However, given that work in this chapter revealed no alteration in the percentage of Treg cells or FOXP3 expression by TGF-β_1 in activated CD4$^+$ T cells, this probably does not represent the mechanism by which TGF-β_1 inhibits the LTR in these cells.

Work in this chapter analysed the impact of TGF-β_1 on phenotypic activation status of CD4$^+$ T cells. In highly activated cells, after 24 hours of TGF-β_1 treatment, overall no substantial effect was seen on expression of some canonical surface activation markers, but expression of the

genes encoding CD38 and CD154 were reduced. Further flow cytometric analysis revealed decreased expression of CD38 two and five days post-TGF-β_1, and of CD25 at day five. However, TGF-β_1 had no impact on these markers in lesser activated $CD4^+$ T cells cultured with allogeneic MDDCs – an alternative assay system used in Chapter 4 to study HIV-1 replication. These data indicate that one mechanism by which TGF-β_1 inhibits HIV-1 replication in $CD4^+$ T cells may be through a reduction in cell activation status, although only in cells that are highly activated in the first place.

This chapter also found TGF-β_1 to stem proliferation of highly activated $CD4^+$ T cells, leaving overall cell numbers reduced, with no effect on cell viability and survival. In an experiment attempting to discern whether the inhibitory effect of TGF-β_1 on HIV-1 replication is more dependent on its effects on cell activation status or on cellular proliferation, an experiment was devised using a reduced activation stimulus. This experiment attempted to mimic the same reduction in cell activation state as that induced by TGF-β_1 in highly stimulated cells, without impacting cell proliferation, before infecting cells in an HIV-1 replication assay. In highly activated cells, TGF-β_1 reduced cell activation status, proliferation, and inhibited HIV-1 replication, in line with previous findings in this thesis. On the other hand, the reduced activation stimulus decreased cell activation status without impacting proliferation, and HIV-1 replication was still inhibited to the same degree, indicating that the reduced cell activation status (and other associated effects on the intracellular environment) induced by TGF-β_1 are likely more crucial for its effects on HIV-1 replication, than are its effects on cellular proliferation. However, more extensive analysis using cells from a greater number of donors is certainly needed before firmer conclusions can be drawn.

A caveat of this experiment is the number of confounding variables created by using a reduced CD3/CD28 activation stimulus as a means of achieving reduced cell activation status. A

reduced activation stimulus has many diverse effects beyond simply impacting cellular phenotypic activation state, such as the differential regulation of thousands of genes including ISGs[573–576]. In future, an alternative experiment could take a proliferation-targeted approach, rather than one targeting activation state. Such an experiment could take highly stimulated, TGF-β_1-treated cells under standard HIV-1 replication assay conditions and attempt to reverse the TGF-β_1 dampening of proliferation, then analysing whether this impacts TGF-β_1-mediated HIV-1 restriction. One way by which TGF-β_1 stems T cell proliferation is through induction of cell cycle inhibitors such as p15[667], so such an experiment could utilise short interfering RNA to silence p15 and/or p57, which is reported to restore proliferation of epithelial cells that is inhibited by TGF-β_1[668]. To give further clues as to whether the inhibitory effects of TGF-β_1 on HIV-1 replication are dependent on its effects on cellular proliferation, future work could also assess whether TGF-β_1 affects the proliferation of $CD4^+$ cells co-cultured with allogeneic MDDCs, given that in Chapter 4, the cytokine had no effect on HIV-1 replication in this assay system.

In summary, data in this chapter has elucidated several mechanisms by which TGF-β_1 likely does and does not inhibit HIV-1 replication. TGF-β_1, along with activin A and BMP-2, does not induce canonical HIV-restrictive genes in activated $CD4^+$ T cells. And TGF-β_1 has minimal effects on the Th subset bias in these cells under these activation conditions, although it may inhibit HIV-1 replication in $CD4^+$ T cells to some extent by reducing the proportion of Th17 and Th17-like follicular cells in the Tem compartment, and, against R5-tropic strains, by inducing CCL5. Notably, TGF-β_1 decreases cell activation state and proliferation. Although the latter may not be essential for its antiviral activity, TGF-β_1 reduces transcription from the HIV-1 LTR, an effect that may putatively be mediated via effects on cellular activation state and associated alterations in activity of transcription factors such as NF-κB. Further work is needed to more deeply explore this – but of all the hypotheses tested, it seems the most likely to provide the

main explanation for the fact that TGF-β_1 inhibits HIV-1 replication in $CD4^+$ T cells in a manner that is highly dependent on cellular activation status.

Chapter 6

Summary and future perspectives

6.1 Summary

Four major objectives were addressed in this thesis. First, I sought to determine whether TGF-β superfamily cytokines are systemically perturbed in HIV-1 infection *in vivo*, and if so, what the cellular sources of production of these cytokines may be (explored in Chapter 3). Second, I investigated the impact of these cytokines on HIV-1 replication *in vitro*, and whether any effects observed were contingent on viral strain or cell type (explored in Chapter 4). Having found that one member of the TGF-β superfamily studied did impact on HIV-1 replication, TGF-β_1, my third objective was to examine the mechanism(s) by which this inhibition was mediated (covered in Chapter 5). Finally, a fourth objective was to explore any intersection of the type I IFN system and TGF-β superfamily cytokines in the modulation of HIV-1 replication (covered by work in Chapters 4 and 5).

In Chapter 3, it was shown that TGF-β_1 is rapidly systemically induced in AHI and remains upregulated throughout subacute and chronic infection, with plasma TGF-β_1 levels increasing between subacute and chronic infection. Overall, no substantial systemic upregulation of other members of the TGF-β superfamily, including activins A and B or BMP-2, was detected, although there was a trend for an increase in plasma activin A levels from subacute to chronic infection. Overall, with the exception of TGF-β_1, these findings disproved my hypothesis in Chapter 1 that TGF-β superfamily cytokines are likely to be induced in HIV-1 infection.

Using *in vitro* assays, it was deduced that DC subsets are unlikely to be sources of the elevated TGF-β_1 levels observed *in vivo*, owing to the lack of production of this cytokine upon stimulation of these cells with HIV-1 (either following isolation, or within total PBMCs). DCs and PBMCs also were not induced to produce activins A and B, or BMP-2 upon HIV-1 stimulation *in vitro*,

providing a possible explanation for the lack of their induction *in vivo.* However there remains scope for further work to re-examine this, carrying out experiments involving co-culture of selected cell subsets (e.g. pDCs together with mDCs or pDCs together with $CD4^+$ Treg cells[241]) and reading out cytokine production at a greater breadth of timepoints to ensure indirect mechanisms of HIV-mediated elicitation of TGF-β superfamily cytokine induction from PBMC subsets are not overlooked. However, one likely key source of TGF-β_1 release in HIV-1 infection is platelets, owing to the correlation observed between the plasma concentration of the cytokine and a marker of platelet degranulation in infected individuals. Together, these findings suggest that TGF-β_1 may be the only TGF-β superfamily cytokine that is substantially upregulated during natural HIV-1 infection, highlighting a need to understand the role(s) it may play in modulating virus replication (and associated pathogenesis), and providing a rationale for exploring putative antiviral effects of other TGF-β superfamily cytokines to determine their potential for therapeutic exploitation.

Experiments performed in Chapter 4 showed that *in vitro*, TGF-β_1 inhibited the replication of both X4- and R5-tropic strains of HIV-1 in activated $CD4^+$ T cells, including that of patient TF and 6-month consensus sequence-matched viruses. However, inhibition of virus replication was only observed in highly activated $CD4^+$ T cells, and not $CD4^+$ T cells with a more resting phenotype or macrophages, and virus production from 293FT cells was also not reduced. Activin A and BMP-2 had no effect on HIV-1 replication in any of the cell types tested, despite a precedent for activins and BMPs to restrict the replication of other viruses in hepatocytes and epithelial cell lines[363,413], disproving another hypothesis made in Chapter 1: that these cytokines would inhibit HIV-1 replication *in vitro*.

In Chapter 5, mechanistic work elucidated that TGF-β_1 does not upregulate expression of antiviral genes known to restrict HIV-1 replication in activated $CD4^+$ T cells. TGF-β_1 was found

to have no effect on Treg cell numbers or FOXP3 expression in pre-activated CD4+ T cells but may possibly reduce the percentage of Tem Th17 cells and Tem Th17-like follicular cells, which could contribute to reduction of HIV-1 replication. A comprehensive examination of the step(s) in the HIV-1 replication cycle impacted by TGF-β_1 was not performed, but it was shown to significantly reduce transcription from the HIV-1 LTR. Experiments examining the effects of TGF-β_1 on NF-κB activity under the cellular conditions used for viral replication assays were inconclusive. Additional work in this chapter found TGF-β_1 to decrease phenotypic cell activation status and cellular proliferation. Given the high importance of CD4+ T cell activation status in determining the ability of these cells to support productive HIV-1 replication[77,570] it is hypothesised that is likely to be the main mechanism underlying its HIV-inhibitory capacity. This could also provide an explanation for the lack of effect of TGF-β_1 on HIV-1 replication in more resting CD4+ T cells and macrophages. Overall, the work in this chapter indicates that the mechanisms of TGF-β_1-mediated inhibition of HIV-1 replication are very different from those of other innate cytokines that have direct antiviral activity.

In line with this, experiments in Chapters 4 and 5 illuminated that in activated CD4+ T cells, TGF-β_1 and IFN-α additively inhibit HIV-1 replication to a greater degree than either alone, suggesting distinct, independent mechanisms of viral restriction. Blockade of cell surface receptor-mediated signalling revealed that TGF-β_1 and IFN-α inhibit HIV-1 replication in a fashion that is mutually independent of intact signalling of one another. At the transcriptional level, neither TGF-β_1, nor activin A and BMP-2 were found to induce the transcription of canonical antiviral genes upregulated by type I IFNs in CD4+ T cells, nor any genes involved in type I IFN signalling, again despite a precedent for activins and BMPs to induce genes of both kinds in non-leukocyte cells[363,413,415,416], and disproving my final hypothesis in Chapter 1, that these cytokines would induce antiviral genes and/or modulate genes involved in type I IFN signalling. In line with these latter findings, the pre-priming of cells with activin A/BMP-2 had

no effect on enhancing IFN-α-mediated HIV-1 restriction, and the converse (IFN-α pre-treatment) did not uncover any untapped HIV-restrictive activity of those two cytokines. These findings provide a broader novel insight into the antiviral activity of TGF-β superfamily cytokines, revealing that their ability to modulate the expression of canonical antiviral genes via type I IFN-independent and -dependent mechanisms is cell-type dependent.

6.2 Future perspectives

Future *in vitro* work should focus on strengthening preliminary observations made in this thesis as well as building on some of the conclusions drawn. In particular, a greater focus is needed on the mechanisms by which TGF-β_1 inhibits HIV-1 replication.

Although data in this thesis showed TGF-β_1 and IFN-α to differentially regulate largely distinct gene sets in activated $CD4^+$ T cells, further work is needed to address the broader question of whether any other crosstalk exists between these two systems in this cell type (e.g. at the signalling protein level). Therefore, future work could examine the possibility of SMAD-STAT signalling crosstalk using flow cytometry, as is seen for example in HuH7.5 cells, where BMP-6 is documented to upregulate pSTAT1, and to enhance pSTAT1 MFI induced by IFN-α[363].

Further work is also needed to expand upon the effects of TGF-β_1 on Th cell phenotype bias in activated cells, to definitively conclude whether the cytokine does indeed reduce the percentage of Th17 cells in the Tem compartment. Given the inhibition of HIV-1 replication by TGF-β_1 *in vitro* assays apparent as early as three days post-infection, this likely does not represent the main mechanism by which the cytokine is acting. Nonetheless, experiments with purified Th subsets may more conclusively demonstrate the significance of this effect.

Further work should also delineate whether the effects of TGF-β_1 on T cell proliferation is required to exert the entirety of its antiviral effect. Similarly, although this thesis revealed little-to-no phenotypic activation of $CD4^+$ T cells infected in an alternative HIV-1 replication assay system utilising MDDC-mediated transmission, it remains to be elucidated whether the $CD4^+$ T cells in this system go on to proliferate, and if so, to what extent compared to highly activated cells in the standard HIV-1 replication assay. If $CD4^+$ T cells in the MDDC system go on to proliferate to the same extent, it will be interesting to know whether TGF-β_1 has any effect on

this proliferation under these settings, given that in this system, TGF-β_1 does not inhibit HIV-1 replication. This will give further clues to understanding whether the HIV-1 restrictive activity of this cytokine is contingent upon also inhibiting cellular proliferation or is more dependent upon modulation of the cellular activation state.

The dampening of $CD4^+$ T cell activation status remains the most likely mechanism by which TGF-β_1 mediates inhibition of HIV-1 replication. Modulation of cell activation state could inhibit numerous stages of the viral life cycle, and further work is required to determine which stages are principally affected by TGF-β_1. Expression levels of viral coreceptors were analysed, and modulation of these by TGF-β_1, which could reduce HIV-1 entry, was ruled out as a mechanism. To investigate whether post-entry early steps in the viral life cycle are affected, the earliest products of reverse transcription could be analysed, such as "strong stop" products, using the qRT-PCR methods of others[669]. The effect of TGF-β_1 could also be measured on viral integration using the popular nested *Alu*-PCR technique that detects conserved *gag* sequences alongside *Alu* elements that are repetitively dispersed throughout the human genome[670]. Importantly, work in this thesis has revealed an effect on transcription from the HIV-1 LTR, which will inevitably result in a reduction in overall viral RNA levels, subsequent viral protein production and virion release, therefore it is probably not worth assessing these. However, the infectivity of released virions could be assessed in an infectivity assay.

To expand on the LTR work, a greater exploration of the role of alterations in NF-κB activity in TGF-β_1-mediated inhibition of HIV-1 replication in activated $CD4^+$ T cells is required. This could involve using modified reporter viruses lacking NF-κB binding sites in the LTR region to see if TGF-β_1 still reduces transcription from the LTR, which has been done by others, but not in $CD4^+$ T cells[603]. In examining the effects of TGF-β_1 on NF-κB activation in primary $CD4^+$ T cells, a more sensitive assay such one using an NF-κB-responsive reporter gene construct could be

considered. Effects of TGF-β_1 on other transcription factors that modulate LTR activity, e.g. NFAT, which binds overlapping sites with those of NF-κB in the HIV-1 LTR, could also be considered.

In addition to a greater mechanistic understanding of TGF-β_1-mediated HIV-1 restriction in $CD4^+$ T cells, further investigation is warranted into the antiviral activity of TGF-β superfamily cytokines more broadly. Firstly, data in this thesis has implied a cell-type specific nature of the ability of these cytokines to initiate an antiviral state, perhaps akin to that of type III IFNs. However, unlike type III IFNs, whose tissue restriction is largely dictated by receptor expression levels[114], both $CD4^+$ T cells and macrophages were shown in this thesis to be capable of triggering receptor-driven SMAD signalling following activin and BMP exposure, yet the transcriptional response was profoundly different to that previously observed in other cell types. The lack of any differential gene expression by activin A or BMP-2 in activated $CD4^+$ T cells despite SMAD signalling could be explained by cell type-restricted downstream modulations of the pathway that affect SMAD spatiotemporal localisation, degradation or transcriptional activity. These include modulation of SMAD nuclear translocation by MAPK pathway proteins, ubiquitination of SMADs, and the presence of transcriptional co-activators or co-repressors[671,672], all of which could be further explored in $CD4^+$ T cells and macrophages in future work.

Secondly, a greater analysis of the activity of TGF-β superfamily cytokines against other viruses is also warranted. To date, antiviral activity of members of the TGF-β superfamily has been documented mostly against hepatotropic viruses. In the case of activins and BMPs, this is due to direct induction of antiviral genes or enhancement of the type I IFN response[363,413], and in the case of TGF-β_1, is due to other, incompletely understood mechanisms[559–562]. One reason for this apparent hepatotropic bias may be that TGF-β superfamily cytokines play

crucial roles in liver physiology. Hepatocytes both heavily produce and respond to BMPs and activins, in which the cytokines regulate numerous processes, including iron homeostasis through the induction of hepcidin[673], an acute phase protein systemically induced in infectious and inflammatory conditions[674]. However, BMP-mediated inhibition of a murine gammaherpesvirus[414] and activin A-mediated inhibition of Zika virus are also documented[363]. Given this, and the induction of canonical antiviral genes by various TGF-β superfamily cytokines in a broad range of cell types[363,415,416,485,486], it is likely that these cytokines restrict the replication of other many viruses of human and animal than is currently appreciated. Exploration of this, as well as the aforementioned tissue-restrictive nature of this activity, is warranted.

The findings relating to the antiviral activity of TGF-β_1 against HIV-1 in this thesis must be contextualised in the wider *in vivo* picture, especially given the complicated, contentious issue of the protective versus pathogenic nature of TGF-β_1 in HIV-1 infection in published literature[233,238,675,676]. TGF-β_1 may limit harmful excessive immune activation, exemplified by its systemic upregulation in non-pathogenic animal models of SIV infection[238]. However, it may also limit HIV-specific adaptive immunity[184,353,354], contributing to the establishment of persistent infection. And, in the later stages of infection, TGF-β_1 mediates fibrosis of secondary lymphoid tissues[349] as well as other non-AIDS morbidities. In line with this, TGF-β_1 is modestly systemically upregulated in pathogenic models in very early infection, and persists into chronicity, differentiating its kinetics from non-pathogenic models, in which induction of the cytokine is of a higher magnitude but relatively rapidly reversed following acute infection[238]. Data in this thesis demonstrating similar TGF-β_1 kinetics in patient samples clarifies the validity of the RM animal model, whilst adding support for a potential host-protective role for TGF-β_1 by restricting HIV-1 replication at the cellular level in highly activated $CD4^+$ T cells.

Although data in this thesis has revealed that they inhibit HIV-1 replication through different mechanisms, parallels can be drawn between TGF-β and type I IFNs. The latter are also induced early in AHI[63], and their ISG transcriptional signatures persist in chronicity[182,183,200], reflecting ongoing immune activation. Type I IFNs restrict HIV-1 replication in infected cells, but chronic type I IFN exposure results in loss of T cell homeostasis and increased apoptosis[195,201]. It is therefore likely that similar to type I IFNs, whether or not TGF-β_1 protects the host in HIV-1 infection depends upon the nuances of timing and cellular context.

The role of TGF-β_1 in HIV-1 infection ultimately leads to a question of whether the cytokine, or modulation of its activity, can be harnessed as part of prophylactic or therapeutic strategies. On this note, it can be concluded from work in this thesis that activin A and BMP-2 likely have no use in limiting viral replication (although they could still have effects on pathogenesis, given their immunomodulatory roles[375,381,399,402]). In line with this, soluble ACVR2.Fc ligand traps (made by the fusion of ACVR2 protein with immunoglobulin Fc, giving an improved serum half-life) have been trialled in SIV-infected RMs as a potential means of improving muscle wastage, with no effect was noted on viral load or $CD4^+$ T cell count[677]. ACVR2 is bound by GDF-8 (also known as myostatin, a member of the TGF-β superfamily that limits myogenesis) but also by activin A and BMP-2[678].

With a view to reducing the pathogenicity of HIV-1 infection to more closely mimic what is seen in SIV-infected AGMs versus that seen in macaques, one therapeutic angle could involve enhancing the activity or production of TGF-β_1 in patients in the very earliest stages of AHI. This could limit the initiation of a cascade of ongoing harmful immune activation, which does not fully abate even in the presence of ART[11,12], as well as potentially limiting HIV-1 replication at the cellular level in more activated $CD4^+$ T cells, extrapolating from *in vitro* findings of this thesis. In this manner, recombinant TGF-β_1, or a drug that enhances the activity of TGF-β_1

could form part of a combined HAART regimen given immediately after suspected or known HIV-1 exposure (e.g. occupational needlestick injuries or known high-risk sex acts), forming a novel post-exposure prophylactic strategy. A multidrug approach, as is recommended for HAART, decreases the likelihood of the development of viral escape and subsequent therapy resistance[679].

Similarly, TGF-β_1 could be harnessed as part of pre-exposure prophylaxis, an approach currently successfully used with ART drugs[680]. However, the consequences of sustained TGF-β_1 administration on establishment of systemic infection following mucosal viral challenge (and the levels of viral replication and subsequent disease progression) would need to be tested in SIV models. This work has been done for type I IFNs, where treated macaques initially showed greater resistance to SIV infection, but in those that acquired infection, disease progression was more rapid due to desensitisation of the IFN system[185].

In chronic infection, it is likely that therapeutic modulation of TGF-β_1 levels or TGF-β-mediated SMAD signalling would need to focus on dampening such activity, given its persistence in natural HIV-1 infection and in SIV-infected RMs, compared to a return to baseline levels in non-pathogenic models. Recent studies suggest such interventions targeting type I IFN activity reduce viral load[207], improve anti-HIV $CD8^+$ T cell responses[207] and reduce generalised type I IFN-driven inflammation[208]. However, it may be that systemic TGF-β_1 in chronic infection could serve to benefit the host in continuing to limit immune hyperactivation, and that the persistent TGF-β_1 signature is actually a reflection of a refractory state in which inhibitory SMAD7 is upregulated and SMAD4 is downregulated, given that these SMAD perturbations are observed in SIV-infected RMs[454].

One study has examined the effect of modulating SMAD2/3 signalling on SIV infection in RMs using pirfenidone, an anti-fibrotic, anti-inflammatory agent used to treat idiopathic pulmonary

fibrosis in people, the precise mechanisms of action of which are incompletely understood[681], but which has been shown to reduce TGF-β-mediated type I collagen synthesis and SMAD3 signalling in fibroblasts[682]. In this two-armed study[350], the authors treated SIV-infected RMs with pirfenidone and/or a HAART drug cocktail at the time of viral inoculation (and throughout acute infection), or in a separate arm, commenced treatments in chronic infection. Overall, pirfenidone in acute infection was found to reduce lymphoid tissue fibrosis and preserve total blood and lymphoid $CD4^+$ T cell numbers independently of ART. These findings may be explained by the fact that lymphoid fibrosis directly predicts a reduced capacity to preserve $CD4^+$ T cell count[95]. Pirfenidone commenced in chronic infection reduced fibrosis but had no effect on T cell numbers.

In the aforementioned study[350], pirfenidone was found to have no effect on viral load or on the percentage of peripheral blood $CD4^+$ T cells expressing the activation marker Ki67, which on the surface may suggest that the TGF-β production elicited during natural infection does not have a substantial impact on these parameters *in vivo*. However, whilst the authors of this study found pirfenidone to significantly lower expression of pSMAD2/3 in the paracortical T cell zone of lymphoid tissue sections (as measured by immunohistochemistry), the drug had no effect on TGF-β expression[350]. Given that TGF-β signals through many other non-SMAD pathways[298], it may be that whilst the modulation of SMAD2/3 signalling has no effect on control of viral replication (and in fact may accelerate lymphoid fibrosis and attrition of $CD4^+$ T cell numbers), modulating levels of TGF-β (or TGF-β-induced non-SMAD signalling pathways) may have more profound effects.

6.3 Final statement

In conclusion, TGF-β_1 is systemically induced in all stages of HIV-1 infection *in vivo.* The cytokine inhibits HIV-1 replication *in vitro* in activated $CD4^+$ T cells in a type I IFN-independent manner, acting (at least in part) by inducing a reduction in transcription from the viral promoter likely through a reduction cellular activation state. Further work is needed to elucidate these mechanisms in greater depth. The possibility of harnessing TGF-β_1 or the modulation of its activity for HIV-1 prophylaxis or therapy should also be explored in future.

BMP-2 and activin A are not substantially induced in HIV-1 infection *in vivo*, do not inhibit HIV-1 replication *in vitro*, and do not induce a type I IFN-like transcriptional signature in activated $CD4^+$ T cells. This is despite a precedent for these cytokines to inhibit different viruses in other cell types through the upregulation of antiviral genes and/or boosting the type I IFN response. A broader exploration of the effects of TGF-β superfamily cytokines against more viruses, and the potential tissue-specific nature of this activity remain exciting, unexplored directions for future innate immunity research.

Appendices

Appendix I

Genes differentially expressed (adjusted P value <0.05) in activated $CD4^+$ T cells relative to non-activated cells

Appendix I is provided as a .pdf file.

Appendix II

Genes differentially expressed (adjusted P value <0.05) in IFN-α-treated activated CD4+ T cells relative to untreated activated cells

Gene	Log2 fold change	Log2 counts per million	Unadjusted P value	Adjusted P value
TRIM25	2.16801249	6.66904394	3.28E-21	4.29E-17
MX2	2.94813387	7.02654807	6.48E-21	4.29E-17
EIF2AK2	3.49722942	5.32150794	3.49E-20	1.54E-16
MX1	4.39869569	8.15070924	9.08E-20	2.81E-16
TRIM22	1.8757894	8.32827067	1.06E-19	2.81E-16
CMTR1	1.29889043	6.80580997	2.09E-19	4.11E-16
IFI6	4.74015321	8.51769258	2.17E-19	4.11E-16
UNC93B1	2.0992172	4.87596253	2.88E-19	4.77E-16
IRF7	2.92375452	6.62029208	1.11E-18	1.64E-15
NT5C3A	2.40516761	6.42546123	2.92E-18	3.87E-15
PARP12	2.31652542	6.06988052	4.28E-18	5.16E-15
IFI27	5.19702994	3.6922363	5.20E-18	5.75E-15
IFI35	2.49359498	6.09096511	8.84E-18	9.02E-15
PNPT1	2.32422774	4.77890917	1.04E-17	9.82E-15
HELZ2	3.47816486	6.72198283	2.18E-17	1.92E-14
LAP3	2.11482762	7.14106976	6.72E-17	5.57E-14
SPATS2L	2.58551513	4.70074433	1.35E-16	1.05E-13
LGALS9	2.75516482	6.62711122	6.25E-16	4.60E-13
DDX60L	2.53267732	5.69799423	8.64E-16	6.03E-13
ADAR	1.36164797	8.85324303	9.59E-16	6.08E-13
PLSCR1	3.1353333	5.53106953	9.62E-16	6.08E-13
SP100	1.73651857	7.03520805	1.12E-15	6.76E-13
ZBP1	2.9423464	4.7154915	1.29E-15	7.43E-13
CNP	1.38718454	6.5274311	1.81E-15	9.63E-13
IFIT5	2.46969866	6.27504707	1.82E-15	9.63E-13
CHMP5	1.45249537	6.00946539	3.75E-15	1.87E-12
SP110	1.7003736	6.09680298	3.80E-15	1.87E-12
ECE1	1.40955471	6.55629244	8.91E-15	4.22E-12
LY6E	2.74533184	8.46430407	1.11E-14	4.91E-12
USP18	5.22067498	4.78951364	1.11E-14	4.91E-12
SAMD9	2.38083658	6.20916735	1.70E-14	7.28E-12
CHST12	1.4850937	5.11637196	3.74E-14	1.55E-11
TRIM21	1.48903901	6.25905157	5.60E-14	2.25E-11
PML	1.40059302	6.20652656	7.88E-14	3.07E-11
TDRD7	2.13226548	4.57954911	8.73E-14	3.31E-11
N4BP1	1.30289494	7.13755797	1.25E-13	4.59E-11
MYD88	0.96048132	6.90320237	1.57E-13	5.62E-11
IFI16	1.53356004	7.38742461	1.66E-13	5.80E-11
APOL6	1.54334219	7.64735479	1.99E-13	6.77E-11
BST2	1.70616033	7.78800868	2.22E-13	7.35E-11
ISG15	4.26639858	7.70412468	2.33E-13	7.53E-11
DTX3L	1.96012723	7.35174278	2.69E-13	8.49E-11
LGALS3BP	1.89062292	6.56470298	3.95E-13	1.22E-10
PARP9	2.34441122	7.17159909	4.41E-13	1.33E-10
OAS3	4.08130297	7.44457005	4.52E-13	1.33E-10
IFI44	3.9684153	6.32454493	6.95E-13	2.00E-10
TREX1	1.57824568	5.38636779	7.31E-13	2.06E-10
WDFY1	0.92712719	6.20351214	9.29E-13	2.57E-10
HSH2D	2.06132967	5.07997702	9.89E-13	2.67E-10
ENDOD1	1.21854902	5.25158972	1.01E-12	2.67E-10
IFI44L	5.22364898	7.02843778	1.11E-12	2.87E-10

CMPK2	5.29122513	5.49401611	1.12E-12	2.87E-10
NMI	1.48492963	6.17024817	1.27E-12	3.17E-10
TRAFD1	1.0116126	7.16887656	1.65E-12	4.00E-10
PARP10	1.94688938	6.97067119	1.68E-12	4.00E-10
STAT2	2.07388382	7.10557892	1.69E-12	4.00E-10
MOV10	1.35280587	5.99062457	1.89E-12	4.39E-10
SSTR3	1.94164767	5.55359847	2.02E-12	4.57E-10
AGRN	1.83377405	4.96701375	2.03E-12	4.57E-10
TRIM38	1.05470678	5.76406305	2.40E-12	5.30E-10
SIDT1	0.84313009	5.45588909	2.47E-12	5.37E-10
IFITM1	2.24482645	9.14144819	2.54E-12	5.43E-10
SAMD9L	2.62415055	6.47313867	4.87E-12	1.02E-09
XAF1	3.30637898	5.47122538	5.64E-12	1.17E-09
ZNFX1	1.36058765	7.17513463	5.75E-12	1.17E-09
BCL2L14	2.79559599	3.25710273	8.11E-12	1.61E-09
ISG20	1.98104835	8.15295722	8.16E-12	1.61E-09
IFIT1	6.28589148	6.57938359	8.55E-12	1.67E-09
ZCCHC2	1.49726014	5.55811558	1.60E-11	3.08E-09
NEXN	3.34862949	1.27822214	2.27E-11	4.30E-09
HIRA	0.71476093	5.69795781	2.98E-11	5.56E-09
OGFR	0.77687345	6.53998144	3.06E-11	5.64E-09
OTOF	2.43178212	2.07918689	4.25E-11	7.72E-09
TRIM26	0.68718769	6.79889872	5.73E-11	1.03E-08
SCARB2	1.03949619	4.96034621	6.71E-11	1.19E-08
IFIT2	4.42890149	7.07636588	7.30E-11	1.27E-08
SLC18B1	1.00624634	4.41970729	8.23E-11	1.42E-08
PHF11	1.22592169	6.25514881	8.99E-11	1.51E-08
XRN1	1.08254593	7.35598764	8.99E-11	1.51E-08
IFIH1	2.5492602	5.93143373	1.00E-10	1.66E-08
MT2A	1.29741556	7.06155978	1.05E-10	1.72E-08
IRS1	1.82366032	2.8709933	1.08E-10	1.75E-08
SHISA5	0.96384533	8.07970523	1.17E-10	1.84E-08
ETV7	1.79069207	3.62884224	1.17E-10	1.84E-08
SMCHD1	1.04204854	8.23795726	1.18E-10	1.84E-08
NUB1	1.00457207	7.2335768	1.26E-10	1.95E-08
FBXO6	1.77562721	4.58100516	1.30E-10	1.98E-08
IFIT3	5.59536017	7.68106957	1.66E-10	2.50E-08
NAPA	1.15259368	6.53817784	1.68E-10	2.50E-08
EPSTI1	2.41574678	6.7924903	1.70E-10	2.51E-08
ZNF620	1.38297012	1.65509	1.73E-10	2.52E-08
OASL	4.5166033	6.64525899	2.13E-10	3.07E-08
OAS1	4.50495464	6.92139119	2.20E-10	3.14E-08
TNFSF10	1.84338562	6.62459743	2.23E-10	3.15E-08
GTPBP2	0.80486801	5.49737966	2.28E-10	3.15E-08
LAMP3	2.1214766	6.58110248	2.28E-10	3.15E-08
NCOA7	0.93695197	5.99234914	3.35E-10	4.58E-08
USP15	0.73100039	6.41029237	3.86E-10	5.22E-08
PPM1K	1.51315663	6.90945727	4.39E-10	5.86E-08
BAG1	0.70805185	6.09988148	4.43E-10	5.86E-08
PARP14	1.68734721	6.40303098	4.48E-10	5.86E-08
C19orf66	1.57164057	5.69688687	4.51E-10	5.86E-08
C5orf56	1.2026519	4.40576122	4.87E-10	6.26E-08
TARBP1	1.24840641	4.89617698	5.56E-10	7.09E-08
LOC100133669	3.00187844	0.78068441	5.83E-10	7.36E-08
RBM43	1.237798	4.21948521	5.91E-10	7.39E-08
DHX58	2.32366503	5.39022842	6.30E-10	7.80E-08
PGAP1	2.14714306	4.86928802	7.18E-10	8.77E-08
SCAMP1-AS1	1.09661754	3.6260774	7.21E-10	8.77E-08
SCLT1	1.07459264	3.2113986	7.62E-10	9.19E-08
HERC6	2.98908061	5.7401473	8.83E-10	1.05E-07

UBE2L6	1.5134243	8.12376841	8.91E-10	1.05E-07
TRIM5	1.43023299	5.29112487	8.98E-10	1.05E-07
CD38	1.34641671	4.43450376	1.00E-09	1.17E-07
RPL5	-0.7975936	10.9380684	1.07E-09	1.23E-07
GPR180	0.66712155	4.60436496	1.97E-09	2.25E-07
CARD17	1.70786315	1.53310637	2.97E-09	3.36E-07
SLFN5	1.4226325	7.85783509	3.31E-09	3.72E-07
OAS2	2.737033	8.09944955	3.38E-09	3.77E-07
CTSS	0.67149058	7.34978362	3.45E-09	3.81E-07
TNK2	1.43186581	6.29644055	3.64E-09	3.99E-07
TMEM110	0.91743902	5.01929649	3.74E-09	4.06E-07
DDX60	3.36434227	6.57553111	3.76E-09	4.06E-07
MDK	1.96158322	1.78009356	4.20E-09	4.49E-07
TGM1	2.59436205	0.69482734	4.47E-09	4.74E-07
PRKD2	1.14433437	6.39768401	4.54E-09	4.74E-07
PI4K2B	1.41570335	5.92049269	4.54E-09	4.74E-07
RBCK1	1.02880916	6.70757821	5.32E-09	5.51E-07
GTPBP1	0.90297056	7.00006807	5.40E-09	5.54E-07
SMG7	0.51917579	6.60908062	5.46E-09	5.54E-07
IFITM3	2.20409051	4.79873729	5.48E-09	5.54E-07
RNF31	0.76239777	6.20924619	5.54E-09	5.57E-07
DDX58	2.55553438	6.16365054	5.63E-09	5.61E-07
PARP11	0.94165466	5.46424823	6.96E-09	6.88E-07
RSAD2	5.71717346	6.76968037	9.35E-09	9.18E-07
TAP2	0.98634241	8.08363815	9.57E-09	9.33E-07
PRR5	0.82330298	4.58704396	9.80E-09	9.48E-07
CD164	0.87023767	8.71052745	1.25E-08	1.20E-06
GBP1P1	2.24709983	1.42071412	1.39E-08	1.32E-06
RBM11	1.40140843	1.54519378	1.46E-08	1.38E-06
SP140	0.9737565	6.30073762	1.74E-08	1.64E-06
HERC5	3.57355645	6.52168801	1.88E-08	1.76E-06
STOM	0.5206267	6.93976644	2.05E-08	1.90E-06
BISPR	1.80086831	4.3365889	2.25E-08	2.07E-06
TRIM14	1.07556578	6.83353262	2.28E-08	2.09E-06
EIF3L	-0.9917523	9.05753498	2.57E-08	2.34E-06
USP30-AS1	1.00835795	3.21174408	2.78E-08	2.51E-06
RTP4	2.48082098	4.5108961	3.23E-08	2.89E-06
SAT1	1.3496525	7.30142625	3.55E-08	3.16E-06
SNX6	0.48043476	6.80606805	3.69E-08	3.26E-06
ODF2L	0.76811441	4.65002795	3.92E-08	3.44E-06
LRRC3	1.37325524	1.87204564	4.03E-08	3.52E-06
TRANK1	1.63233907	7.43233385	4.12E-08	3.57E-06
RPS3A	-0.7414369	9.8893975	4.75E-08	4.09E-06
LINC01260	2.32398056	1.22094916	5.78E-08	4.95E-06
DRAP1	1.16961197	8.21031159	6.23E-08	5.29E-06
ANKFY1	1.06917352	5.85217652	6.38E-08	5.37E-06
TTC21A	2.3207608	0.63463531	6.40E-08	5.37E-06
PSMB8	0.50691484	8.48566329	1.03E-07	8.61E-06
ARHGEF3	0.72305886	7.12076464	1.27E-07	1.05E-05
RPL4	-0.798881	11.5033751	1.37E-07	1.13E-05
LAG3	1.32126452	6.40099837	1.43E-07	1.17E-05
SETX	0.60344183	6.93181559	1.52E-07	1.24E-05
HELB	0.95431861	4.5321826	1.56E-07	1.26E-05
SLFN12	1.08140092	2.10842023	1.59E-07	1.27E-05
GMPR	1.50232033	1.18630018	1.61E-07	1.29E-05
JAK2	1.01683078	4.70120738	1.74E-07	1.38E-05
ABCD1	0.89314977	3.98991854	2.12E-07	1.67E-05
AMBRA1	0.63067568	5.37637843	2.16E-07	1.69E-05
NRSN2-AS1	1.46963964	1.19426389	2.18E-07	1.70E-05
EHD4	1.1366953	6.67313924	2.21E-07	1.71E-05

TMEM140	1.30326041	6.0852516	2.29E-07	1.76E-05
RPS7	-0.659231	7.99717347	2.48E-07	1.90E-05
TMEM62	0.84918756	3.23311894	2.49E-07	1.90E-05
KLF5	1.25038037	2.68631437	2.53E-07	1.92E-05
CASP10	0.76661647	4.93946969	2.95E-07	2.22E-05
FLJ32255	0.81236365	5.71439236	2.99E-07	2.24E-05
ALOX5AP	0.72695535	7.06282158	3.09E-07	2.30E-05
STAT1	1.21102954	10.5612971	3.23E-07	2.39E-05
IL23A	-0.958416	4.129506	3.25E-07	2.40E-05
BHLHE40-AS1	-1.0017223	2.70165145	3.74E-07	2.74E-05
MKRN1	0.52977535	7.67993849	4.14E-07	3.02E-05
SLC35A4	0.45937746	6.84780155	4.23E-07	3.06E-05
EIF3F	-0.5764708	8.22586088	4.48E-07	3.23E-05
SLC37A1	0.56190751	5.00177462	4.63E-07	3.32E-05
RPL3	-0.7664669	12.3554849	4.67E-07	3.33E-05
JADE2	0.46185985	7.79865491	5.23E-07	3.69E-05
EEF1B2	-0.707024	9.17983913	5.25E-07	3.69E-05
MIR4426	-0.6484746	10.2386287	5.26E-07	3.69E-05
CARD16	0.78064324	4.6908323	5.46E-07	3.81E-05
DYNLT1	0.85280572	5.52727504	5.57E-07	3.87E-05
CIB2	0.78104721	1.96637524	5.77E-07	3.97E-05
HERPUD2	0.54052982	6.51720891	5.78E-07	3.97E-05
USP25	0.4627891	5.95101197	5.87E-07	4.00E-05
FRMD3	2.44033193	0.7179145	5.89E-07	4.00E-05
C12orf57	-0.6023066	7.30961545	6.14E-07	4.15E-05
SLC25A28	0.9644306	5.19433965	6.27E-07	4.20E-05
TMEM170A	0.34416361	5.5915906	6.28E-07	4.20E-05
CFB	1.94571786	0.76309228	6.54E-07	4.36E-05
IFITM2	1.04086873	6.80743146	6.60E-07	4.38E-05
AZI2	0.86716714	5.40725093	6.71E-07	4.42E-05
ATP6V1H	0.42654634	4.94569003	6.73E-07	4.42E-05
RPS6	-0.6964136	11.8538119	6.86E-07	4.48E-05
RPL6	-0.7213931	9.76339983	6.92E-07	4.50E-05
SCML4	0.68504243	5.73613011	7.13E-07	4.61E-05
EEF2	-0.6187583	12.0112253	7.34E-07	4.72E-05
TRAK2	0.39068858	6.18101376	7.59E-07	4.86E-05
IRF9	1.07814093	6.60942468	8.01E-07	5.11E-05
C6orf62	0.43968762	7.52095624	8.33E-07	5.28E-05
PARP8	0.48943913	6.78710732	9.01E-07	5.69E-05
SLC38A5	0.94574745	5.54744626	9.67E-07	6.05E-05
LOC101927181	2.07741352	1.22192451	9.67E-07	6.05E-05
RPL10	-0.5995533	11.3056421	1.08E-06	6.70E-05
CEBPD	1.04865839	2.63609669	1.11E-06	6.86E-05
RPL21	-0.6448685	7.96699944	1.12E-06	6.93E-05
PABPC1	-0.5202239	11.1959267	1.20E-06	7.34E-05
C4orf33	0.76251293	2.6626964	1.27E-06	7.78E-05
NAP1L1	-0.4193098	9.93698669	1.35E-06	8.18E-05
RPS8	-0.6308753	11.3842019	1.45E-06	8.77E-05
KDELC2	0.5994807	4.82050436	1.46E-06	8.79E-05
EEF1A1	-0.672537	13.3690598	1.60E-06	9.59E-05
GIMAP2	0.76247173	7.4870455	1.71E-06	0.00010232
STAP1	0.99135852	2.30023668	1.94E-06	0.00011544
HFE	1.43267832	1.21839494	2.01E-06	0.00011895
RASGRP3	1.49551198	3.90669623	2.03E-06	0.00011985
LRRC75A-AS1	-0.5408496	9.19414795	2.12E-06	0.0001241
QKI	0.52403559	6.72154764	2.26E-06	0.00013173
HAPLN3	0.74450599	6.59544586	2.47E-06	0.00014361
APOL1	1.41832471	5.62272766	2.55E-06	0.00014787
RPLP0	-0.687295	11.108895	2.70E-06	0.00015586
GADD45B	0.47214342	6.79837909	2.77E-06	0.00015923

ZNF107	0.7739557	4.95787476	2.83E-06	0.00016177
RPS27A	-0.6730385	9.58922513	2.92E-06	0.00016612
TLR3	1.53280391	1.20262237	3.01E-06	0.00017004
GJA4	2.17862265	-0.3113662	3.03E-06	0.00017004
RPS5	-0.6404859	10.5243374	3.03E-06	0.00017004
HLA-E	0.47290115	11.6649593	3.05E-06	0.00017045
COX4I1	-0.4621697	9.23219855	3.20E-06	0.00017781
MLKL	0.75679269	4.09729282	3.21E-06	0.00017781
RPS4X	-0.6059363	11.6641461	3.22E-06	0.00017781
C12orf43	-0.4699854	4.32787996	3.45E-06	0.00018969
LOC101927027	0.88121818	3.51616278	3.51E-06	0.00019242
RPS3	-0.6043088	12.5905865	3.56E-06	0.00019401
TAP1	0.79375322	9.26501705	3.65E-06	0.00019812
DBF4B	0.77011052	2.7797246	3.68E-06	0.00019886
MICB	0.66112017	5.38075139	3.75E-06	0.0002021
NELL2	-0.6777135	7.80445193	3.79E-06	0.00020366
TTC39B	0.94125538	4.61518237	4.09E-06	0.00021883
SARDH	-0.6208118	3.77205071	4.26E-06	0.00022666
IL1RN	1.46968376	3.09277196	4.31E-06	0.0002284
PVRIG	0.52712095	6.13482798	4.35E-06	0.00022993
CASP7	0.54148783	5.05355133	4.48E-06	0.00023559
EEF1G	-0.6529913	10.5294857	4.50E-06	0.00023559
TTC38	0.72933075	3.62491423	4.51E-06	0.00023559
CHI3L2	0.99969767	3.27649965	4.62E-06	0.00024036
CCR1	1.6657414	3.45491953	4.69E-06	0.00024259
KPNB1	0.52689874	7.89803827	4.71E-06	0.00024259
NECAP1	0.35388135	5.37017336	4.72E-06	0.00024259
BRD2	0.34335069	8.15889759	4.76E-06	0.00024338
RPL13A	-0.5499473	11.8371344	4.84E-06	0.00024611
VCPIP1	0.45400204	6.58018428	4.85E-06	0.00024611
ASB1	-0.3589116	5.54809555	5.01E-06	0.00025346
GLTSCR2	-0.5333176	10.8388878	5.30E-06	0.00026697
TBC1D1	0.57044926	6.07361428	5.41E-06	0.00027167
RPL23	-0.573607	10.4725322	5.54E-06	0.00027695
CCDC9	0.70008552	4.88888098	6.11E-06	0.00030436
SERPINB9P1	1.25226098	2.16744684	6.27E-06	0.00031132
FMR1	0.49880784	5.60497709	6.95E-06	0.00034388
RPL18	-0.5496941	11.0876887	7.06E-06	0.00034796
PNPLA4	-0.633155	3.14085978	7.32E-06	0.00035917
KIAA0040	0.50018989	6.54228472	7.39E-06	0.0003614
RPL13AP5	-0.5624017	12.7496024	7.72E-06	0.00037635
NRBP1	0.38334983	7.01773398	8.44E-06	0.00040995
CD2AP	0.6707996	5.55051778	8.48E-06	0.00041041
ELF1	0.45863507	8.57913395	9.25E-06	0.00044606
ANXA2R	0.64830537	5.7869308	9.32E-06	0.0004474
HM13	0.51024194	6.63524303	9.49E-06	0.00045434
PLEKHN1	1.10956392	1.11071707	9.85E-06	0.00046974
IPO5	-0.40988	7.02717788	9.89E-06	0.00046997
KLRB1	-0.7648466	6.95152617	1.02E-05	0.00048282
MYEOV2	-0.4539794	5.66865892	1.07E-05	0.00050548
GPRC5B	1.74860749	0.31868933	1.12E-05	0.00052546
RPS16	-0.556224	11.4986238	1.20E-05	0.00056161
BRCA2	0.67607	2.39853268	1.29E-05	0.00059979
FHL1	-0.4094882	4.80897673	1.29E-05	0.00060004
FAM46A	1.11174865	3.65033557	1.32E-05	0.00061275
RPL8	-0.4850607	11.7959928	1.34E-05	0.00061819
CFLAR	0.43484772	7.64405847	1.34E-05	0.00061819
ANKIB1	0.73759407	5.32989731	1.48E-05	0.00067687
ODF3B	1.14587729	3.39048396	1.49E-05	0.00067948
RPL27	-0.4812043	11.1896501	1.50E-05	0.00068521

RPL13	-0.5527666	11.9092074	1.56E-05	0.00070892
MIR3654	-0.6862837	8.69970881	1.63E-05	0.00073912
ATP13A1	0.51182864	5.72742343	1.68E-05	0.00075631
CDKL1	0.81687529	1.83064793	1.75E-05	0.00078358
DANCR	-1.0070082	4.48562209	1.75E-05	0.00078358
MVP	0.44005873	7.75196359	1.76E-05	0.00078358
PITPNA-AS1	-0.5457127	3.66926348	1.91E-05	0.00084972
STX17	0.51087914	5.53883579	1.98E-05	0.0008791
IER3	-0.555603	4.35504538	2.08E-05	0.00092091
MICA	0.60305688	4.35494607	2.10E-05	0.0009257
SQRDL	0.45813327	6.82416123	2.13E-05	0.00093353
RIPK3	0.67308339	3.5881641	2.15E-05	0.00094276
RPS18	-0.5056357	11.6703552	2.18E-05	0.00095223
TMEM123	0.50756107	10.1446374	2.25E-05	0.00097997
SMTNL1	1.59730751	0.75887949	2.27E-05	0.00098256
C3AR1	1.1941295	3.80487871	2.28E-05	0.00098256
RPL22	-0.5030769	9.66747634	2.35E-05	0.00101072
PDE8A	0.42117937	3.93129226	2.37E-05	0.0010173
RPL26	-0.4764248	10.1841497	2.39E-05	0.00101952
RPL10A	-0.5954605	10.7317633	2.39E-05	0.00101952
RGS1	0.67088159	8.3016792	2.50E-05	0.00105948
PRKAG2	0.58654133	5.44330507	2.50E-05	0.00105948
USP42	0.42168903	4.43888653	2.54E-05	0.00107221
IDH3A	0.57130531	5.63361743	2.66E-05	0.00111775
TPT1	-0.4968075	13.1457009	2.70E-05	0.00113069
DCTN2	-0.3140272	6.4422977	2.74E-05	0.00114555
TESPA1	0.4359134	7.19164177	2.76E-05	0.00115162
CASP1	0.8978045	5.223901	2.86E-05	0.00118724
NADK	0.35797668	5.43932519	2.95E-05	0.00122005
RPS15A	-0.5238436	11.0058648	3.00E-05	0.0012388
WIPF1	0.39312144	9.24174013	3.01E-05	0.00123928
RPS13	-0.4802281	9.9845656	3.07E-05	0.00125981
SLA2	0.72519808	6.20220004	3.10E-05	0.00126895
DCLRE1C	0.44554335	4.326254	3.11E-05	0.00127024
RPS21	-0.4321998	10.1547383	3.26E-05	0.00132584
PRKCE	0.83869021	3.9058454	3.42E-05	0.00138631
C17orf67	0.61876454	2.43158811	3.50E-05	0.0014146
RBM7	0.37500711	5.941775	3.52E-05	0.00141917
LOC101927482	-0.7006734	3.25202692	3.62E-05	0.00145613
TMEM187	0.85021922	4.25986293	3.70E-05	0.00148113
RPS2	-0.5260789	11.3575329	3.72E-05	0.00148457
PCGF5	0.41892857	7.46442268	3.83E-05	0.0015231
UBA7	0.896065	6.335379	3.84E-05	0.0015231
CACNA1A	1.30252784	0.31357778	3.88E-05	0.00153561
KCNA3	0.56101188	7.57725874	3.91E-05	0.00154171
BIVM	-0.6490771	2.65318467	3.98E-05	0.00156416
NCOA3	0.34764339	6.77211007	4.05E-05	0.00158963
GBP1	1.23227128	7.67598987	4.13E-05	0.00161206
IMPDH2	-0.4988593	7.83124169	4.14E-05	0.00161206
NEURL3	1.22535268	1.18545702	4.15E-05	0.00161206
LGALS17A	1.85428318	0.4778821	4.25E-05	0.00164621
RAD9A	0.50237189	4.47910013	4.26E-05	0.00164621
SNHG5	-0.5481776	9.25748208	4.36E-05	0.00168187
OPTN	0.33452983	7.42485971	4.46E-05	0.00171251
EIF4B	-0.4564175	10.1057416	4.48E-05	0.00171482
KIAA0226	0.4296105	5.5288196	4.49E-05	0.0017171
TYMP	1.11276309	6.73616623	4.58E-05	0.00174593
LARP7	0.36169378	4.76929361	4.80E-05	0.0018222
PSMB9	0.66350933	8.58455348	4.86E-05	0.00184184
YEATS2	0.67962767	6.31788129	4.92E-05	0.00185635

CCDC146	1.54169259	1.09245461	4.93E-05	0.00185701
RNF213	0.91435728	8.80837204	5.02E-05	0.00188563
GCNT1	0.67716445	4.30950968	5.12E-05	0.00191609
VSIG10L	1.10580707	1.18808703	5.21E-05	0.00194373
RPLP1	-0.4502593	11.8213198	5.25E-05	0.00195635
RPL7A	-0.5422443	10.480621	5.50E-05	0.0020432
USE1	-0.336119	5.03761272	5.54E-05	0.00205275
VPS51	-0.4555329	7.77667056	5.62E-05	0.00207373
CREBRF	0.36474315	6.54812405	5.64E-05	0.00207528
MRPL45	-0.5037603	5.45472649	5.65E-05	0.00207528
DPH5	-0.5856816	5.51256528	6.13E-05	0.00224387
SLC25A6	-0.5488833	9.84521062	6.25E-05	0.0022812
FAM175A	0.41806547	5.2601378	6.28E-05	0.0022878
PHB2	-0.4569152	8.18730084	7.18E-05	0.00260754
HINT1	-0.4673418	8.52151992	7.21E-05	0.00261171
UQCRB	-0.4531969	8.39180427	7.41E-05	0.00267633
CERK	-0.4710422	7.8252199	7.55E-05	0.00272024
UBQLN2	0.50404111	6.36213905	7.68E-05	0.00275794
ZFYVE26	0.58445597	4.48530163	8.02E-05	0.00287161
CPEB2	0.56422643	3.94953944	8.13E-05	0.00290649
HTRA2	-0.3402423	5.09014667	8.24E-05	0.00293649
RPS17	-0.4870886	11.1624965	8.86E-05	0.00314779
APOBEC3F	0.50899301	3.85715339	8.88E-05	0.00314779
RPL7	-0.6452491	10.1715281	9.10E-05	0.00321767
RPS23	-0.4380401	11.3185904	9.25E-05	0.00325348
IL15RA	0.65993578	4.12351053	9.25E-05	0.00325348
ARID5A	0.36008616	7.31741468	9.28E-05	0.00325348
PAPD7	0.38970388	5.06960835	9.55E-05	0.00333898
HADHA	-0.4221541	7.56359704	9.68E-05	0.00337576
MCL1	0.48539378	10.1421479	1.00E-04	0.00347769
CEACAM1	0.89213092	2.62692753	0.0001021	0.00354316
ALKBH7	-0.4559294	6.45575377	0.00010314	0.00356975
TMEM139	0.80733631	0.66656968	0.00010431	0.00360097
C1GALT1	0.57579709	6.28704409	0.00010541	0.00362925
SERPING1	1.50710008	2.33524008	0.00010723	0.00367555
CCDC85B	0.52067074	6.41192354	0.00010731	0.00367555
PSMA6	0.31594699	7.42347943	0.00010953	0.00374202
AFF1	0.46275923	6.53396202	0.00011025	0.00374914
RPL34	-0.4416594	10.8793282	0.0001103	0.00374914
TRIM56	0.99782361	5.10117177	0.00011422	0.00386697
EIF4E3	0.41454814	6.61600547	0.00011435	0.00386697
AKT2	0.31222613	7.46416287	0.00011784	0.0039747
NAPSB	1.48455452	2.53362663	0.00011889	0.00400011
ZBTB42	0.53679916	3.85089697	0.00011935	0.00400506
INAFM1	0.74438544	3.10360054	0.00011964	0.00400506
PRADC1	-0.3896507	3.92454573	0.00012059	0.00402666
QARS	-0.5279936	7.36061556	0.00012408	0.00413272
TMEM106A	0.80307417	2.6056483	0.00012536	0.0041649
EPB41L5	0.56345949	2.78286635	0.00012785	0.00423695
ALPK1	0.75266102	4.04558291	0.0001317	0.00435377
CEP78	-0.400422	3.85677987	0.00013223	0.00436044
XPO6	0.30693412	8.13507938	0.0001343	0.0044176
KRT7	-1.1633446	1.5272228	0.00013742	0.00450885
ELK4	0.41084536	7.17096287	0.00013956	0.0045678
MAD2L1BP	0.42529536	4.94771776	0.00014078	0.0045823
IL6ST	0.30356199	7.72548909	0.00014096	0.0045823
GORASP1	0.38368272	4.58855678	0.00014104	0.0045823
GJB2	-0.7897039	2.86654446	0.00014239	0.00461501
CNDP2	0.43944759	7.06054481	0.00014514	0.0046926
DNAJA1	0.53928101	7.58306471	0.00014885	0.00480077

DNMT1	0.40194106	6.75676585	0.00014939	0.00480668
RPL37	-0.40896	10.9443473	0.00015056	0.00483237
IPCEF1	0.58558426	6.54939972	0.00015103	0.00483602
UBE4B	-0.2645769	5.85158389	0.00015141	0.00483634
HOPX	-0.9260612	4.43290336	0.00015431	0.00491725
ATP10A	0.9460612	4.80929133	0.00015482	0.00492172
NACA	-0.4404765	10.0594541	0.00015656	0.00496504
KLHDC7B	0.93560724	5.09527652	0.00015866	0.00501683
C12orf10	-0.3576593	5.72020523	0.00015895	0.00501683
RPL15	-0.4593398	10.3134305	0.00016102	0.00507009
FAM173B	-0.5199423	3.29777769	0.00016388	0.00514791
COX7A2L	-0.3297263	7.04786802	0.00016656	0.00521965
TLK2	0.2786233	4.802305	0.00016921	0.00529027
CLEC2D	0.50768276	8.2111287	0.00018149	0.00566089
CSF2	-0.9383054	2.48746055	0.00018693	0.00581668
KIAA1324	-0.4187939	4.11177991	0.00018748	0.00582025
TIPIN	0.60485655	3.62438196	0.00018962	0.00587302
GPBP1	0.39715986	7.30594212	0.00019018	0.00587666
MAN2B1	-0.4662022	7.43259268	0.00019468	0.00600145
SAMHD1	0.53441154	7.75856268	0.00019806	0.00609151
LOC440461	0.91830035	1.67220172	0.00020406	0.00626164
DNAJC18	-0.5753174	4.03991567	0.00020527	0.00628429
ADO	-0.3133888	5.45143367	0.00022144	0.00674846
EIF3K	-0.4525782	7.84849973	0.00022236	0.00674846
GCH1	0.44743748	5.80198946	0.00022239	0.00674846
CD68	0.99127236	4.7361398	0.00022247	0.00674846
ADPGK	0.27918805	6.26007359	0.00022446	0.00679319
CXCL10	2.55264296	3.20592033	0.000228	0.00687557
RABGGTA	0.3796534	4.81237962	0.00022822	0.00687557
RPS14	-0.482054	12.057733	0.0002336	0.00702174
NTNG2	1.16368563	2.21900505	0.0002393	0.00717679
FAM168B	-0.2824894	7.43481119	0.00024216	0.00724224
CMTM4	-0.887213	1.32570992	0.00024257	0.00724224
PABPC4	-0.4721274	7.65265736	0.00024629	0.00733653
GNA12	-0.3908048	5.92170904	0.00025074	0.00745259
RPS25	-0.3544323	10.8121278	0.00025186	0.00746918
HLA-C	0.39291582	11.9666434	0.00025437	0.00752672
ZZZ3	0.24546069	5.44785402	0.00025621	0.00756404
PARP6	0.59972703	5.08862617	0.00025758	0.00758766
HLA-B	0.31768792	12.8197552	0.00025889	0.00760944
SUMF1	-0.4642111	3.88052389	0.00025983	0.00762012
ITM2C	-0.4740595	6.61574903	0.00026138	0.00764872
DOPEY1	0.47228812	3.98605873	0.00026814	0.00782929
DNAJC13	0.46430265	5.2028162	0.00027264	0.00792861
RPL35A	-0.379976	11.0779488	0.00027274	0.00792861
NTRK2	-0.7140429	2.36214779	0.00027414	0.00795182
EEF1D	-0.477032	9.71167937	0.00027751	0.00802561
CD47	0.28521233	7.72006442	0.00027789	0.00802561
WARS	0.64415685	7.55000919	0.00028382	0.00817909
AHCY	-0.5633288	6.45021652	0.00028594	0.00822205
NUDT5	-0.3189439	5.26937616	0.00029113	0.00835337
STAP2	0.66363588	2.29783897	0.00029416	0.00842208
ATP5L	-0.3750375	8.03608002	0.0003052	0.0087193
EIF3E	-0.4370654	9.31681448	0.00031027	0.00884512
ZNRF3	-1.0771561	0.94545106	0.00031148	0.00886044
SLFN12L	0.93156982	2.14066321	0.00031504	0.0089319
DAP3	-0.3854631	6.96111186	0.00031534	0.0089319
MRPS27	-0.383727	6.06665727	0.0003178	0.0089823
MATK	-0.7954015	3.82282568	0.00032261	0.00909893
ERGIC3	-0.420504	7.37319876	0.0003276	0.00922

RPL27A	-0.3911309	9.34329467	0.00033723	0.00947095
RPL19	-0.4324943	11.3247785	0.00033917	0.0095053
PRF1	0.49024261	5.46772737	0.00034198	0.00956401
CTSO	0.43096212	4.65178786	0.00034338	0.00957278
RPL37A	-0.4416461	10.6153856	0.00034374	0.00957278
LOC100506548	-0.4762943	5.63821558	0.00034623	0.00962194
RPL24	-0.3434154	9.71981391	0.00035429	0.00982519
GGH	-0.4102978	3.83351787	0.00035645	0.00986456
SHMT2	-0.4205574	7.69782051	0.00035765	0.00987715
HLF	-0.7258907	3.75829067	0.00036877	0.01016305
ITGA3	0.53465293	3.79010352	0.00037606	0.01033886
ATP5A1	-0.3222635	8.68342333	0.00037671	0.01033886
KIAA0430	0.31515517	7.27073428	0.00037749	0.01033898
LOC728743	0.54625006	5.01118082	0.00039007	0.0106614
SEC61B	-0.3076442	7.04406416	0.00039312	0.0107117
THTPA	0.46516506	3.16239929	0.00039353	0.0107117
C18orf25	0.30704728	5.93232523	0.0003959	0.01074806
GJB6	-1.2630402	2.22491634	0.00039723	0.01074806
RPL31	-0.3660372	11.5895823	0.0003973	0.01074806
NSMCE1	-0.3407662	6.1906053	0.00039993	0.01079726
GCNT2	1.00001781	1.41310397	0.00040543	0.01092348
CASP4	0.37241958	6.4271739	0.00041814	0.01123312
GBP5	0.71837708	8.7175499	0.00041862	0.01123312
UNQ6494	-0.994414	2.63201653	0.0004295	0.01148195
RPL11	-0.3700671	11.5065368	0.00042962	0.01148195
DSC1	-0.9495888	1.09702111	0.00043295	0.01154777
GPX4	-0.3701717	7.8864477	0.00043411	0.0115553
TRIM44	0.43191208	6.34734685	0.00043744	0.01162055
SLFN11	-0.3480164	5.7393811	0.00043903	0.01163955
UBR2	0.30011284	6.2597404	0.00044872	0.01187259
MRPS15	-0.4354466	5.44750898	0.00045267	0.01195341
CBX7	-0.4258236	7.60562639	0.00045511	0.01197786
NFATC2IP	0.26038975	5.98993812	0.0004554	0.01197786
LOC100506844	-0.5301284	3.93468911	0.00046025	0.01208134
IL10	1.02323156	3.0220754	0.00046231	0.01211147
TAPBP	0.5194682	8.13852551	0.00046393	0.01212998
TUFM	-0.2700665	7.46357553	0.00046823	0.0122182
VASH1	-0.6878389	3.44905029	0.00046979	0.01223481
MR1	0.31062641	6.13128306	0.00047217	0.01227281
RIPK1	0.49753181	6.00995413	0.00048851	0.01267254
TATDN2	0.29530652	7.02889299	0.00050828	0.01315956
GANC	0.36398953	3.5726652	0.00051553	0.01332141
COMMD6	-0.3842867	6.74919478	0.00051982	0.01340227
LOC100506990	0.48009507	3.68710144	0.00052068	0.01340227
TCIRG1	0.51847882	6.09676852	0.00052322	0.01341895
IGF2R	-0.2942184	7.29796982	0.00052336	0.01341895
TOMM7	-0.439578	8.58970825	0.00052784	0.01350794
BZRAP1-AS1	-0.3813199	4.6576431	0.00053956	0.01378102
HES4	1.38339925	0.81178962	0.00054242	0.01382741
AP1S2	-0.3687864	5.29038202	0.00054359	0.01383064
MORC3	0.32930557	6.61107204	0.00054652	0.01387872
DNPEP	0.36671835	5.79702552	0.00055156	0.01397977
RPS20	-0.4543801	11.3745968	0.00055827	0.01410723
RSL1D1	-0.2999795	7.54114241	0.00055871	0.01410723
RAB8A	0.34375816	6.79596329	0.00056289	0.01418575
FAHD2B	-0.5115095	3.68939466	0.00056636	0.0142461
UBA52	-0.3719346	10.9825652	0.00057051	0.01432319
GRN	0.46063314	6.27752159	0.0005745	0.01439619
EIF3D	-0.3739718	8.37480853	0.00057695	0.01443023
COL6A3	-0.9675903	3.96726344	0.00058093	0.01450252

PXYLP1	0.45641808	3.85000651	0.00058929	0.01468352
C7orf49	0.26751336	4.67424659	0.00059669	0.01481676
ST13P4	-0.4080869	4.6150847	0.00059687	0.01481676
DCP1A	0.27633256	5.88156432	0.00060053	0.01487971
RPL32	-0.3783629	10.8556254	0.00060848	0.01504862
HDX	1.40132194	-0.3760237	0.00061183	0.01510313
SLFN13	1.07254212	4.33893574	0.00061305	0.01510518
BAZ1A	0.38902234	5.78924481	0.00061866	0.01521508
SPTLC2	0.66821526	6.32930168	0.00062735	0.0154004
RPL17	-0.5383183	4.29929943	0.00063653	0.01559681
CDK18	0.97545429	1.61125823	0.00063852	0.01561654
FHL3	0.69783282	3.24696849	0.00064281	0.01569256
DHRS1	0.38005846	3.98804239	0.00064601	0.01574174
A1BG	-0.5633499	3.86868535	0.00066225	0.01610705
NUTM2B-AS1	-0.5040188	2.82063353	0.00066343	0.01610705
DLL1	0.92398758	2.04923723	0.00066538	0.01612479
FAM64A	-0.5158929	2.3426623	0.00067167	0.01624746
SYNE1	0.26195225	6.77851054	0.00067592	0.01632056
C2orf76	-0.5794733	2.8457539	0.00067936	0.01637382
TIPARP	0.32866727	6.66781929	0.00068062	0.01637451
GLO1	-0.2746316	7.08732501	0.00069471	0.01668301
LOC101243545	-0.4056282	10.6368606	0.00069857	0.01674542
ADGRL1	0.4304437	4.78322937	0.0007057	0.01688591
NEFM	-0.611267	1.31346021	0.0007135	0.01704162
FBL	-0.4127799	8.89097131	0.00071678	0.01708925
P2RX7	0.41289466	3.95755398	0.00071808	0.01708962
RPL29	-0.4334816	9.76859652	0.00072275	0.0171699
CRTAP	-0.3992036	6.56362939	0.00072413	0.01717183
TBK1	0.27926416	5.09912075	0.00072574	0.01717941
RDH14	0.44856518	3.1830784	0.00073881	0.01745745
RPSAP58	-0.4788888	10.0854559	0.00074323	0.01753079
PFDN5	-0.3725691	8.56450606	0.0007519	0.01769943
PTMS	0.50522062	5.14573857	0.00075305	0.01769943
TMEM200A	-0.7180476	2.40769815	0.00075484	0.01771004
NOD1	0.5729878	4.27717091	0.00076503	0.01788896
GAS5	-0.4025678	6.7969018	0.00076517	0.01788896
GPR68	-0.4041147	6.19180791	0.0007783	0.01816398
USPL1	0.43340887	4.86095162	0.00078251	0.01823015
R3HCC1L	0.28810614	4.49613792	0.00078769	0.01831855
FAM122C	0.74454759	3.30016037	0.00081314	0.01887744
SPATA13	0.34786539	7.52306881	0.00081552	0.01889957
PNRC2	0.22032697	7.86488917	0.00082286	0.01903633
STARD10	-0.5024367	4.76452867	0.00083105	0.01917553
ARAP2	0.34238046	6.17003675	0.00083459	0.01917553
ZNF592	0.27178415	5.79621046	0.00083498	0.01917553
KDM6A	0.3586258	5.509226	0.00083557	0.01917553
LGALS8	0.30032813	6.66052157	0.00083611	0.01917553
VRK2	0.36683312	4.04722344	0.00083957	0.0192217
ZNF350	0.28046335	3.91910439	0.00084441	0.01929908
LOC113230	-0.9215223	0.99942396	0.00084796	0.0193469
CCDC34	-0.502529	3.71941391	0.00085164	0.01939749
RPL23A	-0.4281297	7.96254127	0.00087184	0.01982344
PPARG	-0.6787239	1.2850248	0.00087522	0.01986624
TMEM14C	-0.3668222	5.79306635	0.00087739	0.01988155
OLA1	-0.3982595	6.06976803	0.00088461	0.02001088
IL5	-1.3690884	1.40295418	0.0009001	0.02032661
BAIAP2-AS1	-0.4742549	2.65050866	0.00091287	0.02057998
LRRC16A	0.99099942	1.97726212	0.00092417	0.02079934
MAMLD1	0.84979682	1.08975195	0.00094303	0.02118771
ZNF619	0.3671424	3.1328344	0.00094699	0.02121515

AMZ1	-0.9011	0.65697384	0.00094745	0.02121515
OTUD7B	0.29591384	4.02366067	0.00095571	0.02136319
SLC25A5	-0.4395204	8.07884714	0.00095728	0.02136319
CXCL11	2.4901665	1.05674194	0.00096361	0.02146826
KDM5A	0.29556254	6.83063421	0.00097348	0.02165169
CDKN2AIPNL	-0.2868289	4.59789067	0.00099867	0.02214704
TINF2	0.44175453	6.45806941	0.00100021	0.02214704
CAPN2	0.75347361	7.11947804	0.00100076	0.02214704
RPL35	-0.3502843	11.2759781	0.00100318	0.02216362
GNG4	-1.3404369	1.95673203	0.00100718	0.02221489
ADAM19	0.34356351	6.98827285	0.00101101	0.02226233
TAPT1	0.31149889	5.48080615	0.00101767	0.0223719
RPS19	-0.4203957	11.3490611	0.00103689	0.02275657
DCTN4	0.33919463	5.37910403	0.00105635	0.02314531
ITGAE	-0.5697664	5.27983915	0.00105892	0.0231524
UTRN	0.85749474	5.50633431	0.00106016	0.0231524
IL12RB2	0.55226747	5.08218796	0.00106743	0.02327278
SLC30A4	0.617252	1.67411059	0.00108238	0.02355991
SACS	-0.348966	5.0514738	0.00108883	0.02366053
ACOT9	0.30874615	4.88734782	0.00109059	0.02366053
CAST	0.43331567	6.92329741	0.00109235	0.02366053
ALDH5A1	-0.365929	4.38553099	0.00110262	0.02384397
NPM3	-0.4427548	5.41670967	0.0011197	0.02417375
POLR2L	-0.3997669	5.50737363	0.00112504	0.0242032
SBK1	0.54884229	5.22634561	0.00112645	0.0242032
LOC100294362	1.32116866	0.31607865	0.00112654	0.0242032
NDUFB1	-0.3032138	5.58378013	0.00113367	0.02431696
LOC643733	0.86060232	2.87785889	0.00115916	0.02482359
SUPT3H	0.54585791	3.71643387	0.00117922	0.02521244
B3GNT2	0.40701894	5.79072987	0.00118258	0.02524354
LOC100419583	0.54377769	6.64932894	0.00118869	0.02533332
TCTN1	-0.8185871	1.28445437	0.00119933	0.02551898
RPS18P9	-0.5989923	2.58616617	0.00120611	0.02562204
SSR2	-0.3147154	8.26758096	0.00121052	0.02566894
TIPARP-AS1	0.67359034	1.1270685	0.00121527	0.02566894
LAIR1	-0.4055214	4.52630347	0.00121607	0.02566894
MRPL33	-0.254086	5.27954138	0.00121695	0.02566894
GIMAP6	0.67749546	8.29755411	0.001218	0.02566894
GBP3	0.75302348	4.74389611	0.00122886	0.02585682
KIAA1671	0.54708453	4.68027236	0.00123308	0.02590453
EIF3H	-0.381118	8.4945765	0.00125704	0.02636605
TOMM22	-0.3587163	6.39030295	0.00126539	0.02649933
BTF3	-0.3711462	9.43285124	0.00127451	0.02664812
SLC25A3	-0.391596	8.35072369	0.0012864	0.02685432
RPL23P8	-0.6125078	2.27613279	0.00129377	0.02696578
TAGAP	0.54122566	7.26600371	0.00129601	0.02696995
ZNF710	0.45692706	3.97077858	0.00130104	0.0270322
POLR1E	-0.4129942	5.7529639	0.00131882	0.02734778
RPS9	-0.4221065	11.6418054	0.00132081	0.02734778
RPLP2	-0.3219842	11.1787803	0.00132241	0.02734778
CD48	0.36063386	9.31887674	0.00133192	0.02750154
RPSA	-0.4617493	10.4742978	0.00134329	0.02769304
LAX1	0.48304588	5.15694137	0.00135457	0.02786043
ELOVL7	1.03484905	0.87481934	0.00135561	0.02786043
MRPL52	-0.2751004	5.26949905	0.00138321	0.02838359
COX5A	0.31982003	6.68694727	0.00142754	0.02924796
BAD	-0.333668	4.93670124	0.00145342	0.02972266
NCCRP1	-1.1527023	1.97967092	0.00145519	0.02972266
GPATCH11	-0.5819703	5.16216211	0.00145945	0.02972391
RPL30	-0.3269521	11.6586699	0.00145974	0.02972391

CXorf21	0.86525756	3.11768333	0.00148153	0.03012147
FAM84B	0.49400189	5.31569947	0.00149031	0.03022565
FNDC3A	0.52245231	5.79720724	0.00149122	0.03022565
NT5DC2	-0.7394934	3.85372408	0.0014946	0.03024794
F3	-1.4967487	-0.5260457	0.00151	0.030513
CALCOCO2	0.29595602	6.57283107	0.0015174	0.03061594
ZSCAN12	0.36550294	2.997765	0.00153262	0.03087593
UXT	-0.4029587	6.29976013	0.00153931	0.03096365
XCL1	-0.6077914	1.89880881	0.00157356	0.03160462
TIA1	0.31384164	5.94402246	0.00158191	0.03170622
PTK2B	0.3148339	7.29181174	0.00158574	0.03170622
TAF9B	-0.3384637	5.54146305	0.00158838	0.03170622
MORN4	-0.7716508	1.10965906	0.00159229	0.03170622
ATP5O	-0.3090417	7.43853189	0.0015929	0.03170622
XIAP	0.33789727	6.05276194	0.00159674	0.03170622
SMCO4	-0.4604999	4.32788299	0.00159707	0.03170622
MVD	-0.2666968	5.52769522	0.00159832	0.03170622
.MARCH8	0.21913555	6.5271731	0.00160136	0.03170622
HMGB3	-0.5274185	4.11336289	0.00160253	0.03170622
POU2F1	0.39909455	5.04917059	0.00161415	0.03188853
LRRN2	1.57183053	0.38440851	0.00161803	0.03191749
HPSE	0.47321369	4.78061462	0.00165055	0.0325107
NPM1	-0.3530929	9.57952986	0.00165853	0.0326194
ACP2	0.5042424	4.02281233	0.00166176	0.03263444
SECTM1	0.46881865	4.77662603	0.00169671	0.0332716
FAM201A	-0.9375753	0.73623551	0.00170583	0.03340098
TMEM218	-0.4235707	3.71450673	0.00172025	0.03363372
REEP2	-0.8160686	1.30816593	0.00172536	0.03368387
C14orf159	0.73580863	5.23754977	0.00172999	0.03370804
BRPF3	0.29983788	5.40653575	0.00173168	0.03370804
C12orf45	-0.3759743	4.0253412	0.00173815	0.03378429
LRP10	0.26781601	7.83692448	0.0017593	0.03414536
NLE1	-0.4114671	4.27599174	0.00176729	0.03425035
DSTN	-0.2412451	6.19608742	0.00177278	0.03428613
CARD11	0.52132599	7.01017328	0.00177543	0.03428613
KCTD2	0.26545269	5.85545383	0.0017769	0.03428613
ATP5F1	-0.3148161	7.09857313	0.00183821	0.0354176
GPR89B	0.43068041	2.58641488	0.00184346	0.0354266
KPNA5	0.37284781	3.91770447	0.00184402	0.0354266
SOCS7	-0.3321368	4.88686399	0.00189137	0.03628365
CHRNB1	0.49577269	4.48660794	0.00189696	0.0363382
LAPTM5	-0.2379161	10.4344105	0.00190547	0.0363466
SCO2	0.82975026	0.16375062	0.00190609	0.0363466
SRD5A1	0.3265652	3.28252165	0.00190632	0.0363466
RCN2	-0.3644123	5.1876124	0.00190836	0.0363466
RASGEF1A	-0.6631482	1.34022414	0.00191176	0.03635909
CCSAP	0.33379883	5.1127088	0.00192535	0.03647413
C4orf3	0.25208975	8.71736857	0.00192599	0.03647413
SGK1	-0.7047937	5.27055471	0.00192606	0.03647413
ATP1B1	-0.7416391	2.88092405	0.0019371	0.03663074
FAM215A	1.01753149	-0.2697415	0.00194957	0.03681419
PROCR	0.80964253	0.83247306	0.00195948	0.03691038
KLHL26	0.3002708	4.19853896	0.00196024	0.03691038
RPS11	-0.4009924	12.0722628	0.00198642	0.03734208
CLUAP1	0.51869261	4.60065753	0.0019888	0.03734208
RPS12	-0.3209413	10.7746646	0.00200881	0.03766447
CD37	0.35356588	8.15333852	0.00202396	0.03789496
ITIH1	-1.3297173	0.16672711	0.002032	0.03794775
CS	-0.2865013	7.45016029	0.00203251	0.03794775
HTT	0.24410348	6.05284738	0.00203795	0.03799595

APOL3	0.40746885	7.48722974	0.00204583	0.03808922
SUSD3	0.4057843	5.87237391	0.00207481	0.03857453
ELF4	0.44100425	6.37579983	0.00208497	0.03870916
SOCS1	0.46883303	6.28364354	0.00208953	0.03873837
NAA25	0.41002739	4.89417954	0.00209239	0.03873837
RPS4Y1	-0.3983189	9.24363192	0.00210257	0.03887266
MGAT5B	-0.8369355	1.63334223	0.00211198	0.03899216
UBL7-AS1	-0.4364746	2.79072516	0.0021264	0.03920017
LTA4H	-0.3928769	7.07758048	0.00212916	0.03920017
TM7SF3	-0.2849813	5.6848823	0.00214743	0.03948171
ALDH4A1	-0.6453415	2.09188815	0.0021597	0.03965227
TLDC2	0.65987486	1.153722	0.00217736	0.03992126
.SEPT8	-0.300517	4.02788138	0.00219891	0.04026069
GRK5	0.4460044	5.87883048	0.00222206	0.04062854
IMMP1L	-0.45113	2.44376481	0.00227215	0.04145153
NDUFA9	0.32631002	5.86319788	0.00227506	0.04145153
FKBP5	0.30064311	7.54894503	0.00227646	0.04145153
KLRG1	-0.4430516	3.24130212	0.00228359	0.04152441
PRPS2	0.36916317	5.92241272	0.00231363	0.04196198
TRMT10A	-0.353127	2.6107918	0.00231399	0.04196198
LINC00881	-0.8242717	0.11218327	0.00236011	0.04273984
SMIM10L2A	-0.6224996	1.28266935	0.00236384	0.04274904
ZBTB43	0.32540814	4.82900004	0.00237246	0.04284648
TMEM229B	1.16297415	4.42051622	0.0023768	0.04286653
PCNX	0.2973542	7.12882573	0.00238475	0.0429515
PTDSS1	-0.2206432	7.69040457	0.0024724	0.04442221
TRPC4AP	0.18221847	6.66286291	0.00247585	0.04442221
RANBP10	0.22420357	4.96372931	0.00247646	0.04442221
PFDN4	-0.3821348	4.63225512	0.00248035	0.04443172
MYL12A	0.41692996	8.75328818	0.00248711	0.04449283
ACTG1	-0.38704	11.9378191	0.00250232	0.04470452
BAK1	0.31543781	6.13087862	0.00251871	0.04493668
ZC3H7B	0.28658167	6.00302625	0.0025609	0.04562815
LOC100996286	-0.5481659	3.09759845	0.00256785	0.04569048
LINC00278	1.09901827	-0.1194004	0.00259564	0.0461064
COLGALT2	-0.7796177	1.42564868	0.00259818	0.0461064
E2F5	0.64509608	0.76729702	0.0026039	0.04614609
MASTL	0.66583514	4.57367767	0.00260762	0.04615043
STAU1	0.30551594	6.6109756	0.00261726	0.04625927
SWT1	0.41944778	3.22501335	0.00263106	0.04638332
L3MBTL3	0.63881347	4.35278002	0.00263128	0.04638332
NAPA-AS1	-0.6113927	1.76311008	0.0026371	0.04641584
SNHG8	-0.2934192	6.49881509	0.00264013	0.04641584
ZNF287	-0.2859758	3.63364904	0.00264655	0.04646706
CCT6P1	0.41984658	3.16004727	0.00270695	0.04746123
NDUFA10	-0.3034898	6.31169626	0.00271033	0.04746123
IRAK1BP1	-0.5501646	1.94988417	0.00272552	0.04766427
PASK	-0.293628	7.43126242	0.00273736	0.0477535
DGCR2	0.24609341	6.69325824	0.00273783	0.0477535
GATA3-AS1	-1.1180729	-0.0137694	0.0027473	0.04785575
MRPL36	-0.2915849	4.57349044	0.00275136	0.04786348
ORMDL3	0.34220614	7.15310373	0.00282326	0.04905002
LDHB	-0.328704	9.72981663	0.00283536	0.04919569
SDHAF3	-0.2952525	4.63291304	0.00286263	0.04960395
NFKBIE	0.34112967	5.01593443	0.0028795	0.04983115

Appendix III

Genes differentially expressed (adjusted P value <0.05) in TGF-β_1-treated activated $CD4^+$ T cells relative to untreated activated cells

Gene	Log_2 fold change	Log_2 counts per million	Unadjusted P value	Adjusted P value
CLIC3	2.62646965	3.00335544	1.49E-14	1.48E-10
SARDH	1.46074223	3.77205071	2.26E-14	1.48E-10
OCIAD2	1.23836772	6.96927928	3.34E-14	1.48E-10
C1orf106	3.60633088	0.75746106	4.95E-13	1.64E-09
SIAH3	3.83885094	0.92080919	6.94E-13	1.84E-09
RGS16	2.21480529	4.73885761	2.43E-12	5.37E-09
ROM1	1.87902226	2.35983192	9.22E-12	1.75E-08
YPEL2	0.80554718	6.19143953	2.34E-11	3.87E-08
APOD	3.08087965	0.50560657	6.38E-11	9.40E-08
RABGAP1L	0.55163525	6.65947017	7.19E-11	9.53E-08
VASH1	1.6522867	3.44905029	8.39E-11	1.01E-07
LDLRAD4	1.2409196	6.84100937	1.23E-10	1.36E-07
SLC25A53	1.11135401	3.28546262	1.53E-10	1.56E-07
ZCCHC18	1.21034777	1.61976281	1.71E-10	1.62E-07
LINC01128	0.64837871	4.38648482	1.09E-09	9.63E-07
F2RL1	1.3196256	3.69583567	1.51E-09	1.25E-06
SMAD7	1.48879666	5.96307358	2.08E-09	1.62E-06
USP35	0.91303657	3.81163559	3.57E-09	2.63E-06
NKD1	2.29856279	2.80122622	3.86E-09	2.69E-06
SMOX	1.79847783	3.28789808	4.65E-09	3.08E-06
PDCD4	0.48779013	8.61538405	5.18E-09	3.27E-06
FBXO34	0.5778175	6.14147226	5.46E-09	3.29E-06
DBH-AS1	2.33103758	1.66620321	6.95E-09	4.00E-06
CCL5	0.93665314	7.69095228	8.36E-09	4.62E-06
KIAA1671	1.19989281	4.68027236	9.22E-09	4.89E-06
CTSL	2.766968	6.21541353	1.07E-08	5.45E-06
IL17F	-1.8629203	3.83848069	1.16E-08	5.60E-06
PLEKHO1	0.62704278	7.00347875	1.18E-08	5.60E-06
AQP1	2.43938556	1.62184136	1.75E-08	8.00E-06
DBH	2.10877978	1.10133607	1.83E-08	8.07E-06
STMND1	2.1618161	0.40582106	2.40E-08	1.03E-05
ERBB2IP	0.46765706	6.59606602	2.60E-08	1.08E-05
PLAT	1.28290775	3.15051216	2.78E-08	1.12E-05
LRRC2	1.9147684	0.62836309	4.13E-08	1.57E-05
PMEPA1	2.75561574	5.30256647	4.15E-08	1.57E-05
MYO7A	1.94742558	0.15170487	4.55E-08	1.68E-05
PIK3IP1	0.770776	9.38774131	5.19E-08	1.86E-05
LINC01281	1.65296193	2.1155095	6.08E-08	2.07E-05
ARRDC2	0.48328684	7.47514779	6.09E-08	2.07E-05
GRAP	0.94857124	5.58449167	7.03E-08	2.33E-05
KLHL25	0.98654751	3.70324784	7.35E-08	2.37E-05
TNFRSF25	0.75780988	6.45076793	7.51E-08	2.37E-05
SKIL	1.82983804	6.03076291	9.37E-08	2.89E-05
MMP2	1.96749937	1.49869309	1.46E-07	4.41E-05
UPP1	0.68744246	5.66577403	1.50E-07	4.42E-05
ITGA1	1.05622161	3.78518418	2.13E-07	6.14E-05
STRIP2	1.10954054	2.59709216	2.22E-07	6.25E-05
CD101	1.2488922	2.29210783	2.84E-07	7.84E-05
BIRC2	0.62678924	6.7728399	3.11E-07	8.42E-05
BEX1	2.36080978	0.69595084	3.22E-07	8.53E-05

ELN	2.90584253	-0.2063033	4.09E-07	0.00010635
RNF157-AS1	1.28176125	1.32198963	4.53E-07	0.00011431
STARD3	0.50629381	6.56771832	4.57E-07	0.00011431
TGFA	1.90872617	1.8388096	4.72E-07	0.00011575
ZNF764	0.48522498	4.78940877	5.23E-07	0.00012616
AHCYL2	0.6582578	4.9134725	5.82E-07	0.00013731
CSF2	-1.4166422	2.48746055	5.90E-07	0.00013731
FMNL3	0.78438958	5.74768718	7.33E-07	0.00016752
EML3	0.72549488	6.86323677	7.50E-07	0.00016861
CYS1	1.71169979	0.06258157	8.32E-07	0.00018387
SNTA1	0.97486454	4.24768071	1.42E-06	0.00030767
EPHA1	0.8105687	3.49970428	1.44E-06	0.00030767
TBC1D16	1.36312177	2.5665599	1.68E-06	0.00035445
FBLN7	1.14744531	6.06094727	1.94E-06	0.00039486
NKILA	1.23085857	1.18722973	1.94E-06	0.00039486
AMPD3	0.46358879	5.25918394	2.13E-06	0.00042778
STC2	-0.9188717	1.63553384	2.34E-06	0.00045952
QPCT	2.13450088	1.80236455	2.38E-06	0.00045952
EMB	0.41118479	8.17108822	2.39E-06	0.00045952
IL9	1.90215679	2.57685575	2.47E-06	0.00046407
SPOCK2	0.44085556	10.6372873	2.51E-06	0.00046407
DEF6	0.44778408	7.06245643	2.52E-06	0.00046407
IKZF4	0.95126988	4.33430963	2.98E-06	0.00054133
FBXO31	0.39865747	5.93490997	3.46E-06	0.00061958
ADAMTSL2	1.66438766	-0.3424912	3.79E-06	0.0006704
IL22	-1.6036144	2.57887433	3.88E-06	0.00067756
CTSA	0.42110421	6.66354979	4.06E-06	0.00069862
SS18	0.50099862	6.12755654	4.15E-06	0.00070529
CDK5RAP1	0.48346193	4.61535785	5.40E-06	0.00090672
BMF	1.00058438	4.93546405	5.67E-06	0.00093968
STK17A	0.51892541	7.72161023	5.74E-06	0.00094011
ITGAE	0.84867126	5.27983915	6.57E-06	0.00106223
MTHFD2	-0.40875	6.94991867	6.81E-06	0.00108754
SPSB1	1.48089155	4.29976353	7.05E-06	0.00109515
TMEM173	0.40678867	7.42081624	7.07E-06	0.00109515
SUOX	1.07311971	2.3710752	7.10E-06	0.00109515
KCTD17	0.42628088	4.67594814	9.00E-06	0.00137077
PDLIM1	-0.7711481	2.77981475	9.80E-06	0.0014603
CTSB	0.50427919	8.42724001	9.80E-06	0.0014603
FNBP1L	1.1387129	2.78514424	1.04E-05	0.00152817
BTG1	0.43084356	9.90299595	1.08E-05	0.00157529
SCML1	0.91780921	3.51940923	1.11E-05	0.00159276
TSPAN14	0.51415734	7.76553112	1.13E-05	0.00160677
CIB1	0.48409022	8.03080066	1.16E-05	0.00163161
CD6	0.48798058	9.26443778	1.19E-05	0.0016577
ADGRG6	2.03211668	-0.2413029	1.22E-05	0.00168345
GAL3ST4	1.13194928	2.28183162	1.26E-05	0.00172122
PLK3	0.6061225	5.97806394	1.38E-05	0.00185244
ATP1B1	1.09425403	2.88092405	1.40E-05	0.00185244
RASAL3	0.39524514	6.88017864	1.42E-05	0.00185244
NLRC3	0.70646815	6.11012584	1.43E-05	0.00185244
BMPR2	0.78266489	5.70719663	1.43E-05	0.00185244
MXD4	0.54895061	6.4145267	1.44E-05	0.00185244
DKK3	1.15707989	0.88538354	1.58E-05	0.00198013
CCDC74A	1.53488778	1.05646713	1.58E-05	0.00198013
PGLYRP2	1.1996642	0.92339737	1.58E-05	0.00198013
DAPK2	1.2234711	1.47272682	1.61E-05	0.00199003
TUFT1	0.91184751	3.27764407	1.63E-05	0.00200469
TOX2	0.89297476	2.54092568	1.75E-05	0.00213309
CDC6	-0.4685301	4.60960931	1.86E-05	0.00223652

DNPH1	0.6290997	6.55343154	1.92E-05	0.00229379
RHOU	0.82376792	3.28295041	1.98E-05	0.00234927
FAM132B	-1.4888905	-0.0491045	2.05E-05	0.00241022
ADAMTS14	-1.5269086	0.10715129	2.39E-05	0.00277608
CHMP7	0.3274547	7.82130937	2.44E-05	0.00280507
E2F1	-0.4449597	4.95472982	2.45E-05	0.00280507
CCL2	2.34997926	-0.3538463	2.48E-05	0.00281348
HIC1	-0.7665243	5.64278335	2.76E-05	0.00308031
COL6A3	1.20172479	3.96726344	2.77E-05	0.00308031
GPR35	0.86278362	2.85231012	2.86E-05	0.00315991
CHI3L2	0.8825053	3.27649965	2.95E-05	0.00323351
ZBED2	0.56675827	5.74818822	3.09E-05	0.00336263
GALNT10	0.82314455	6.13636513	3.16E-05	0.00340928
ERVH48-1	1.28590853	1.79577742	3.20E-05	0.00342009
IL2RB	0.67174872	8.62699891	3.28E-05	0.00347678
DSCC1	-0.5705472	3.61495625	3.32E-05	0.00349464
ADARB2	2.17987849	0.6329074	3.45E-05	0.00360095
FHL3	0.88540175	3.24696849	3.61E-05	0.00373978
LZTS3	0.63863756	4.73124379	3.67E-05	0.00377275
EVA1C	0.58958664	3.06425395	3.70E-05	0.00377327
HTRA3	1.8349522	-0.3804438	3.93E-05	0.00397077
RGS1	0.64947342	8.3016792	3.95E-05	0.00397077
ARHGEF7	0.35076438	6.19511741	4.22E-05	0.00420231
C22orf29	0.42644733	4.9306557	4.45E-05	0.00439728
KLF10	0.6876864	6.38483561	4.93E-05	0.00484565
CYTH3	0.96186349	4.45867188	5.00E-05	0.00486983
TGFBR2	0.38048573	8.17497468	5.06E-05	0.00489911
ZNF853	1.10888215	2.29676535	5.48E-05	0.0052369
MZB1	-1.0573681	1.84735549	5.49E-05	0.0052369
TLE3	0.48727554	6.97773548	5.97E-05	0.00565394
MYL12B	0.36870645	8.42148112	6.08E-05	0.00571146
PDGFB	1.24865222	2.72186288	6.19E-05	0.00573929
CEP112	0.97956055	0.48927007	6.19E-05	0.00573929
GMNN	-0.357784	4.51173395	6.30E-05	0.00573929
XCL1	-0.8193658	1.89880881	6.33E-05	0.00573929
DHRS2	1.92667874	0.35248498	6.35E-05	0.00573929
MAGED2	0.73983726	6.74371574	6.36E-05	0.00573929
FAM102A	0.63367669	8.89090144	7.02E-05	0.00628966
RGS10	0.47926025	7.43275669	7.97E-05	0.00708695
SASH3	0.27444189	7.59455426	8.10E-05	0.0071547
C12orf79	0.66260227	2.80306525	8.39E-05	0.00736434
GZMA	-1.1060753	6.24751461	9.46E-05	0.0082529
ZCCHC14	0.41717403	4.53812202	9.81E-05	0.00849742
AQP3	0.4644378	7.67878759	0.00010076	0.0086728
ARID5A	0.35663137	7.31741468	0.00010494	0.00897473
SKI	0.63250121	6.98381495	0.00010841	0.00921243
FAM172BP	0.89478523	3.58995087	0.00011212	0.00946627
RHOF	0.48802359	4.89133798	0.00011692	0.00979666
GALNT2	0.37576541	6.6997327	0.00011856	0.00979666
ABLIM1	0.61855621	8.99189704	0.00011883	0.00979666
FAM160B1	0.39898534	5.55589638	0.00011898	0.00979666
PIM2	-0.5335354	8.42496272	0.00013356	0.01092861
CLSTN3	0.39009975	6.04055455	0.00013551	0.01102005
ESPN	0.79488184	1.29712413	0.00013674	0.01105243
HRH2	-0.8427105	1.38292199	0.00013859	0.01113385
SMPD1	0.46911271	5.58900938	0.00014022	0.01119753
S1PR1	0.67313507	8.60911127	0.00014316	0.01136342
CDCA5	-0.3600776	6.21901247	0.0001523	0.01201705
PPARG	0.74869483	1.2850248	0.0001675	0.0131384
SEMA7A	0.70437307	4.92384658	0.00017059	0.01330165

CPNE7	1.3439556	2.70716599	0.00017237	0.01336232
RORC	0.5257486	4.12145259	0.00017537	0.0135154
CERK	0.43858561	7.8252199	0.00018013	0.01380206
KCTD11	0.87483	5.34417042	0.00018287	0.01385588
LINC00674	0.29637672	5.59990238	0.00018292	0.01385588
IRF2BPL	0.38465411	6.14210828	0.00019046	0.01434479
PLLP	1.27962137	0.91653555	0.0002007	0.01503132
CD40LG	-0.3621797	5.92416065	0.00020631	0.01535557
CHIC2	0.32910744	5.14355594	0.00020735	0.01535557
DUSP4	0.72008342	7.8362468	0.00020931	0.01541465
GPR25	0.81449762	2.03277288	0.00021628	0.01583963
GPR161	1.33150123	0.24416259	0.00022289	0.01623455
FES	-0.6957429	2.75104969	0.00022644	0.01635206
CCL20	0.71738572	3.39537079	0.00022697	0.01635206
GIT2	0.23027422	6.5112103	0.00023178	0.01660805
RAB38	-0.7252979	1.5335408	0.0002384	0.01699047
LSR	0.35098473	6.34013838	0.00024071	0.01706369
CD38	-0.6522527	4.43450376	0.00024954	0.01758848
ABHD13	0.52540287	5.89679646	0.00025077	0.01758848
SLC20A2	0.55720869	4.44657263	0.00026426	0.01840248
CDK5R1	0.83707465	4.7176854	0.00026557	0.01840248
REEP2	0.92286942	1.30816593	0.00026654	0.01840248
RNPEPL1	0.28039998	6.7301049	0.00027444	0.01878254
SPON1	1.00863538	5.21330257	0.00027488	0.01878254
SRGAP3	1.09780442	1.61646008	0.00029445	0.02001662
IRS1	0.77774423	2.8709933	0.0003046	0.02060122
PSMG1	-0.4071497	4.69312288	0.00031661	0.02130422
HPRT1	-0.2448644	5.79812552	0.0003222	0.02157096
DLGAP4	0.2583904	5.50878497	0.00032567	0.02169402
ELOVL6	-0.861773	1.86237155	0.00033843	0.02235498
DIRAS1	-1.3358203	0.06833155	0.00033897	0.02235498
TRAF4	-0.5138523	5.83233295	0.00034591	0.02269987
KRAS	0.33867487	6.73895698	0.00035501	0.02318249
FBLN2	1.89392735	0.62246783	0.00035684	0.02318763
ZFP36L1	0.39708467	7.79541707	0.00036012	0.02328648
OLFM2	0.98668331	4.94362426	0.00036475	0.02347176
JUN	1.73207996	8.50365174	0.00037381	0.023938
MAP3K4	0.26895206	5.39968984	0.00037913	0.02416248
IGFBP2	0.58559539	4.93545627	0.00038299	0.02429166
KDM7A	0.44142816	7.12356634	0.00038541	0.02432843
BCL9L	0.54771453	7.32411336	0.00038984	0.02449133
IL17A	-0.7504995	2.5916594	0.00040024	0.02502608
FAM214A	0.37430947	4.86336049	0.00041137	0.0255712
GDF15	-1.4776035	1.73752053	0.00041281	0.0255712
PLEK2	0.99706237	1.40543073	0.00042062	0.02591417
ABAT	0.83723364	3.63966048	0.00042226	0.02591417
NYNRIN	1.13269314	0.68610133	0.00044726	0.02732224
TMEM200A	0.72454726	2.40769815	0.00046139	0.02801529
CHST15	1.16195568	2.16143281	0.00046287	0.02801529
KCTD21	0.90729489	3.83384421	0.00046495	0.02801529
GBP6	-0.7345651	2.36315712	0.00049879	0.02991846
ZBTB32	-0.8344614	3.60040993	0.00051527	0.0307677
FAM174B	0.8603227	2.04881223	0.00052769	0.03126437
POLQ	-0.4721835	3.00851269	0.00052831	0.03126437
PLAU	1.35392476	-0.0265642	0.00053987	0.0318069
TEX30	-0.4539046	3.9735632	0.00054333	0.03186884
ST6GALNAC6	0.39738138	6.32212173	0.00054881	0.03204847
NOTCH1	0.54653018	5.95006157	0.00056544	0.03279073
HVCN1	0.48449365	2.44986733	0.00056647	0.03279073
RAB19	0.96895795	1.37356007	0.00057933	0.03338927

CBFB	0.24334264	7.39123395	0.00058576	0.03356379
GRAP2	0.33834044	6.9976272	0.00058856	0.03356379
RAB33A	0.57354411	5.19619295	0.00058995	0.03356379
NMB	0.62650449	2.5439803	0.00059831	0.03389424
RASGRP4	0.76269647	3.31163698	0.00063857	0.03602105
BACH1	0.29577876	5.75935407	0.00064906	0.03645737
TGFB1	0.43609917	8.47646338	0.00065286	0.03651595
GINS4	-0.3579935	4.08495498	0.00066982	0.03730713
LINC00673	1.00907991	0.87780319	0.00067713	0.03755651
DNM3	0.96826531	0.69662276	0.00068078	0.03760166
HAGHL	0.83583313	2.35419942	0.00071598	0.03938176
ATG14	0.43698016	4.65658882	0.00073137	0.04006233
FLT3LG	0.40040644	6.69011555	0.00074332	0.04054907
MN1	1.58318787	-0.2979383	0.00074875	0.04067775
NLN	-0.4892448	3.04331188	0.00075207	0.04069137
BACH2	0.30637781	6.6191446	0.00075693	0.04078827
ID3	0.55455756	5.70600204	0.00078138	0.04193525
PRF1	-0.4553811	5.46772737	0.00079225	0.04234684
ZDHHC3	0.22710067	5.67007269	0.00079881	0.04252595
PRMT2	0.27169832	7.36552832	0.00081003	0.04289797
XRCC2	-0.6384915	1.67402783	0.00081227	0.04289797
ATAD2	-0.3241252	5.97702999	0.00081784	0.04302087
B3GAT3	0.28274592	5.60867108	0.00082901	0.04343474
PDE4DIP	0.58130203	5.59726248	0.00083226	0.04343474
GDF11	-0.4505654	4.36938811	0.00084833	0.04393328
ANKRD35	-1.1516509	0.12606369	0.00084844	0.04393328
ABCG1	0.74179229	5.39644473	0.00089062	0.04593778
HOPX	-0.783703	4.43290336	0.00091115	0.04681459
MINA	-0.4801839	4.13725463	0.00091822	0.04699573
FLJ32255	0.45618298	5.71439236	0.00093648	0.04772712
CST7	-0.5063878	5.77213632	0.00093971	0.04772712
BUB1	-0.3703825	5.33530373	0.000952	0.04816691
PSD	0.40920193	4.07455101	0.00097855	0.04932176

Appendix IV

Genes differentially expressed (based on unadjusted P value <0.05) in activin A-treated activated CD4+ T cells relative to untreated activated cells

Gene	Log_2 fold change	Log_2 counts per million	Unadjusted P value	Adjusted P value
SARDH	0.45253748	3.77205071	0.00024587	0.99983114
OCIAD2	0.35923146	6.96927928	0.00055566	0.99983114
SIAH3	1.2538824	0.92080919	0.00074779	0.99983114
CEP57L1	-0.3996783	2.27250874	0.00120622	0.99983114
APOD	1.03026099	0.50560657	0.00255481	0.99983114
HTRA3	1.2875488	-0.3804438	0.00258109	0.99983114
CACHD1	-0.9275187	0.24965048	0.00279942	0.99983114
GOLGB1	-0.7628038	3.96923082	0.00316231	0.99983114
ANG	0.81108652	-0.3815971	0.0041153	0.99983114
AGAP6	-0.6486758	1.6712128	0.00420955	0.99983114
SETD5	-0.2997512	5.92526024	0.00499035	0.99983114
LIPE-AS1	0.67403547	0.12183175	0.00525578	0.99983114
RBP5	-1.0767875	-0.1792337	0.00594599	0.99983114
ROM1	0.52343206	2.35983192	0.00638462	0.99983114
ARL10	-0.4764825	2.50060183	0.00657143	0.99983114
KMT2C	-0.3797683	5.75526704	0.00688082	0.99983114
BDP1	-0.4836456	4.43038835	0.00723015	0.99983114
RAD54L2	-0.3443541	3.42754685	0.00789775	0.99983114
STMND1	0.83347354	0.40582106	0.00798582	0.99983114
LINC00342	-1.4485815	-0.1011117	0.0081247	0.99983114
LOC105747689	-0.9065072	0.09137502	0.00835081	0.99983114
MKI67	-0.7976503	4.20939361	0.00886315	0.99983114
YPEL2	0.22029546	6.19143953	0.00923969	0.99983114
PIP5KL1	-0.9000803	-0.0201264	0.00935687	0.99983114
MTRNR2L8	-0.7116367	0.01287131	0.00971908	0.99983114
RNF43	-1.0256504	-0.1069352	0.00995607	0.99983114
ZNF408	0.24053461	4.22430459	0.0099863	0.99983114
FOXD2	-0.4193484	1.273485	0.01012584	0.99983114
KMT2A	-0.3881547	6.6718109	0.01013861	0.99983114
CCDC71	0.23335285	4.65192298	0.01028767	0.99983114
KIF5A	-0.7585244	-0.1694368	0.01091559	0.99983114
PRRC2C	-0.560551	6.45195207	0.01182392	0.99983114
ARFGEF3	-0.9927017	-0.3723647	0.01207736	0.99983114
KMT2B	-0.3594437	6.04374718	0.01274261	0.99983114
TCEB3-AS1	0.69809852	0.25560359	0.01303983	0.99983114
HUWE1	-0.256287	7.30087779	0.01318406	0.99983114
LOC102723824	0.68071242	0.20691537	0.01371189	0.99983114
LPPR2	-0.4565298	1.94763408	0.01388758	0.99983114
AQP1	0.83971683	1.62184136	0.0140297	0.99983114
HKDC1	0.70558735	0.94458341	0.0142542	0.99983114
LOC100129917	-0.704059	0.46536815	0.01446347	0.99983114
BOD1L1	-0.594921	4.07422985	0.01449816	0.99983114
MGST3	0.19290275	5.14196971	0.01471667	0.99983114
PDCD4	0.15724192	8.61538405	0.01500969	0.99983114
ZNF285	0.51778828	0.3592049	0.01554821	0.99983114
GNRH1	-0.6855529	-0.1264656	0.01559498	0.99983114
ZNF335	-0.3916631	4.39669939	0.01606363	0.99983114
PDXDC2P	-0.6067607	2.68707144	0.01636952	0.99983114
USP49	-0.3095579	2.87016368	0.01667612	0.99983114
LOC100507006	-0.8120743	0.70953536	0.01669724	0.99983114
RGS16	0.49005771	4.73885761	0.01696317	0.99983114

SH3BP5-AS1	-0.526684	2.08699599	0.01719431	0.99983114
ADARB2	1.19556598	0.6329074	0.01728792	0.99983114
GOLGA4	-0.640634	3.35639102	0.0190443	0.99983114
AKAP9	-0.7353756	3.53509473	0.01924927	0.99983114
SEMA4G	-0.3729662	1.06534279	0.01942819	0.99983114
WWTR1	0.65561276	0.24010617	0.01966145	0.99983114
NBPF12	-0.3378055	3.6900844	0.01968421	0.99983114
UBR4	-0.282391	6.93664971	0.01969589	0.99983114
FAM132B	-0.6773819	-0.0491045	0.01985027	0.99983114
KSR1	-0.2127447	4.11381529	0.01998447	0.99983114
F3	-1.02532	-0.5260457	0.02015076	0.99983114
GPR35	0.43296894	2.85231012	0.02028726	0.99983114
C1orf106	0.77610808	0.75746106	0.02037616	0.99983114
PIK3C2B	-0.2077483	5.56242312	0.02089155	0.99983114
IGSF9B	-0.5248429	3.38855714	0.02099375	0.99983114
SLC7A5P1	-0.420908	1.63063325	0.02138115	0.99983114
DYNC1H1	-0.2261502	7.07652013	0.02159348	0.99983114
MIR4697HG	-0.4344225	3.61565879	0.02166801	0.99983114
GLRX3	0.17103529	5.77551288	0.02183962	0.99983114
CCDC122	0.53311307	0.39884525	0.0219021	0.99983114
PLLP	0.74405371	0.91653555	0.02252812	0.99983114
RABGAP1L	0.13682982	6.65947017	0.02270895	0.99983114
GLI1	-0.7404569	-0.0990366	0.02275372	0.99983114
EIF2AK3	-0.1921859	4.74733379	0.02370293	0.99983114
UNKL	-0.223971	4.40299306	0.02387476	0.99983114
LRP2BP	-0.6295537	-0.3695816	0.02388243	0.99983114
NKTR	-0.4523848	5.56734031	0.02399258	0.99983114
DDTL	-0.5765412	0.30982215	0.02415987	0.99983114
STK17A	0.22476258	7.72161023	0.02432203	0.99983114
ELAC1	0.24571672	3.01979711	0.0245473	0.99983114
STARD5	-0.3456205	3.47557851	0.02467769	0.99983114
SH3PXD2A	-0.268756	5.44689148	0.02531148	0.99983114
PPFIA4	-0.6300446	4.17715031	0.02553877	0.99983114
MYO18B	-0.8015574	-0.1890346	0.02588043	0.99983114
ZNF767P	-0.5528615	2.68203579	0.02605673	0.99983114
DNAJC17	0.21819058	3.15765387	0.02633416	0.99983114
ANKRD23	-0.6993148	1.21970351	0.02651997	0.99983114
TOX2	0.41292068	2.54092568	0.0267051	0.99983114
MAP3K13	0.23272431	3.88028613	0.02672163	0.99983114
PSMB8-AS1	0.28210867	4.88035485	0.02766979	0.99983114
LINC00969	-0.7637993	0.38051499	0.02781338	0.99983114
SYNE2	-0.6949999	6.17980105	0.02822718	0.99983114
EP400	-0.3124467	5.48729474	0.02878171	0.99983114
TMEM176A	0.68237444	1.24619522	0.02921491	0.99983114
LOC441155	-0.3381071	1.4020629	0.02935757	0.99983114
PLEKHO1	0.18584872	7.00347875	0.02982507	0.99983114
KLHL17	-0.3894652	2.60244475	0.02996016	0.99983114
SKIL	0.58904574	6.03076291	0.03041324	0.99983114
ITSN1	-0.4051864	0.60560842	0.03043481	0.99983114
CLIP3	-0.4553763	0.80455316	0.03049978	0.99983114
SLC45A1	0.66250333	-0.1899818	0.03088664	0.99983114
TUBG2	-0.373133	2.3780465	0.03105108	0.99983114
LOC440434	-0.3504876	2.3024969	0.03117959	0.99983114
PFN1P2	-0.791625	-0.1328019	0.03141144	0.99983114
TPRG1L	0.12453087	6.35727715	0.03155146	0.99983114
NEUROG3	-0.7896684	-0.7541755	0.03175271	0.99983114
RPUSD2	0.2766041	4.54430502	0.03183574	0.99983114
SH3PXD2B	-0.7729845	-0.1131589	0.03201722	0.99983114
CNTRL	-0.5170665	4.18972807	0.03215482	0.99983114
CYB5D2	0.26666761	3.98058198	0.03302152	0.99983114

REV3L	-0.2879528	4.02671038	0.03318098	0.99983114
BRCA2	-0.2949672	2.39853268	0.03337517	0.99983114
NKILA	0.47556511	1.18722973	0.03348389	0.99983114
MPP5	-0.2092141	3.98662836	0.03430348	0.99983114
CASC5	-0.3679255	2.62000086	0.03463457	0.99983114
MSTO2P	-0.5363891	1.06132484	0.03478217	0.99983114
USP51	-0.3184469	1.54187107	0.03490193	0.99983114
PAK3	-0.6620521	0.44180513	0.03519412	0.99983114
TBCE	0.167858	3.514069	0.03534691	0.99983114
MMP2	0.65055404	1.49869309	0.03537544	0.99983114
ZNF818P	-0.5738966	1.42870163	0.03541439	0.99983114
MON2	-0.1514078	5.45083529	0.03549374	0.99983114
CCDC142	-0.3557956	2.34434569	0.03556427	0.99983114
BEX1	0.83220283	0.69595084	0.03576763	0.99983114
HDAC8	0.28099797	3.22133419	0.0358883	0.99983114
ZMYND10	-0.5580078	-0.1930506	0.03634802	0.99983114
ADAMTS13	-0.7148189	-0.1739678	0.03643183	0.99983114
NDUFB2-AS1	-0.5539244	-0.0505766	0.03663002	0.99983114
DOT1L	-0.3061974	4.90455384	0.03704511	0.99983114
KMT2D	-0.3868879	6.26023743	0.03724695	0.99983114
LINC00957	-0.3108846	1.98914017	0.03758909	0.99983114
PLXNB2	-0.4378368	4.01186088	0.03771551	0.99983114
KDM5D	-0.2682723	5.42828734	0.03773723	0.99983114
SDHAP3	-0.5372504	0.69875494	0.03774745	0.99983114
FNBP4	-0.3244239	5.85530308	0.03805318	0.99983114
SRRM2	-0.4436933	8.0522014	0.0381665	0.99983114
AHNAK	-0.3728837	8.84105697	0.03826758	0.99983114
GNB3	-0.6941205	-0.10435	0.03830443	0.99983114
CHMP7	0.14265483	7.82130937	0.03869336	0.99983114
ZNF785	-0.3653309	1.95802021	0.03899188	0.99983114
NCOR1	-0.2860486	5.94449304	0.03945484	0.99983114
ACTG1P20	-0.5895441	0.74288274	0.0395904	0.99983114
CCZ1	0.24814721	3.99919513	0.03969175	0.99983114
FAM72C	0.4311235	0.39120817	0.0406986	0.99983114
PRKRIP1	-0.4090049	0.75834464	0.04077684	0.99983114
FAM133DP	0.24042576	2.76966501	0.0413194	0.99983114
TMEM53	0.41437813	0.98461831	0.04139099	0.99983114
CTSL	0.71967006	6.21541353	0.04168949	0.99983114
MACF1	-0.5625273	5.84233523	0.0417904	0.99983114
TAGLN	-0.4095004	1.85283562	0.04180352	0.99983114
DTHD1	-0.6700609	0.32291183	0.04190434	0.99983114
FAM86B3P	-0.5727575	0.02711967	0.04200805	0.99983114
FAM153C	-0.81915	-0.3794583	0.04217773	0.99983114
C2CD3	-0.2198883	4.28701639	0.04265539	0.99983114
TPR	-0.3160067	5.86222506	0.04266526	0.99983114
SZT2	-0.3812742	5.06241796	0.04284977	0.99983114
BAZ2A	-0.1872869	7.39469042	0.04307882	0.99983114
GRAP	0.28339173	5.58449167	0.04357904	0.99983114
ZNF14	0.17823252	4.76743709	0.043885	0.99983114
ST20-AS1	0.40484347	2.05295182	0.04425709	0.99983114
CEP350	-0.2918211	5.25663952	0.04426304	0.99983114
C16orf74	0.7039604	0.47314904	0.04431113	0.99983114
SPEN	-0.3983876	5.61705638	0.0445566	0.99983114
USP6NL	-0.2572566	2.73761955	0.04497769	0.99983114
LOC202181	-0.5556318	0.63310323	0.04529237	0.99983114
ZNF559	0.20091163	4.20143197	0.04578862	0.99983114
RSRP1	-0.3574759	4.94696822	0.04580691	0.99983114
URGCP	0.14121801	5.02719991	0.04597917	0.99983114
SEC16A	-0.1677632	6.71351263	0.04599134	0.99983114
HSF4	-0.8826093	1.17824249	0.04644963	0.99983114

ADAMDEC1	-0.5670704	0.17993567	0.04666179	0.99983114
USP32P1	-0.875285	1.3489802	0.04666637	0.99983114
DIRAS1	-0.6559613	0.06833155	0.04676404	0.99983114
PTPN23	-0.2036232	5.19667649	0.04707001	0.99983114
UBL7	0.14184048	5.71584523	0.04707651	0.99983114
TAF6L	0.19040738	3.74759171	0.04714556	0.99983114
GLB1L3	-0.6096476	-0.0741502	0.04736726	0.99983114
BCAN	0.60166332	-0.6297644	0.04752535	0.99983114
CD300C	0.90695402	0.20388468	0.04752548	0.99983114
TRAPPC2B	0.22392764	2.91502712	0.04753493	0.99983114
CHIC2	0.16138834	5.14355594	0.04810062	0.99983114
DNAJC25	-0.2708564	2.53909035	0.0484184	0.99983114
COX14	0.15386531	5.51229823	0.0484996	0.99983114
PRRT2	-0.7993322	-0.0213113	0.04928349	0.99983114
GOLGA2	-0.222058	4.95341415	0.04953988	0.99983114

Appendix V

Genes differentially expressed (based on unadjusted P value <0.05) in BMP-2-treated activated CD4+ T cells relative to untreated activated cells

Gene	Log_2 fold change	Log_2 counts per million	Unadjusted P value	Adjusted P value
ZNF208	-1.0211197	0.40476821	0.00179909	0.99989942
ID3	0.44195034	5.70600204	0.00572228	0.99989942
ANKRD36	-0.6140961	1.96791162	0.0064903	0.99989942
C1orf106	0.92202315	0.75746106	0.00677874	0.99989942
FAM153C	-1.1335657	-0.3794583	0.00769363	0.99989942
CLIP3	-0.5682731	0.80455316	0.00848607	0.99989942
SCARNA9	-0.8184659	-0.1016169	0.0086699	0.99989942
ITSN1	-0.4922856	0.60560842	0.01025449	0.99989942
C5orf45	-0.3033685	2.82288852	0.01165355	0.99989942
GLI1	-0.7945511	-0.0990366	0.01561108	0.99989942
LGALSL	0.69133526	-0.0443614	0.01563575	0.99989942
MKI67	-0.7245195	4.20939361	0.01641716	0.99989942
PDK2	0.21135871	4.76854479	0.01788757	0.99989942
ZNF397	-0.3554219	3.01904661	0.01893459	0.99989942
ZNF767P	-0.5764471	2.68203579	0.02085203	0.99989942
LOC105747689	-0.7754759	0.09137502	0.0210235	0.99989942
SELO	-0.230144	4.24978942	0.02180098	0.99989942
NBPF12	-0.3314981	3.6900844	0.02200403	0.99989942
PIGB	-0.2177648	3.27386652	0.02209067	0.99989942
LINC00342	-1.1951981	-0.1011117	0.02248116	0.99989942
LPPR2	-0.4170547	1.94763408	0.02351776	0.99989942
MEF2BNB	0.35378897	2.04907355	0.02363768	0.99989942
SRR	-0.2744333	2.28198813	0.02393855	0.99989942
WDR90	-0.3338327	2.62096093	0.02538154	0.99989942
GOLGB1	-0.552134	3.96923082	0.02637147	0.99989942
ANKRD36C	-0.6574972	1.02357066	0.02649139	0.99989942
LIPE-AS1	0.52665125	0.12183175	0.02650346	0.99989942
MST1P2	-0.8088423	0.10178612	0.02748472	0.99989942
LOC100506985	0.17908597	4.76567032	0.02922185	0.99989942
PLEKHM1	0.19677073	5.60912494	0.02922514	0.99989942
ZNF573	-0.4893907	1.22504097	0.02958255	0.99989942
RFESD	0.48648073	0.66138359	0.0299017	0.99989942
LOC729683	0.22844268	5.33066189	0.03008041	0.99989942
AMT	-0.7275557	1.25084063	0.03098997	0.99989942
SGK494	-0.8629846	1.19405009	0.03145939	0.99989942
SCO2	-0.5944331	0.16375062	0.03161216	0.99989942
PDXDC2P	-0.5352854	2.68707144	0.03194007	0.99989942
BOD1L1	-0.5130905	4.07422985	0.03240829	0.99989942
ZBTB11-AS1	-0.3351083	1.55978131	0.0329159	0.99989942
UPF3B	-0.3140256	3.41868621	0.03361658	0.99989942
AK1	-0.6576431	2.76310864	0.03362353	0.99989942
TMEM53	0.43344181	0.98461831	0.03382275	0.99989942
CHMP6	0.13973796	4.72220179	0.03453983	0.99989942
GNRH1	-0.5856394	-0.1264656	0.03635525	0.99989942
RSRC2	-0.1601305	5.72784876	0.03651951	0.99989942
DDTL	-0.5307979	0.30982215	0.03706795	0.99989942
TCF7L2	-0.4941545	1.27955889	0.03775297	0.99989942
CBWD6	-0.6224551	-0.1572249	0.03805187	0.99989942
MALAT1	-0.6153415	7.56515819	0.03861027	0.99989942
CCDC130	-0.2383886	4.3409168	0.03871093	0.99989942
SEMA4G	-0.3269485	1.06534279	0.03871261	0.99989942

USP49	-0.2634871	2.87016368	0.03905856	0.99989942
SH3BP5-AS1	-0.4494392	2.08699599	0.03909033	0.99989942
KANK2	0.29376341	1.83958989	0.03987847	0.99989942
POTEE	0.62631455	0.18407394	0.03990251	0.99989942
KLF3-AS1	-0.5818502	0.19010825	0.04048434	0.99989942
SCNN1D	-1.00742	0.04339372	0.04059541	0.99989942
COMMD3	-0.2032266	3.45028969	0.04066209	0.99989942
HSF4	-0.9062428	1.17824249	0.04116102	0.99989942
PLLP	0.66642834	0.91653555	0.04216665	0.99989942
CEP112	0.46005795	0.48927007	0.04223367	0.99989942
ZBED1	0.14758783	6.11138581	0.04263431	0.99989942
PANK1	0.47842207	1.28703003	0.0431738	0.99989942
TGFB1I1	-0.57064	-0.1980223	0.0442907	0.99989942
PPFIA4	-0.5604363	4.17715031	0.04437648	0.99989942
CCDC122	0.46339291	0.39884525	0.04480863	0.99989942
SOCS1	0.2895625	6.28364354	0.04620362	0.99989942
ZNF883	-0.5066509	0.13913153	0.0464351	0.99989942
GOLGA4	-0.5353737	3.35639102	0.04660234	0.99989942
UBAP1L	-0.5155695	0.0911912	0.04682578	0.99989942
NPIPA5	-0.726378	-0.4880045	0.0468907	0.99989942
EFHC1	0.45531218	1.01024777	0.04733686	0.99989942
AGAP6	-0.4300919	1.6712128	0.04735438	0.99989942
FGFR1OP	-0.1935396	3.85785973	0.04876364	0.99989942
MIR3181	0.79225001	-0.0180083	0.04922492	0.99989942
C8orf76	-0.4111906	0.92441592	0.04946147	0.99989942

References

1. UNAIDS. UNAIDS data 2019. Published 2019. Accessed on October 8, 2020. https://www.unaids.org/sites/default/files/media_asset/2019-UNAIDS-data_en.pdf
2. World Health Organisation. Ten threats to global health in 2019, 13th General Programme of Work. Published 2019. Accessed on October 8, 2020. https://www.who.int/news-room/spotlight/ten-threats-to-global-health-in-2019
3. Sharp PM, Hahn BH. Origins of HIV and the AIDS pandemic. *Cold Spring Harb Perspect Med*. 2011;1(1):a006841.
4. Nyamweya S, Hegedus A, Jaye A, Rowland-Jones S, Flanagan KL, Macallan DC. Comparing HIV-1 and HIV-2 infection: Lessons for viral immunopathogenesis. *Rev Med Virol*. 2013;23(4):221–40.
5. Greene WC. A history of AIDS: looking back to see ahead. *Eur J Immunol*. 2007;37 Suppl 1:S94-102.
6. Quinn TC, Overbaugh J. HIV/AIDS in women: an expanding epidemic. *Science*. 2005;308(5728):1582–3.
7. Shaw GM, Hunter E. HIV transmission. *Cold Spring Harb Perspect Med*. 2012;2(11):a006965.
8. UNAIDS. Miles to go: closing gaps, breaking barriers, righting injustices. Published 2018. Accessed on October 8, 2020. https://www.unaids.org/sites/default/files/media_asset/miles-to-go_en.pdf
9. Trickey A, May MT, Vehreschild JJ, et al. Survival of HIV-positive patients starting antiretroviral therapy between 1996 and 2013: a collaborative analysis of cohort studies. *Lancet HIV*. 2017;4(8):e349-56.
10. Posse M, Meheus F, Asten H, Ven A, Baltussen R. Barriers to access to antiretroviral treatment in developing countries: a review. *Trop Med Int Health*. 2008;13(7):904–13.
11. Keating SM, Golub ET, Nowicki M, et al. The effect of HIV infection and HAART on inflammatory biomarkers in a population-based cohort of women. *AIDS*. 2011;25(15):1823–32.
12. Fernandez S, Tanaskovic S, Helbig K, et al. CD4+ T cell deficiency in HIV patients responding to antiretroviral therapy is associated with increased expression of interferon-stimulated genes in CD4+ T cells. *J Infect Dis*. 2011;204(12):1927–35.
13. Deeks SG, Lewin SR, Havlir DV. The end of AIDS: HIV infection as a chronic disease. *Lancet*. 2013;382(9903):1525–33.
14. Bangsberg DR, Moss AR, Deeks SG. Paradoxes of adherence and drug resistance to HIV antiretroviral therapy. *J Antimicrob Chemother*. 2004;53(5):696–9.
15. Finzi D, Blankson J, Siliciano JD, et al. Latent infection of CD4+ T cells provides a mechanism for lifelong persistence of HIV-1, even in patients on effective combination therapy. *Nat Med*. 1999;5(5):512–7.
16. Haynes BF, Shaw GM, Korber B, et al. HIV-host interactions: implications for vaccine design. *Cell Host Microbe*. 2016;19(3):292–303.
17. Barouch DH, Deeks SG. Immunologic strategies for HIV-1 remission and eradication. *Science*. 2014;345(6193):169–74.

18. Bbosa N, Kaleebu P, Ssemwanga D. HIV subtype diversity worldwide. *Curr Opin HIV AIDS*. 2019;14(3):153–60.

19. Geretti AM, Harrison L, Green H, et al. Effect of HIV-1 subtype on virologic and immunologic response to starting highly active antiretroviral therapy. *Clin Infect Dis*. 2009;48(9):1296–305.

20. Wilen CB, Tilton JC, Doms RW. HIV: cell binding and entry. *Cold Spring Harb Perspect Med*. 2012;2(8):a006866.

21. Engelman A, Cherepanov P. The structural biology of HIV-1: mechanistic and therapeutic insights. *Nat Rev Microbiol*. 2012;10(4):279–90.

22. Malim MH, Bieniasz PD. HIV restriction factors and mechanisms of evasion. *Cold Spring Harb Perspect Med*. 2012;2(5):a006940.

23. Prévost J, Edgar CR, Richard J, et al. HIV-1 vpu downregulates TIM-3 from the surface of infected CD4+ T cells. *J Virol*. 2020;94(7):e01999-19.

24. Usami Y, Wu Y, Göttlinger HG. SERINC3 and SERINC5 restrict HIV-1 infectivity and are counteracted by Nef. *Nature*. 2015;526(7572):218–23.

25. Shum KT, Zhou J, Rossi JJ. Aptamer-based therapeutics: new approaches to combat human viral diseases. *Pharmaceuticals (Basel)*. 2013;6(12):1507–42.

26. Zhu P, Chertova E, Bess J, et al. Electron tomography analysis of envelope glycoprotein trimers on HIV and simian immunodeficiency virus virions. *Proc Natl Acad Sci USA*. 2003;100(26):15812–7.

27. Yamaguchi M, Danev R, Nishiyama K, Sugawara K, Nagayama K. Zernike phase contrast electron microscopy of ice-embedded influenza A virus. *J Struct Biol*. 2008;162(2):271–6.

28. Prasad VM, Miller AS, Klose T, et al. Structure of the immature Zika virus at 9 Å resolution. *Nat Struct Mol Biol*. 2017;24(2):184–6.

29. Grünewald K, Desai P, Winkler DC, et al. Three-dimensional structure of herpes simplex virus from cryo-electron tomography. *Science*. 2003;302(5649):1396–8.

30. Strebel K. HIV accessory proteins versus host restriction factors. *Curr Opin Virol*. 2013;3(6):692–9.

31. Jeeninga RE, Hoogenkamp M, Armand-Ugon M, Baar M, Verhoef K, Berkhout B. Functional differences between the long terminal repeat transcriptional promoters of human immunodeficiency virus type 1 subtypes A through G. *J Virol*. 2000;74(8):3740–51.

32. Los Alamos National Laboratory. HIV sequence database. Last modified 2017. Accessed on October 8, 2020. https://www.hiv.lanl.gov/content/sequence/HIV/MAP/landmark.html

33. Jacques DA, McEwan WA, Hilditch L, Price AJ, Towers GJ, James LC. HIV-1 uses dynamic capsid pores to import nucleotides and fuel encapsidated DNA synthesis. *Nature*. 2016;536(7616):349–53.

34. Towers GJ, Noursadeghi M. Interactions between HIV-1 and the cell-autonomous innate immune system. *Cell Host Microbe*. 2014;16(1):10–8.

35. Craigie R, Bushman FD. HIV DNA integration. *Cold Spring Harb Perspect Med*. 2012;2(7):a006890.

36. Siliciano RF, Greene WC. HIV latency. *Cold Spring Harb Perspect Med*. 2011;1(1):a007096.

37. Pan X, Baldauf HM, Keppler OT, Fackler OT. Restrictions to HIV-1 replication in resting CD4+ T lymphocytes. *Cell Res*. 2013;23(7):876–85.

38. Nabel G, Baltimore D. An inducible transcription factor activates expression of human immunodeficiency virus in T cells. *Nature*. 1987;326(6114):711–3.

39. Mbonye U, Karn J. Control of HIV latency by epigenetic and non-epigenetic mechanisms. *Curr HIV Res*. 2011;9(8):554–67.

40. Karn J, Stoltzfus CM. Transcriptional and posttranscriptional regulation of HIV-1 gene expression. *Cold Spring Harb Perspect Med*. 2012;2(2):a006916.

41. Freed EO. HIV-1 assembly, release and maturation. *Nat Rev Microbiol*. 2015;13(8):484–96.

42. Schacker T, Collier AC, Hughes J, Shea T, Corey L. Clinical and epidemiologic features of primary HIV infection. *Ann Intern Med*. 1996;125(4):257–64.

43. Medley GF, Anderson RM, Cox DR, Billard L. Incubation period of AIDS in patients infected via blood transfusion. *Nature*. 1987;328(6132):719–21.

44. Lewthwaite P, Wilkins E. Natural history of HIV/AIDS. *Medicine*. 2005;33(6):10–13.

45. Burdo TH, Lackner A, Williams KC. Monocyte/macrophages and their role in HIV neuropathogenesis. *Immunol Rev*. 2013;254(1):102–13.

46. Simon V, Ho DD, Abdool Karim Q. HIV/AIDS epidemiology, pathogenesis, prevention, and treatment. *Lancet*. 2006;368(9534):489–504.

47. Sabin CA, Lundgren JD. The natural history of HIV infection. *Curr Opin HIV AIDS*. 2013;8(4):311–7.

48. Okulicz JF, Marconi VC, Landrum ML, et al. Clinical outcomes of elite controllers, viremic controllers, and long-term nonprogressors in the US Department of Defense HIV natural history study. *J Infect Dis*. 2009;200(11):1714–23.

49. Kolodkin-Gal D, Hulot SL, Korioth-Schmitz B, et al. Efficiency of cell-free and cell-associated virus in mucosal transmission of human immunodeficiency virus type 1 and simian immunodeficiency virus. *J Virol*. 2013;87(24):13589–97.

50. Quinn TC, Wawer MJ, Sewankambo N, et al. Viral load and heterosexual transmission of human immunodeficiency virus type 1. Rakai Project Study Group. *N Engl J Med*. 2000;342(13):921–9.

51. Patel P, Borkowf CB, Brooks JT, Lasry A, Lansky A, Mermin J. Estimating per-act HIV transmission risk: a systematic review. *AIDS*. 2014;28(10):1509–19.

52. Cuevas JM, Geller R, Garijo R, López-Aldeguer J, Sanjuán R. Extremely high mutation rate of HIV-1 in vivo. *PLoS Biol*. 2015;13(9):e1002251.

53. Korber B, Gaschen B, Yusim K, Thakallapally R, Kesmir C, Detours V. Evolutionary and immunological implications of contemporary HIV-1 variation. *Br Med Bull*. 2001;58:19–42.

54. Salazar-Gonzalez JF, Bailes E, Pham KT, et al. Deciphering human immunodeficiency virus type 1 transmission and early envelope diversification by single-genome amplification and sequencing. *J Virol*. 2008;82(8):3952–70.

55. Keele BF, Giorgi EE, Salazar-Gonzalez JF, et al. Identification and characterization of transmitted and early founder virus envelopes in primary HIV-1 infection. *Proc Natl Acad Sci USA*. 2008;105(21):7552–7.

56. Parrish NF, Gao F, Li H, et al. Phenotypic properties of transmitted founder HIV-1. *Proc Natl Acad Sci USA*. 2013;110(17):6626–33.

57. Fenton-May AE, Dibben O, Emmerich T, et al. Relative resistance of HIV-1 founder viruses to control by interferon-alpha. *Retrovirology*. 2013;10(146).

58. Iyer SS, Bibollet-Ruche F, Sherrill-Mix S, et al. Resistance to type 1 interferons is a major determinant of HIV-1 transmission fitness. *Proc Natl Acad Sci USA*. 2017;114(4):E590-E599.

59. Shankarappa R, Margolick JB, Gange SJ, et al. Consistent viral evolutionary changes associated with the progression of human immunodeficiency virus type 1 infection. *J Virol*. 1999;73(12):10489–502.

60. Haase AT. Targeting early infection to prevent HIV-1 mucosal transmission. *Nature*. 2010;464(7286):217–23.

61. Hatziioannou T, Evans DT. Animal models for HIV/AIDS research. *Nat Rev Microbiol*. 2012;10(12):852–67.

62. Miller CJ, Li Q, Abel K, et al. Propagation and dissemination of infection after vaginal transmission of simian immunodeficiency virus. *J Virol*. 2005;79(14):9217–27.

63. Stacey AR, Norris PJ, Qin L, et al. Induction of a striking systemic cytokine cascade prior to peak viremia in acute human immunodeficiency virus type 1 infection, in contrast to more modest and delayed responses in acute hepatitis B and C virus infections. *J Virol*. 2009;83(8):3719–33.

64. Gasper-Smith N, Crossman DM, Whitesides JF, et al. Induction of plasma (TRAIL), TNFR-2, Fas ligand, and plasma microparticles after human immunodeficiency virus type 1 (HIV-1) transmission: implications for HIV-1 vaccine design. *J Virol*. 2008;82(15):7700–10.

65. Konrad BP, Taylor D, Conway JM, Ogilvie GS, Coombs D. On the duration of the period between exposure to HIV and detectable infection. *Epidemics*. 2017;20:73–83.

66. Little SJ, McLean AR, Spina CA, Richman DD, Havlir DV. Viral dynamics of acute HIV-1 infection. *J Exp Med*. 1999;190(6):841–50.

67. Whitney JB, Hill AL, Sanisetty S, et al. Rapid seeding of the viral reservoir prior to SIV viraemia in rhesus monkeys. *Nature*. 2014;512(7512):74–7.

68. Lifson JD, Rossio JL, Arnaout R, et al. Containment of simian immunodeficiency virus infection: cellular immune responses and protection from rechallenge following transient postinoculation antiretroviral treatment. *J Virol*. 2000;74(6):2584–93.

69. Borrow P, Lewicki H, Hahn BH, Shaw GM, Oldstone MB. Virus-specific CD8+ cytotoxic T-lymphocyte activity associated with control of viremia in primary human immunodeficiency virus type 1 infection. *J Virol*. 1994;68(9):6103–10.

70. Koup RA, Safrit JT, Cao Y, et al. Temporal association of cellular immune responses with the initial control of viremia in primary human immunodeficiency virus type 1 syndrome. *J Virol*. 1994;68(7):4650–5.

71. Mellors JW, Rinaldo CR, Gupta P, White RM, Todd JA, Kingsley LA. Prognosis in HIV-1 infection predicted by the quantity of virus in plasma. *Science*. 1996;272(5265):1167–70.

72. Sterling TR, Vlahov D, Astemborski J, Hoover DR, Margolick JB, Quinn TC. Initial plasma HIV-1 RNA levels and progression to AIDS in women and men. *N Engl J Med*. 2001;344(10):720–5.

73. Fiebig EW, Wright DJ, Rawal BD, et al. Dynamics of HIV viremia and antibody seroconversion in plasma donors: implications for diagnosis and staging of primary HIV infection. *AIDS*. 2003;17(13):1871–9.

74. Tough RH, McLaren PJ. Interaction of the Host and Viral Genome and Their Influence on HIV Disease. *Front Genet*. 2018;9(720).

75. Guadalupe M, Reay E, Sankaran S. Severe CD4+ T cell depletion in gut lymphoid tissue during primary human immunodeficiency virus type 1 infection and substantial delay in restoration following highly active antiretroviral therapy. *J Virol*. 2003;77(21):11708–17.

76. Brenchley JM, Schacker TW, Ruff LE, et al. CD4+ T cell depletion during all stages of HIV disease occurs predominantly in the gastrointestinal tract. *J Exp Med*. 2004;200(6):749–59.

77. Rato S, Rausell A, Muñoz M, Telenti A, Ciuffi A. Single-cell analysis identifies cellular markers of the HIV permissive cell. *PLoS Pathog*. 2017;13(10):e1006678.

78. Zhang Z, Schuler T, Zupancic M, et al. Sexual transmission and propagation of SIV and HIV in resting and activated CD4+ T cells. *Science*. 1999;286(5443):1353–7.

79. Li Q, Duan L, Estes JD, et al. Peak SIV replication in resting memory CD4+ T cells depletes gut lamina propria CD4+ T cells. *Nature*. 2005;434(7037):1148–52.

80. Meng G, Sellers MT, Mosteller-Barnum M, Rogers TS, Shaw GM, Smith PD. Lamina propria lymphocytes, not macrophages, express CCR5 and CXCR4 and are the likely target cell for human immunodeficiency virus type 1 in the intestinal mucosa. *J Infect Dis*. 2000;182(3):785–91.

81. Vijayan KKV, Karthigeyan KP, Tripathi SP, Hanna LE. Pathophysiology of CD4+ T cell depletion in HIV-1 and HIV-2 infections. *Front Immunol*. 2017;8(580).

82. Dockrell DH, Badley AD, Algeciras-Schimnich A, et al. Activation-induced CD4+ T cell death in HIV-positive individuals correlates with Fas susceptibility, CD4+ T cell count, and HIV plasma viral copy number. *AIDS Res Hum Retroviruses*. 1999;15(17):1509–18.

83. Yates A, Stark J, Klein N, Antia R, Callard R. Understanding the slow depletion of memory CD4+ T cells in HIV infection. *PLoS Med*. 2007;4(5):e177.

84. Goonetilleke N, Liu MK, Salazar-Gonzalez JF, et al. The first T cell response to transmitted/founder virus contributes to the control of acute viremia in HIV-1 infection. *J Exp Med*. 2009;206(6):1253–72.

85. Doitsh G, Galloway NL, Geng X, et al. Cell death by pyroptosis drives CD4 T cell depletion in HIV-1 infection. *Nature*. 2014;505(7484):509–14.

86. Sousa AE, Carneiro J, Meier-Schellersheim M, Grossman Z, Victorino RM. CD4 T cell depletion is linked directly to immune activation in the pathogenesis of HIV-1 and HIV-2 but only indirectly to the viral load. *J Immunol*. 2002;169(6):3400–6.

87. Paiardini M, Müller-Trutwin M. HIV-associated chronic immune activation. *Immunol Rev*. 2013;254(1):78–101.

88. Day CL, Kaufmann DE, Kiepiela P, et al. PD-1 expression on HIV-specific T cells is associated with T cell exhaustion and disease progression. *Nature*. 2006;443(7109):350–4.

89. Boasso A, Shearer GM, Chougnet C. Immune dysregulation in human immunodeficiency virus infection: know it, fix it, prevent it. *J Intern Med*. 2009;265(1):78–96.

90. Brenchley JM, Douek DC. HIV infection and the gastrointestinal immune system. *Mucosal Immunol*. 2008;1(1):23–30.

91. Brenchley JM, Price DA, Schacker TW, et al. Microbial translocation is a cause of systemic immune activation in chronic HIV infection. *Nat Med*. 2006;12(12):1365–71.

92. Lurain NS, Hanson BA, Hotton AL, Weber KM, Cohen MH, Landay AL. The association of human cytomegalovirus with biomarkers of inflammation and immune activation in HIV-1-infected women. *AIDS Res Hum Retroviruses*. 2016;32(2):134–43.

93. Freeman ML, Lederman MM, Gianella S, et al. Partners in Crime: The role of CMV in immune dysregulation and clinical outcome during HIV infection. *Curr HIV/AIDS Rep*. 2016;13(1):10–9.

94. Douek DC, Picker LJ, Koup RA. T cell dynamics in HIV-1 infection. *Annu Rev Immunol*. 2003;21:265–304.

95. Schacker TW, Reilly C, Beilman GJ, et al. Amount of lymphatic tissue fibrosis in HIV infection predicts magnitude of HAART-associated change in peripheral CD4 cell count. *AIDS*. 2005;19(18):2169–71.

96. Doria A, Zen M, Bettio S, et al. Autoinflammation and autoimmunity: bridging the divide. *Autoimmun Rev*. 2012;12(1):22–30.

97. Gasteiger G, D'Osualdo A, Schubert DA, Weber A, Bruscia EM, Hartl D. Cellular innate immunity: an old game with new players. *J Innate Immun*. 2017;9(2):111–25.

98. Seong SY, Matzinger P. Hydrophobicity: an ancient damage-associated molecular pattern that initiates innate immune responses. *Nat Rev Immunol*. 2004;4(6):469–78.

99. Brown GD, Willment JA, Whitehead L. C-type lectins in immunity and homeostasis. *Nat Rev Immunol*. 2018;18(6):374–89.

100. Mogensen TH. Pathogen recognition and inflammatory signaling in innate immune defenses. *Clin Microbiol Rev*. 2009;22(2):240–73.

101. Holdsworth SR, Gan P. Cytokines: names and numbers you should care about. *Clin J Am Soc Nephrol*. 2015;10(12):2243–54.

102. Steinman RM. Decisions about dendritic cells: past, present, and future. *Annu Rev Immunol*. 2012;30:1–22.

103. Holling TM, Stoep N, Quinten E, Elsen PJ. Activated human T cells accomplish MHC class II expression through T cell-specific occupation of class II transactivator promoter III. *J Immunol*. 2002;168(2):763–70.

104. Joffre OP, Segura E, Savina A, Amigorena S. Cross-presentation by dendritic cells. *Nat Rev Immunol*. 2012;12(8):557–69.

105. Fujii S, Liu K, Smith C, Bonito AJ, Steinman RM. The linkage of innate to adaptive immunity via maturing dendritic cells in vivo requires CD40 ligation in addition to antigen presentation and CD80/86 costimulation. *J Exp Med*. 2004;199(12):1607–18.

106. McNab F, Mayer-Barber K, Sher A, Wack A, O'Garra A. Type I interferons in infectious disease. *Nat Rev Immunol*. 2015;15(2):87–103.

107. da Silva, AJ, Brickelmaier, M, Majeau, GR, et al. Comparison of gene expression patterns induced by treatment of human umbilical vein endothelial cells with IFN-alpha 2b vs. IFN-beta 1a: understanding the functional relationship between distinct type I

interferons that act through a common receptor. *J Interferon Cytokine Res*. 2002;22(2):173–88.

108. Moll HP, Maier T, Zommer A, Lavoie T, Brostjan C. The differential activity of interferon-α subtypes is consistent among distinct target genes and cell types. *Cytokine*. 2011;53(1):52–9.

109. Tamura T, Yanai H, Savitsky D, Taniguchi T. The IRF family transcription factors in immunity and oncogenesis. *Annu Rev Immunol*. 2008;26:535–84.

110. Izaguirre A, Barnes BJ, Amrute S, et al. Comparative analysis of IRF and IFN-alpha expression in human plasmacytoid and monocyte-derived dendritic cells. *J Leukoc Biol*. 2003;74(6):1125–38.

111. Speer SD, Li Z, Buta S, et al. ISG15 deficiency and increased viral resistance in humans but not mice. *Nat Commun*. 2016;7(11496).

112. Samuel CE. Antiviral actions of interferons. *Clin Microbiol Rev*. 2001;14(4):778–809.

113. Zhou JH, Wang YN, Chang QY, Ma P, Hu Y, Cao X. Type III interferons in viral infection and antiviral immunity. *Cell Physiol Biochem*. 2018;51(1):173–85.

114. Sommereyns C, Paul S, Staeheli P, Michiels T. IFN-lambda (IFN-lambda) is expressed in a tissue-dependent fashion and primarily acts on epithelial cells in vivo. *PLoS Pathog*. 2008;4(3):e1000017.

115. Pervolaraki K, Rastgou Talemi S, Albrecht D, et al. Differential induction of interferon stimulated genes between type I and type III interferons is independent of interferon receptor abundance. *PLoS Pathog*. 2018;14(11):e1007420.

116. Hou W, Wang X, Ye L, et al. Lambda interferon inhibits human immunodeficiency virus type 1 infection of macrophages. *J Virol*. 2009;83(8):3834–42.

117. Santer DM, Minty GES, Golec DP, et al. Differential expression of interferon-lambda receptor 1 splice variants determines the magnitude of the antiviral response induced by interferon-lambda 3 in human immune cells. *PLoS Pathog*. 2020;16(4):e1008515.

118. Market E, Papavasiliou FN. V(D)J recombination and the evolution of the adaptive immune system. *PLoS Biol*. 2003;1(1):E16.

119. Hogquist KA, Baldwin TA, Jameson SC. Central tolerance: learning self-control in the thymus. *Nat Rev Immunol*. 2005;5(10):772–82.

120. Guidotti LG, Borrow P, Brown A, McClary H, Koch R, Chisari FV. Noncytopathic clearance of lymphocytic choriomeningitis virus from the hepatocyte. *J Exp Med*. 1999;189(10):1555–64.

121. Soghoian DZ, Streeck H. Cytolytic CD4(+) T cells in viral immunity. *Expert Rev Vaccines*. 2010;9(12):1453–63.

122. Smith-Garvin JE, Koretzky GA, Jordan MS. T cell activation. *Annu Rev Immunol*. 2009;27:591–619.

123. Martinez-Sanchez ME, Huerta L, Alvarez-Buylla ER, Villarreal Luján C. Role of cytokine combinations on CD4+ T cell differentiation, partial polarization, and plasticity: continuous network modeling approach. *Front Physiol*. 2018;9(877).

124. Gasper DJ, Tejera MM, Suresh M. CD4 T-cell memory generation and maintenance. *Crit Rev Immunol*. 2014;34(2):121–46.

125. Nurieva RI, Chung Y. Understanding the development and function of T follicular helper cells. *Cell Mol Immunol*. 2010;7(3):190–7.

126. Fontenot JD, Gavin MA, Rudensky AY. FOXP3 programs the development and function of CD4+CD25+ regulatory T cells. *Nat Immunol*. 2003;4(4):330–6.

127. Schmidt A, Oberle N, Krammer PH, et al. Molecular mechanisms of Treg-mediated T cell suppression. *Front Immunol*. 2012;3(51).

128. Vignali DA, Collison LW, Workman CJ. How regulatory T cells work. *Nat Rev Immunol*. 2008;8(7):523–32.

129. Dhamne C, Chung Y, Alousi AM, Cooper LJ, Tran DQ. Peripheral and thymic FOXP3+ regulatory T cells in search of origin, distinction, and function. *Front Immunol*. 2013;4(253).

130. Thornton AM, Korty PE, Tran DQ, et al. Expression of Helios, an Ikaros transcription factor family member, differentiates thymic-derived from peripherally induced FOXP3+ T regulatory cells. *J Immunol*. 2010;184(7):3433–41.

131. Oukka M. Th17 cells in immunity and autoimmunity. *Ann Rheum Dis*. 2008;67 Suppl 3:iii26-9.

132. Stritesky GL, Yeh N, Kaplan MH, et al. IL-23 promotes maintenance but not commitment to the Th17 lineage. *J Immunol*. 2008;181(9):5948–55.

133. Guéry L, Hugues S. Th17 Cell Plasticity and Functions in Cancer Immunity. *Biomed Res Int*. 2015;2015(314620):314620.

134. Ivanov II, McKenzie BS, Zhou L, et al. The orphan nuclear receptor RORgammat directs the differentiation program of proinflammatory IL-17+ T helper cells. *Cell*. 2006;126(6):1121–33.

135. Wei L, Laurence A, Elias KM, O'Shea JJ. IL-21 is produced by Th17 cells and drives IL-17 production in a STAT3-dependent manner. *J Biol Chem*. 2007;282(48):34605–10.

136. McGeachy MJ, Bak-Jensen KS, Chen Y, et al. TGF-beta and IL-6 drive the production of IL-17 and IL-10 by T cells and restrain Th17 cell-mediated pathology. *Nat Immunol*. 2007;8(12):1390–7.

137. Lee Y, Awasthi A, Yosef N, et al. Induction and molecular signature of pathogenic Th17 cells. *Nat Immunol*. 2012;13(10):991–9.

138. Zhou L, Lopes JE, Chong MM, et al. TGF-beta-induced FOXP3 inhibits Th17 cell differentiation by antagonizing RORgammat function. *Nature*. 2008;453(7192):236–40.

139. Wilson NJ, Boniface K, Chan J, et al. Development, cytokine profile and function of human interleukin 17-producing helper T cells. *Nat Immunol*. 2007;8(9):950–7.

140. Acosta-Rodriguez EV, Napolitani G, Lanzavecchia A, Sallusto F. Interleukins 1beta and 6 but not transforming growth factor-beta are essential for the differentiation of interleukin 17-producing human T helper cells. *Nat Immunol*. 2007;8(9):942–9.

141. Hatton RD. TGF-beta in Th17 cell development: the truth is out there. *Immunity*. 2011;34(3):288–90.

142. Zhang S. The role of transforming growth factor beta in T helper 17 differentiation. *Immunology*. 2018;155(1):24–35.

143. Manel N, Unutmaz D, Littman DR. The differentiation of human Th17 cells requires transforming growth factor-beta and induction of the nuclear receptor RORgammat. *Nat Immunol*. 2008;9(6):641–9.

144. Volpe E, Servant N, Zollinger R, et al. A critical function for transforming growth factor-beta, interleukin 23 and proinflammatory cytokines in driving and modulating human T(H)-17 responses. *Nat Immunol*. 2008;9(6):650–7.

145. Ghoreschi K, Laurence A, Yang XP, et al. Generation of pathogenic T(H)17 cells in the absence of TGF-beta signalling. *Nature*. 2010;467(7318):967–71.

146. Gutcher I, Donkor MK, Ma Q, Rudensky AY, Flavell RA, Li MO. Autocrine transforming growth factor-beta1 promotes in vivo Th17 cell differentiation. *Immunity*. 2011;34(3):396–408.

147. Borrow P. Innate immunity in acute HIV-1 infection. *Curr Opin HIV AIDS*. 2011;6(5):353–63.

148. Miller E, Bhardwaj N. Dendritic cell dysregulation during HIV-1 infection. *Immunol Rev*. 2013;254(1):170–89.

149. Li Q, Estes JD, Schlievert PM, et al. Glycerol monolaurate prevents mucosal SIV transmission. *Nature*. 2009;458(7241):1034–8.

150. Kadowaki N, Ho S, Antonenko S, et al. Subsets of human dendritic cell precursors express different toll-like receptors and respond to different microbial antigens. *J Exp Med*. 2001;194(6):863–9.

151. Beignon AS, McKenna K, Skoberne M, et al. Endocytosis of HIV-1 activates plasmacytoid dendritic cells via Toll-like receptor-viral RNA interactions. *J Clin Invest*. 2005;115(11):3265–75.

152. Yan N, Regalado-Magdos AD, Stiggelbout B, Lee-Kirsch MA, Lieberman J. The cytosolic exonuclease TREX1 inhibits the innate immune response to human immunodeficiency virus type 1. *Nat Immunol*. 2010;11(11):1005–13.

153. Solis M, Nakhaei P, Jalalirad M, et al. RIG-I-mediated antiviral signaling is inhibited in HIV-1 infection by a protease-mediated sequestration of RIG-I. *J Virol*. 2011;85(3):1224–36.

154. Doehle BP, Chang K, Rustagi A, McNevin J, McElrath MJ, Gale M. Vpu mediates depletion of interferon regulatory factor 3 during HIV infection by a lysosome-dependent mechanism. *J Virol*. 2012;86(16):8367–74.

155. Cocchi F, DeVico AL, Garzino-Demo A, Arya SK, Gallo RC, RANTES LPI. MIP-1 alpha, and MIP-1 beta as the major HIV-suppressive factors produced by CD8+ T cells. *Science*. 1995;270(5243):1811–5.

156. Florentin J, Aouar B, Dental C, et al. HCV glycoprotein E2 is a novel BDCA-2 ligand and acts as an inhibitor of IFN production by plasmacytoid dendritic cells. *Blood*. 2012;120(23):4544–51.

157. Mitchell JL, Takata H, Muir R, et al. Plasmacytoid dendritic cells sense HIV replication before detectable viremia following treatment interruption. *J Clin Invest*. 2020;130(6):2845-2858.

158. Geijtenbeek TB, Kwon DS, Torensma R, et al. DC-SIGN, a dendritic cell-specific HIV-1-binding protein that enhances trans-infection of T cells. *Cell*. 2000;100(5):587–97.

159. de Witte L, Nabatov A, Pion M, et al. Langerin is a natural barrier to HIV-1 transmission by Langerhans cells. *Nat Med*. 2007;13(3):367–71.

160. Dinter J, Duong E, Lai NY, et al. Variable processing and cross-presentation of HIV by dendritic cells and macrophages shapes CTL immunodominance and immune escape. *PLoS Pathog*. 2015;11(3):e1004725.

161. Coulon PG, Richetta C, Rouers A, et al. HIV-Infected Dendritic Cells Present Endogenous MHC Class II-Restricted Antigens to HIV-Specific CD4+ T Cells. *J Immunol*. 2016;197(2):517–32.

162. Sabado RL, O'Brien M, Subedi A, et al. Evidence of dysregulation of dendritic cells in primary HIV infection. *Blood*. 2010;116(19):3839–52.

163. Chehimi J, Campbell DE, Azzoni L, et al. Persistent decreases in blood plasmacytoid dendritic cell number and function despite effective highly active antiretroviral therapy and increased blood myeloid dendritic cells in HIV-infected individuals. *J Immunol*. 2002;168(9):4796–801.

164. Barron MA, Blyveis N, Palmer BE, MaWhinney S, Wilson CC. Influence of plasma viremia on defects in number and immunophenotype of blood dendritic cell subsets in human immunodeficiency virus 1-infected individuals. *J Infect Dis*. 2003;187(1):26–37.

165. Frleta D, Ochoa CE, Kramer HB, et al. HIV-1 infection-induced apoptotic microparticles inhibit human DCs via CD44. *J Clin Invest*. 2012;122(12):4685–97.

166. Donaghy H, Gazzard B, Gotch F, Patterson S. Dysfunction and infection of freshly isolated blood myeloid and plasmacytoid dendritic cells in patients infected with HIV-1. *Blood*. 2003;101(11):4505–11.

167. Fonteneau JF, Larsson M, Beignon AS, et al. Human immunodeficiency virus type 1 activates plasmacytoid dendritic cells and concomitantly induces the bystander maturation of myeloid dendritic cells. *J Virol*. 2004;78(10):5223–32.

168. Baxter AE, Russell RA, Duncan CJ, et al. Macrophage infection via selective capture of HIV-1-infected CD4+ T cells. *Cell Host Microbe*. 2014;16(6):711–21.

169. Cashin K, Roche M, Sterjovski J, et al. Alternative coreceptor requirements for efficient CCR5- and CXCR4-mediated HIV-1 entry into macrophages. *J Virol*. 2011;85(20):10699–709.

170. Groot F, Welsch S, Sattentau QJ. Efficient HIV-1 transmission from macrophages to T cells across transient virological synapses. *Blood*. 2008;111(9):4660–3.

171. Shen R, Richter HE, Clements RH, et al. Macrophages in vaginal but not intestinal mucosa are monocyte-like and permissive to human immunodeficiency virus type 1 infection. *J Virol*. 2009;83(7):3258–67.

172. Ochsenbauer C, Edmonds TG, Ding H, et al. Generation of transmitted/founder HIV-1 infectious molecular clones and characterization of their replication capacity in CD4 T lymphocytes and monocyte-derived macrophages. *J Virol*. 2012;86(5):2715–28.

173. Davies LC, Taylor PR. Tissue-resident macrophages: then and now. *Immunology*. 2015;144(4):541–8.

174. Barton K, Winckelmann A, Palmer S. HIV-1 reservoirs during suppressive therapy. *Trends Microbiol*. 2016;24(5):345–55.

175. Igarashi T, Brown CR, Endo Y, et al. Macrophage are the principal reservoir and sustain high virus loads in rhesus macaques after the depletion of CD4+ T cells by a highly pathogenic simian immunodeficiency virus/HIV type 1 chimera (SHIV): Implications for HIV-1 infections of humans. *Proc Natl Acad Sci USA*. 2001;98(2):658–63.

176. Kramer HB, Lavender KJ, Qin L, et al. Elevation of intact and proteolytic fragments of acute phase proteins constitutes the earliest systemic antiviral response in HIV-1 infection. *PLoS Pathog*. 2010;6(5):e1000893.

177. Muema DM, Akilimali NA, Ndumnego OC, et al. Association between the cytokine storm, immune cell dynamics, and viral replicative capacity in hyperacute HIV infection. *BMC Med*. 2020;18(1):81.

178. Blackwell SE, Krieg AM. CpG-A-induced monocyte IFN-gamma-inducible protein-10 production is regulated by plasmacytoid dendritic cell-derived IFN-alpha. *J Immunol*. 2003;170(8):4061–8.

179. Schroder K, Hertzog PJ, Ravasi T, Hume DA. Interferon-gamma: an overview of signals, mechanisms and functions. *J Leukoc Biol*. 2004;75(2):163–89.

180. Biancotto A, Grivel JC, Iglehart SJ, et al. Abnormal activation and cytokine spectra in lymph nodes of people chronically infected with HIV-1. *Blood*. 2007;109(10):4272–9.

181. Osuji FN, Onyenekwe CC, Ahaneku JE, Ukibe NR. The effects of highly active antiretroviral therapy on the serum levels of pro-inflammatory and anti-inflammatory cytokines in HIV infected subjects. *J Biomed Sci*. 2018;25(1):88.

182. Jacquelin B, Mayau V, Targat B, et al. Nonpathogenic SIV infection of African green monkeys induces a strong but rapidly controlled type I IFN response. *J Clin Invest*. 2009;119(12):3544–55.

183. Bosinger SE, Li Q, Gordon SN, et al. Global genomic analysis reveals rapid control of a robust innate response in SIV-infected sooty mangabeys. *J Clin Invest*. 2009;119(12):3556–72.

184. Barouch DH, Ghneim K, Bosche WJ, et al. Rapid inflammasome activation following mucosal SIV infection of rhesus monkeys. *Cell*. 2016;165(3):656–67.

185. Sandler NG, Bosinger SE, Estes JD, et al. Type I interferon responses in rhesus macaques prevent SIV infection and slow disease progression. *Nature*. 2014;511(7511):601–5.

186. Mangeat B, Turelli P, Caron G, Friedli M, Perrin L, Trono D. Broad antiretroviral defence by human APOBEC3G through lethal editing of nascent reverse transcripts. *Nature*. 2003;424(6944):99–103.

187. Chen K, Huang J, Zhang C, et al. Alpha interferon potently enhances the anti-human immunodeficiency virus type 1 activity of APOBEC3G in resting primary CD4 T cells. *J Virol*. 2006;80(15):7645–57.

188. Sakuma R, Mael AA, Ikeda Y. Alpha interferon enhances TRIM5alpha-mediated antiviral activities in human and rhesus monkey cells. *J Virol*. 2007;81(18):10201–6.

189. Jimenez-Guardeño JM, Apolonia L, Betancor G, Malim MH. Immunoproteasome activation enables human TRIM5α restriction of HIV-1. *Nat Microbiol*. 2019;4(6):933–40.

190. Kane M, Yadav SS, Bitzegeio J, et al. MX2 is an interferon-induced inhibitor of HIV-1 infection. *Nature*. 2013;502(7472):563–6.

191. Pincetic A, Kuang Z, Seo EJ, Leis J. The interferon-induced gene ISG15 blocks retrovirus release from cells late in the budding process. *J Virol*. 2010;84(9):4725–36.

192. Lu J, Pan Q, Rong L, He W, Liu SL, Liang C. The IFITM proteins inhibit HIV-1 infection. *J Virol*. 2011;85(5):2126–37.

193. Neil SJ, Zang T, Bieniasz PD. Tetherin inhibits retrovirus release and is antagonized by HIV-1 Vpu. *Nature*. 2008;451(7177):425–30.

194. Utay NS, Douek DC. Interferons and HIV Infection: The Good, the bad, and the ugly. *Pathog Immun*. 2016;1(1):107–16.

195. Le Saout C, Hasley RB, Imamichi H, et al. Chronic exposure to type-I IFN under lymphopenic conditions alters CD4 T cell homeostasis. *PLoS Pathog*. 2014;10(3):e1003976.

196. Skillman DR, Malone JL, Decker CF, et al. Phase I trial of interferon alfa-n3 in early-stage human immunodeficiency virus type 1 disease: evidence for drug safety, tolerance, and antiviral activity. *J Infect Dis*. 1996;173(5):1107–14.

197. Tavel JA, Huang CY, Shen J, et al. Interferon-alpha produces significant decreases in HIV load. *J Interferon Cytokine Res*. 2010;30(7):461–4.

198. Haas DW, Lavelle J, Nadler JP, et al. A randomized trial of interferon alpha therapy for HIV type 1 infection. *AIDS Res Hum Retroviruses*. 2000;16(3):183–90.

199. Krown SE. AIDS-associated Kaposi's sarcoma: is there still a role for interferon alfa? *Cytokine Growth Factor Rev*. 2007;18(5-6):395–402.

200. Lederer S, Favre D, Walters KA, et al. Transcriptional profiling in pathogenic and non-pathogenic SIV infections reveals significant distinctions in kinetics and tissue compartmentalization. *PLoS Pathog*. 2009;5(2):e1000296.

201. Fraietta JA, Mueller YM, Yang G, et al. Type I interferon upregulates Bak and contributes to T cell loss during human immunodeficiency virus (HIV) infection. *PLoS Pathog*. 2013;9(10):e1003658.

202. Hardy GA, Sieg S, Rodriguez B, et al. Interferon-alpha is the primary plasma type-I IFN in HIV-1 infection and correlates with immune activation and disease markers. *PLoS ONE*. 2013;8(2):e56527.

203. Meier A, Chang JJ, Chan ES, et al. Sex differences in the Toll-like receptor-mediated response of plasmacytoid dendritic cells to HIV-1. *Nat Med*. 2009;15(8):955–9.

204. Evans JS, Nims T, Cooley J, et al. Serum levels of virus burden in early-stage human immunodeficiency virus type 1 disease in women. *J Infect Dis*. 1997;175(4):795–800.

205. Farzadegan H, Hoover DR, Astemborski J, et al. Sex differences in HIV-1 viral load and progression to AIDS. *Lancet*. 1998;352(9139):1510–4.

206. Massanella M, Tural C, Papagno L, et al. Changes in T cell subsets in HIV-HCV-coinfected patients during pegylated interferon-alpha2a plus ribavirin treatment. *Antivir Ther*. 2010;15(3):333–42.

207. Zhen A, Rezek V, Youn C, et al. Targeting type I interferon-mediated activation restores immune function in chronic HIV infection. *J Clin Invest*. 2017;127(1):260–8.

208. Nganou-Makamdop K, Billingsley JM, Yaffe Z, et al. Type I IFN signaling blockade by a PASylated antagonist during chronic SIV infection suppresses specific inflammatory pathways but does not alter T cell activation or virus replication. *PLoS Pathog*. 2018;14(8):e1007246.

209. Tomaras GD, Haynes BF. HIV-1-specific antibody responses during acute and chronic HIV-1 infection. *Curr Opin HIV AIDS*. 2009;4(5):373–9.

210. Wei X, Decker JM, Wang S, et al. Antibody neutralization and escape by HIV-1. *Nature*. 2003;422(6929):307–12.

211. Mikell I, Sather DN, Kalams SA, Altfeld M, Alter G, Stamatatos L. Characteristics of the earliest cross-neutralizing antibody response to HIV-1. *PLoS Pathog*. 2011;7(1):e1001251.

212. Moir S, Fauci AS. B cell exhaustion in HIV infection: the role of immune activation. *Curr Opin HIV AIDS*. 2014;9(5):472–7.

213. McMichael AJ, Borrow P, Tomaras GD, Goonetilleke N, Haynes BF. The immune response during acute HIV-1 infection: clues for vaccine development. *Nat Rev Immunol*. 2010;10(1):11–23.

214. Levy JA. Discovery of another anti-HIV protein in the search for the CD8+ cell anti-HIV Factor. *Proc Natl Acad Sci USA*. 2015;112(26):7888–9.

215. Matano T, Shibata R, Siemon C, Connors M, Lane HC, Martin MA. Administration of an anti-CD8 monoclonal antibody interferes with the clearance of chimeric simian/human immunodeficiency virus during primary infections of rhesus macaques. *J Virol*. 1998;72(1):164–9.

216. Borrow P, Lewicki H, Wei X, et al. Antiviral pressure exerted by HIV-1-specific cytotoxic T lymphocytes (CTLs) during primary infection demonstrated by rapid selection of CTL escape virus. *Nat Med*. 1997;3(2):205–11.

217. Shankar P, Russo M, Harnisch B, Patterson M, Skolnik P, Lieberman J. Impaired function of circulating HIV-specific CD8+ T cells in chronic human immunodeficiency virus infection. *Blood*. 2000;96(9):3094–101.

218. Jin X, Bauer DE, Tuttleton SE, et al. Dramatic rise in plasma viremia after CD8(+) T cell depletion in simian immunodeficiency virus-infected macaques. *J Exp Med*. 1999;189(6):991–8.

219. Schieffer M, Jessen HK, Oster AF, et al. Induction of Gag-specific CD4 T cell responses during acute HIV infection is associated with improved viral control. *J Virol*. 2014;88(13):7357–66.

220. Rosenberg ES, Billingsley JM, Caliendo AM, et al. Vigorous HIV-1-specific CD4+ T cell responses associated with control of viremia. *Science*. 1997;278(5342):1447–50.

221. Douek DC, Brenchley JM, Betts MR, et al. HIV preferentially infects HIV-specific CD4+ T cells. *Nature*. 2002;417(6884):95–8.

222. Chevalier MF, Weiss L. The split personality of regulatory T cells in HIV infection. *Blood*. 2013;121(1):29–37.

223. Pion M, Jaramillo-Ruiz D, Martínez A, Muñoz-Fernández MA, Correa-Rocha R. HIV infection of human regulatory T cells downregulates FOXP3 expression by increasing DNMT3b levels and DNA methylation in the FOXP3 gene. *AIDS*. 2013;27(13):2019–29.

224. Simonetta F, Lecuroux C, Girault I, et al. Early and long-lasting alteration of effector CD45RA-FOXP3high regulatory T cell homeostasis during HIV infection. *J Infect Dis*. 2012;205(10):1510–9.

225. Angin M, Kwon DS, Streeck H, et al. Preserved function of regulatory T cells in chronic HIV-1 infection despite decreased numbers in blood and tissue. *J Infect Dis*. 2012;205(10):1495–500.

226. Eggena MP, Barugahare B, Jones N, et al. Depletion of regulatory T cells in HIV infection is associated with immune activation. *J Immunol*. 2005;174(7):4407–14.

227. Ndhlovu LC, Loo CP, Spotts G, Nixon DF, Hecht FM. FOXP3 expressing CD127lo CD4+ T cells inversely correlate with CD38+ CD8+ T cell activation levels in primary HIV-1 infection. *J Leukoc Biol*. 2008;83(2):254–62.

228. Rallón NI, López M, Soriano V, et al. Level, phenotype and activation status of CD4+FOXP3+ regulatory T cells in patients chronically infected with human immunodeficiency virus and/or hepatitis C virus. *Clin Exp Immunol*. 2009;155(1):35–43.

229. Bi X, Suzuki Y, Gatanaga H, Oka S. High frequency and proliferation of CD4+ FOXP3+ Treg in HIV-1-infected patients with low CD4 counts. *Eur J Immunol*. 2009;39(1):301–9.

230. Shaw JM, Hunt PW, Critchfield JW, et al. Increased frequency of regulatory T cells accompanies increased immune activation in rectal mucosae of HIV-positive noncontrollers. *J Virol*. 2011;85(21):11422–34.

231. Epple HJ, Loddenkemper C, Kunkel D, et al. Mucosal but not peripheral FOXP3+ regulatory T cells are highly increased in untreated HIV infection and normalize after suppressive HAART. *Blood*. 2006;108(9):3072–8.

232. Brenchley JM, Paiardini M, Knox KS, et al. Differential Th17 CD4 T cell depletion in pathogenic and nonpathogenic lentiviral infections. *Blood*. 2008;112(7):2826–35.

233. Estes JD, Li Q, Reynolds MR, et al. Premature induction of an immunosuppressive regulatory T cell response during acute simian immunodeficiency virus infection. *J Infect Dis*. 2006;193(5):703–12.

234. Caruso MP, Falivene J, Holgado MP, et al. Impact of HIV-ART on the restoration of Th17 and Treg cells in blood and female genital mucosa. *Sci Rep*. 2019;9(1):1978.

235. Kmieciak M, Gowda M, Graham L, et al. Human T cells express CD25 and FOXP3 upon activation and exhibit effector/memory phenotypes without any regulatory/suppressor function. *J Transl Med*. 2009;7(89).

236. Kinter AL, Hennessey M, Bell A, et al. CD25+CD4+ regulatory T cells from the peripheral blood of asymptomatic HIV-infected individuals regulate CD4+ and CD8+ HIV-specific T cell immune responses in vitro and are associated with favorable clinical markers of disease status. *J Exp Med*. 2004;200(3):331–43.

237. Gaardbo JC, Ronit A, Hartling HJ, et al. Immunoregulatory T cells may be involved in preserving CD4 T cell counts in HIV-infected long-term nonprogressors and controllers. *J Acquir Immune Defic Syndr*. 2014;65(1):10–8.

238. Kornfeld C, Ploquin MJ, Pandrea I, et al. Antiinflammatory profiles during primary SIV infection in African green monkeys are associated with protection against AIDS. *J Clin Invest*. 2005;115(4):1082–91.

239. Kinter A, McNally J, Riggin L, Jackson R, Roby G, Fauci AS. Suppression of HIV-specific T cell activity by lymph node CD25+ regulatory T cells from HIV-infected individuals. *Proc Natl Acad Sci USA*. 2007;104(9):3390–5.

240. Kinter AL, Horak R, Sion M, et al. CD25+ regulatory T cells isolated from HIV-infected individuals suppress the cytolytic and nonlytic antiviral activity of HIV-specific CD8+ T cells in vitro. *AIDS Res Hum Retroviruses*. 2007;23(3):438–50.

241. Manches O, Munn D, Fallahi A, et al. HIV-activated human plasmacytoid DCs induce Tregs through an indoleamine 2,3-dioxygenase-dependent mechanism. *J Clin Invest*. 2008;118(10):3431–9.

242. Cecchinato V, Trindade CJ, Laurence A, et al. Altered balance between Th17 and Th1 cells at mucosal sites predicts AIDS progression in simian immunodeficiency virus-infected macaques. *Mucosal Immunol*. 2008;1(4):279–88.

243. Sun H, Kim D, Li X, et al. Th1/17 Polarization of CD4 T Cells Supports HIV-1 Persistence during Antiretroviral Therapy. *J Virol*. 2015;89(22):11284–93.

244. Klatt NR, Brenchley JM. Th17 cell dynamics in HIV infection. *Curr Opin HIV AIDS*. 2010;5(2):135–40.

245. Alvarez Y, Tuen M, Shen G, et al. Preferential HIV infection of CCR6+ Th17 cells is associated with higher levels of virus receptor expression and lack of CCR5 ligands. *J Virol*. 2013;87(19):10843–54.

246. El Hed A, Khaitan A, Kozhaya L, et al. Susceptibility of human Th17 cells to human immunodeficiency virus and their perturbation during infection. *J Infect Dis*. 2010;201(6):843–54.

247. Christensen-Quick A, Lafferty M, Sun L, Marchionni L, DeVico A, Garzino-Demo A. Human Th17 Cells Lack HIV-Inhibitory RNases and Are Highly Permissive to Productive HIV Infection. *J Virol*. 2016;90(17):7833–47.

248. Seeger P, Musso T, Sozzani S. The TGF-β superfamily in dendritic cell biology. *Cytokine Growth Factor Rev*. 2015;26(6):647–57.

249. Anzano MA, Roberts AB, Meyers CA, et al. Synergistic interaction of two classes of transforming growth factors from murine sarcoma cells. *Cancer Res*. 1982;42(11):4776–8.

250. Grafe I, Alexander S, Peterson J, et al. TGF-β Family Signaling in Mesenchymal Differentiation. *Cold Spring Harb Perspect Biol*. 2018;10(5).

251. Kahata K, Dadras MS, Moustakas A. TGF-β Family Signaling in Epithelial Differentiation and Epithelial-Mesenchymal Transition. *Cold Spring Harb Perspect Biol*. 2018;10(1):a022194.

252. Meyers EA, Kessler JA. TGF-β Family Signaling in Neural and Neuronal Differentiation, Development, and Function. *Cold Spring Harb Perspect Biol*. 2017;9(8):a022244.

253. Okado T, Terada Y, Tanaka H, Inoshita S, Nakao A, Sasaki S. SMAD7 mediates transforming growth factor-beta-induced apoptosis in mesangial cells. *Kidney Int*. 2002;62(4):1178–86.

254. Sanjabi S, Oh SA, Li MO. Regulation of the Immune Response by TGF-β: From Conception to Autoimmunity and Infection. *Cold Spring Harb Perspect Biol*. 2017;9(6):a022236.

255. Thompson HG, Mih JD, Krasieva TB, Tromberg BJ, George SC. Epithelial-derived TGF-beta2 modulates basal and wound-healing subepithelial matrix homeostasis. *Am J Physiol Lung Cell Mol Physiol*. 2006;291(6):L1277-85.

256. Li MO, Flavell RA. TGF-beta: a master of all T cell trades. *Cell*. 2008;134(3):392–404.

257. Oh SA, Li MO. TGF-β: guardian of T cell function. *J Immunol*. 2013;191(8):3973–9.

258. Kondaiah P, Sands MJ, Smith JM, et al. Identification of a novel transforming growth factor-beta (TGF-beta 5) mRNA in Xenopus laevis. *J Biol Chem*. 1990;265(2):1089–93.

259. Jakowlew SB, Dillard PJ, Sporn MB, Roberts AB. Complementary deoxyribonucleic acid cloning of an mRNA encoding transforming growth factor-beta 2 from chicken embryo chondrocytes. *Growth Factors*. 1990;2(2-3):123–33.

260. Halper J, Burt DW, Romanov MN. On reassessment of the chicken TGFB4 gene as TGFB1. *Growth Factors*. 2004;22(2):121–2.

261. Flanders KC, Yang YA, Herrmann M, et al. Quantitation of TGF-β proteins in mouse tissues shows reciprocal changes in TGF-β1 and TGF-β3 in normal vs neoplastic mammary epithelium. *Oncotarget*. 2016;7(25):38164–79.

262. Ask K, Bonniaud P, Maass K, et al. Progressive pulmonary fibrosis is mediated by TGF-beta isoform 1 but not TGF-beta3. *Int J Biochem Cell Biol*. 2008;40(3):484–95.

263. Gato A, Martinez ML, Tudela C, et al. TGF-beta-3-induced chondroitin sulphate proteoglycan mediates palatal shelf adhesion. *Dev Biol*. 2002;250(2):393–405.

264. Cheifetz S, Weatherbee JA, Tsang ML, et al. The transforming growth factor-beta system, a complex pattern of cross-reactive ligands and receptors. *Cell*. 1987;48(3):409–15.

265. Ogawa Y, Schmidt DK, Dasch JR, Chang RJ, Glaser CB. Purification and characterization of transforming growth factor-beta 2.3 and -beta 1.2 heterodimers from bovine bone. *J Biol Chem*. 1992;267(4):2325–8.

266. Ling N, Ying SY, Ueno N, et al. Pituitary FSH is released by a heterodimer of the beta-subunits from the two forms of inhibin. *Nature*. 1986;321(6072):779–82.

267. Tuuri T, Erämaa M, Hildén K, Ritvos O. The tissue distribution of activin beta A- and beta B-subunit and follistatin messenger ribonucleic acids suggests multiple sites of action for the activin-follistatin system during human development. *J Clin Endocrinol Metab*. 1994;78(6):1521–4.

268. Namwanje M, Brown CW. Activins and inhibins: roles in development, physiology, and disease. *Cold Spring Harb Perspect Biol*. 2016;8(7):a021881.

269. Thompson TB, Cook RW, Chapman SC, Jardetzky TS, Woodruff TK. Beta A versus beta B: is it merely a matter of expression. *Mol Cell Endocrinol*. 2004;225(1-2):9–17.

270. Matzuk MM, Kumar TR, Vassalli A, et al. Functional analysis of activins during mammalian development. *Nature*. 1995;374(6520):354–6.

271. Vassalli A, Matzuk MM, Gardner HA, Lee KF, Jaenisch R. Activin/inhibin beta B subunit gene disruption leads to defects in eyelid development and female reproduction. *Genes Dev*. 1994;8(4):414–27.

272. Ludlow H, Phillips DJ, Myers M, et al. A new “total” activin B enzyme-linked immunosorbent assay (ELISA): development and validation for human samples. *Clin Endocrinol (Oxf)*. 2009;71(6):867–73.

273. Wang EA, Rosen V, Cordes P, et al. Purification and characterization of other distinct bone-inducing factors. *Proc Natl Acad Sci USA*. 1988;85(24):9484–8.

274. Bragdon B, Moseychuk O, Saldanha S, King D, Julian J, Nohe A. Bone morphogenetic proteins: a critical review. *Cell Signal*. 2011;23(4):609–20.

275. Little SC, Mullins MC. Bone morphogenetic protein heterodimers assemble heteromeric type I receptor complexes to pattern the dorsoventral axis. *Nat Cell Biol*. 2009;11(5):637–43.

276. Wozney JM. The bone morphogenetic protein family and osteogenesis. *Mol Reprod Dev*. 1992;32(2):160–7.

277. Harrison CA, Al-Musawi SL, Walton KL. Prodomains regulate the synthesis, extracellular localisation and activity of TGF-β superfamily ligands. *Growth Factors*. 2011;29(5):174–86.

278. Derynck R, Budi EH. Specificity, versatility, and control of TGF-β family signaling. *Sci Signal*. 2019;12(570):eaav5183.

279. Robertson IB, Horiguchi M, Zilberberg L, Dabovic B, Hadjiolova K, Rifkin DB. Latent TGF-β-binding proteins. *Matrix Biol*. 2015;47:44–53.

280. Miyazono K, Olofsson A, Colosetti P, Heldin CH. A role of the latent TGF-beta 1-binding protein in the assembly and secretion of TGF-beta 1. *EMBO J*. 1991;10(5):1091–101.

281. Robertson IB, Rifkin DB. Regulation of the Bioavailability of TGF-β and TGF-β-Related Proteins. *Cold Spring Harb Perspect Biol*. 2016;8(6):a021907.

282. Crawford SE, Stellmach V, Murphy-Ullrich JE, et al. Thrombospondin-1 is a major activator of TGF-beta1 in vivo. *Cell*. 1998;93(7):1159–70.

283. Kobayashi T, Kim H, Liu X, et al. Matrix metalloproteinase-9 activates TGF-β and stimulates fibroblast contraction of collagen gels. *Am J Physiol Lung Cell Mol Physiol*. 2014;306(11):L1006-15.

284. Amarnath S, Dong L, Li J, Wu Y, Chen W. Endogenous TGF-beta activation by reactive oxygen species is key to FOXP3 induction in TCR-stimulated and HIV-1-infected human CD4+CD25- T cells. *Retrovirology*. 2007;4(57).

285. Worthington JJ, Klementowicz JE, Travis MA. TGFβ: a sleeping giant awoken by integrins. *Trends Biochem Sci*. 2011;36(1):47–54.

286. Dong X, Zhao B, Iacob RE, et al. Force interacts with macromolecular structure in activation of TGF-β. *Nature*. 2017;542(7639):55–9.

287. Mu D, Cambier S, Fjellbirkeland L, et al. The integrin alpha(v)beta8 mediates epithelial homeostasis through MT1-MMP-dependent activation of TGF-beta1. *J Cell Biol*. 2002;157(3):493–507.

288. Weiss A, Attisano L. The TGFbeta superfamily signaling pathway. *Wiley Interdiscip Rev Dev Biol*. 2013;2(1):47–63.

289. Lawler S, Feng XH, Chen RH, et al. The type II transforming growth factor-beta receptor autophosphorylates not only on serine and threonine but also on tyrosine residues. *J Biol Chem*. 1997;272(23):14850–9.

290. Heldin CH, Moustakas A. Signaling Receptors for TGF-β Family Members. *Cold Spring Harb Perspect Biol*. 2016;8(8):a022053.

291. López-Casillas F, Wrana JL, Massagué J. Betaglycan presents ligand to the TGF beta signaling receptor. *Cell*. 1993;73(7):1435–44.

292. Lee NY, Kirkbride KC, Sheu RD, Blobe GC. The transforming growth factor-beta type III receptor mediates distinct subcellular trafficking and downstream signaling of activin-like kinase (ALK)3 and ALK6 receptors. *Mol Biol Cell*. 2009;20(20):4362–70.

293. Aykul S, Martinez-Hackert E. Transforming Growth Factor-β Family Ligands Can Function as Antagonists by Competing for Type II Receptor Binding. *J Biol Chem*. 2016;291(20):10792–804.

294. Gamer LW, Nove J, Levin M, Rosen V. BMP-3 is a novel inhibitor of both activin and BMP-4 signaling in Xenopus embryos. *Dev Biol*. 2005;285(1):156–68.

295. Melé M, Ferreira PG, Reverter F, et al. Human genomics. The human transcriptome across tissues and individuals. *Science*. 2015;348(6235):660–5.

296. Roelen BA, Rooijen MA, Mummery CL. Expression of ALK-1, a type 1 serine/threonine kinase receptor, coincides with sites of vasculogenesis and angiogenesis in early mouse development. *Dev Dyn*. 1997;209(4):418–30.

297. Bondestam J, Huotari MA, Morén A, et al. cDNA cloning, expression studies and chromosome mapping of human type I serine/threonine kinase receptor ALK7 (ACVR1C. *Cytogenet Cell Genet*. 2001;95(3-4):157–62.

298. Zhang YE. Non-SMAD pathways in TGF-beta signaling. *Cell Res*. 2009;19(1):128–39.

299. Martin-Malpartida P, Batet M, Kaczmarska Z, et al. Structural basis for genome wide recognition of 5-bp GC motifs by SMAD transcription factors. *Nat Commun*. 2017;8(1):2070.

300. Hill CS. Transcriptional Control by the SMADs. *Cold Spring Harb Perspect Biol*. 2016;8(10):a022079.

301. Miyazawa K, Miyazono K. Regulation of TGF-β family signaling by inhibitory Smads. *Cold Spring Harb Perspect Biol.* 2017;9(3):a022095.

302. Ma J, Sanchez-Duffhues G, Goumans MJ, Ten Dijke P. TGF-β-induced endothelial to mesenchymal transition in disease and tissue engineering. *Front Cell Dev Biol.* 2020;8:260.

303. Goumans MJ, Valdimarsdottir G, Itoh S, Rosendahl A, Sideras P, Dijke P. Balancing the activation state of the endothelium via two distinct TGF-beta type I receptors. *EMBO J*. 2002;21(7):1743–53.

304. Daly AC, Randall RA, Hill CS. Transforming growth factor beta-induced SMAD1/5 phosphorylation in epithelial cells is mediated by novel receptor complexes and is essential for anchorage-independent growth. *Mol Cell Biol*. 2008;28(22):6889–902.

305. Kamato D, Do BH, Osman N, et al. SMAD linker region phosphorylation is a signalling pathway in its own right and not only a modulator of canonical TGF-β signalling. *Cell Mol Life Sci*. 2020;77(2):243–51.

306. Wynn TA, Barron L. Macrophages: master regulators of inflammation and fibrosis. *Semin Liver Dis*. 2010;30(3):245–57.

307. Grotendorst GR, Smale G, Pencev D, et al. Production of transforming growth factor beta by human peripheral blood monocytes and neutrophils. *J Cell Physiol*. 1989;140(2):396–402.

308. Li J, Huang ZF, Xiong G, et al. Distribution, characterization, and induction of CD8+ regulatory T cells and IL-17-producing CD8+ T cells in nasopharyngeal carcinoma. *J Transl Med*. 2011;9(189).

309. Lee KM, Stott RT, Zhao G, et al. TGF-β-producing regulatory B cells induce regulatory T cells and promote transplantation tolerance. *Eur J Immunol*. 2014;44(6):1728–36.

310. Li MO, Sanjabi S, Flavell RA. Transforming growth factor-beta controls development, homeostasis, and tolerance of T cells by regulatory T cell-dependent and -independent mechanisms. *Immunity*. 2006;25(3):455–71.

311. Liu Y, Zhang P, Li J, Kulkarni AB, Perruche S, Chen W. A critical function for TGF-beta signaling in the development of natural CD4+CD25+Foxp3+ regulatory T cells. *Nat Immunol*. 2008;9(6):632–40.

312. Doisne JM, Bartholin L, Yan KP, et al. iNKT cell development is orchestrated by different branches of TGF-beta signaling. *J Exp Med*. 2009;206(6):1365–78.

313. Tamayo E, Alvarez P, Merino R. TGF-β superfamily members as regulators of B cell development and function-implications for autoimmunity. *Int J Mol Sci*. 2018;19(12):E3928.

314. Ouyang W, Oh SA, Ma Q, Bivona MR, Zhu J, Li MO. TGF-β cytokine signaling promotes CD8+ T cell development and low-affinity CD4+ T cell homeostasis by regulation of interleukin-7 receptor α expression. *Immunity*. 2013;39(2):335–46.

315. Bradley LM, Haynes L, Swain SL. IL-7: maintaining T cell memory and achieving homeostasis. *Trends Immunol*. 2005;26(3):172–6.

316. Johnson LD, Jameson SC. TGF-β sensitivity restrains CD8+ T cell homeostatic proliferation by enforcing sensitivity to IL-7 and IL-15. *PLoS ONE*. 2012;7(8):e42268.

317. Lucas PJ, Kim SJ, Melby SJ, Gress RE. Disruption of T cell homeostasis in mice expressing a T cell-specific dominant negative transforming growth factor beta II receptor. *J Exp Med*. 2000;191(7):1187–96.

318. Schmitt N, Liu Y, Bentebibel SE, et al. The cytokine TGF-β co-opts signaling via STAT3-STAT4 to promote the differentiation of human Tfh cells. *Nat Immunol*. 2014;15(9):856–65.

319. Kel JM, Girard-Madoux MJ, Reizis B, Clausen BE. TGF-beta is required to maintain the pool of immature Langerhans cells in the epidermis. *J Immunol*. 2010;185(6):3248–55.

320. Lin JT, Martin SL, Xia L, Gorham JD. TGF-beta 1 uses distinct mechanisms to inhibit IFN-gamma expression in CD4+ T cells at priming and at recall: differential involvement of STAT4 and T-bet. *J Immunol*. 2005;174(10):5950–8.

321. Gorelik L, Fields PE, Flavell RA. Cutting edge: TGF-beta inhibits Th type 2 development through inhibition of GATA-3 expression. *J Immunol*. 2000;165(9):4773–7.

322. Mani V, Bromley SK, Äijö T, et al. Migratory DCs activate TGF-β to precondition naïve CD8+ T cells for tissue-resident memory fate. *Science*. 2019;366(6462):eaav5728.

323. Chen CH, Seguin-Devaux C, Burke NA, et al. Transforming growth factor beta blocks Tec kinase phosphorylation, Ca2+ influx, and NFATc translocation causing inhibition of T cell differentiation. *J Exp Med*. 2003;197(12):1689–99.

324. Thomas DA, Massagué J. TGF-beta directly targets cytotoxic T cell functions during tumor evasion of immune surveillance. *Cancer Cell*. 2005;8(5):369–80.

325. Brabletz T, Pfeuffer I, Schorr E, Siebelt F, Wirth T, Serfling E. Transforming growth factor beta and cyclosporin A inhibit the inducible activity of the interleukin-2 gene in T cells through a noncanonical octamer-binding site. *Mol Cell Biol*. 1993;13(2):1155–62.

326. Dickson MC, Martin JS, Cousins FM, Kulkarni AB, Karlsson S, Akhurst RJ. Defective haematopoiesis and vasculogenesis in transforming growth factor-beta 1 knock out mice. *Development*. 1995;121(6):1845–54.

327. Christ M, McCartney-Francis NL, Kulkarni AB, et al. Immune dysregulation in TGF-beta 1-deficient mice. *J Immunol*. 1994;153(5):1936–46.

328. Letterio JJ, Geiser AG, Kulkarni AB, et al. Autoimmunity associated with TGF-beta1-deficiency in mice is dependent on MHC class II antigen expression. *J Clin Invest*. 1996;98(9):2109–19.

329. Kobayashi S, Yoshida K, Ward JM, et al. Beta 2-microglobulin-deficient background ameliorates lethal phenotype of the TGF-beta 1 null mouse. *J Immunol*. 1999;163(7):4013–9.

330. Marie JC, Liggitt D, Rudensky AY. Cellular mechanisms of fatal early-onset autoimmunity in mice with the T cell-specific targeting of transforming growth factor-beta receptor. *Immunity*. 2006;25(3):441–54.

331. Laouar Y, Sutterwala FS, Gorelik L, Flavell RA. Transforming growth factor-beta controls T helper type 1 cell development through regulation of natural killer cell interferon-gamma. *Nat Immunol*. 2005;6(6):600–7.

332. Castriconi R, Cantoni C, Della Chiesa M, et al. Transforming growth factor beta 1 inhibits expression of NKp30 and NKG2D receptors: consequences for the NK-mediated killing of dendritic cells. *Proc Natl Acad Sci USA*. 2003;100(7):4120–5.

333. Zhang F, Wang H, Wang X, et al. TGF-β induces M2-like macrophage polarization via SNAIL-mediated suppression of a pro-inflammatory phenotype. *Oncotarget*. 2016;7(32):52294–306.

334. Wiseman DM, Polverini PJ, Kamp DW, Leibovich SJ. Transforming growth factor-beta (TGF beta) is chemotactic for human monocytes and induces their expression of angiogenic activity. *Biochem Biophys Res Commun*. 1988;157(2):793–800.

335. Sato K, Kawasaki H, Nagayama H, et al. TGF-beta 1 reciprocally controls chemotaxis of human peripheral blood monocyte-derived dendritic cells via chemokine receptors. *J Immunol*. 2000;164(5):2285–95.

336. Han G, Li F, Singh TP, Wolf P, Wang XJ. The pro-inflammatory role of TGFβ1: a paradox. *Int J Biol Sci*. 2012;8(2):228–35.

337. Li AG, Wang D, Feng XH, Wang XJ. Latent TGFbeta1 overexpression in keratinocytes results in a severe psoriasis-like skin disorder. *EMBO J*. 2004;23(8):1770–81.

338. Wiercińska-Drapalo A, Flisiak R, Jaroszewicz J, Prokopowicz D. Increased plasma transforming growth factor-beta1 is associated with disease progression in HIV-1-infected patients. *Viral Immunol*. 2004;17(1):109–13.

339. Liovat AS, Rey-Cuillé MA, Lécuroux C, et al. Acute plasma biomarkers of T cell activation set-point levels and of disease progression in HIV-1 infection. *PLoS ONE*. 2012;7(10):e46143.

340. Ahmad R, Sindhu ST, Toma E, Morisset R, Ahmad A. Elevated levels of circulating interleukin-18 in human immunodeficiency virus-infected individuals: role of peripheral blood mononuclear cells and implications for AIDS pathogenesis. *J Virol*. 2002;76(24):12448–56.

341. Valdivia A, Ly J, Gonzalez L, et al. Restoring cytokine balance in HIV-positive individuals with low CD4 T cell counts. *AIDS Res Hum Retroviruses*. 2017;33(9):905–18.

342. Maina EK, Abana CZ, Bukusi EA, Sedegah M, Lartey M, Ampofo WK. Plasma concentrations of transforming growth factor beta 1 in non-progressive HIV-1 infection correlates with markers of disease progression. *Cytokine*. 2016;81:109–16.

343. Malherbe G, Steel HC, Cassol S, et al. Circulating biomarkers of immune activation distinguish viral suppression from nonsuppression in HAART-treated patients with advanced HIV-1 subtype C infection. *Mediators Inflamm*. 2014;2014(198413):198413.

344. Márquez M, Romero-Cores P, Montes-Oca M, et al. Immune activation response in chronic HIV-infected patients: influence of Hepatitis C virus coinfection. *PLoS ONE*. 2015;10(3):e0119568.

345. Morris D, Guerra C, Donohue C, Oh H, Khurasany M, Venketaraman V. Unveiling the mechanisms for decreased glutathione in individuals with HIV infection. *Clin Dev Immunol*. 2012;2012(734125).

346. Makhubele TG, Steel HC, Anderson R, Dyk G, Theron AJ, Rossouw TM. Systemic immune activation profiles of HIV-1 subtype C-infected children and their mothers. *Mediators Inflamm*. 2016;2016(9026573).

347. Cumont MC, Monceaux V, Viollet L, et al. TGF-beta in intestinal lymphoid organs contributes to the death of armed effector CD8 T cells and is associated with the absence of virus containment in rhesus macaques infected with the simian immunodeficiency virus. *Cell Death Differ*. 2007;14(10):1747–58.

348. Arakelyan A, Petersen JD, Blazkova J, Margolis L. Macrophage-derived HIV-1 carries bioactive TGF-beta. *Sci Rep*. 2019;9(1):19100.

349. Zeng M, Smith AJ, Wietgrefe SW, et al. Cumulative mechanisms of lymphoid tissue fibrosis and T cell depletion in HIV-1 and SIV infections. *J Clin Invest*. 2011;121(3):998–1008.

350. Estes JD, Reilly C, Trubey CM, et al. Antifibrotic therapy in simian immunodeficiency virus infection preserves CD4+ T cell populations and improves immune reconstitution with antiretroviral therapy. *J Infect Dis*. 2015;211(5):744–54.

351. Tinoco R, Alcalde V, Yang Y, Sauer K, Zuniga EI. Cell-intrinsic transforming growth factor-beta signaling mediates virus-specific CD8+ T cell deletion and viral persistence in vivo. *Immunity*. 2009;31(1):145–57.

352. Garba ML, Pilcher CD, Bingham AL, Eron J, Frelinger JA. HIV antigens can induce TGF-beta1-producing immunoregulatory CD8+ T cells. *J Immunol*. 2002;168(5):2247–54.

353. Jelicic K, Cimbro R, Nawaz F, et al. The HIV-1 envelope protein gp120 impairs B cell proliferation by inducing TGF-β1 production and FcRL4 expression. *Nat Immunol*. 2013;14(12):1256–65.

354. Kekow J, Wachsman W, McCutchan JA, et al. Transforming growth factor-beta and suppression of humoral immune responses in HIV infection. *J Clin Invest*. 1991;87(3):1010–6.

355. Sharkey DJ, Macpherson AM, Tremellen KP, Mottershead DG, Gilchrist RB, Robertson SA. TGF-β mediates proinflammatory seminal fluid signaling in human cervical epithelial cells. *J Immunol.* 2012;189(2):1024-35.

356. Robertson SA, Ingman WV, O'Leary S, Sharkey DJ, Tremellen KP. Transforming growth factor beta–a mediator of immune deviation in seminal plasma. *J Reprod Immunol*. 2002;57(1-2):109–28.

357. Yang HG, Jiao YM, Huang HH, et al. Transforming growth factor-β promotes the function of HIV-specific CXCR5+ CD8 T cells. *Microbiol Immunol*. 2020;64(6):458-468.

358. Leong YA, Chen Y, Ong HS, et al. CXCR5+ follicular cytotoxic T cells control viral infection in B cell follicles. *Nat Immunol*. 2016;17(10):1187–96.

359. Nakamura K, Kitani A, Fuss I, et al. TGF-beta 1 plays an important role in the mechanism of CD4+CD25+ regulatory T cell activity in both humans and mice. *J Immunol*. 2004;172(2):834–42.

360. Aleman-Muench GR, Soldevila G, et al. When versatility matters: activins/inhibins as key regulators of immunity. *Immunol Cell Biol*. 2012;90(2):137–48.

361. Morianos I, Papadopoulou G, Semitekolou M, Xanthou G. Activin A in the regulation of immunity in health and disease. *J Autoimmun*. 2019;104(102314):102314.

362. Phillips DJ, de Kretser DM, Hedger MP. Activin and related proteins in inflammation: not just interested bystanders. *Cytokine Growth Factor Rev*. 2009;20(2):153–64.

363. Eddowes LA, Al-Hourani K, Ramamurthy N, et al. Antiviral activity of bone morphogenetic proteins and activins. *Nat Microbiol*. 2019;4(2):339–51.

364. Reeves MB, Compton T. Inhibition of inflammatory interleukin-6 activity via extracellular signal-regulated kinase-mitogen-activated protein kinase signaling antagonizes human cytomegalovirus reactivation from dendritic cells. *J Virol*. 2011;85(23):12750–8.

365. Jones KL, Brauman JN, Groome NP, Kretser DM, Phillips DJ. Activin A release into the circulation is an early event in systemic inflammation and precedes the release of follistatin. *Endocrinology*. 2000;141(5):1905–8.

366. Harrington AE, Morris-Triggs SA, Ruotolo BT, Robinson CV, Ohnuma S, Hyvönen M. Structural basis for the inhibition of activin signalling by follistatin. *EMBO J*. 2006;25(5):1035–45.

367. Jones KL, Mansell A, Patella S, et al. Activin A is a critical component of the inflammatory response, and its binding protein, follistatin, reduces mortality in endotoxemia. *Proc Natl Acad Sci USA*. 2007;104(41):16239–44.

368. Wu H, Chen Y, Winnall WR, Phillips DJ, Hedger MP. Acute regulation of activin A and its binding protein, follistatin, in serum and tissues following lipopolysaccharide treatment of adult male mice. *Am J Physiol Regul Integr Comp Physiol*. 2012;303(6):R665-75.

369. Chen Y, Wu H, Winnall WR, et al. Tumour necrosis factor-α stimulates human neutrophils to release preformed activin A. *Immunol Cell Biol*. 2011;89(8):889–96.

370. Qi Y, Ge J, Ma C, Wu N, Cui X, Liu Z. Activin A regulates activation of mouse neutrophils by SMAD3 signalling. *Open Biol*. 2017;7(5):160342.

371. Salogni L, Musso T, Bosisio D, et al. Activin A induces dendritic cell migration through the polarized release of CXC chemokine ligands 12 and 14. *Blood*. 2009;113(23):5848–56.

372. Scutera S, Riboldi E, Daniele R, et al. Production and function of activin A in human dendritic cells. *Eur Cytokine Netw*. 2008;19(1):60–8.

373. Musso T, Scutera S, Vermi W, et al. Activin A induces Langerhans cell differentiation in vitro and in human skin explants. *PLoS ONE*. 2008;3(9):e3271.

374. Robson NC, Phillips DJ, McAlpine T, et al. Activin-A: a novel dendritic cell-derived cytokine that potently attenuates CD40 ligand-specific cytokine and chemokine production. *Blood*. 2008;111(5):2733–43.

375. Seeger P, Bosisio D, Parolini S, et al. Activin A as a mediator of NK-dendritic cell functional interactions. *J Immunol*. 2014;192(3):1241–8.

376. Robson NC, Wei H, McAlpine T, Kirkpatrick N, Cebon J, Maraskovsky E. Activin A attenuates several human natural killer cell functions. *Blood*. 2009;113(14):3218–25.

377. Rautela J, Dagley LF, Oliveira CC, et al. Therapeutic blockade of activin A improves NK cell function and antitumor immunity. *Sci Signal*. 2019;12(596):eaat7527.

378. Ebert S, Zeretzke M, Nau R, Michel U. Microglial cells and peritoneal macrophages release activin A upon stimulation with Toll-like receptor agonists. *Neurosci Lett*. 2007;413(3):241–4.

379. Sugama S, Takenouchi T, Kitani H, Fujita M, Hashimoto M. Activin as an anti-inflammatory cytokine produced by microglia. *J Neuroimmunol*. 2007;192(1-2):31–9.

380. Sugatani T, Alvarez UM, Hruska KA. Activin A stimulates IkappaB-alpha/NFkappaB and RANK expression for osteoclast differentiation, but not AKT survival pathway in osteoclast precursors. *J Cell Biochem*. 2003;90(1):59–67.

381. Ge J, Wang Y, Feng Y, et al. Direct effects of activin A on the activation of mouse macrophage RAW264.7 cells. *Cell Mol Immunol*. 2009;6(2):129–33.

382. Wang Y, Cui X, Tai G, et al. A critical role of activin A in maturation of mouse peritoneal macrophages in vitro and in vivo. *Cell Mol Immunol*. 2009;6(5):387–92.

383. Li N, Cui X, Ge J, et al. Activin A inhibits activities of lipopolysaccharide-activated macrophages via TLR4, not of TLR2. *Biochem Biophys Res Commun*. 2013;435(2):222–8.

384. Nüsing RM, Barsig J. Induction of prostanoid, nitric oxide, and cytokine formation in rat bone marrow derived macrophages by activin A. *Br J Pharmacol*. 1999;127(4):919–26.

385. Zhang XJ, Li Y, Tai GX, et al. Effects of activin A on the activities of the mouse peritoneal macrophages. *Cell Mol Immunol*. 2005;2(1):63–7.

386. Ohguchi M, Yamato K, Ishihara Y, et al. Activin A regulates the production of mature interleukin-1beta and interleukin-1 receptor antagonist in human monocytic cells. *J Interferon Cytokine Res*. 1998;18(7):491–8.

387. Zhou J, Tai G, Liu H, et al. Activin A down-regulates the phagocytosis of lipopolysaccharide-activated mouse peritoneal macrophages in vitro and in vivo. *Cell Immunol*. 2009;255(1-2):69–75.

388. Locci M, Wu JE, Arumemi F, et al. Activin A programs the differentiation of human Tfh cells. *Nat Immunol*. 2016;17(8):976–84.

389. Ogawa K, Funaba M, Chen Y, Tsujimoto M. Activin A functions as a Th2 cytokine in the promotion of the alternative activation of macrophages. *J Immunol*. 2006;177(10):6787–94.

390. Hardy CL, O'Connor AE, Yao J, et al. Follistatin is a candidate endogenous negative regulator of activin A in experimental allergic asthma. *Clin Exp Allergy*. 2006;36(7):941–50.

391. Karagiannidis C, Hense G, Martin C, et al. Activin A is an acute allergen-responsive cytokine and provides a link to TGF-beta-mediated airway remodeling in asthma. *J Allergy Clin Immunol*. 2006;117(1):111–8.

392. Hardy CL, Lemasurier JS, Olsson F, et al. Interleukin-13 regulates secretion of the tumor growth factor-beta superfamily cytokine activin A in allergic airway inflammation. *Am J Respir Cell Mol Biol*. 2010;42(6):667–75.

393. Semitekolou M, Alissafi T, Aggelakopoulou M, et al. Activin-A induces regulatory T cells that suppress T helper cell immune responses and protect from allergic airway disease. *J Exp Med*. 2009;206(8):1769–85.

394. Huber S, Stahl FR, Schrader J, et al. Activin a promotes the TGF-beta-induced conversion of CD4+CD25- T cells into FOXP3+ induced regulatory T cells. *J Immunol*. 2009;182(8):4633–40.

395. Aoki F, Kurabayashi M, Hasegawa Y, Kojima I. Attenuation of bleomycin-induced pulmonary fibrosis by follistatin. *Am J Respir Crit Care Med*. 2005;172(6):713–20.

396. Ogawa K, Funaba M, Tsujimoto M. A dual role of activin A in regulating immunoglobulin production of B cells. *J Leukoc Biol*. 2008;83(6):1451–8.

397. Lee HJ, Seo GY, Kim HA, Kim PH. Activin A stimulates IgA expression in mouse B cells. *Biochem Biophys Res Commun*. 2008;366(2):574–8.

398. Cejalvo T, Sacedón R, Hernández-López C, et al. Bone morphogenetic protein-2/4 signalling pathway components are expressed in the human thymus and inhibit early T cell development. *Immunology*. 2007;121(1):94–104.

399. Martínez VG, Sacedón R, Hidalgo L, et al. The BMP pathway participates in human naive CD4+ T cell activation and homeostasis. *PLoS ONE*. 2015;10(6):e0131453.

400. Lu L, Ma J, Wang X, et al. Synergistic effect of TGF-beta superfamily members on the induction of FOXP3+ Treg. *Eur J Immunol*. 2010;40(1):142–52.

401. Capucha T, Koren N, Nassar M, et al. Sequential BMP7/TGF-β1 signaling and microbiota instruct mucosal Langerhans cell differentiation. *J Exp Med*. 2018;215(2):481–500.

402. Yoshioka Y, Ono M, Osaki M, Konishi I, Sakaguchi S. Differential effects of inhibition of bone morphogenic protein (BMP) signalling on T cell activation and differentiation. *Eur J Immunol*. 2012;42(3):749–59.

403. Varas A, Valencia J, Lavocat F, et al. Blockade of bone morphogenetic protein signaling potentiates the pro-inflammatory phenotype induced by interleukin-17 and tumor necrosis factor-α combination in rheumatoid synoviocytes. *Arthritis Res Ther*. 2015;17(192).

404. Sivertsen EA, Huse K, Hystad ME, Kersten C, Smeland EB, Myklebust JH. Inhibitory effects and target genes of bone morphogenetic protein 6 in Jurkat TAg cells. *Eur J Immunol*. 2007;37(10):2937–48.

405. Huse K, Bakkebø M, Oksvold MP, et al. Bone morphogenetic proteins inhibit CD40L/IL-21-induced Ig production in human B cells: differential effects of BMP-6 and BMP-7. *Eur J Immunol*. 2011;41(11):3135–45.

406. Kersten C, Sivertsen EA, Hystad ME, Forfang L, Smeland EB, Myklebust JH. BMP-6 inhibits growth of mature human B cells; induction of SMAD phosphorylation and upregulation of Id1. *BMC Immunol*. 2005;6(9).

407. Gould SE, Day M, Jones SS, Dorai H. BMP-7 regulates chemokine, cytokine, and hemodynamic gene expression in proximal tubule cells. *Kidney Int*. 2002;61(1):51–60.

408. Hagen M, Fagan K, Steudel W, et al. Interaction of interleukin-6 and the BMP pathway in pulmonary smooth muscle. *Am J Physiol Lung Cell Mol Physiol*. 2007;292(6):L1473-9.

409. Lee MJ, Yang CW, Jin DC, Chang YS, Bang BK, Kim YS. Bone morphogenetic protein-7 inhibits constitutive and interleukin-1 beta-induced monocyte chemoattractant protein-1 expression in human mesangial cells: role for JNK/AP-1 pathway. *J Immunol*. 2003;170(5):2557–63.

410. Martínez VG, Hidalgo L, Valencia J, et al. Autocrine activation of canonical BMP signaling regulates PD-L1 and PD-L2 expression in human dendritic cells. *Eur J Immunol*. 2014;44(4):1031–8.

411. Robson NC, Hidalgo L, Mc Alpine T, et al. Optimal effector functions in human natural killer cells rely upon autocrine bone morphogenetic protein signaling. *Cancer Res*. 2014;74(18):5019–31.

412. Rowe IA, Galsinh SK, Wilson GK, et al. Paracrine signals from liver sinusoidal endothelium regulate hepatitis C virus replication. *Hepatology*. 2014;59(2):375–84.

413. Sakamoto N, Yoshimura M, Kimura T, et al. Bone morphogenetic protein-7 and interferon-alpha synergistically suppress hepatitis C virus replicon. *Biochem Biophys Res Commun*. 2007;357(2):467–73.

414. Liu SY, Sanchez DJ, Aliyari R, Lu S, Cheng G. Systematic identification of type I and type II interferon-induced antiviral factors. *Proc Natl Acad Sci USA*. 2012;109(11):4239–44.

415. Sanchez-Casanova S, Martin-Saavedra FM, Escudero-Duch C, et al. Local delivery of bone morphogenetic protein-2 from near infrared-responsive hydrogels for bone tissue regeneration. *Biomaterials*. 2020;241(119909).

416. Olsavszky V, Ulbrich F, Singh S, et al. GATA4 and LMO3 balance angiocrine signaling and autocrine inflammatory activation by BMP2 in liver sinusoidal endothelial cells. *Gene*. 2017;627:491–9.

417. Caldwell RL, Gadipatti R, Lane KB, Shepherd VL. HIV-1 Tat represses transcription of the bone morphogenic protein receptor-2 in U937 monocytic cells. *J Leukoc Biol*. 2006;79(1):192–201.

418. Liu Y, Sun R, Lin X, Liang D, Deng Q, Lan K. Kaposi's sarcoma-associated herpesvirus-encoded microRNA miR-K12-11 attenuates transforming growth factor beta signaling through suppression of SMAD5. *J Virol*. 2012;86(3):1372–81.

419. Durrington HJ, Upton PD, Hoer S, et al. Identification of a lysosomal pathway regulating degradation of the bone morphogenetic protein receptor type II. *J Biol Chem*. 2010;285(48):37641–9.

420. Xia L, Wang S, Zhang H, et al. The HBx and HBc of hepatitis B virus can influence Id1 and Id3 by reducing their transcription and stability. *Virus Res*. 2020;284(197973).

421. Tousa S, Semitekolou M, Morianos I, et al. Activin-A co-opts IRF4 and AhR signaling to induce human regulatory T cells that restrain asthmatic responses. *Proc Natl Acad Sci USA*. 2017;114(14):E2891-E2900.

422. Forero A, Moore PS, Sarkar SN. Role of IRF4 in IFN-stimulated gene induction and maintenance of Kaposi sarcoma-associated herpesvirus latency in primary effusion lymphoma cells. *J Immunol*. 2013;191(3):1476–85.

423. Xu P, Bailey-Bucktrout S, Xi Y, et al. Innate antiviral host defense attenuates TGF-β function through IRF3-mediated suppression of Smad signaling. *Mol Cell*. 2014;56(6):723–37.

424. Qing J, Liu C, Choy L, Wu RY, Pagano JS, Derynck R. Transforming growth factor beta/SMAD3 signaling regulates IRF-7 function and transcriptional activation of the beta interferon promoter. *Mol Cell Biol*. 2004;24(3):1411–25.

425. Cocolakis E, Dai M, Drevet L, et al. Smad signaling antagonizes STAT5-mediated gene transcription and mammary epithelial cell differentiation. *J Biol Chem*. 2008;283(3):1293–307.

426. Uddin S, Lekmine F, Sassano A, Rui H, Fish EN, Platanias LC. Role of STAT5 in type I interferon-signaling and transcriptional regulation. *Biochem Biophys Res Commun*. 2003;308(2):325–30.

427. Tsai MH, Pai LM, Lee CK. Fine-Tuning of Type I Interferon Response by STAT3. *Front Immunol*. 2019;10(1448).

428. Yoon JH, Sudo K, Kuroda M, et al. Phosphorylation status determines the opposing functions of SMAD2/SMAD3 as STAT3 cofactors in Th17 differentiation. *Nat Commun*. 2015;6(7600).

429. Johnson DE, O'Keefe RA, Grandis J, et al. Targeting the IL-6/JAK/STAT3 signalling axis in cancer. *Nat Rev Clin Oncol*. 2018;15(4):234–48.

430. Makino Y, Yoon JH, Bae E, et al. Repression of SMAD3 by STAT3 and c-Ski/SnoN induces gefitinib resistance in lung adenocarcinoma. *Biochem Biophys Res Commun*. 2017;484(2):269–77.

431. Starsíchová A, Lincová E, Pernicová Z, Kozubík A, Soucek K. TGF-beta1 suppresses IL-6-induced STAT3 activation through regulation of Jak2 expression in prostate epithelial cells. *Cell Signal*. 2010;22(11):1734–44.

432. Hertoghs N, Nijmeijer BM, Teijlingen NH, et al. Sexually transmitted founder HIV-1 viruses are relatively resistant to Langerhans cell-mediated restriction. *PLoS ONE*. 2019;14(12):e0226651.

433. Fairbanks VF, Tefferi A. Normal ranges for packed cell volume and hemoglobin concentration in adults: relevance to "apparent polycythemia." *Eur J Haematol*. 2000;65(5):285–96.

434. Matrosovich M, Matrosovich T, Garten W, Klenk HD. New low-viscosity overlay medium for viral plaque assays. *Virol J*. 2006;3(63).

435. Matrosovich M, Matrosovich T, Carr J, Roberts NA, Klenk HD. Overexpression of the alpha-2,6-sialyltransferase in MDCK cells increases influenza virus sensitivity to neuraminidase inhibitors. *J Virol*. 2003;77(15):8418–25.

436. Dobin A, Davis CA, Schlesinger F, et al. STAR: ultrafast universal RNA-seq aligner. *Bioinformatics*. 2013;29(1):15–21.

437. Robinson MD, McCarthy DJ, Smyth GK. edgeR: a Bioconductor package for differential expression analysis of digital gene expression data. *Bioinformatics*. 2010;26(1):139–40.

438. Livak KJ, Schmittgen TD. Analysis of relative gene expression data using real-time quantitative PCR and the 2(-Delta Delta C(T)) method. *Methods*. 2001;25(4):402–8.

439. Penna I, Vella S, Gigoni A, Russo C, Cancedda R, Pagano A. Selection of candidate housekeeping genes for normalization in human postmortem brain samples. *Int J Mol Sci*. 2011;12(9):5461–70.

440. Armitage AE, Stacey AR, Giannoulatou E, et al. Distinct patterns of hepcidin and iron regulation during HIV-1, HBV, and HCV infections. *Proc Natl Acad Sci USA*. 2014;111(33):12187–92.

441. Roberts L, Passmore JA, Williamson C, et al. Plasma cytokine levels during acute HIV-1 infection predict HIV disease progression. *AIDS*. 2010;24(6):819–31.

442. Vingert B, Benati D, Lambotte O, et al. HIV controllers maintain a population of highly efficient Th1 effector cells in contrast to patients treated in the long term. *J Virol*. 2012;86(19):10661–74.

443. Lugli E, Goldman CK, Perera LP, et al. Transient and persistent effects of IL-15 on lymphocyte homeostasis in nonhuman primates. *Blood*. 2010;116(17):3238–48.

444. Hasan MS, Kallas EG, Thomas EK, Looney J, Campbell M, Evans TG. Effects of interleukin-15 on in vitro human T cell proliferation and activation. *J Interferon Cytokine Res*. 2000;20(2):119–23.

445. Monsuez JJ, Escaut L, Teicher E, Charniot JC, Vittecoq D. Cytokines in HIV-associated cardiomyopathy. *Int J Cardiol*. 2007;120(2):150–7.

446. Sevigny JJ, Albert SM, McDermott MP, et al. Evaluation of HIV RNA and markers of immune activation as predictors of HIV-associated dementia. *Neurology*. 2004;63(11):2084–90.

447. Ross MJ, Fan C, Ross MD, et al. HIV-1 infection initiates an inflammatory cascade in human renal tubular epithelial cells. *J Acquir Immune Defic Syndr*. 2006;42(1):1–11.

448. Ansari AA, Mayne AE, Sundstrom JB, et al. Administration of recombinant rhesus interleukin-12 during acute simian immunodeficiency virus (SIV) infection leads to decreased viral loads associated with prolonged survival in SIVmac251-infected rhesus macaques. *J Virol*. 2002;76(4):1731–43.

449. Mueller YM, Do DH, Altork S, et al. IL-15 treatment during acute simian immunodeficiency virus (SIV) infection increases viral set point and accelerates disease progression despite the induction of stronger SIV-specific CD8+ T cell responses. *J Immunol*. 2008;180(1):350–60.

450. Picker LJ, Reed-Inderbitzin EF, Hagen SI, et al. IL-15 induces CD4 effector memory T cell production and tissue emigration in nonhuman primates. *J Clin Invest*. 2006;116(6):1514–24.

451. Garrido C, Abad-Fernandez M, Tuyishime M, et al. Interleukin-15-stimulated natural killer cells clear HIV-1-infected cells following latency reversal ex vivo. *J Virol*. 2018;92(12):e00235-18.

452. Keating SM, Jacobs ES, Norris PJ, et al. Soluble mediators of inflammation in HIV and their implications for therapeutics and vaccine development. *Cytokine Growth Factor Rev*. 2012;23(4-5):193–206.

453. Katsikis PD, Mueller YM, Villinger F. The cytokine network of acute HIV infection: a promising target for vaccines and therapy to reduce viral set-point. *PLoS Pathog*. 2011;7(8):e1002055.

454. Ploquin MJ, Desoutter JF, Santos PR, et al. Distinct expression profiles of TGF-beta1 signaling mediators in pathogenic SIVmac and non-pathogenic SIVagm infections. *Retrovirology*. 2006;3(37).

455. Boulassel MR, Young M, Routy JP, Sekaly RP, Tremblay C, Rouleau D. Circulating levels of IL-7 but not IL-15, IGF-1, and TGF-beta are elevated during primary HIV-1 infection. *HIV Clin Trials*. 2004;5(5):357–9.

456. Blackard JT, Kang M, St Clair JB, et al. Viral factors associated with cytokine expression during HCV/HIV co-infection. *J Interferon Cytokine Res*. 2007;27(4):263–9.

457. Izadi A, Asadikaram G, Nakhaee N, Hadizadeh S, Ayatollahi Mousavi A. Plasma levels of Transforming Growth Factor Beta in HIV-1 patients with oral candidiasis. *Curr Med Mycol*. 2015;1(1):22–5.

458. Hu R, Oyaizu N, Than S, Kalyanaraman VS, Wang XP, Pahwa S. HIV-1 gp160 induces transforming growth factor-beta production in human PBMC. *Clin Immunol Immunopathol*. 1996;80(3 Pt 1):283–9.

459. Cupp C, Taylor JP, Khalili K, Amini S. Evidence for stimulation of the transforming growth factor beta 1 promoter by HIV-1 Tat in cells derived from CNS. *Oncogene*. 1993;8(8):2231–6.

460. Zauli G, Davis BR, Re MC, Visani G, Furlini G, La Placa M. tat protein stimulates production of transforming growth factor-beta 1 by marrow macrophages: a potential

mechanism for human immunodeficiency virus-1-induced hematopoietic suppression. *Blood*. 1992;80(12):3036–43.

461. Gibellini D, Zauli G, Re MC, et al. Recombinant human immunodeficiency virus type-1 (HIV-1) Tat protein sequentially up-regulates IL-6 and TGF-beta 1 mRNA expression and protein synthesis in peripheral blood monocytes. *Br J Haematol*. 1994;88(2):261–7.

462. Fang DY, Lu B, Hayward S, Kretser DM, Cowan PJ, Dwyer KM. The Role of activin A and B and the benefit of follistatin treatment in renal ischemia-reperfusion injury in mice. *Transplant Direct*. 2016;2(7):e87.

463. Reis FM, Cobellis L, Tameirão LC, et al. Serum and tissue expression of activin A in postmenopausal women with breast cancer. *J Clin Endocrinol Metab*. 2002;87(5):2277–82.

464. Michel U, Ebert S, Phillips D, Nau R. Serum concentrations of activin and follistatin are elevated and run in parallel in patients with septicemia. *Eur J Endocrinol*. 2003;148(5):559–64.

465. Patella S, Phillips DJ, Kretser DM, Evans LW, Groome NP, Sievert W. Characterization of serum activin-A and follistatin and their relation to virological and histological determinants in chronic viral hepatitis. *J Hepatol*. 2001;34(4):576–83.

466. Refaat B, Ashshi AM, El-Shemi AG, AlZanbagi A. Effects of chronic hepatitis C genotype 1 and 4 on serum activins and follistatin in treatment naïve patients and their correlations with interleukin-6, tumour necrosis factor-α, viral load and liver damage. *Clin Exp Med*. 2015;15(3):293–302.

467. Takei Y, Takahashi S, Nakasatomi M, et al. Urinary Activin A is a novel biomarker reflecting renal inflammation and tubular damage in ANCA-associated vasculitis. *PLoS ONE*. 2019;14(10):e0223703.

468. Ebert S, Phillips DJ, Jenzewski P, Nau R, O'Connor AE, Michel U. Activin A concentrations in human cerebrospinal fluid are age-dependent and elevated in meningitis. *J Neurol Sci*. 2006;250(1-2):50–7.

469. Gribi R, Tanaka T, Harper-Summers R, Yu J. Expression of activin A in inflammatory arthropathies. *Mol Cell Endocrinol*. 2001;180(1-2):163–7.

470. Snijders A, Kalinski P, Hilkens CM, Kapsenberg ML. High-level IL-12 production by human dendritic cells requires two signals. *Int Immunol*. 1998;10(11):1593–8.

471. Mattei F, Schiavoni G, Belardelli F, Tough DF. IL-15 is expressed by dendritic cells in response to type I IFN, double-stranded RNA, or lipopolysaccharide and promotes dendritic cell activation. *J Immunol*. 2001;167(3):1179–87.

472. Hémont C, Neel A, Heslan M, Braudeau C, Josien R. Human blood mDC subsets exhibit distinct TLR repertoire and responsiveness. *J Leukoc Biol*. 2013;93(4):599–609.

473. Reis e Sousa C. Toll-like receptors and dendritic cells: for whom the bug tolls. *Semin Immunol*. 2004;16(1):27–34.

474. Heil F, Hemmi H, Hochrein H, et al. Species-specific recognition of single-stranded RNA via toll-like receptor 7 and 8. *Science*. 2004;303(5663):1526–9.

475. Gay C, Dibben O, Anderson JA, et al. Cross-sectional detection of acute HIV infection: timing of transmission, inflammation and antiretroviral therapy. *PLoS ONE*. 2011;6(5):e19617.

476. von Sydow M, Sonnerborg A, Gaines H, Strannegard O. Interferon-alpha and tumor necrosis factor-alpha in serum of patients in various stages of HIV-1 infection. *AIDS Res Hum Retroviruses*. 1991;7(4):375–80.

477. Nyamweya S, Townend J, Zaman A, et al. Are plasma biomarkers of immune activation predictive of HIV progression: a longitudinal comparison and analyses in HIV-1 and HIV-2 infections. *PLoS ONE*. 2012;7(9):e44411.

478. Langford SE, Ananworanich J, Cooper DA, et al. Predictors of disease progression in HIV infection: a review. *AIDS Res Ther*. 2007;4(11).

479. Blair P, Flaumenhaft R. Platelet alpha-granules: basic biology and clinical correlates. *Blood Rev*. 2009;23(4):177–89.

480. Thomas JM, Pos Z, Reinboth J, et al. Differential responses of plasmacytoid dendritic cells to influenza virus and distinct viral pathogens. *J Virol*. 2014;88(18):10758–66.

481. Hoene V, Peiser M, Wanner R. Human monocyte-derived dendritic cells express TLR9 and react directly to the CpG-A oligonucleotide D19. *J Leukoc Biol*. 2006;80(6):1328–36.

482. Schattenberg D, Schott M, Reindl G, et al. Response of human monocyte-derived dendritic cells to immunostimulatory DNA. *Eur J Immunol*. 2000;30(10):2824–31.

483. Gendelman HE, Baca LM, Kubrak CA, et al. Induction of IFN-alpha in peripheral blood mononuclear cells by HIV-infected monocytes. Restricted antiviral activity of the HIV-induced IFN. *J Immunol*. 1992;148(2):422–9.

484. Sturlan S, Sachet M, Baumann S, Kuznetsova I, Spittler A, Bergmann M. Influenza a virus induces an immediate cytotoxic activity in all major subsets of peripheral blood mononuclear cells. *PLoS ONE*. 2009;4(1):e4122.

485. Wang H, Tang F, Bian E, et al. IFITM3/STAT3 axis promotes glioma cells invasion and is modulated by TGF-β. *Mol Biol Rep*. 2020;47(1):433–41.

486. Woodby BL, Songock WK, Scott ML, Raikhy G, Bodily JM. Induction of interferon kappa in human papillomavirus 16 infection by transforming growth factor beta-induced promoter demethylation. *J Virol*. 2018;92(8):e01714-17.

487. Khan SA, Joyce J, Tsuda T. Quantification of active and total transforming growth factor-β levels in serum and solid organ tissues by bioassay. *BMC Res Notes*. 2012;5(636).

488. Skogstrand K. Multiplex assays of inflammatory markers, a description of methods and discussion of precautions - our experience through the last ten years. *Methods*. 2012;56(2):204–12.

489. de Jager W, Bourcier K, Rijkers GT, Prakken BJ, Seyfert-Margolis V. Prerequisites for cytokine measurements in clinical trials with multiplex immunoassays. *BMC Immunol*. 2009;10(52).

490. Flower L, Ahuja RH, Humphries SE, Mohamed-Ali V. Effects of sample handling on the stability of interleukin 6, tumour necrosis factor-alpha and leptin. *Cytokine*. 2000;12(11):1712–6.

491. Aziz N, Nishanian P, Mitsuyasu R, Detels R, Fahey JL. Variables that affect assays for plasma cytokines and soluble activation markers. *Clin Diagn Lab Immunol*. 1999;6(1):89–95.

492. Biancotto A, Feng X, Langweiler M, Young NS, McCoy JP. Effect of anticoagulants on multiplexed measurement of cytokine/chemokines in healthy subjects. *Cytokine*. 2012;60(2):438–46.

493. Grainger DJ, Mosedale DE, Metcalfe JC. TGF-beta in blood: a complex problem. *Cytokine Growth Factor Rev*. 2000;11(1-2):133–45.

494. Grainger DJ, Heathcote K, Chiano M, et al. Genetic control of the circulating concentration of transforming growth factor type beta1. *Hum Mol Genet*. 1999;8(1):93–7.

495. Morrell CN, Aggrey AA, Chapman LM, Modjeski KL. Emerging roles for platelets as immune and inflammatory cells. *Blood*. 2014;123(18):2759–67.

496. Semple JW, Italiano JE, Freedman J. Platelets and the immune continuum. *Nat Rev Immunol*. 2011;11(4):264–74.

497. Chaipan C, Soilleux EJ, Simpson P, et al. DC-SIGN and CLEC-2 mediate human immunodeficiency virus type 1 capture by platelets. *J Virol*. 2006;80(18):8951–60.

498. Maurice A, Marchand-Arvier M, Edert D, Le Faou A, Gondrexon G, Vigneron C. The virucidal effect of platelet concentrates: preliminary study and first conclusions. *Platelets*. 2002;13(4):219–22.

499. Parker ZF, Rux AH, Riblett AM, et al. Platelet factor 4 inhibits and enhances HIV-1 infection in a concentration-dependent manner by modulating viral attachment. *AIDS Res Hum Retroviruses*. 2016;32(7):705–17.

500. Koupenova M, Vitseva O, MacKay CR, et al. Platelet-TLR7 mediates host survival and platelet count during viral infection in the absence of platelet-dependent thrombosis. *Blood*. 2014;124(5):791–802.

501. Assinger A, Kral JB, Yaiw KC, et al. Human cytomegalovirus-platelet interaction triggers toll-like receptor 2-dependent proinflammatory and proangiogenic responses. *Arterioscler Thromb Vasc Biol*. 2014;34(4):801–9.

502. Sipe JB, Zhang J, Waits C, Skikne B, Garimella R, Anderson HC. Localization of bone morphogenetic proteins (BMPs)-2, -4, and -6 within megakaryocytes and platelets. *Bone*. 2004;35(6):1316–22.

503. Osada M, Inoue O, Ding G, et al. Platelet activation receptor CLEC-2 regulates blood/lymphatic vessel separation by inhibiting proliferation, migration, and tube formation of lymphatic endothelial cells. *J Biol Chem*. 2012;287(26):22241–52.

504. Kalen A, Wahlstrom O, Linder CH, Magnusson P. The content of bone morphogenetic proteins in platelets varies greatly between different platelet donors. *Biochem Biophys Res Commun*. 2008;375(2):261–4.

505. Coupes BM, Williams S, Roberts IS, Short CD, Brenchley PE. Plasma transforming growth factor beta(1) and platelet activation: implications for studies in transplant recipients. *Nephrol Dial Transplant*. 2001;16(2):361–7.

506. Ahnadi CE, Sabrinah Chapman E, Lépine M, et al. Assessment of platelet activation in several different anticoagulants by the Advia 120 Hematology System, fluorescence flow cytometry, and electron microscopy. *Thromb Haemost*. 2003;90(5):940–8.

507. Mussbacher M, Schrottmaier WC, Salzmann M, et al. Optimized plasma preparation is essential to monitor platelet-stored molecules in humans. *PLoS ONE*. 2017;12(12):e0188921.

508. Kaplan KL, Owen J. Plasma levels of beta-thromboglobulin and platelet factor 4 as indices of platelet activation in vivo. *Blood*. 1981;57(2):199–202.

509. Dubrac A, Quemener C, Lacazette E, et al. Functional divergence between 2 chemokines is conferred by single amino acid change. *Blood*. 2010;116(22):4703–11.

510. Rucinski B, Niewiarowski S, Strzyzewski M, Holt JC, Mayo KH. Human platelet factor 4 and its C-terminal peptides: heparin binding and clearance from the circulation. *Thromb Haemost*. 1990;63(3):493–8.

511. Rucinski B, Knight LC, Niewiarowski S. Clearance of human platelet factor 4 by liver and kidney: its alteration by heparin. *Am J Physiol*. 1986;251(4 Pt 2):H800-7.

512. Mancini D, Monteagudo J, Suárez-Fariñas M, et al. New methodologies to accurately assess circulating active transforming growth factor-β1 levels: implications for evaluating heart failure and the impact of left ventricular assist devices. *Transl Res*. 2018;192:15–29.

513. FitzGerald GA, Smith B, Pedersen AK, Brash AR. Increased prostacyclin biosynthesis in patients with severe atherosclerosis and platelet activation. *N Engl J Med*. 1984;310(17):1065–8.

514. Jonnalagadda D, Izu LT, Whiteheart SW. Platelet secretion is kinetically heterogeneous in an agonist-responsive manner. *Blood*. 2012;120(26):5209–16.

515. Rex S, Beaulieu LM, Perlman DH, et al. Immune versus thrombotic stimulation of platelets differentially regulates signalling pathways, intracellular protein-protein interactions, and alpha-granule release. *Thromb Haemost*. 2009;102(1):97–110.

516. Wakefield LM, Letterio JJ, Chen T, et al. Transforming growth factor-beta1 circulates in normal human plasma and is unchanged in advanced metastatic breast cancer. *Clin Cancer Res*. 1995;1(1):129–36.

517. Mayne E, Funderburg NT, Sieg SF, et al. Increased platelet and microparticle activation in HIV infection: upregulation of P-selectin and tissue factor expression. *J Acquir Immune Defic Syndr*. 2012;59(4):340–6.

518. Mesquita EC, Hottz ED, Amancio RT, et al. Persistent platelet activation and apoptosis in virologically suppressed HIV-infected individuals. *Sci Rep*. 2018;8(1):14999.

519. Holme PA, Müller F, Solum NO, Brosstad F, Frøland SS, Aukrust P. Enhanced activation of platelets with abnormal release of RANTES in human immunodeficiency virus type 1 infection. *FASEB J*. 1998;12(1):79–89.

520. O'Halloran JA, Dunne E, Gurwith M, et al. The effect of initiation of antiretroviral therapy on monocyte, endothelial and platelet function in HIV-1 infection. *HIV Med*. 2015;16(10):608–19.

521. Nkambule BB, Davison GM, Ipp H. The evaluation of platelet indices and markers of inflammation, coagulation and disease progression in treatment-naïve, asymptomatic HIV-infected individuals. *Int J Lab Hematol*. 2015;37(4):450–8.

522. Tunjungputri RN, Van Der Ven AJ, Schonsberg A, et al. Reduced platelet hyperreactivity and platelet-monocyte aggregation in HIV-infected individuals receiving a raltegravir-based regimen. *AIDS*. 2014;28(14):2091–6.

523. Taylor KA, Smyth E, Rauzi F, et al. Pharmacological impact of antiretroviral therapy on platelet function to investigate human immunodeficiency virus-associated cardiovascular risk. *Br J Pharmacol*. 2019;176(7):879–89.

524. Boilard E, Paré G, Rousseau M, et al. Influenza virus H1N1 activates platelets through FcγRIIA signaling and thrombin generation. *Blood*. 2014;123(18):2854–63.

525. Fusegawa H, Shiraishi K, Ogasawara F, et al. Platelet activation in patients with chronic hepatitis C. *Tokai J Exp Clin Med*. 2002;27(4):101–6.

526. Chao CH, Wu WC, Lai YC, et al. Dengue virus nonstructural protein 1 activates platelets via Toll-like receptor 4, leading to thrombocytopenia and hemorrhage. *PLoS Pathog*. 2019;15(4):e1007625.

527. Metcalf Pate KA, Lyons CE, Dorsey JL, et al. Platelet activation and platelet-monocyte aggregate formation contribute to decreased platelet count during acute simian immunodeficiency virus infection in pig-tailed macaques. *J Infect Dis*. 2013;208(6):874–83.

528. Yun SH, Sim EH, Goh RY, Park JI, Han JY. Platelet activation: the mechanisms and potential biomarkers. *Biomed Res Int*. 2016;2016(9060143).

529. Wang J, Zhang W, Nardi MA, Li Z. HIV-1 Tat-induced platelet activation and release of CD154 contribute to HIV-1-associated autoimmune thrombocytopenia. *J Thromb Haemost*. 2011;9(3):562–73.

530. Davidson DC, Hirschman MP, Spinelli SL, et al. Antiplatelet activity of valproic acid contributes to decreased soluble CD40 ligand production in HIV type 1-infected individuals. *J Immunol*. 2011;186(1):584–91.

531. Davidson DC, Hirschman MP, Sun A, Singh MV, Kasischke K, Maggirwar SB. Excess soluble CD40L contributes to blood brain barrier permeability in vivo: implications for HIV-associated neurocognitive disorders. *PLoS ONE*. 2012;7(12):e51793.

532. Banerjee M, Huang Y, Joshi S, et al. Platelets endocytose viral particles and are activated via TLR (toll-like receptor) signaling. *Arterioscler Thromb Vasc Biol*. 2020;40(7):1635–50.

533. Vaidya SA, Korner C, Sirignano MN, et al. Tumor necrosis factor α is associated with viral control and early disease progression in patients with HIV type 1 infection. *J Infect Dis*. 2014;210(7):1042–6.

534. Piguet PF, Vesin C, Da Kan C. Activation of platelet caspases by TNF and its consequences for kinetics. *Cytokine*. 2002;18(4):222–30.

535. Claushuis TAM, Van Der Veen AIP, Horn J, et al. Platelet Toll-like receptor expression and activation induced by lipopolysaccharide and sepsis. *Platelets*. 2019;30(3):296–304.

536. Cognasse F, Hamzeh-Cognasse H, Lafarge S, et al. Toll-like receptor 4 ligand can differentially modulate the release of cytokines by human platelets. *Br J Haematol*. 2008;141(1):84–91.

537. Tsoupras AB, Chini M, Mangafas N, et al. Platelet-activating factor and its basic metabolic enzymes in blood of naive HIV-infected patients. *Angiology*. 2012;63(5):343–52.

538. Aliahmadi E, Gramlich R, Grützkau A, et al. TLR2-activated human Langerhans cells promote Th17 polarization via IL-1beta, TGF-beta and IL-23. *Eur J Immunol*. 2009;39(5):1221–30.

539. Dumitriu IE, Dunbar DR, Howie SE, Sethi T, Gregory CD. Human dendritic cells produce TGF-beta 1 under the influence of lung carcinoma cells and prime the differentiation of CD4+CD25+Foxp3+ regulatory T cells. *J Immunol*. 2009;182(5):2795–807.

540. Morelli AE, Zahorchak AF, Larregina AT, et al. Cytokine production by mouse myeloid dendritic cells in relation to differentiation and terminal maturation induced by lipopolysaccharide or CD40 ligation. *Blood*. 2001;98(5):1512–23.

541. Bonnefoy F, Couturier M, Clauzon A, et al. TGF-beta-exposed plasmacytoid dendritic cells participate in Th17 commitment. *J Immunol*. 2011;186(11):6157–64.

542. Li J, Mbow ML, Sun L, et al. Induction of dendritic cell maturation by IL-18. *Cell Immunol*. 2004;227(2):103–8.

543. Wang J, Guan E, Roderiquez G, Norcross MA. Synergistic induction of apoptosis in primary CD4+ T cells by macrophage-tropic HIV-1 and TGF-beta1. *J Immunol*. 2001;167(6):3360–6.

544. Peterson PK, Gekker G, Chao CC, Schut R, Molitor TW, Balfour HH. Cocaine potentiates HIV-1 replication in human peripheral blood mononuclear cell cocultures. Involvement of transforming growth factor-beta. *J Immunol*. 1991;146(1):81–4.

545. Poli G, Kinter AL, Justement JS, Bressler P, Kehrl JH, Fauci AS. Transforming growth factor beta suppresses human immunodeficiency virus expression and replication in infected cells of the monocyte/macrophage lineage. *J Exp Med*. 1991;173(3):589–97.

546. Moriuchi M, Moriuchi H. Cell-type-dependent effect of transforming growth factor beta, a major cytokine in breast milk, on human immunodeficiency virus type 1 infection of mammary epithelial MCF-7 cells or macrophages. *J Virol*. 2004;78(23):13046–52.

547. Iannello A, Boulassel MR, Samarani S, et al. HIV-1 causes an imbalance in the production of interleukin-18 and its natural antagonist in HIV-infected individuals: implications for enhanced viral replication. *J Infect Dis*. 2010;201(4):608–17.

548. Chen S, Tuttle DL, Oshier JT, et al. Transforming growth factor-beta1 increases CXCR4 expression, stromal-derived factor-1alpha-stimulated signalling and human immunodeficiency virus-1 entry in human monocyte-derived macrophages. *Immunology*. 2005;114(4):565–74.

549. Lazdins JK, Klimkait T, Woods-Cook K, et al. In vitro effect of transforming growth factor-beta on progression of HIV-1 infection in primary mononuclear phagocytes. *J Immunol*. 1991;147(4):1201–7.

550. Lima RG, Van Weyenbergh J, Saraiva EM, Barral-Netto M, Galvão-Castro B, Bou-Habib DC. The replication of human immunodeficiency virus type 1 in macrophages is enhanced after phagocytosis of apoptotic cells. *J Infect Dis*. 2002;185(11):1561–6.

551. Poli G, Kinter AL, Justement JS, Bressler P, Kehrl JH, Fauci AS. Retinoic acid mimics transforming growth factor beta in the regulation of human immunodeficiency virus expression in monocytic cells. *Proc Natl Acad Sci USA*. 1992;89(7):2689–93.

552. Shen R, Meng G, Ochsenbauer C, et al. Stromal down-regulation of macrophage CD4/CCR5 expression and NF-κB activation mediates HIV-1 non-permissiveness in intestinal macrophages. *PLoS Pathog.* 2011;7(5):e1002060.

553. Czubala MA, Finsterbusch K, Ivory MO, et al. TGFβ induces a SAMHD1-independent post-entry restriction to HIV-1 infection of human epithelial Langerhans cells. *J Invest Dermatol*. 2016;136(10):1981–9.

554. Goldstone DC, Ennis-Adeniran V, Hedden JJ, et al. HIV-1 restriction factor SAMHD1 is a deoxynucleoside triphosphate triphosphohydrolase. *Nature*. 2011;480(7377):379–82.

555. McCann KL, Imani F. Transforming growth factor beta enhances respiratory syncytial virus replication and tumor necrosis factor alpha induction in human epithelial cells. *J Virol*. 2007;81(6):2880–6.

556. Thomas BJ, Lindsay M, Dagher H, et al. Transforming growth factor-beta enhances rhinovirus infection by diminishing early innate responses. *Am J Respir Cell Mol Biol*. 2009;41(3):339–47.

557. Bedke N, Sammut D, Green B, et al. Transforming growth factor-beta promotes rhinovirus replication in bronchial epithelial cells by suppressing the innate immune response. *PLoS ONE*. 2012;7(9):e44580.

558. Denney L, Branchett W, Gregory LG, Oliver RA, Lloyd CM. Epithelial-derived TGF-β1 acts as a pro-viral factor in the lung during influenza A infection. *Mucosal Immunol*. 2018;11(2):523–35.

559. Chou YC, Chen ML, Hu CP, et al. Transforming growth factor-beta1 suppresses hepatitis B virus replication primarily through transcriptional inhibition of pregenomic RNA. *Hepatology*. 2007;46(3):672–81.

560. Liang G, Liu G, Kitamura K, et al. TGF-β suppression of HBV RNA through AID-dependent recruitment of an RNA exosome complex. *PLoS Pathog*. 2015;11(4):e1004780.

561. Park SO, Kumar M, Gupta S, et al. TGF-β and iron differently alter HBV replication in human hepatocytes through TGF-β/BMP signaling and cellular microRNA expression. *PLoS ONE*. 2012;7(6):e39276.

562. Murata T, Ohshima T, Yamaji M, et al. Suppression of hepatitis C virus replicon by TGF-beta. *Virology*. 2005;331(2):407–17.

563. Tu E, Chia CPZ, Chen W, et al. T cell receptor-regulated TGF-β type I receptor expression determines T cell quiescence and activation. *Immunity*. 2018;48(4):745–759.

564. Halder SK, Beauchamp RD, Datta PK. A specific inhibitor of TGF-beta receptor kinase, SB-431542, as a potent antitumor agent for human cancers. *Neoplasia*. 2005;7(5):509–21.

565. Boergermann JH, Kopf J, Yu PB, Knaus P. Dorsomorphin and LDN-193189 inhibit BMP-mediated Smad, p38 and Akt signalling in C2C12 cells. *Int J Biochem Cell Biol*. 2010;42(11):1802–7.

566. Shirazi Y, Pitha PM. Alpha interferon inhibits early stages of the human immunodeficiency virus type 1 replication cycle. *J Virol*. 1992;66(3):1321–8.

567. Dube PR, Birnbaumer L, Vazquez G. Evidence for constitutive bone morphogenetic protein-2 secretion by M1 macrophages: Constitutive auto/paracrine osteogenic signaling by BMP-2 in M1 macrophages. *Biochem Biophys Res Commun*. 2017;491(1):154–8.

568. Champagne CM, Takebe J, Offenbacher S, Cooper LF. Macrophage cell lines produce osteoinductive signals that include bone morphogenetic protein-2. *Bone*. 2002;30(1):26–31.

569. Foster TL, Wilson H, Iyer SS, et al. Resistance of transmitted founder HIV-1 to IFITM-mediated restriction. *Cell Host Microbe*. 2016;20(4):429–42.

570. Oswald-Richter K, Grill SM, Leelawong M, Unutmaz D. HIV infection of primary human T cells is determined by tunable thresholds of T cell activation. *Eur J Immunol*. 2004;34(6):1705–14.

571. Chavez L, Calvanese V, Verdin E. HIV latency is established directly and early in both resting and activated primary CD4 T cells. *PLoS Pathog*. 2015;11(6):e1004955.

572. Alexaki A, Liu Y, Wigdahl B, et al. Cellular reservoirs of HIV-1 and their role in viral persistence. *Curr HIV Res*. 2008;6(5):388–400.

573. Bedford JG, O'Keeffe M, Reading PC, Wakim LM. Rapid interferon independent expression of IFITM3 following T cell activation protects cells from influenza virus infection. *PLoS ONE*. 2019;14(1):e0210132.

574. Dondi E, Rogge L, Lutfalla G, Uzé G, Pellegrini S. Down-modulation of responses to type I IFN upon T cell activation. *J Immunol*. 2003;170(2):749–56.

575. Oliva H, Pacheco R, Martinez-Navio JM, et al. Increased expression with differential subcellular location of cytidine deaminase APOBEC3G in human CD4+ T cell activation and dendritic cell maturation. *Immunol Cell Biol*. 2016;94(7):689–700.

576. Rausell A, Muñoz M, Martinez R, Roger T, Telenti A, Ciuffi A. Innate immune defects in HIV permissive cell lines. *Retrovirology*. 2016;13(1):43.

577. Baldauf HM, Pan X, Erikson E, et al. SAMHD1 restricts HIV-1 infection in resting CD4+ T cells. *Nat Med*. 2012;18(11):1682–7.

578. Plesa G, Dai J, Baytop C, Riley JL, June CH, O'Doherty U. Addition of deoxynucleosides enhances human immunodeficiency virus type 1 integration and 2LTR formation in resting CD4+ T cells. *J Virol*. 2007;81(24):13938–42.

579. Roux A, Leroy H, De Muylder B, et al. FOXO1 transcription factor plays a key role in T cell-HIV-1 interaction. *PLoS Pathog*. 2019;15(5):e1007669.

580. Reddy M, Eirikis E, Davis C, Davis HM, Prabhakar U. Comparative analysis of lymphocyte activation marker expression and cytokine secretion profile in stimulated human peripheral blood mononuclear cell cultures: an in vitro model to monitor cellular immune function. *J Immunol Methods*. 2004;293(1-2):127–42.

581. Sandoval-Montes C, Santos-Argumedo L. CD38 is expressed selectively during the activation of a subset of mature T cells with reduced proliferation but improved potential to produce cytokines. *J Leukoc Biol*. 2005;77(4):513–21.

582. Yamamoto T, Tsunetsugu-Yokota Y, Mitsuki YY, et al. Selective transmission of R5 HIV-1 over X4 HIV-1 at the dendritic cell-T cell infectious synapse is determined by the T cell activation state. *PLoS Pathog*. 2009;5(1):e1000279.

583. Inada M, Izawa G, Kobayashi W, Ozawa M. 293 cells express both epithelial as well as mesenchymal cell adhesion molecules. *Int J Mol Med*. 2016;37(6):1521–7.

584. Pang S, Yu D, An DS, et al. Human immunodeficiency virus Env-independent infection of human CD4(-) cells. *J Virol*. 2000;74(23):10994–1000.

585. Viñals F, Pouysségur J. Transforming growth factor beta1 (TGF-beta1) promotes endothelial cell survival during in vitro angiogenesis via an autocrine mechanism implicating TGF-alpha signaling. *Mol Cell Biol*. 2001;21(21):7218–30.

586. Gorrell RE, Totten MH, Schoerning LJ, et al. Identification of a bone morphogenetic protein type 2 receptor neutralizing antibody. *BMC Res Notes*. 2019;12(331).

587. Zhang Y, Bao YL, Yang MT, et al. Activin A induces SLC5A8 expression through the Smad3 signaling pathway in human colon cancer RKO cells. *Int J Biochem Cell Biol*. 2010;42(12):1964–72.

588. Rich EA, Chen IS, Zack JA, Leonard ML, O'Brien WA. Increased susceptibility of differentiated mononuclear phagocytes to productive infection with human immunodeficiency virus-1 (HIV-1). *J Clin Invest*. 1992;89(1):176–83.

589. Schuitemaker H, Kootstra NA, Koppelman MH, et al. Proliferation-dependent HIV-1 infection of monocytes occurs during differentiation into macrophages. *J Clin Invest*. 1992;89(4):1154–60.

590. Yu X, Buttgereit A, Lelios I, et al. The Cytokine TGF-β Promotes the Development and Homeostasis of Alveolar Macrophages. *Immunity*. 2017;47(5):903–912.

591. Butovsky O, Jedrychowski MP, Moore CS, et al. Identification of a unique TGF-β-dependent molecular and functional signature in microglia. *Nat Neurosci*. 2014;17(1):131–43.

592. Nasr N, Alshehri AA, Wright TK, et al. Mechanism of interferon-stimulated gene induction in HIV-1-infected macrophages. *J Virol*. 2017;91(20):e00744-17.

593. Pichlmair A, Lassnig C, Eberle CA, et al. IFIT1 is an antiviral protein that recognizes 5'-triphosphate RNA. *Nat Immunol*. 2011;12(7):624–30.

594. Goujon C, Malim MH. Characterization of the alpha interferon-induced postentry block to HIV-1 infection in primary human macrophages and T cells. *J Virol*. 2010;84(18):9254–66.

595. Ashokkumar M, Sonawane A, Sperk M, Tripathy SP, Neogi U, Hanna LE. In vitro replicative fitness of early Transmitted founder HIV-1 variants and sensitivity to Interferon alpha. *Sci Rep*. 2020;10(1):2747.

596. Lin AH, Burrascano C, Pettersson PL, Ibañez CE, Gruber HE, Jolly DJ. Blockade of type I interferon (IFN) production by retroviral replicating vectors and reduced tumor cell responses to IFN likely contribute to tumor selectivity. *J Virol*. 2014;88(17):10066–77.

597. Noser JA, Mael AA, Sakuma R, et al. The RAS/Raf1/MEK/ERK signaling pathway facilitates VSV-mediated oncolysis: implication for the defective interferon response in cancer cells. *Mol Ther*. 2007;15(8):1531–6.

598. Orlova-Fink N, Chowdhury FZ, Sun X, et al. Preferential susceptibility of Th9 and Th2 CD4+ T cells to X4-tropic HIV-1 infection. *AIDS*. 2017;31(16):2211–5.

599. Ledru E, Lecoeur H, Garcia S, Debord T, Gougeon ML. Differential susceptibility to activation-induced apoptosis among peripheral Th1 subsets: correlation with Bcl-2 expression and consequences for AIDS pathogenesis. *J Immunol*. 1998;160(7):3194–206.

600. van Opijnen, T, Kamoschinski, J, Jeeninga, RE, Berkhout, B. The human immunodeficiency virus type 1 promoter contains a CATA box instead of a TATA box for optimal transcription and replication. *J Virol*. 2004;78(13):6883–90.

601. Shukla RR, Kumar A, Kimmel PL. Transforming growth factor beta increases the expression of HIV-1 gene in transfected human mesangial cells. *Kidney Int*. 1993;44(5):1022–9.

602. Coyle-Rink J, Sweet T, Abraham S, et al. Interaction between TGFbeta signaling proteins and C/EBP controls basal and Tat-mediated transcription of HIV-1 LTR in astrocytes. *Virology*. 2002;299(2):240–7.

603. Li JM, Shen X, Hu PP, Wang XF. Transforming growth factor beta stimulates the human immunodeficiency virus 1 enhancer and requires NF-kappaB activity. *Mol Cell Biol*. 1998;18(1):110–21.

604. Hokello J, Sharma AL, Tyagi M. Efficient non-epigenetic activation of HIV latency through the Tcell receptor signalosome. *Viruses*. 2020;12(8):E868.

605. Grant C, Oh U, Fugo K, et al. FOXP3 represses retroviral transcription by targeting both NF-kappaB and CREB pathways. *PLoS Pathog*. 2006;2(4):e33.

606. Selliah N, Zhang M, White S, et al. FOXP3 inhibits HIV-1 infection of CD4 T cells via inhibition of LTR transcriptional activity. *Virology*. 2008;381(2):161–7.

607. Holmes D, Knudsen G, Mackey-Cushman S, Su L. FOXP3 enhances HIV-1 gene expression by modulating NFkappaB occupancy at the long terminal repeat in human T cells. *J Biol Chem*. 2007;282(22):15973–80.

608. Oeckinghaus A, Ghosh S. The NF-kappaB family of transcription factors and its regulation. *Cold Spring Harb Perspect Biol*. 2009;1(4):a000034.

609. Liu T, Zhang L, Joo D, Sun SC. NF-κB signaling in inflammation. *Signal Transduct Target Ther*. 2017;2(17023).

610. Chen LF, Greene WC. Shaping the nuclear action of NF-kappaB. *Nat Rev Mol Cell Biol*. 2004;5(5):392–401.

611. Dorrington MG, Fraser IDC. NF-κB Signaling in macrophages: dynamics, crosstalk, and signal integration. *Front Immunol*. 2019;10(705).

612. Ernst O, Vayttaden SJ, Fraser IDC. Measurement of NF-κB activation in TLR-activated macrophages. *Methods Mol Biol*. 2018;1714:67–78.

613. Azuma M, Motegi K, Aota K, Yamashita T, Yoshida H, Sato M. TGF-beta1 inhibits NF-kappaB activity through induction of IkappaB-alpha expression in human salivary gland cells: a possible mechanism of growth suppression by TGF-beta1. *Exp Cell Res*. 1999;250(1):213–22.

614. Badr CE, Niers JM, Tjon-Kon-Fat LA, Noske DP, Wurdinger T, Tannous BA. Real-time monitoring of nuclear factor kappaB activity in cultured cells and in animal models. *Mol Imaging*. 2009;8(5):278–90.

615. Luo K. Signaling Cross Talk between TGF-β/SMAD and Other Signaling Pathways. *Cold Spring Harb Perspect Biol*. 2017;9(1):a022137.

616. Freudlsperger C, Bian Y, Contag Wise S, et al. TGF-β and NF-κB signal pathway cross-talk is mediated through TAK1 and SMAD7 in a subset of head and neck cancers. *Oncogene*. 2013;32(12):1549–59.

617. Yeh YY, Chiao CC, Kuo WY, et al. TGF-beta1 increases motility and alphavbeta3 integrin up-regulation via PI3K, Akt and NF-kappaB-dependent pathway in human chondrosarcoma cells. *Biochem Pharmacol*. 2008;75(6):1292–301.

618. Arsura M, Panta GR, Bilyeu JD, et al. Transient activation of NF-kappaB through a TAK1/IKK kinase pathway by TGF-beta1 inhibits AP-1/SMAD signaling and apoptosis: implications in liver tumor formation. *Oncogene*. 2003;22(3):412–25.

619. Sovak MA, Arsura M, Zanieski G, Kavanagh KT, Sonenshein GE. The inhibitory effects of transforming growth factor beta1 on breast cancer cell proliferation are mediated through regulation of aberrant nuclear factor-kappaB/Rel expression. *Cell Growth Differ*. 1999;10(8):537–44.

620. Monteleone G, Mann J, Monteleone I, et al. A failure of transforming growth factor-beta1 negative regulation maintains sustained NF-kappaB activation in gut inflammation. *J Biol Chem*. 2004;279(6):3925–32.

621. Cottrez F, Groux H. Regulation of TGF-beta response during T cell activation is modulated by IL-10. *J Immunol*. 2001;167(2):773–8.

622. Tu E, Bourges D, Gleeson PA, Ang DK, Driel IR. Pathogenic T cells persist after reversal of autoimmune disease by immunosuppression with regulatory T cells. *Eur J Immunol*. 2013;43(5):1286–96.

623. Tiemessen MM, Kunzmann S, Schmidt-Weber CB, et al. Transforming growth factor-beta inhibits human antigen-specific CD4+ T cell proliferation without modulating the cytokine response. *Int Immunol*. 2003;15(12):1495–504.

624. Walsh D, Mathews MB, Mohr I. Tinkering with translation: protein synthesis in virus-infected cells. *Cold Spring Harb Perspect Biol*. 2013;5(1):a012351.

625. Duan D, Derynck R. Transforming growth factor-β (TGF-β)-induced up-regulation of TGF-β receptors at the cell surface amplifies the TGF-β response. *J Biol Chem*. 2019;294(21):8490–504.

626. Brunschwig EB, Wilson K, Mack D, et al. PMEPA1, a transforming growth factor-beta-induced marker of terminal colonocyte differentiation whose expression is maintained in primary and metastatic colon cancer. *Cancer Res*. 2003;63(7):1568–75.

627. Guzzo C, Fox J, Lin Y, et al. The CD8-derived chemokine XCL1/lymphotactin is a conformation-dependent, broad-spectrum inhibitor of HIV-1. *PLoS Pathog*. 2013;9(12):e1003852.

628. Lei Y, Takahama Y. XCL1 and XCR1 in the immune system. *Microbes Infect*. 2012;14(3):262–7.

629. National Center for Biotechnology Information, NIH, USA. Gene. Accessed on October 8, 2020. https://www.ncbi.nlm.nih.gov/gene/

630. Masuda K, Ripley B, Nishimura R, et al. Arid5a controls IL-6 mRNA stability, which contributes to elevation of IL-6 level in vivo. *Proc Natl Acad Sci USA*. 2013;110(23):9409–14.

631. Hogan KA, Chini CCS, Chini EN. The multi-faceted ecto-enzyme CD38: roles in immunomodulation, cancer, aging, and metabolic diseases. *Front Immunol*. 2019;10(1187).

632. Becher B, Tugues S, Greter M. GM-CSF: from growth factor to central mediator of tissue inflammation. *Immunity*. 2016;45(5):963–73.

633. Ding L, Wang Z, Yan J, et al. Human four-and-a-half LIM family members suppress tumor cell growth through a TGF-beta-like signaling pathway. *J Clin Invest*. 2009;119(2):349–61.

634. Zhao G, Na R, Li L, et al. Vasohibin-1 inhibits angiogenesis and suppresses tumor growth in renal cell carcinoma. *Oncol Rep*. 2017;38(2):1021–8.

635. Szarek M, Bergmann M, Konrad L, et al. Activin A target genes are differentially expressed between normal and neoplastic adult human testes: clues to gonocyte fate choice. *Andrology*. 2019;7(1):31–41.

636. Hollnagel A, Oehlmann V, Heymer J, Rüther U, Nordheim A. Id genes are direct targets of bone morphogenetic protein induction in embryonic stem cells. *J Biol Chem*. 1999;274(28):19838–45.

637. Miossec P, Kolls JK. Targeting IL-17 and Th17 cells in chronic inflammation. *Nat Rev Drug Discov*. 2012;11(10):763–76.

638. Colin P, Bénureau Y, Staropoli I, et al. HIV-1 exploits CCR5 conformational heterogeneity to escape inhibition by chemokines. *Proc Natl Acad Sci USA*. 2013;110(23):9475–80.

639. Szabo PA, Goswami A, Mazzuca DM, et al. Rapid and rigorous IL-17A production by a distinct subpopulation of effector memory T lymphocytes constitutes a novel mechanism of toxic shock syndrome immunopathology. *J Immunol*. 2017;198(7):2805–18.

640. Nath AP, Braun A, Ritchie SC, et al. Comparative analysis reveals a role for TGF-β in shaping the residency-related transcriptional signature in tissue-resident memory CD8+ T cells. *PLoS One*. 2019;14(2):e0210495.

641. Kim BO, Liu Y, Zhou BY, He JJ. Induction of C chemokine XCL1 (lymphotactin/single C motif-1 alpha/activation-induced, T cell-derived and chemokine-related cytokine) expression by HIV-1 Tat protein. *J Immunol*. 2004;172(3):1888–95.

642. Korn T, Bettelli E, Oukka M, Kuchroo VK. IL-17 and Th17 Cells. *Annu Rev Immunol*. 2009;27:485–517.

643. Riley JL, Levine BL, Craighead N, et al. Naïve and memory CD4 T cells differ in their susceptibilities to human immunodeficiency virus type 1 infection following CD28 costimulation: implications for transmission and pathogenesis. *J Virol*. 1998;72(10):8273–80.

644. Koch S, Larbi A, Derhovanessian E, Ozcelik D, Naumova E, Pawelec G. Multiparameter flow cytometric analysis of CD4 and CD8 T cell subsets in young and old people. *Immun Ageing*. 2008;5(6).

645. Mousset CM, Hobo W, Woestenenk R, Preijers F, Dolstra H, Waart AB. Comprehensive phenotyping of T cells using flow cytometry. *Cytometry A*. 2019;95(6):647–54.

646. Silveira-Mattos PS, Narendran G, Akrami K, et al. Differential expression of CXCR3 and CCR6 on CD4+ T-lymphocytes with distinct memory phenotypes characterizes tuberculosis-associated immune reconstitution inflammatory syndrome. *Sci Rep*. 2019;9(1):1502.

647. Fonseca VR, Romão VC, Agua-Doce A, et al. The ratio of blood T follicular regulatory cells to T follicular helper cells marks ectopic lymphoid structure formation while activated follicular helper T cells indicate disease activity in primary Sjögren's syndrome. *Arthritis Rheumatol*. 2018;70(5):774–84.

648. Morita R, Schmitt N, Bentebibel SE, et al. Human blood CXCR5(+)CD4(+) T cells are counterparts of T follicular cells and contain specific subsets that differentially support antibody secretion. *Immunity*. 2011;34(1):108–21.

649. Allan SE, Crome SQ, Crellin NK, et al. Activation-induced FOXP3 in human T effector cells does not suppress proliferation or cytokine production. *Int Immunol*. 2007;19(4):345–54.

650. Mohr A, Malhotra R, Mayer G, Gorochov G, Miyara M. Human FOXP3+ T regulatory cell heterogeneity. *Clin Transl Immunology*. 2018;7(1):e1005.

651. Bonyhadi M, Frohlich M, Rasmussen A, et al. In vitro engagement of CD3 and CD28 corrects T cell defects in chronic lymphocytic leukemia. *J Immunol*. 2005;174(4):2366–75.

652. Liu R, Paxton WA, Choe S, et al. Homozygous defect in HIV-1 coreceptor accounts for resistance of some multiply exposed individuals to HIV-1 infection. *Cell*. 1996;86(3):367–77.

653. Motamedi M, Xu L, Elahi S. Correlation of transferrin receptor (CD71) with Ki67 expression on stimulated human and mouse T cells: The kinetics of expression of T cell activation markers. *J Immunol Methods*. 2016;437:43–52.

654. Schumann J, Stanko K, Schliesser U, Appelt C, Sawitzki B. Differences in cd44 surface expression levels and function discriminates IL-17 and IFN-γ producing helper T cells. *PLoS ONE*. 2015;10(7):e0132479.

655. Yan ZH, Zheng XF, Yi L, et al. CD137 is a useful marker for identifying CD4+ T cell responses to Mycobacterium tuberculosis. *Scand J Immunol*. 2017;85(5):372–80.

656. Daoussis D, Antonopoulos I, Andonopoulos AP, Liossis SN. Increased expression of CD154 (CD40L) on stimulated T cells from patients with psoriatic arthritis. *Rheumatology (Oxford)*. 2007;46(2):227–31.

657. Zaunders JJ, Munier ML, Seddiki N, et al. High levels of human antigen-specific CD4+ T cells in peripheral blood revealed by stimulated coexpression of CD25 and CD134 (OX40). *J Immunol*. 2009;183(4):2827–36.

658. Rusconi S, La Seta Catamancio S, Citterio P, et al. Combination of CCR5 and CXCR4 inhibitors in therapy of human immunodeficiency virus type 1 infection: in vitro studies of mixed virus infections. *J Virol*. 2000;74(19):9328–32.

659. Mosier DE, Picchio GR, Gulizia RJ, et al. Highly potent RANTES analogues either prevent CCR5-using human immunodeficiency virus type 1 infection in vivo or rapidly select for CXCR4-using variants. *J Virol*. 1999;73(5):3544–50.

660. Ganesan M, Poluektova LY, Kharbanda KK, Osna NA. Liver as a target of human immunodeficiency virus infection. *World J Gastroenterol*. 2018;24(42):4728–37.

661. Takai S, Schlom J, Tucker J, Tsang KY, Greiner JW. Inhibition of TGF-β1 signaling promotes central memory T cell differentiation. *J Immunol*. 2013;191(5):2299–307.

662. Ma C, Zhang N. Transforming growth factor-β signaling is constantly shaping memory T-cell population. *Proc Natl Acad Sci USA*. 2015;112(35):11013–7.

663. Groot F, Capel TM, Schuitemaker J, Berkhout B, Jong EC. Differential susceptibility of naïve, central memory and effector memory T cells to dendritic cell-mediated HIV-1 transmission. *Retrovirology*. 2006;3(52).

664. Lim HW, Lee J, Hillsamer P, Kim CH. Human Th17 cells share major trafficking receptors with both polarized effector T cells and FOXP3+ regulatory T cells. *J Immunol*. 2008;180(1):122–9.

665. Zhao XP, Huang YY, Huang Y, et al. Transforming growth factor-beta1 upregulates the expression of CXC chemokine receptor 4 (CXCR4) in human breast cancer MCF-7 cells. *Acta Pharmacol Sin*. 2010;31(3):347–54.

666. Mohammadi P, Desfarges S, Bartha I, et al. 24 hours in the life of HIV-1 in a T cell line. *PLoS Pathog*. 2013;9(1):e1003161.

667. Dahmani A, Delisle JS. TGF-β in T cell biology: implications for cancer immunotherapy. *Cancers (Basel)*. 2018;10(6):194.

668. Chen Z, Li DQ, Tong L, Stewart P, Chu C, Pflugfelder SC. Targeted inhibition of p57 and p15 blocks transforming growth factor beta-inhibited proliferation of primary cultured human limbal epithelial cells. *Mol Vis*. 2006;12:983–94.

669. Zhuang X, Pedroza-Pacheco I, Nawroth I, et al. Hypoxic microenvironment shapes HIV-1 replication and latency. *Commun Biol*. 2020;3(1):376.

670. Brussel A, Delelis O, Sonigo P. Alu-LTR real-time nested PCR assay for quantifying integrated HIV-1 DNA. *Methods Mol Biol*. 2005;304:139–54.

671. Zhang Y, Derynck R. Regulation of Smad signalling by protein associations and signalling crosstalk. *Trends Cell Biol*. 1999;9(7):274–9.

672. ten Dijke, P, Miyazono, K, Heldin, CH. Signaling inputs converge on nuclear effectors in TGF-beta signaling. *Trends Biochem Sci*. 2000;25(2):64–70.

673. Herrera B, Addante A, Sánchez A. BMP signalling at the crossroad of liver fibrosis and regeneration. *Int J Mol Sci*. 2017;19(1):39.

674. Armitage AE, Eddowes LA, Gileadi U, et al. Hepcidin regulation by innate immune and infectious stimuli. *Blood*. 2011;118(15):4129–39.

675. López-Abente J, Correa-Rocha R, Pion M. Functional mechanisms of Treg in the context of HIV infection and the Janus face of immune suppression. *Front Immunol*. 2016;7:192.

676. Theron AJ, Anderson R, Rossouw TM, Steel HC. The role of transforming growth factor beta-1 in the progression of HIV/AIDS and development of non-AIDS-defining fibrotic disorders. *Front Immunol*. 2017;8:1461.

677. O'Connell KE, Guo W, Serra C, et al. The effects of an ActRIIb receptor Fc fusion protein ligand trap in juvenile simian immunodeficiency virus-infected rhesus macaques. *FASEB J*. 2015;29(4):1165–75.

678. Sako D, Grinberg AV, Liu J, et al. Characterization of the ligand binding functionality of the extracellular domain of activin receptor type IIb. *J Biol Chem*. 2010;285(27):21037–48.

679. Saag MS, Benson CA, Gandhi RT, et al. Antiretroviral drugs for treatment and prevention of HIV infection in adults: 2018 recommendations of the International Antiviral Society-USA panel. *JAMA*. 2018;320(4):379–96.

680. Spinner CD, Boesecke C, Zink A, et al. HIV pre-exposure prophylaxis (PrEP): a review of current knowledge of oral systemic HIV PrEP in humans. *Infection*. 2016;44(2):151–8.

681. Cho ME, Kopp JB. Pirfenidone: an anti-fibrotic therapy for progressive kidney disease. *Expert Opin Investig Drugs*. 2010;19(2):275–83.

682. Conte E, Gili E, Fagone E, Fruciano M, Iemmolo M, Vancheri C. Effect of pirfenidone on proliferation, TGF-β-induced myofibroblast differentiation and fibrogenic activity of primary human lung fibroblasts. *Eur J Pharm Sci*. 2014;58:13–9.

Publications

Dickinson M, Kliszczak AE, Giannoulatou E, et al. Dynamics of TGF-β superfamily cytokines during HIV-1 infection are distinct from other innate cytokines. *Front Immunol*. 2020;11(596841).

Borrmann H, Davies R, Dickinson M, et al. Pharmacological activation of the circadian component REV-ERB inhibits HIV-1 replication. *Sci Rep.* 2020;10(1):13271.